



Cape Peninsula
University of Technology

**PROPOSED MITIGATION TECHNIQUES FOR NON-COMPLIANCE CHALLENGES
OF A GRID-CONNECTED PHOTOVOLTAIC PLANT**

by

THEUNIS JOHANNES DUVENHAGE

Dissertation submitted in partial fulfilment of the requirements for the degree

Master of Engineering in Energy

Faculty of Engineering and the Built Environment

Cape Peninsula University of Technology

Supervisor: Prof. Khaled Mohamed Aboalez

Bellville Campus


May 2022

CPUT copyright information

The dissertation/thesis may not be published either in part (in scholarly, scientific or technical journals), or as a whole (as a monograph), unless permission has been obtained from the University

DECLARATION

I, Theunis Johannes Duvenhage, declare that the contents of this dissertation/thesis represent my own unaided work, and that the dissertation/thesis has not previously been submitted for academic examination towards any qualification. Furthermore, it represents my own opinions and not necessarily those of the Cape Peninsula University of Technology.



Signed

04 May 2022

Date

ABSTRACT

South Africa has a need for renewable energy generation as the utility struggles to maintain base load requirements for the country, leaving most of the customers without electricity for hours a day. Detailed information regarding the requirements for connecting a solar photovoltaic plant (SPP) to the South African (SA) utility grid, including legal aspects and boundaries will be presented in a legislative context for grid code compliance (GCC). A network model will be created in DIgSILENT PowerFactory, which includes the utility grid and the connection of a grid-connected SPP. The values of the equipment will be obtained from industry standards and the software program PowerFactory, which the model will be implemented to determine whether there are non-compliance factors during steady-state conditions. A primary objective of this dissertation will be to test the performance of a static inverter model within a designed network for possible non-compliance factors for a Category B SPP with a capacity of 9 MW, located close to an existing Eskom 22 kV network. In addition to providing insight into possible mitigation techniques that can be used by independent power producers (IPPs) to overcome non-compliance with a proposed SPP. The following compliance factor was investigated: 1. Reactive power compliance, 2. Voltage capability requirements, and 3. Power quality. The investigation could provide valuable insight into what methods could be implemented to avoid violations in the GCC. A description of the main electrical equipment for a grid-connected SPP installation is provided, along with a list of the components applicable to a grid-connected SPP installation. Control strategies play a crucial role in assisting SPP inverters in performing according to the grid code to avoid the mitigation of non-compliance factors, which is why the dissertation also provides an understanding on different types of control measures. The simulation requirements for the South African renewable energy grid code (SAREGC) simulations will be discussed and analysed. This is to provide a comprehensive set of simulation requirements that may be defined for grid-connected SPPs in steady-state environments. An analysis of the SPP network model will indicate the necessary steps to conduct reactive compliance simulations at the point of connection (POC) and how the study can be completed by means of adding additional inverters to increase the generation capacity. As part of the steady-state performance simulations, the voltage capability requirements and compliance issues will also be scrutinized for possible issues related to non-compliance. Studies will also focus on fault level inverter contributions and their effect on the utility grid when the utility grid is subjected to maximum and minimum fault level conditions. The power quality requirements will be done for the SPP at the POC with the modelling done in terms of steady-state requirements for the SAREGC. There are several power quality issues challenges that can result in the SPPs producing a non-compliance issue, such as harmonic distortion and can be mitigated by installing a harmonic filter in the SPP network. In the area of grid codes, observational studies are now being used to develop methods of mitigation for violations or non-compliances to be encountered when violations or

non-compliances are observed. The impact of proposing the mitigation techniques will result in the following: 1. Achieving grid code compliance, 2. Optimizing plant performance, and 3. Increasing the lifespan of electrical equipment. Consequently, it is possible to gain a deeper understanding of the main challenges associated with grid code compliance. A comparison of the mitigation techniques implemented and their impact on achieving compliance will be carried out during the studies.

ACKNOWLEDGEMENTS

I wish to thank:

- God the Father, Son and Holy Spirit to whom I owe all that I am;
- Professor Khaled Mohamed Aboalez, my supervisor, for his guidance, support and expert advice throughout this project;
- My parents Theuns and Sophia Duvenhage who always believed in me;
- My wife Anschke and our children Matthew and Mila Duvenhage for allowing me the time and support to pursue my passion.

DEDICATION

For my family

TABLE OF CONTENTS

DECLARATION	ii
ABSTRACT	iii
ACKNOWLEDGEMENTS	v
DEDICATION	vi
TABLE OF CONTENTS	vii
LIST OF FIGURES	x
LIST OF TABLES	xvii
GLOSSARY	xix
ABBREVIATIONS AND SYMBOLS	xx
CHAPTER ONE: INTRODUCTION	1
1.1 Background of the research	1
1.2 Significance of the study	4
1.3 Problem statement	6
1.4 Research methodology	6
1.5 Scope and limitations	8
1.6 Outline of dissertation	8
1.7 Summary	9
CHAPTER TWO: LITERATURE REVIEW	10
2.1 Introduction	10
2.2 Subsystem components of a SPP	10
2.2.1 Solar PV modules	11
2.2.2 DC-link capacitor	12
2.2.3 Inverter (voltage source converter)	13
2.2.4 LCL filter	14
2.3 Topologies of a SPP	15
2.4 Control strategy of a grid-connected SPP	16
2.4.1 Reactive power (Q) control strategy	17
2.4.2 Power factor control strategy	22
2.4.3 Voltage control strategy	28
2.5 Power Quality requirements for grid compliance	34
2.6 Control function requirements for grid compliance	37
2.6.1 Reactive power (Q) control function requirement.....	37
2.6.2 Power factor control function requirement	38
2.6.3 Voltage control function requirement	38
2.7 Steady-state compliance studies for a grid-connected SPP	39
2.7.1 Reactive power requirements	40
2.7.2 Voltage requirement capability	42
2.7.3 Power quality requirements.....	43

2.8	Summary	44
CHAPTER THREE: MODELLING AND SIMULATION OF A SOLAR PHOTOVOLTAIC PLANT		45
3.1	Introduction	45
3.2	Network model	46
3.3	Overview of SPP model in PowerFactory	48
3.3.1	Utility network	48
3.3.2	AC voltage source for harmonic simulations	50
3.3.3	Power park controller	50
3.3.4	Primary incomer and secondary feeder cables	52
3.3.5	Grid box of a SPP	54
3.1.6	Step-up transformers	55
3.1.7	Inverter model	59
3.4	Studies to be conducted in steady-state analysis	66
3.4.1	Reactive capability simulation	69
3.4.2	Voltage capability requirements simulation	71
3.4.3	Fault level study simulation	73
3.4.4	Power quality studies simulation	76
3.5	Summary	83
CHAPTER FOUR: NON-COMPLIANCE IDENTIFICATION OF A SOLAR PHOTOVOLTAIC PLANT		84
4.1	Introduction	84
4.2	Grid code compliance studies	85
4.2.1	SPP reactive power capability	85
4.2.2	SPP voltage capability	88
4.2.3	SPP fault level study	92
4.2.4	Power quality	93
4.3	Summary	98
CHAPTER FIVE: MITIGATION TECHNIQUES FOR NON-COMPLIANCE FACTORS		99
5.1	Introduction	99
5.2	Mitigation techniques for grid code compliance	100
5.3	Grid code compliance studies including the proposed mitigation techniques	100
5.3.1	Case study 1 - SPP reactive power capability and voltage capability requirement mitigation techniques	101
5.3.2	Case study 2 - SPP reactive power capability and voltage capability requirement mitigation techniques	104
5.3.3	Comparative analysis between case study 1 and case study 2	107
5.3.4	SPP power quality mitigation techniques	108
5.4	Summary	113
CHAPTER SIX: CONCLUSIONS AND FUTURE WORKS		115

6.1	Conclusions.....	115
6.2	Future works.....	116
	REFERENCES	117
	APPENDICES	123
	APPENDIX A: PUBLICATION SELECTION WITH THE ABSTRACTS.....	123
	APPENDIX B: POWERFACTORY NETWORK MODEL DATA	124
	APPENDIX C: POWERFACTORY NETWORK MODEL RESULTS	137

LIST OF FIGURES

Figure 1.1: Single line representation of different point of connections	8
Figure 2.1: Subsystems of a SPP	10
Figure 2.2: Equivalent circuit of a PV array	11
Figure 2.3: DC-link circuit illustration	12
Figure 2.4: Three-phase DC-AC inverter	13
Figure 2.5: LCL filter illustration	14
Figure 2.6: Inverter topologies	15
Figure 2.7: Grid-connected SPP control strategy	16
Figure 2.8: PQ capability curve indicating a variable DC voltage	17
Figure 2.9: Variable modulation index of a PQ capability curve	18
Figure 2.10: Control strategy for Q control	19
Figure 2.11: Variable PQ and ambient conditions of the Q_{PPT} operation for absorption of reactive power	20
Figure 2.12: Variable PQ and ambient conditions of the Q_{PPT} operation for injection of reactive power	21
Figure 2.13: Logic function of reactive power control strategy	21
Figure 2.14: Simplified PF control strategy architecture	23
Figure 2.15: PF solar irradiance curve.....	24
Figure 2.16: PF closed-loop system	25
Figure 2.17: PI control algorithm for PF control	26
Figure 2.18: Simplified PF control cycle loop.....	27
Figure 2.19: LVC - Q (V) droop characteristics.....	29
Figure 2.20: (a) Q (V) droop partial rectification on overvoltage conditions, (b) Q support by the inverters of the SPP relative to the collector group distance	30
Figure 2.21: Adaptive Q(V) droop control for SPP	31
Figure 2.22: Adaptive Q(V) droop control for SPP.....	34
Figure 2.23: Q control for a SPP.....	38
Figure 2.24: Voltage control for a SPP	39

Figure 2.25: Reactive power capability requirements at the POC (Q_{min} and Q_{max} are voltage dependent)	41
Figure 2.26: Reactive power capability requirements at the POC (for nominal voltage at POC).....	41
Figure 2.27: Reactive power capability requirements at the POC (for nominal voltage at POC).....	42
Figure 3.1: Overview of complete SPP model in PowerFactory	48
Figure 3.2: Network model simplified.....	49
Figure 3.3: AC voltage source for harmonic simulations	50
Figure 3.4: PPC in network model at the POC	51
Figure 3.5: PPCs dialog within the base case PowerFactory model	51
Figure 3.6: Different control modes of the PPC	52
Figure 3.7: Setpoints, orientation and control characteristics in the network model.....	52
Figure 3.8: Distributed parameter model of a cable.....	53
Figure 3.9: Cable analysis in PowerFactory for the SPP	54
Figure 3.10: Grid box in PowerFactory as modelled in the network	54
Figure 3.11: Three-winding equivalent circuit.....	55
Figure 3.12: Three-winding transformer terminal markings	56
Figure 3.13: Three-winding transformer simulation in network model	58
Figure 3.14: Tap positions for the SPP modelling	59
Figure 3.15: Composite control frame of a SPP modelled in PowerFactory.....	60
Figure 3.16: DSL for dq-transformation of voltage and current	62
Figure 3.17: Control frame for Q control functions.....	63
Figure 3.18: Q control for a SPP.....	64
Figure 3.19: V control for a SPP	65
Figure 3.20: Modelling block diagram for PowerFactory	67
Figure 3.21: Flowchart overview of creating a steady-state network model	68
Figure 3.22: Q capability curve in PowerFactory according to the SAREGC	70
Figure 3.23: $Q_{capability}$ assessment flowchart.....	71

Figure 3.24: Voltage capability diagram in PowerFactory according to the SAREGC.....	73
Figure 3.25: IEC 60909 method illustration used for PowerFactory fault level simulations ...	74
Figure 3.26: IEC 60909 impedance correction principles (DIgSILENT GmbH, 2020)	75
Figure 3.27: Flowchart for fault level compliance	76
Figure 3.28: Power quality flowchart to determine non-compliance factors	78
Figure 4.1: Reactive power requirements for $Q = -0.450$ MVar & $P = 0.450$ MW at POC.....	86
Figure 4.2: Full reactive power capability of the SPP	87
Figure 4.2: PPC set to voltage control for SPP inverters.....	88
Figure 4.3: Study pints to confirm SPP voltage capability	89
Figure 4.4: Voltage capability at 1.1 p.u. for $Q = 2.052$ MVar & $P = 9.000$ MW at POC.....	90
Figure 4.5: Full voltage requirement capability of the SPP.....	91
Figure 4.6: Fault current contributions from the SPP to the POC	92
Figure 4.7: Harmonic distortion at the POC for maximum fault level.....	95
Figure 4.8: Harmonic distortion at the POC for minimum fault level.....	95
Figure 4.9: Frequency sweep from the POC	96
Figure 5.1: SPP inverter PTR 8 addition overview	101
Figure 5.2: Case study 1A - full reactive power capability of the SPP	102
Figure 5.3: Case study 1B - full voltage requirement capability of the SPP	104
Figure 5.4: Case study 2 - full reactive power capability of the SPP	105
Figure 5.5: Case study 2 - full voltage requirement capability of the SPP.....	107
Figure 5.6: Case study 3 - harmonic distortion at the POC for maximum fault level with shunt filter 1 installed.....	109
Figure 5.7: Case study 3 - harmonic distortion at the POC for minimum fault level with shunt filter 1 installed.....	110
Figure 5.8: Case study 3 – Gridbox with shunt filter 1 and shunt filter 2 installed	110
Figure 5.8: Case study 3 - harmonic distortion at the POC for maximum fault level with shunt filter 2 installed.....	112
.....	112

Figure 5.9: Case study 3 - harmonic distortion at the POC for minimum fault level with shunt filter 2 installed.....	112
Figure 5.10: Frequency sweep from the POC with shunt filter 2	113
Figure B.1: Three-winding transformer modelling in PowerFactory.....	131
Figure B.2: Script for Q control	131
Figure B.3: Script for current control.....	131
Figure B.4: Script for power frequency reduction	132
Figure B.5: Script for power frequency non-hysteresis.....	132
Figure B.6: Script for protection of SPP inverter	132
Figure B.7: Script for voltage control	133
Figure B.8: SPP inverter defined as static generator in PowerFactory.....	133
Figure B.9: Control frame of inverter measurements and control.....	133
Figure B.10: Q capability operational limits of the SPP inverters	134
Figure B.11: Q capability curve of the SPP inverters.....	134
Figure B.12: Harmonic source type IEC 61000	135
Figure B.13: Flicker data applied in SPP inverter controls	135
Figure B.14: Continuous and switching operations in PowerFactory	135
Figure B.15: Frequency sweep for minimum- and maximum fault current setup	136
Figure B.16: Case study 3 – shunt filter 1 design parameters.....	136
Figure C.1: Reactive power requirements for Q = 0.450 MVar & P = 0.450 MW at POC ...	140
Figure C.2: Reactive power requirements for Q = -2.052 MVar & P = 1.800 MW at POC ..	140
Figure C.3: Reactive power requirements for Q = 2.052 MVar & P = 1.800 MW at POC ...	141
Figure C.4: Reactive power requirements for Q = -2.052 MVar & P = 9.000 MW at POC ..	141
Figure C.5: Reactive power requirements for Q = 2.052 MVar & P = 9.000 MW at POC ...	142
Figure C.6: Voltage capability at 1.0 p.u. for Q = 2.052 MVar & P = 9.000 MW at POC	142
Figure C.7: Voltage capability at 0.9 p.u. for Q = -0.000 MVar & P = 9.000 MW at POC	143
Figure C.8: Voltage capability at 1.1 p.u. for Q = 0.000 MVar & P = 9.000 MW at POC	143
Figure C.9: Voltage capability at 1.0 p.u. for Q = -2.052 MVar & P = 9.000 MW at POC	144
Figure C.10: Voltage capability at 0.9 p.u. for Q = -2.052 MVar & P = 9.000 MW at POC ..	144

Figure C.11: Study point 1 during a voltage of 1.1 p.u. at the POC – inverter voltage overloaded.....	145
Figure C.12: Study point 4 during a voltage of 1.1 p.u. at the POC – inverter voltage overloaded.....	145
Figure C.13: Power factor and voltage requirement at POC indicating underexcited (left) conditions and overexcited conditions (right).....	146
Figure C.14: Fault level study at POC (total contributions).....	146
Figure C.15: THD at POC for maximum fault level.....	147
Figure C.16: THD at POC for minimum fault level.....	147
Figure C.17: Flicker at maximum fault level - Short-term continuous and switching operation results.....	148
Figure C.18: Flicker at maximum fault level - Long-term continuous and switching operation results.....	148
Figure C.19: Flicker at minimum fault level - Short-term continuous and switching operation results.....	149
Figure C.20: Flicker at minimum fault level - Long-term continuous and switching operation results.....	149
Figure C.21: Case study 1 - reactive power requirements for $Q = -0.450$ MVar & $P = 0.450$ MW at POC.....	150
Figure C.22: Case study 1 - reactive power requirements for $Q = 0.450$ MVar & $P = 0.450$ MW at POC.....	150
Figure C.23: Case study 1 - reactive power requirements for $Q = -2.052$ MVar & $P = 1.800$ MW at POC.....	151
Figure C.24: Case study 1 - reactive power requirements for $Q = 2.052$ MVar & $P = 1.800$ MW at POC.....	151
Figure C.25: Case study 1 - reactive power requirements for $Q = -2.052$ MVar & $P = 9.000$ MW at POC.....	152
Figure C.26: Case study 1 - reactive power requirements for $Q = 2.052$ MVar & $P = 9.000$ MW at POC.....	152

Figure C.27: Case study 1 - voltage capability at 1.1 p.u. for $Q = 2.052$ MVar & $P = 9.000$ MW at POC.....	153
Figure C.28: Case study 1 - voltage capability at 1.0 p.u. for $Q = 2.052$ MVar & $P = 9.000$ MW at POC.....	153
Figure C.29: Case study 1 - voltage capability at 0.9 p.u. for $Q = -0.000$ MVar & $P = 9.000$ MW at POC.....	154
Figure C.30: Case study 1 - voltage capability at 1.1 p.u. for $Q = 0.000$ MVar & $P = 9.000$ MW at POC.....	154
Figure C.31: Case study 1 - voltage capability at 1.0 p.u. for $Q = -2.052$ MVar & $P = 9.000$ MW at POC.....	155
Figure C.32: Case study 1 - voltage capability at 0.9 p.u. for $Q = -2.052$ MVar & $P = 9.000$ MW at POC.....	155
Figure C.33: Case study 1 - study point 1 during a voltage of 1.1 p.u. at the POC – inverter voltage within operational requirements	156
Figure C.34: Study case 1 - study point 4 during a voltage of 1.1 p.u. at the POC – inverter voltage within operational requirements	156
Figure C.35: Case study 1 - power factor and voltage requirement at POC indicating under excited (left) conditions and overexcited conditions (right)	157
Figure C.35: Case study 2 - reactive power requirements for $Q = -0.450$ MVar & $P = 0.450$ MW at POC.....	157
Figure C.37: Case study 2 - reactive power requirements for $Q = 0.450$ MVar & $P = 0.450$ MW at POC.....	158
Figure C.38: Case study 2 - reactive power requirements for $Q = -2.052$ MVar & $P = 1.800$ MW at POC.....	158
Figure C.39: Case study 2 - reactive power requirements for $Q = 2.052$ MVar & $P = 1.800$ MW at POC.....	159
Figure C.40: Case study 2 - reactive power requirements for $Q = -2.052$ MVar & $P = 9.000$ MW at POC.....	159

Figure C.41: Case study 2 - reactive power requirements for $Q = 2.052$ MVar & $P = 9.000$ MW at POC.....	160
Figure C.42: Case study 2 - voltage capability at 1.1 p.u. for $Q = 2.052$ MVar & $P = 9.000$ MW at POC.....	160
Figure C.43: Case study 2 - voltage capability at 1.0 p.u. for $Q = 2.052$ MVar & $P = 9.000$ MW at POC.....	161
Figure C.44: Case study 2 - voltage capability at 0.9 p.u. for $Q = -0.000$ MVar & $P = 9.000$ MW at POC.....	161
Figure C.45: Case study 2 - voltage capability at 1.1 p.u. for $Q = 0.000$ MVar & $P = 9.000$ MW at POC.....	162
Figure C.46: Case study 2 - voltage capability at 1.0 p.u. for $Q = -2.052$ MVar & $P = 9.000$ MW at POC.....	162
Figure C.47: Case study 2 - voltage capability at 0.9 p.u. for $Q = -2.052$ MVar & $P = 9.000$ MW at POC.....	163
Figure C.48: Case study 2 - study point 1 during a voltage of 1.1 p.u. at the POC – inverter voltage within operational requirements	163
Figure C.49: Study case 2 - study point 4 during a voltage of 1.1 p.u. at the POC – inverter voltage within operational requirements	164
Figure C.50: Case study 2 - power factor and voltage requirement at POC indicating under excited (left) conditions and overexcited conditions (right)	164
Figure C.51: Case study 3 - THD at POC for maximum fault level with shunt filter 1.....	165
Figure C.52: Case study 3 - THD at POC for minimum fault level with shunt filter 1.....	165
Figure C.53: Case study 3 - THD at POC for maximum fault level with shunt filter 2.....	166
Figure C.54: Case study 3 - THD at POC for minimum fault level with shunt filter 2.....	166

LIST OF TABLES

Table 1.1: Renewable power plant categories.....	7
Table 2.1: Inverter harmonic emission requirements for SPPs	35
Table 3.1: Connection table for star-star-delta transformer	57
Table 4.1: Reactive power requirements and results of the SPP	85
Table 4.2: Requirements and results of voltage capability at the POC	89
Table 4.3: Harmonic emission limits for compliance of the SPP (NRS 048-4, 2004)	93
Table 4.4: Compatibility levels for harmonic voltages for HV and EHV networks (expressed as a percentage of the reference voltage)	94
Table 4.5: Recommended planning levels for harmonic voltages (as a percentage of the rated voltage of the power system).....	94
Table 4.6: Flicker disturbance factors at the POC	97
Table 5.1: Case study 1A - reactive power requirements and results of the SPP	102
Table 5.2: Case study 1B - requirements and results of voltage capability at the POC	103
Table 5.3: Case study 2A - reactive power requirements and results of the SPP	105
Table 5.4: Case study 2B - requirements and results of voltage capability at the POC	106
Table 5.5: Case study 1 versus case study 2 – reactive power and voltage capability	107
Table 5.6: Case study 3 – shunt filter 1 data	109
Table 5.7: Case study 3 – shunt filter 2 data	111
Table B.1: External grid parameters for a SPP in PowerFactory	124
Table B.2: AC voltage source values for steady-state simulations.....	124
Table B.3: Cable data used in the network model (Aberdare, 2008).....	124
Table B.4: Cable lengths in the network model	125
Table B.5: Transformer data for SPP	125
Table B.6: Q capability limits of the SPP inverters provided in p.u. in PowerFactory	125
Table B.7A: Q capability curve matrix for Qmax (export)	126
Table B.7B: Q capability curve matrix for Qmax continued (export).....	126
Table B.8A: Q capability curve matrix for Qmin (import)	127
Table B.8B: Q capability curve matrix for Qmin continued (import).....	127

Table B.9: Voltage capability matrix for the requirements of the SPP in PowerFactory	128
Table B.10A: Case study 2 - Q capability curve matrix for Qmax (export)	129
Table B.10B: Case study 2 - Q capability curve matrix for Qmax continued (export).....	129
Table B.11A: Case study 2 - Q capability curve matrix for Qmin (import)	130
Table B.11B: Case study 2 - Q capability curve matrix for Qmin continued (import).....	130
Table C.1: Harmonic Distortion at maximum and minimum fault level at POC	137
Table C.2: Harmonic Distortion at maximum and minimum fault level at POC with shunt filter 1	138
Table C.3: Harmonic Distortion at maximum and minimum fault level at POC with shunt filter 2.....	139

GLOSSARY

Definition/Explanation

Harmonic- A sinusoidal component of a periodic wave or quantity having a frequency that is an integral multiple of the fundamental frequency (IEEE, 2000).

Harmonic distortion – Distortion of a sinusoidal waveform characterized by indication of the magnitude and order of the Fourier series terms describing the wave (IEEE, 2000).

Independent power producer (IPP) – We define IPPs as power projects that are, in the main, privately developed, constructed, operated and owned; have a significant proportion of private finance; and have long-term power purchase agreements with a utility or another off-taker (Eberhard, et al., 2017).

Integrated resource plan (IRP) – Refers to the co-ordinated schedule for generation expansion and demand-side intervention programmes, taking into consideration multiple criteria to meet electricity demand (DoE, 2019).

Levelised cost of energy (LCOE) – is an economic measure used to compare the lifetime costs of generating electricity across various generation technologies (Raikar & Adamson, 2020).

Point of connection (POC) – The electrical node(s) on the Network Service Provider's network where the Embedded Generator's electrical equipment is physically connected to the Network Service Provider's electrical equipment (Andrew Craib, 2013).

Power park controller (PPC) – Facilitates comprehensive regulation of active and reactive power as well as the voltage of heterogeneous PV systems, enabling fast and stable control at the grid connection point (Meteo Control, 2021).

Renewable energy – Renewable energy is defined as energy that is produced by natural resources, such as sunlight, wind, rain, waves, tides, and geothermal heat, that are naturally replenished within a time span of a few years (Lund, 2010).

Shunt filter – A type of filter that reduces harmonics by providing a low-impedance path to shunt the harmonics from the source away from the system to be protected (IEEE, 2000).

Solar photovoltaic plant (SPP) – A single photovoltaic panel or a group of several photovoltaic panels with associated equipment operating as a power plant (Andrew Craib, 2013).

System Operator (SO) – Usually adopt load following control such as look-ahead short-term unit commitment, real-time economic dispatch and automatic generation control to maintain system balance (Zheng, et al., 2012).

Total harmonic distortion (THD) – The ratio of the root square value of the harmonic content to the root square value of the fundamental quantity, expressed as a percent of the fundamental (IEEE, 2000).

Utility grid – Not consisting of a single entity but an aggregate of multiple networks and multiple power generation companies with multiple operators employing varying levels of communication and coordination, most of which is manually controlled (Bassam, 2021).

ABBREVIATIONS AND SYMBOLS

Abbreviations

AC	Alternating current
BW	Bid window
CIGRE	Council on large electric systems (French acronym)
CIREN	International agency for research on the environment and development (French acronym)
COD	Commercial operation date
CT	Current transformer
CVC	Coordinated voltage control
DC	Direct current
DCUOSA	Distribution connection and use-of-system agreement
DlgSILENT	Digital simulation of electrical networks
DoE	Department of Energy
DPL	DlgSILENT programming language
DSL	DlgSILENT simulation language
EID	Electronic intelligent device
EMC	Electromagnetic compatibility
Eskom	Electrical Supply Commission
FC	Flicker control
GCC	Grid code compliance
GCRPP	Grid connection for renewable power plants
GW	Gigawatt
HMI	Human machine interface
HV	High voltage
IEC	International electrotechnical commission
IEEE	Institute of electrical and electronics Engineers
IGBT	Insulated gate bipolar transistor
IPP	Independent power producer
IRP	Integrated resource plan
kA	Kiloampere
kVA	Kilovolt Ampere
LCOE	Levelized cost of energy
LV	Low voltage
LVC	Local voltage control
MEC	Maximum export capacity

MPPT	Maximum power point tracker
MV	Medium voltage
MVA	Megavolt Ampere
MVar	Megavolt Ampere reactive
NERSA	National Energy Regulator of South Africa
NIPS	National interconnected power system
NRS	National rationalised specification
NSP	Network service provider
OEM	Original equipment manufacturer
PCC	Point of common coupling
PF	Power factor
PGC	Point of generator connection
PI	Proportional integral
PLL	Phase-locked loop
POC	Point of connection
POS	Point of supply
PPA	Power purchase agreement
PPC	Power park controller
PTR	PV and transformer station
PUC	Point of utility connection
PV	Photovoltaic
PWM	Pulse-width modulator
REIPPP	Renewable energy power producer procurement programme
RES	Renewable energy
RETEC	Renewable energy technical evaluation committee
RMS	Root mean square
RPP	Renewable power producer
RVC	Rapid voltage change
SA	South African
SANS	South African national standards
SAREGC	South African renewable energy grid code
SBA	Self-build agreement
SBO	Single buyers office
SCADA	Supervisory control and data acquisition
SO	System operator
SOA	System operating agreement
SPP	Solar PV plant
THD	Total harmonic distortion

TR	Technical report
VT	Voltage transformer
WECC	Western electricity coordinating council

Roman alphabet

C	Capacitance, F
E	Electromagnetic field, V
F_{meas}	Measured frequency, Hz
G_{β}	Solar irradiance on PV array surface, W/m ²
G	Solar irradiation, W/m ²
i_{cap}	DC-link capacitor current, A
i_{conv}	DC converter output current, A
I_D	Diode current, A
I_F	Distributed current source, A
i_{inv}	AC-DC inverter input current, A
I_{K_SPP}	Total fault current from SPP, A
I_{K_Total}	Total fault current contribution at POC, A
$I_{K_Utility_Grid}$	Total existing fault current at POC, A
I_{ph}	Photoelectric current, A
I_{pva}	PV array current, A
I_{sc}	Short-circuit current, A
k_b	Boltzmann constant, J/°K
k_{Isc}	Temperature coefficient of the short-circuit current, %/°C
k_{QV}	Predefined QV droop, %
k_{Voc}	Temperature coefficient of the open-circuit voltage, %/°C
L	Inductance, H
M	Modulation index, no unit
N_C	Common windings, no unit
N_{pp}	Number of parallel connected PV modules, no unit
N_S	Serial windings, no unit
N_{ss}	Number of series connected PV modules, no unit
N_T	Total windings, no unit
PF_{ind}^{min}	Inductive power factor limit, no unit
P_{Gen}	Generation real power, W
P_{meas}	Measured real power, W
P_{MPP}	Maximum real power, W
P_{out}	Real power output of inverter, W

P_R	Exceeded real power, W
P_{ref}	Reference real power, W
P_{SPP}	Real power of the SPP, W
q	Electric charge, C
Q	Reactive power, Var
Q_{max}	Maximum reactive power of inverter, VAR
Q_{meas}	Measured reactive power, VAR
Q_{MPP}	Maximum reactive power, VAR
Q_R	Exceeded reactive power, Var
Q_{ref}	Reference reactive power, VAR
QV	Reactive power and voltage function for droop, %
R_N	Short-circuit resistance at the POC, Ω
R_p	Parallel resistance of the PV array, Ω
R_s	Series resistance of the PV array, Ω
S	Apparent power, VA
S_i	Solar irradiance, W/m ²
S_{max}	Maximum apparent power of inverter, VA
T_a	Ambient temperature, °C
T_n	Nominal temperature of PV module, °C
T_{op}	Operating temperature of PV module, °C
V_a	Phase 'a' of inverter, V
V_b	Phase 'b' of inverter, V
V_c	Phase 'c' of inverter, V
V_{conv}	Conversion voltage, V
V_F	Distributed voltage source, V
V_{grid}	Grid voltage, V
V_{meas}	Measured voltage, V
V_{MPP}	Maximum DC voltage, V
V_{oc}	Open-circuit voltage, V
V_{sm}	Line-to-ground voltage amplitude, V
V_t	Thermic voltage of PV array, V
X	Reactance of the utility grid, Ω
X_C	Capacitance reactance, Ω
X_L	Inductive reactance, Ω
X_N	Short-circuit reactance at the POC, Ω
Z	Impedance, Ω
Z_h	Harmonic impedance, Ω
Z_M	Magnetizing impedance, Ω

P_{st}	Short-term flicker disturbance factor, no unit
P_{lt}	Long-term flicker disturbance factor, no unit
S_k	Short-circuit apparent power of the utility grid, VA

Greek alphabet

β	Angle of tilt of the PV array, Degrees
Δ	Delta, indicates a change in the parameter to which it is attached, no unit
γ	Admittance, Siemens
γ_M	Magnetizing admittance, Siemens
δ	Harmonic attenuation, no unit
ψ_k	Impedance angle, Degrees
ω	Angular frequency, rad/second
G	Conductance, Siemens
G_M	Magnetizing conductance, Siemens

CHAPTER ONE: INTRODUCTION

1.1 Background of the research

Critical components in economic growth and development in any country is to supply energy continuously and sustainably. The challenge is to provide access to affordable and reliable energy in support of socio-economic development needs in the South African (SA) context and reducing the major environmental challenges that the carbon footprint of energy systems shall undergo to deliver clean energy. The Electricity Supply Commission (Eskom) is currently in distress from energy generation capacity problems due to demand exceeding supply as the installed capacity needs to increase from 51 Gigawatt (GW) to 72 GW (Monyei, et al., 2018) (Eskom, 2018). Unplanned utility outages due to dwindling reserve margins from economic expansions, which has not been mirrored in the energy generation sector for development and equipment failure have been blamed for the crisis. As a result, Eskom introduced “load shedding”, that try to prevent a total blackout and preserve the grid when the demand exceeds the supply (Monyei, et al., 2018).

The reliability of energy supply in South Africa is under question due to Eskom’s installed generation capacity deficit by more than 8 GW, renewable energy sources (RES) may be used to complement the demand of the South African electricity network, proving a reliable and sustainable solution to the energy crisis (Eberhard, 2014). The SA utility’s grid energy mix consists of 3.7 GW from RE, 2.7 GW generated from pumped-storage, 1.8 GW from nuclear, 3.8 GW from diesel generators, 1.7 GW from hydroelectric power and 38 GW generated from coal, accumulating installed capacity at 51.7 GW and firm capacity at a base of 45 GW. Electricity generated is transmitted through the Eskom transmission networks to various end users including the municipalities, which distributes the electricity within their own networks. The integrated resource plan (IRP) 2019 indicates that RE will form part of the energy mix till 2030, which will determine if adequate capacity is installed, and the base requirements are met with RESs to the utility grid (Department of Mineral Resources and Energy, 2019).

Energy storage is disrupting the traditional power delivery model as it provides functionality similar to smart grids and will form part of the future bid window (BW) in order to utilize non-dispatchable RE technologies, such as wind and solar photovoltaic (PV). The addition of the energy storage component will contribute to the already installed 6 GW of RE in SA, where the energy can then be evacuated when required. The IRP 2019 indicates an additional 7.5 GW of solar PV will be installed and connected to the utility grid, providing more opportunities for viable compliance techniques (Department of Mineral Resources and Energy, 2019). Integration of renewable energy plants into the national utility grid is therefore a necessity, with

necessary mitigation techniques being required to enable compliance within the SA renewable energy grid code (SAREGC).

With the increasing requirement of renewable energy to support the utility grid a tender process was developed to facilitate the energy needs of the SA energy sector. The SA renewable energy independent power producer procurement programme (REIPPPP) was launched to enable grid-connected RE generation and a total of 6.3 GW of solar PV, wind and other RE technologies have been procured under the programme to date. Each phase of the REIPPPP BW bidding process the independent power producer (IPP) will have to submit a competitive bid, which forms part of a one-series close tender bid comprising of a request for qualification and proposal. Once the IPPs reached preferred bidder status in the tender process from the SA government, a non-negotiable standard 20-year power purchase agreement (PPA) between the off-taker (Eskom) and IPP will be concluded. Direct agreements, which entails the compliance of RE technology connected to the utility grid will also be included between the Department of Energy (DOE), the National Energy Regulator of South Africa (NERSA), IPPs and Eskom to ensure operational technical grid compliance as set out by the system operator agreement (Eberhard & Naude, 2016).

In order to embed the Solar PV Plant (SPP) to the South African grid the solar plant has to comply with the SAREGC and the Eskom Distribution Connection and Use-of-System Agreement with generators (DCUOSA), which comprises of technical requirement within the design of the SPP, mainly for protection, metering and the indication of legal connection points in the system. If a violation of the SAREGC occurs the IPP has the option to apply for a temporary or permanent derogation depending on the seriousness of the offense. Usually, a temporary exemption is granted if the offense can be resolved with the major design criteria of the SPP. When the IPP applies for a permanent exemption the design criteria did not meet the requirements and the project is already in the construction phase. The transmission System Operator (SO) for the SA grid will institute set points in the System Operating Agreement (SOA) within the SPP's power park controller in order not to compromise the grid's integrity. The PPA will constitute the legal requirements that needs to be fulfilled in order to grant generation into the utility grid. The PPA will state what the maximum export capacity (MEC) entails and the contractual construction programme timelines that needs to be adhered to (Smit, 2015). Eskom also provides the developer with a Self-Build Agreement (SBA), which enables the developer to expedite the construction of the integration between the grid and SPP on his own terms (Eskom, 2021).

DlgSILENT PowerFactory will be used as the primary simulation software as required by the utility. In order to reach the Commercial Operational Date (COD), the SPP needs to be simulated and verified on DlgSILENT PowerFactory, once all the simulations and test data is

provided and satisfactory to Eskom, an approval is obtained from the Renewable Energy Technical Evaluation Committee (RETEC) and the SO, a COD can be issued which allows the SPP to generate electricity into the utility grid. During the legal requirements and obligations that needs to be fulfilled according to the PPA (between the Seller, which is represented by the IPP and the Single Buyers Office (SBO – Eskom entity), the contractual agreed timelines shall be met in the PPA. When the COD is postponed, the IPP may be liable for costly penalties imposed on them by the Lenders (Banks) and the SBO. Thus, it is critical that the COD is reached by providing all the necessary simulations and test results.

Solar energy technologies with respect to PV comprise of a unique property of certain semi-conductors, which converts solar radiation into electricity. Wafers used in PV systems made from crystalline silicon produce a direct current when exposed to sunlight or radiation from the sun. A SPP system consists of several electrical components, such as PV arrays, inverters, maximum power point tracker (MPPT) controllers, solar plant controllers, step-up transformers, direct current (DC) cables, alternating current (AC) cables and grid boxes. The electrical components form part of the SPP when operating as a large-embedded generation plant (Dunlop, 2010). When the SPP is geographically located too far from the point of connection (POC) at the utility, the set-points may not be achieved due to the plant not being adequately designed with the calculated/pre-determined set-points under consideration. The solar plant will be connected to the utility grid at a Medium Voltage (MV) level, the distance between the SPP and the POC may need to be reduced or the equipment needs to be upgraded to identify and eliminate the contributing non-compliance factors.

Previous work has been published in regard to compliance studies for “Grid-connected renewable energy sources: Review of the recent integration requirements and control methods” by Al-Shetwi, et al (2020), “Guiding Principles for Grid Code Compliance of Large Utility Scale Renewable Power Plant Integration onto South Africa’s Transmission/Distribution Networks” by Sewchurran and Davidson (2016) and “Study on Grid-connected Renewable Energy Grid Code Compliance” by Yongning, et al. (2019), which also considers further compliance studies with regard to the generation of energy by renewable energy plants.

This study will focus on the SAREGC requirements and simulation studies for one solar plant, connected at a specific point within the South African Eskom utility network. Simulation and identification of non-compliances factors will be done for a SPP.

1.2 Significance of the study

The primary objective of this study will be to identify specific non-compliance factors during steady-state conditions, which may hamper the successful connection of a SPP to the utility grid, using appropriate simulation software. A second objective will be to determine appropriate mitigation techniques for the specified non-compliance factors, thereby enabling successful grid connection and considerable savings for IPPs. Utility grid information will be implemented at the POC to mimic the utility grid performance at the specific connection of the SPP. The information will be evaluated, and the data will be modelled as an external grid to the SPP to accurately simulate the inverter model in the DiGSILENT PowerFactory software. Capabilities of the complete SPP model will be analysed in steady-state operation cases to indicate the possibilities of non-compliance factors according to the SAREGC.

Mandatory minimum guidelines were also developed in 2010 by NERSA and Eskom in order to ensure that any generation facility connected onto the national grid ensures that the integrity of the grid is not compromised and that the grid remains stable (Sewchurran & Davidson, 2017). Before the integration of any generation plant whether state or privately owned, which is intended to be connected onto the electrical grid should provide compliance to the SAREGC requirements and the studies should be provided to the RETEC for approval (Sewchurran & Davidson, 2016). DiGSILENT PowerFactory will be used as the primary simulation software to perform the mathematical analysis required for the steady-state simulations. In order to reach the COD, the solar PV plant needs to be simulated and verified on the simulation software, tested with the presence of the RETEC and the SO, which is governed by Eskom. Once all the simulations and test data are provided and satisfactory to Eskom an approval is obtained from RETEC and the SO, a COD can be issued which allows the solar PV plant to generate power into the grid.

Steady-state studies that is required for the integration of SPPs to the SA grid comprises of reactive power capabilities of the inverters when introduced to the parameters of the existing grid. Existing regulations and studies show that the plant needs to absorb or inject reactive power within the required power factor range, which is dependent on the size of the plant and the maximum export capacity (Sewchurran & Davidson, 2017). Compliance simulation with reactive power capabilities will cover the power factor control of the inverter, which the inverter needs to be within the threshold of the desired parameters whilst delivering the under excitation or over excitation condition to the grid (Yongning, et al., 2019). Reactive power needs to be adjusted continuously when the plant is instructed by national control in order to perform within the ranges of the power factor at the point of connection (POC), this is normally achieved by a Power Park Controller (PPC) (Dinu, et al., 2016). Voltage requirements of the SPP also forms part of the steady-state studies, which needs to be performed in conjunction with the reactive

power capability studies. In the studies performed previously and within the set points of the regulations the voltage requirements are usually not required at the generating plant itself, but at the POC (Kunte, et al., 2012) (Irazabal, et al., 2017). The findings also show that if the grid voltage is unstable and the grid frequency operating limits are compromised the addition of a SPP may provide stabilisation as per the SAREGC requirements (Rodrigues, et al., 2016). Power quality issues within the SPP is also documented and the regulation for the power quality in South Africa is adopted by the National Rationalised Specification (NRS) 048 part 2, which was introduced in 1996 and is regularly revised. Previous studies show that the contributing factor to the harmonic spectrum at the Point of Common Coupling (PCC) or POC has an impact on the inverter's capability to reduce the harmonic emission in the network (Minnaar, et al., 2018) (Bullich-Massague, et al., 2015).

The work will focus on the steady-state simulation of grid code compliance factors that may obstruct the connection of the plant to the national grid of South Africa and provide possible mitigation techniques. Compliance studies may also indicate to the designer of the SPP what design methodologies to introduce to the plant design in order to obtain compliance from RETEC and to avoid any delays that may form part in the design process. The framework of the study will focus on the steady-state SAREGC requirements and simulation studies for one SPP, connected at a specific point within the South African Eskom network. Simulation and identification of non-compliance factors will only be done for Category B (1 MVA – 20 MVA) SPPs. The new knowledge and significance gained during the process of compiling the dissertation will comprise of benefit factors that may result in easier grid integration (grid code compliance).

Contributing factors towards grid code compliance will also be considered by using the NRS, South African national standards (SANS) and the Eskom Standard DST 34-1765. Reactive power capabilities of the plant will be assessed to determine if the SPP can inject or absorb reactive power when the utility grid requires the SPP to comply with the specific control mode provided by the SAREGC. When the reactive power capabilities are performed the study and analysis will also cover the voltage requirements capability of the SPP when connected to the utility grid. Information obtained from simulations for the quality of supply (QoS) will be used to determine the extent to which the harmonic emissions have on the compliance of the SPP. The utilisation of mitigation techniques will enable Eskom and the IPP to benefit from the implementation scenarios. Once Eskom provides the IPP the grid characteristics, the original equipment manufacturer (OEM) of the inverter will have a better interpretation of the expected operational capabilities of the product to ensure that the requirements are achieved for the specific SPP. Eskom may also benefit from this study regarding the contribution of the findings with respect to the electrical energy evacuated to the national grid with the desirable harmonic

emission in-feeds to their network. Different mitigation techniques focussing on steady-state compliance factors will be simulated using DIgSILENT PowerFactory to demonstrate the compliance/non-compliance conditions for a SPP. Eskom may be able to decrease the stress on their existing network with the connection of an approved SPP to the utility's grid. Capital investments will be reduced by both IPP and Eskom, due to a better understanding of the SAREGC.

The objective of the analysis will give the IPP a workable and cost-effective solution to connect a SPP effectively and efficiently to the national grid of the utility, thereby assisting to reduce any possible "shortcomings" in the proposed connection.

1.3 Problem statement

Problem arises in the proposed grid-connected SPPs that may not comply with specific power regulations from the SAREGC and therefore may be denied connection to the utility's grid, or the IPP shall apply for an exemption where the plant needs to comply within a specific timeline when connected to the utility's grid. The IPP needs to evaluate what possible measures can be taken from a techno-economic viable perspective. Proposing appropriate mitigation techniques for the following non-compliance factors is required to ensure grid connection:

- i. Non-compliance factor 1: Reactive power requirements;
- ii. Non-compliance factor 2: Voltage capability requirement;
- iii. Non-compliance factor 3: Power quality.

1.4 Research methodology

The simulations for the SPP will indicate on what the possible non-compliance factors may entail for the integration to the National Interconnected Power System (NIPS) (DoE, 2019) (Sewchurran & Davidson, 2017). The steps below will indicate on how the research design will be approached by performing the following (Sewchurran & Davidson, 2016):

- i. Obtain DCUOSA with Generators from the IPP with the specific requirements to be met as per grid code requirements;
- ii. Utility grid to provide the external grid details of POC;
- iii. Inverter suppliers to provide dynamic inverter model in the PowerFactory execution file format;
- iv. Build the power system network on PowerFactory software and implement all design parameters;

- v. Use the SAREGC and Eskom standard DST 34-1795 as guidelines of what simulations needs to be performed in steady-state conditions;
- vi. Identify non-compliances in the new generation SPP;
- vii. Implement mitigation techniques to resolve or mitigate any non-compliance factors.

The power system network will have to be based on an Eskom side and a facility side (located at the IPP portion of the SPP) in the study, where important definitions need to be defined to understand and to analyse the data for grid code compliance (Sewchurran & Davidson, 2017). The SAREGC has 5 categories as shown in Table 1 that needs to be adhered to when applying for a generation license (Sewchurran & Davidson, 2017).

Table 1.1: Renewable power plant categories (Mchunu, 2020)

Category	Rated Power	Voltage Level
A1	0 - 13.8 kVA	LV Connected
A2	13.8 – 100 kVA	LV Connected
A3	0.1 – 1 MVA	LV Connected
B	1 – 20 MVA	MV Connected
C	≥20 MV	HV Connected

All the simulations and findings will be conducted at the POC as per the SAREGC requirements. Figure 1 shows the demarcation between the IPP (facility side) and Eskom (utility grid side) with the relevant connection points. The following technical connection points are shown below and in Figure 1:

- PCC: Point of Common Coupling;
- POC: Point of Connection;
- PUC: Point of Utility Connection;
- POS: Point of Supply;
- PGC: Point of Generator Connection.

In accordance with the requirements of the SAREGC, the simulations and results of the research will be presented during steady-state analysis. To meet grid compliance requirements, the power system network will have to be modelled as a network model with a utility grid that possess a X/R ratio at the POC. The SPP network contribution from the IPP's facility side will be implemented to determine the impact on the utility grid. All the requirements in terms of compliance to the utility grid will be investigated and information will be gathered to determine the impact, the SPP will have on the utility grid. As the SPP must support the grid

or enhance the performance at the POC, it will be mandatory to present all the findings in terms of non-compliance or compliance to the utility grid.

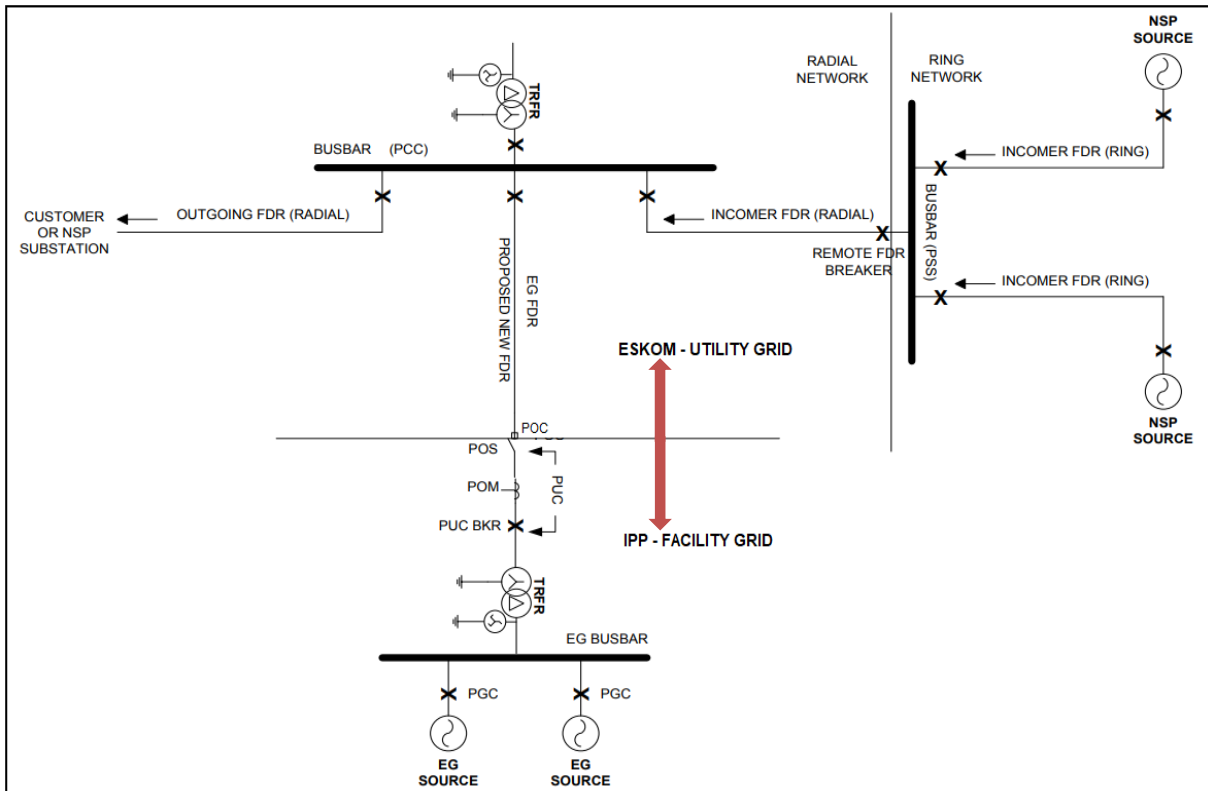


Figure 1.1: Single line representation of different point of connections (Andrew Craib, 2013)

1.5 Scope and limitations

This study will not include compliance studies and requirements for all SPP categories. Signalling, communication, PPC and protection designs will not be considered in this research paper. Simulation tests will only be conducted at the POC and for steady-state conditions in the network model. Also, an exclusion of detailed design of any compensation device for reactive power requirements nor the detailed design of an active or passive filter for power quality enhancements. The composite frame of the inverters which incorporates DlgSILENT Programming Language (DPL) scripts will only be implemented as a generic controller with minor modifications and contributions for reactive power, voltage and power quality in the SPP performance.

1.6 Outline of dissertation

The layout of the remaining part of this dissertation is as follows:

Chapter 2: In this chapter the focus is on the SPP technology that will be used in the plant for the simulations, including the different control strategies that will also

be investigated for the SPP. Requirements and studies that can be carried out in a power system according to the SAREGC for compliance and non-compliance behaviour during steady-state operations.

- Chapter 3: The readably available inverter model in DIgSILENT PowerFactory format will be introduced and explained together with all the network equipment to provide the complete simulation model. The concepts behind the simulations and how they may be performed for steady-state cases will be discussed. All variables required will be clarified and the exact process or steps taken to arrive at the results will be documented.
- Chapter 4: This chapter will incorporate the results obtained from the previous chapter's simulation model, the data will be utilized to describe if the SPP complies to the SAREGC or if there are any non-compliance factors that will inhibit the connection of the grid-connected plant under any steady-state simulation conditions.
- Chapter 5: The aim of this chapter is to provide mitigation techniques and prove compliance in steady-state conditions. A summary of findings of the simulations done will be presented with comparisons made between this chapter and chapter 4s simulation results, with some of the more important points being taken under consideration with a view toward related work.
- Chapter 6: Conclusions and discussions of the possible mitigation techniques are drawn and recommendations toward possible future research are discussed of the study.

1.7 Summary

The aim of chapter 1 was to provide a background to the legal aspects and boundaries of what is required for the connection of a SPP to the SA National utility grid. The network will be modelled to determine whether non-compliance factors may arise. The primary research objective is to test the performance of a static inverter model within the designed network for possible non-compliance factors for a Category B SPP. The research has the potential of providing valuable insight on possible mitigation techniques that may be used to overcome non-compliance of a proposed SPP by an IPP to an off-taker (Eskom – utility grid or private entity), before connecting the RE technology to the national utility grid. Chapter 2 will focus on the solar PV technology that is implemented in the network model for simulation purposes. Also, the theoretical and mathematical aspects of how the SPP is controlled at the POC with different strategies to implement efficient control and mitigate the risk of non-compliance issues that may arise during steady-state conditions.

CHAPTER TWO: LITERATURE REVIEW

2.1 Introduction

This chapter will review and discuss available literature on grid-connected SPPs, the main electrical components will be discussed to understand the simulation model's configuration. The control system of the RE plant will form part of this chapter including the grid code compliance (GCC) studies that permits the integration of RE technology to the utility grid. Designing a utility scale SPP requires detailed involvement, which requires years of design experience and considerable technical knowledge in the solar PV field. The levelized cost of energy (LCOE) in a SPP design criterion is of utmost importance, the SPP should be optimised and scrutinized to provide a techno-economic viable solution. The fundamental building blocks of a SPP is the subsystems consisting of power electronic equipment, also the inverter topology and the control system that forms part of the simulation to identify possible compliance violations during steady-state conditions.

2.2 Subsystem components of a SPP

During the design stage, particularly in the front-end engineering design phase the equipment rating of the SPP is calculated before any simulation for grid code compliance occurs. Fundamental components in Figure 2.1 relating to the subsystem of a SPP is shown and comprises of the solar PV modules, DC-link capacitor, inverters and a LCL filter, which is connected to the AC grid of the off taker (Nwaigwe, et al., 2019).

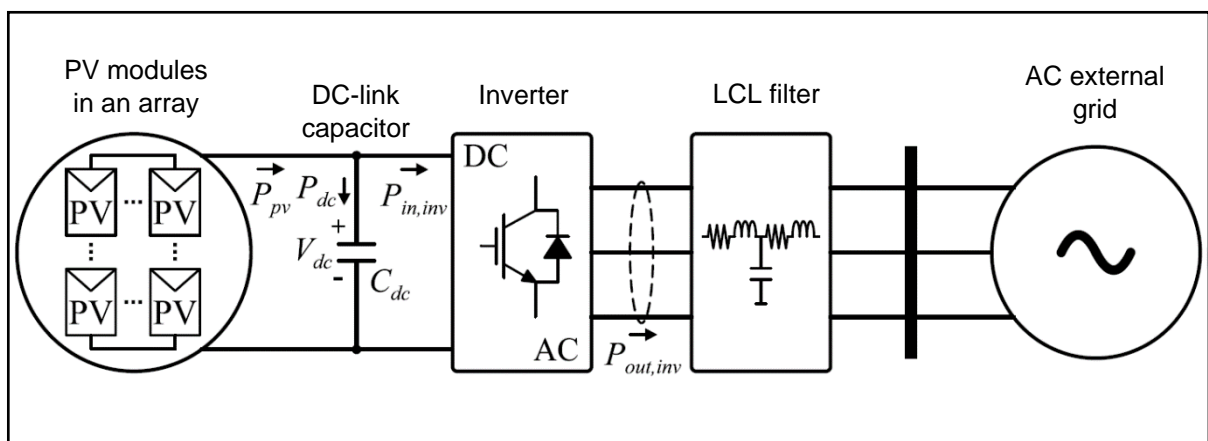


Figure 2.1: Subsystems of a SPP (Feldman & Vasques de Oliveira, 2021)

Specifications pertaining to the equipment will be provided in the form of a technical schedule, the technical schedules will provide information in terms of the electrical and mechanical properties that is required for continuous and safe operation of the electrical system.

2.2.1 Solar PV modules

The solar PV module absorbs the irradiation from the sun, which then converts the source of energy into electricity. When solar PV modules are connected in a group of series-connected PV modules the group is referred to as an PV array, the PV array is connected in parallel to achieve a central inverter topology. PV arrays can be represented as an equivalent circuit with the series-connected and parallel-connected PV modules indicated as N_{ss} and N_{pp} respectively as shown in Figure 2.2 (Castro, et al., 2020).

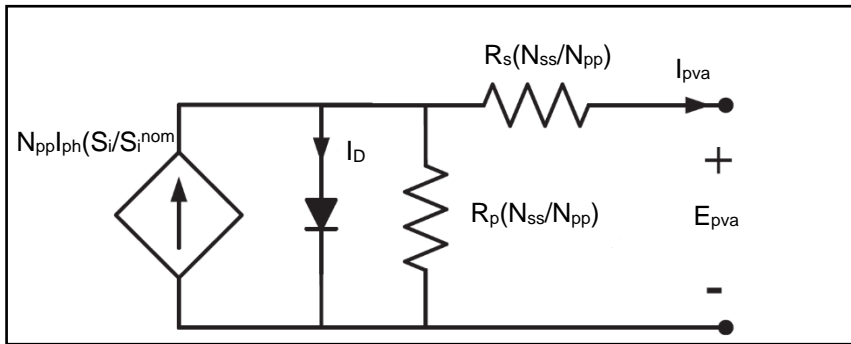


Figure 2.2: Equivalent circuit of a PV array (Diaz-Araujo, et al., 2019)

From the equivalent circuit represented in Figure 2.2, the generated current I_{pva} [A] can be calculated by Equation (1). A known voltage should be applied over the terminals of the equivalent circuit as the nominal photoelectric current I_{ph} [A] is a function of the PV array voltage E_{pva} [V]. With the incident solar irradiance S_i [W/m^2] obtained by the energy provided by the sun, the energy average harvested is the nominal irradiance S_i^{nom} [W/m^2] of the PV array (Castro, et al., 2020).

$$I_{pva} = N_{pp} I_{ph} \left(\frac{S_i}{S_i^{nom}} \right) - N_{pp} I_D (e^{V_x/V_y} - 1) - \frac{V_x}{R_p (N_{ss}/N_{pp})} \quad (2.1)$$

By implementing Equation (2.1) – (2.7) the other variables in Equation (2.11) can be calculated to calculate I_{pva} in the equivalent circuit.

$$V_x = E_{pva} + R_s I_{pva} (N_{ss}/N_{pp}) \quad (2.2)$$

$$V_y = k_d V_t N_s N_{ss} \quad (2.3)$$

$$V_t = k_b T_n / q; \quad (2.4)$$

$$I_{sc} = I_{sc}^{nom} [1 + k_{Isc} (T_{op} - T_n)] \quad (2.5)$$

$$V_{oc} = V_{oc}^{nom} [1 + k_{V_{oc}} (T_{op} - T_n)] \quad (2.6)$$

$$I_D = I_{sc} (e^{V_{oc}/k_a V_t N_s} - 1)^{-1} \quad (2.7)$$

The nominal short-circuit current I_{sc}^{nom} [A] and open-circuit voltage V_{oc}^{nom} [V] is shown in (2.5) and (2.6), both values provided at the module's nominal temperature T_n [°C]. Given the operating temperature T_{op} [°C] of the module, which is implemented to obtain the saturation current of the diode represented by I_D [A]. Where the series and parallel resistance of the PV array is R_s [Ω] and R_p [Ω] respectively and V_t [V] is represented by the nominal PV array thermic voltage. The number of modules per PV array is shown as N_s in the circuit; Boltzmann constant is k_b [J/°K]; electric charge expressed as q [C]; both the short-circuit current I_{sc} [A] and the open-circuit voltage V_{oc} has a temperature coefficient shown as $k_{I_{sc}}$ [%/°C] and $k_{V_{oc}}$ [%/°C] respectively (Castro, et al., 2020).

2.2.2 DC-link capacitor

Power quality has become a primary reason in DC and AC systems to reduce voltage and current oscillations. When a voltage ripple caused by high DC-link voltage oscillation of an inverter requires smoothing of the output power, a DC link capacitor will be implemented in the inverter design to reduce the oscillation voltage as shown in Figure 2.3 (Meral & Celik, 2021). A boost converter is used to control the DC link voltage of the capacitor in order to produce the required signal output by reducing any harmonic emissions. The input voltage of the inverter will be a known voltage source as the inverter has predefined operating range from the input voltage, however the current supplied to the DC-link capacitor can be calculated by Equation (8) (Turksoy, et al., 2018).

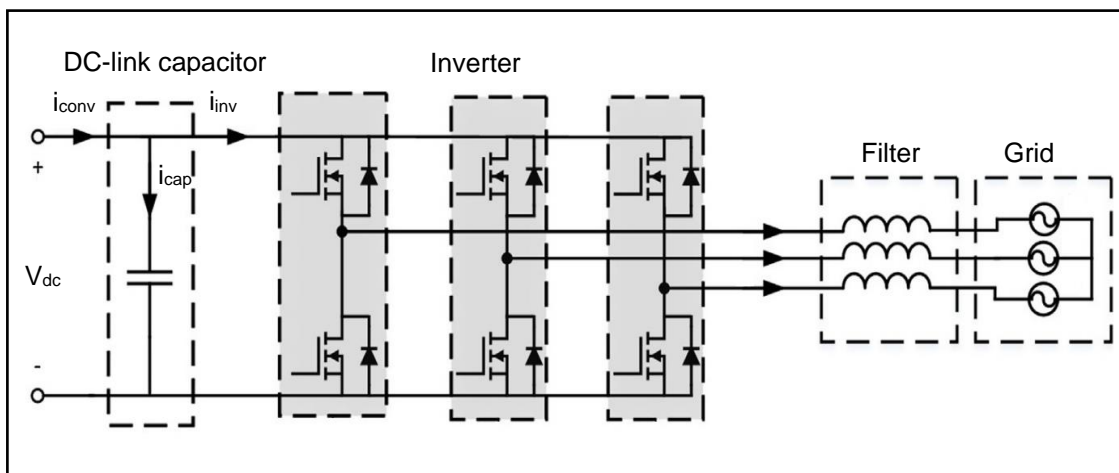


Figure 2.3: DC-link circuit illustration (Turksoy, et al., 2018)

Considering the circuit illustration in Figure 2.3, the current in the DC-link capacitor can be expressed as per Equation (2.8) below.

$$i_{cap} = i_{conv} - i_{inv} \quad (2.8)$$

Where the DC-link capacitor current is shown as i_{cap} , DC converter output current is i_{conv} and the AC – DC inverter input current is indicated as i_{inv} (Dursun & Dosoglu, 2018). By obtaining the current components, which is divided in average and harmonic components the following Equations from (2.9) to (2.11) can be obtained.

$$i_{cap,avg} = i_{conv,avg} - i_{inv,avg} \quad (2.9)$$

$$i_{cap,h} = i_{conv,h} - i_{inv,h} \quad (2.10)$$

$$i_{cap,avg} + i_{cap,h} = i_{conv,avg} + i_{conv,h} - i_{inv,avg} - i_{inv,h} \quad (2.11)$$

When the capacitor current is large enough, the harmonics generated by the inverter's input current is filtered by the DC-link capacitor, resulting in the average capacitor current being zero. The harmonics from the DC-DC converter will be neglected if the output current is filtered by the DC-link capacitor and Equation (2.11) can be simplified as follow (Turksoy, et al., 2018):

$$i_{cap,h} = -i_{inv,h} \quad (2.12)$$

2.2.3 Inverter (voltage source converter)

Inverters are crucial subsystem component of a SPP as the inverter contains the functionality for the conversion of DC- to AC voltage (see Figure 2.4). There are various types of inverters, with the voltage source inverter (VSI) commonly utilised in a utility size SPP, due to the high energy requirements (Alhussainy & Alquthamni, 2020).

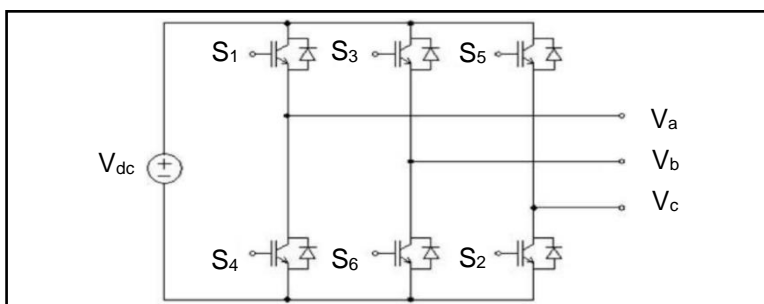


Figure 2.4: Three-phase DC-AC inverter (Rohmat, et al., 2019)

The inverter is designed to be operated as a six-pulse multistage VSI, where the VSI implements the input voltages as the DC voltage (V_{dc}) reference. Control and protection of the AC phase voltages, which is represented by V_a , V_b and V_c will be performed by the six insulated gate bipolar transistors (IGBTs) and diodes (Alhussainy & Alquthamni, 2020) (Rohmat, et al., 2019).

2.2.4 LCL filter

To eliminate high switching frequencies and minimise harmonic currents for sinusoidal shaped signal outputs of the inverter, the application of a filter is introduced in the circuit. Passive filters are designed with an inductive (L) and capacitive (C) component to eliminate the high switching frequencies and reduce second order harmonics. The filters utilised in the subsystem of a SPP is the LCL filter type, which is shown in Figure 2.5 (Dursun & Dosoglu, 2018) (Hussain & Qureshi, 2021).

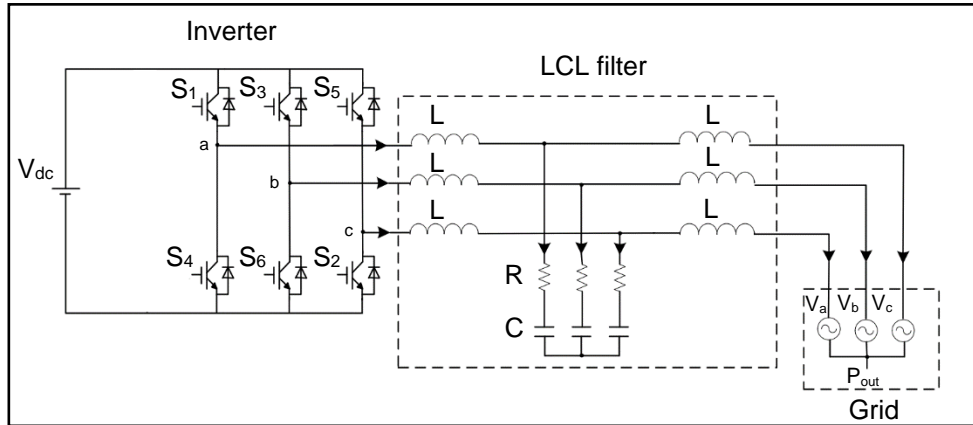


Figure 2.5: LCL filter illustration (Dursun & Dosoglu, 2018)

The power flow complex equation is used to obtain the L and C value of the filter in Equation (2.13), this is to ensure that the generated current does not affect the load with abnormal performance conditions in the AC grid (Rohmat, et al., 2019).

$$P_{out} = \frac{|V_a| |V_b| |V_c|}{X} \cdot \sin(\delta_1 - \delta_2) \quad (2.13)$$

The three-phase voltages from the inverter are represented by V_a , V_b and V_c [V], with the real power output P_{out} [W] indicated as the energy generated and the harmonic attenuation is shown as δ . Harmonics caused by resonance is reduced by the inductive reactance [X_L] and capacitive reactance [X_C] when the reactance's are not equal in value. From Equation (2.14) and (2.15) below, the L and C value can be calculated (Rohmat, et al., 2019).

$$X_L = 2\pi fL \quad (2.14)$$

$$X_C = \frac{1}{2\pi fC} \quad (2.15)$$

Resistors in parallel with the inductors are also implemented in the circuit to reduce part of the switching frequency caused by the ripple current. The parallel resistors should have an impedance value equal to one third of the filter capacitance impedance when compared to the rated resonance frequency (Dursun & Dosoglu, 2018) (Hussain & Qureshi, 2021).

2.3 Topologies of a SPP

The SPP design depends on the end-user requirements in terms of the load demand, efficiency and cost, utility scale plants will usually have an off-taker that consumes large amounts of electricity. Due to technical factors, which includes mismatch losses, solar irradiation and shading a PV system architecture can consists of three types of PV array connections to the inverter system. Configurations that are implemented in SPP designs are shown in Figure 2.6 and consist of central-, string- and multi string inverters (Yilmaz & Dincer, 2017) (Kabalci, 2020).

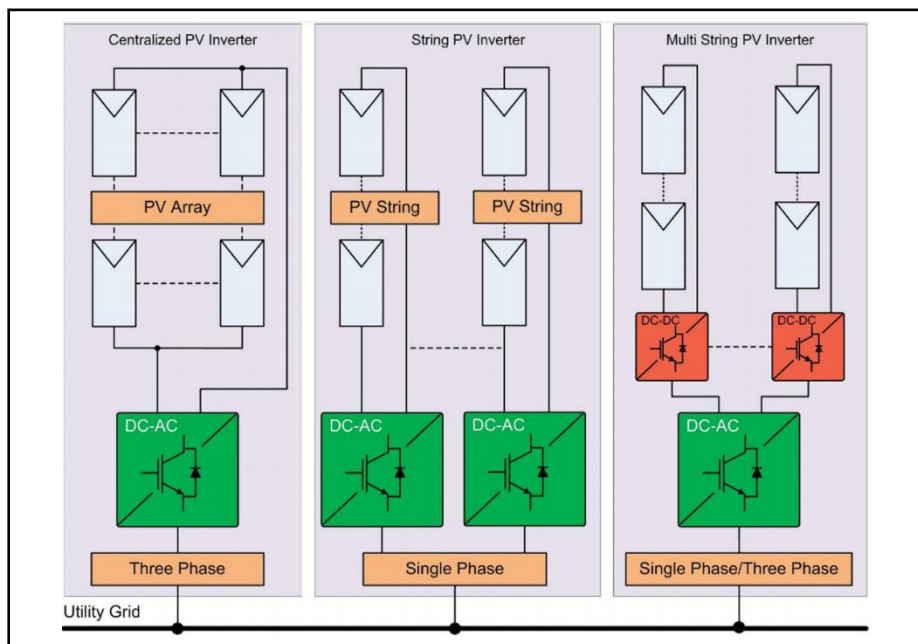


Figure 2.6: Inverter topologies (Kabalci, 2020)

Central inverters are usually the configuration preference for large scale utility integrated SPPs, due to the inverter being three-phase and no additional voltage transformation is required. The centralized system is created by a string of series connected PV panels that are connected in parallel to achieve a single inverter configuration system. The disadvantage of the connection type is the operation of only one MPPT for all PV arrays connected to the centralized inverter, which results in lower energy production and decreased performance of

the inverter system (Yilmaz & Dincer, 2017). The most distinguished reasons for implementing the central inverter system to grid-connected SPPs are the simplicity of installation, robustness, reduced quantity of inverters and competitive cost. Efficiency and performance in terms of energy yield from the MPPTs is 1.5 % less in central inverters compared to string inverters, also with the installation and maintenance cost of the central topology being in the range of 60 % less than the string inverter configuration (Rakhshani, et al., 2019).

2.4 Control strategy of a grid-connected SPP

For grid-connected SPPs, the inverters of the SPP are required to be controlled at the low voltage (LV) inverter output terminals by the PPC. The complete control strategy of a SPP is shown in Figure 2.7 and illustrates the layout of the complete SPP in terms of the subsystem, POC and utility grid (Shi, et al., 2021). Furthermore, the individual control strategies will be discussed in this section to identify the requirements and industry standards for the control of a SPP to avoid non-compliance challenges.

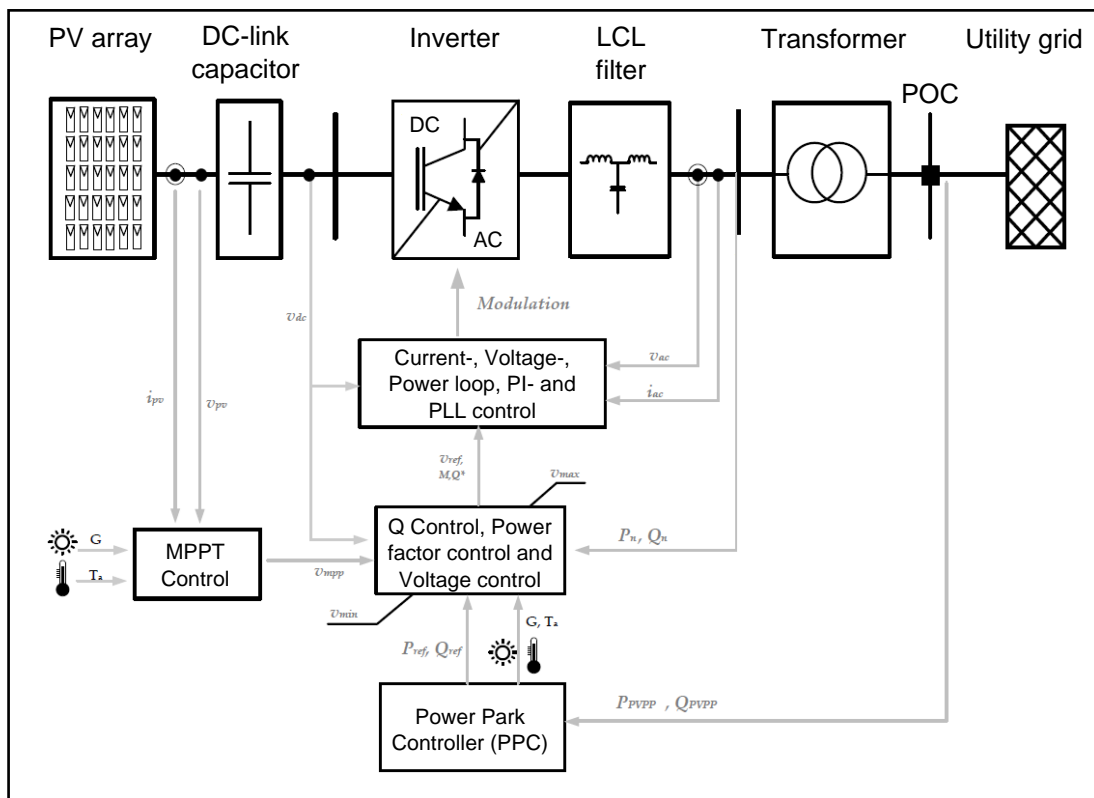


Figure 2.7: Grid-connected SPP control strategy (Cabrera-Tobar, et al., 2019)

Control of a SPP for grid compliance can be achieved by a typical multiple-loop control, which includes voltage loop, power loop, current loop and Phase-locked loop (PLL) control strategies as per Figure 2.7. The proportional-integral (PI) controller strategy is based on the voltage loop control method, which implements the reference DC voltage ($V_{dc,ref}$) to perform accurate tracking from the output of the MPPT.

Variations of PV cell temperature and solar irradiation is controlled by the power loop control to provide maximum yield during the MPPT process. The power factor integration is done by the current control, which forms part of the PI controller. Synchronisation to the grid is achieved by comparing the frequency and phase of the SPP by the PLL control strategy (Shi, et al., 2021). References from the loop controllers are provided to the reactive power-, power factor- and voltage control strategies with the inputs from the network service provider (NSP) or SO to the PPC in order to control the IPP in different control methods and setpoints as required by the grid code (Cabrera-Tobar, et al., 2019).

2.4.1 Reactive power (Q) control strategy

DC voltage applied at the LV terminals of the inverter from the PV array or modulation index, which forms part of inverter internal control and is dependent on the temperature or solar irradiance. The internal control of the inverter will provide an input parameter to the real Power (P) and Reactive power (Q) capability of a SPP. The different variations are illustrated in Figure 2.8 and Figure 2.9 and indicates how these parameters affect the PQ curve from a variable DC voltage and a variable modulation index (Cabrera-Tobar, et al., 2019).

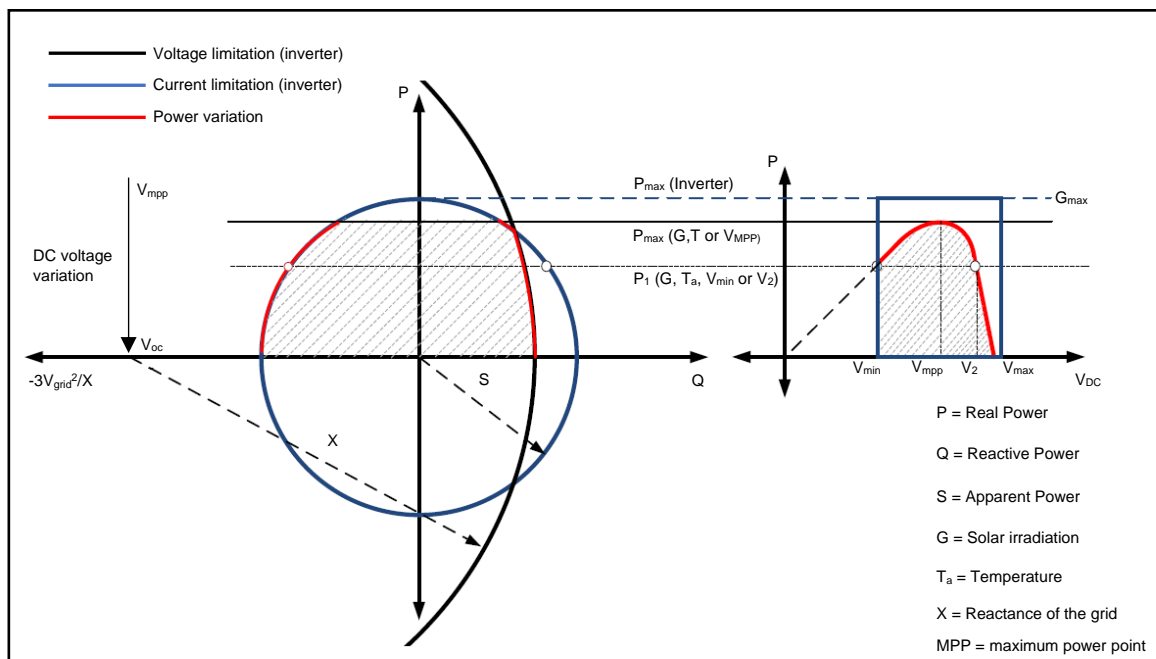


Figure 2.8: PQ capability curve indicating a variable DC voltage (Cabrera-Tobar, et al., 2019)

Both the PQ capability curves represented in Figure 2.8 and Figure 2.9 illustrates the variable DC voltage and variable modulation index control strategy and can be expressed by Equation (2.16) and (2.17).

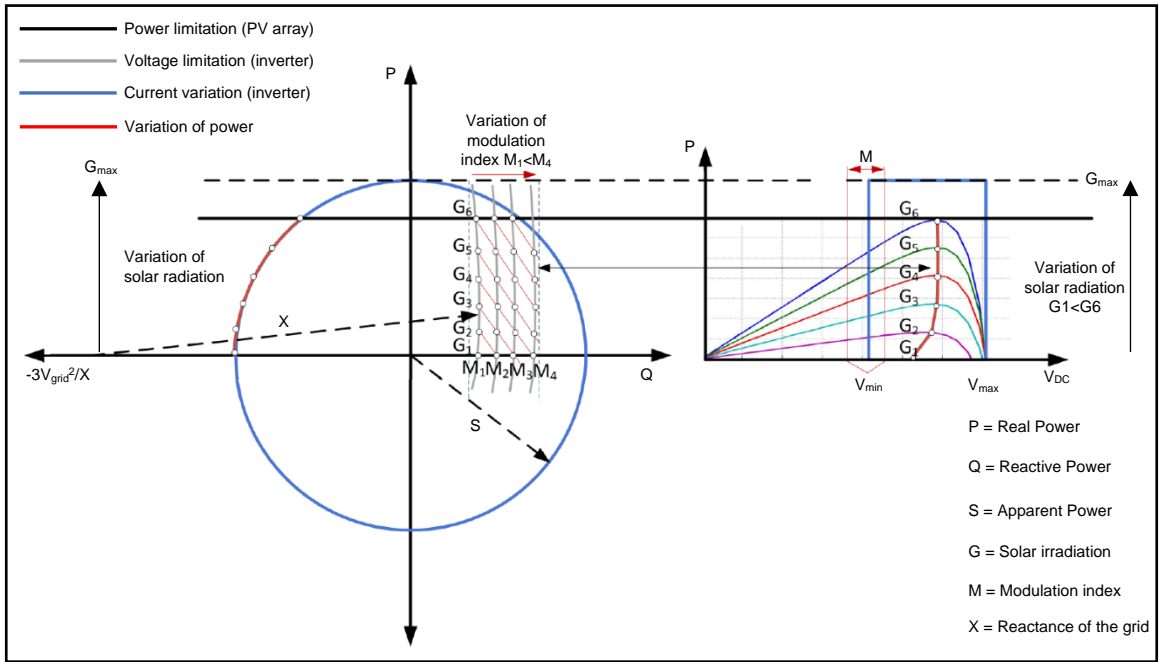


Figure 2.9: Variable modulation index of a PQ capability curve (Cabrera-Tobar, et al., 2019)

The PQ capability curves will follow the input signals provided will control the complete PQ capability of the SPP and will ensure compliance to grid code requirements.

$$P_{ref}^2 = S^2 - Q_{ref}^2 \quad (2.16)$$

$$P_{ref}^2 + \left(Q_{ref} + \frac{3V_{grid}^2}{X}\right)^2 = \left(3 \cdot \frac{V_{grid}V_{conv}}{X}\right)^2 \quad (2.17)$$

Where P_{ref} is the reference real power [W], S is indicated as the apparent power [VA] and Q_{ref} represents the reactive power [VAR] reference in the SPP. The reactance [Ω] of the utility grid is shown as X and the voltages are represented by the voltage grid [V_{grid}] and the voltage conversion [V_{conv}] (Cabrera-Tobar, et al., 2019).

2.4.1.1 Absorption of reactive power control strategy

When the grid code requires the SPP to operate in Q control as a preference, the PQ curve provides the required injection or absorption of reactive power to the utility grid. The control scheme strategy is shown in Figure 2.10, If the SPP is ordered to operate in Q control the PPC is required to determine the maximum possible reactive power (Q_{MPP}). The calculated Q_{MPP} is dependent on the variation in DC voltage and modulation index of the PQ capability curves (Cabrera-Tobar, et al., 2019). Depending on the under excitation or overexcitation of the SPP, the control strategy will be subjected to a performance requirement of reaching the setpoint in 30 seconds (Mchunu, 2020).

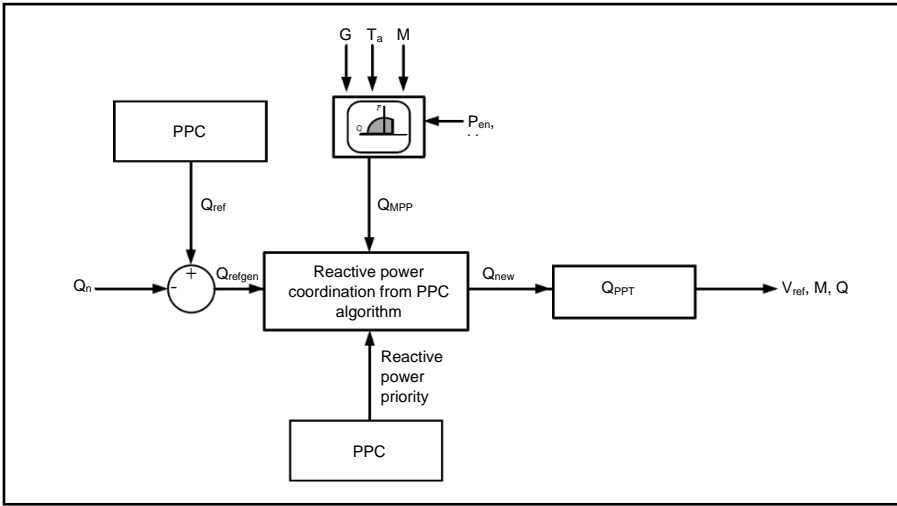


Figure 2.10: Control strategy for Q control (Cabrera-Tobar, et al., 2019)

Operation in the fourth quadrant of the PQ capability curve allows the absorption of reactive power and can be formulated by Equation (2.18) in order to obtain the variation of the maximum power point limitation of the reactive power (Cabrera-Tobar, et al., 2019).

$$Q_{MPP}^2(G, T_a) = S^2 - P_{MPP}^2(G, T_a, V_{MPP}) \quad (2.18)$$

Where Q_{MPP} is the maximum reactive power [Var], S is indicated as the apparent power [VA], P_{MPP} represents the maximum real power [Var] reference in the SPP and T_a represents the ambient temperature [$^{\circ}\text{C}$] and G is the solar irradiation [W/m^2].

If the reference of the absorbed reactive power Q_{ref} , is higher than the Q_{MPP} , the SPP is required to perform absorption of reactive power requirements, absorption of reactive power is done by the variation in DC voltage. Tracking the reactive power point Q_{PPT} each time the solar irradiance value changes and the setpoint remains the same is called the reactive power point tracking in the control strategy. The Q_{MPP} is shown in Figure 2.11, where point A is illustrated as the behaviour of the solar irradiance, at point A, the real power of the SPP is the P_{MPP} that the plant can evacuate into the utility grid. When the reactive power requires the be absorbed, a reference of reactive power is provided to the PPC, however if the Q_{MPP} is lower than the reactive power reference, a new real power reference is calculated (P_{ref1}). If the new reference point is to be achieved, the SPP's reactive power shall be directed to point B where the DC voltage will change from V_{MPP} to V_{ref} . When the setpoint is at point b, the reactive power is equal to the reference at point 3. As the solar irradiance changes during the day, the new PV curve (blue line) is generated and a new real power P_2 is generated. The SPP's reactive power reference will move to a new PV curve at point C and a new PQ curve at point 4. As the PPC will provide a new reference point for the reactive power, the DC should reduce to achieve the reference points at point D and point 3 (Cabrera-Tobar, et al., 2019).

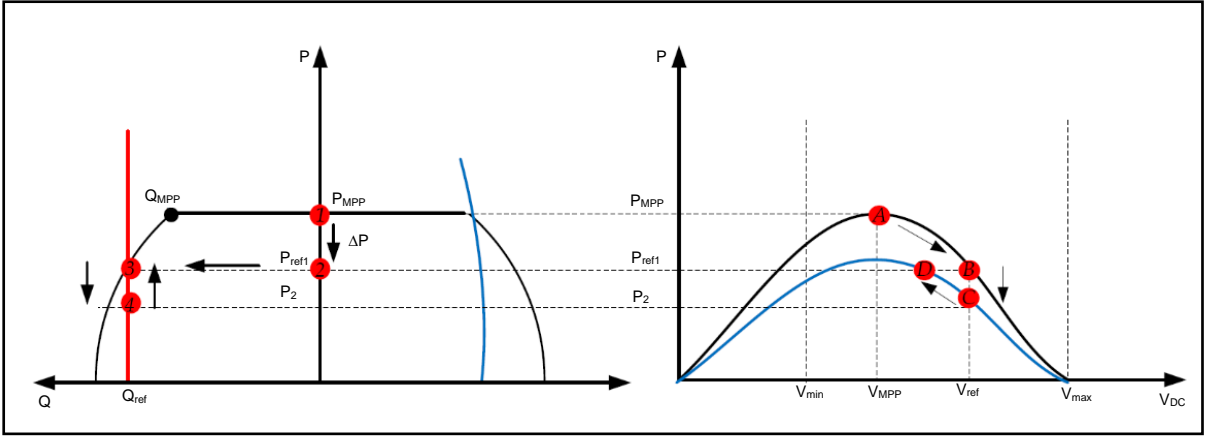


Figure 2.11: Variable PQ and ambient conditions of the Q_{PPT} operation for absorption of reactive power (Cabrera-Tobar, et al., 2019)

Different PQ capabilities and ambient conditions is illustrated in Figure 2.11 during the absorption of reactive power. The graph indicates conditions from (1) - (4), which indicates the following:

- 1) MPP at a specific solar irradiance;
- 2) Real power reference variation;
- 3) Reactive power reference variation;
- 4) New real and reactive power.

2.4.1.2 Injection of reactive power control strategy

For the injection of reactive power into the utility grid, the PQ capability curve requires to operate in the first quadrant, Equation (2.19) provides the variation of the maximum power point limitation of the reactive power (Cabrera-Tobar, et al., 2019).

$$Q_{MPP} = \frac{3\sqrt{3}}{2\sqrt{2}} \cdot \frac{V_{grid} \cdot V_{MPP} \cdot M}{X} \quad (2.19)$$

Where X is the reactance [Ω] of the utility grid, provided by the SO and M is the modulation index, which varies in value between 0 and 1. For the maximum injection of reactive power, the value of M equals 1, this happens when the given V_{MPP} , temperature and solar irradiance is at maximum operational values. By increasing the reactive power value, the injection into the grid at a certain setpoint can require that the modulation index exceed the value of 1, which could result in harmonic violations. In the case where the modulation index is higher than 1, the Q_{MPP} has to be lower than the reference set by the PPC as illustrated in Figure 2.12, this is achieved by the PPC increasing the DC voltage. Point A is on the ambient conditions graph represents the given solar irradiance, which is equal to the real power at the maximum power point P_{MPP} at (1) of the PQ capability curve. When the reference point moves to a point higher

than Q_{MPP} a new reference point must be calculated and the new real power reference point is required to move to point (2) at P_{ref1} in order to increase the reactive power. The PPC will provide a new reference point for the reactive power to achieve P_{ref1} , the DC voltage should change from point (A) to point (B), which is the V_{MPP} and V_{ref} respectively (Cabrera-Tobar, et al., 2019).

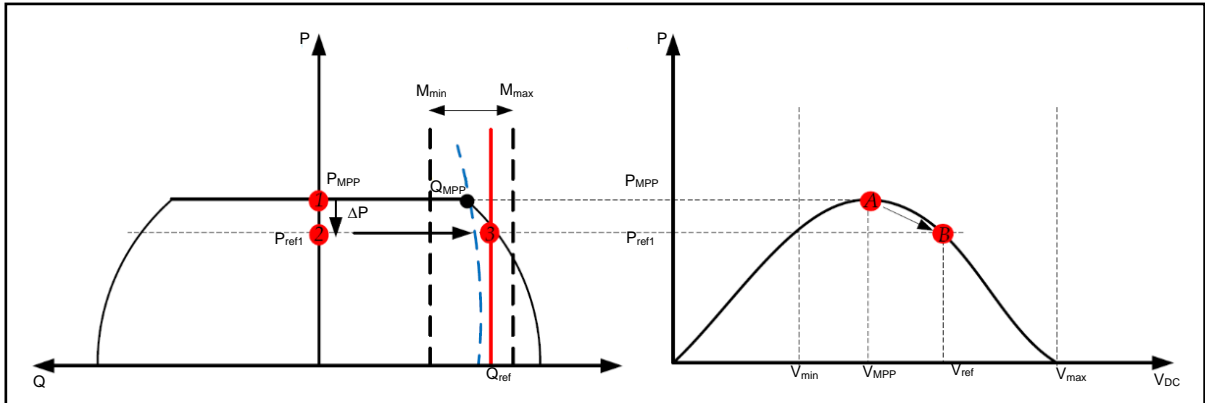


Figure 2.12: Variable PQ and ambient conditions of the Q_{PPT} operation for injection of reactive power (Cabrera-Tobar, et al., 2019)

Conditions from (1) - (3), indicates the following: (1) MPP at a specific solar irradiance; (2) Real power reference variation; (3) Reactive power reference variation.

2.4.1.3 Reactive power control logic function

The logic function of the control strategy in SPPs is illustrated in Figure 2.13 to demonstrate the reactive power control in variable PQ and ambient conditions in relation to the Q_{PPT} limitations for the absorption and injection scenarios.

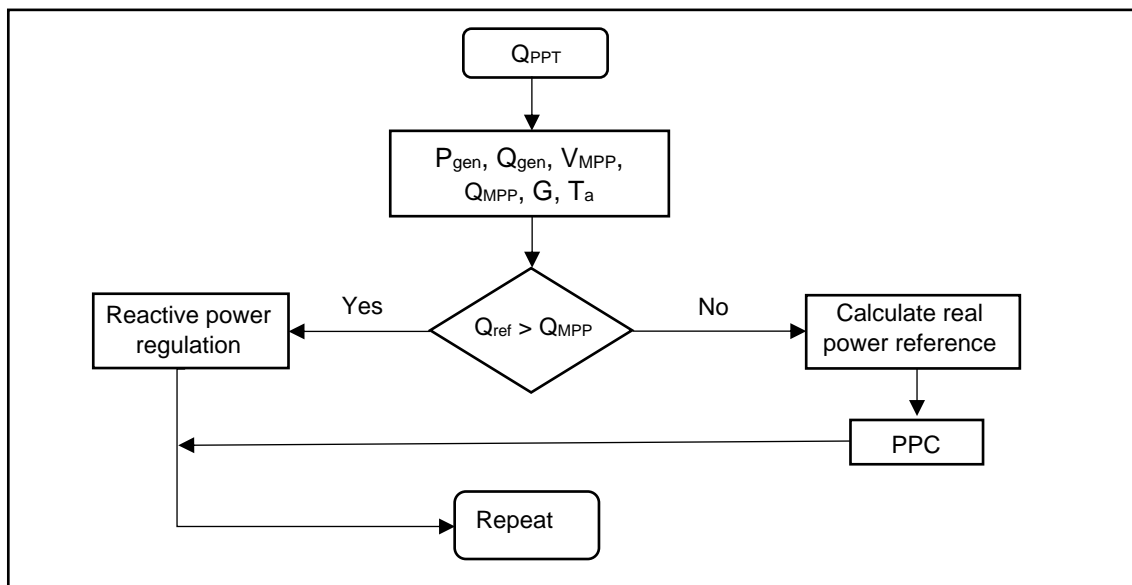


Figure 2.13: Logic function of reactive power control strategy (Cabrera-Tobar, et al., 2019)

2.4.2 Power factor control strategy

Power quality of a SPP is required to be maintained within the SAREGC requirement range, which can be achieved by the common-point power factor (PF) control strategy. Efficiency of the overall utility grid can be improved once the PF has been adjusted to perform within the utility's accepted parameters. The common-point PF of a SPP at the POC may be subjected to unpredictable fluctuations in the grid that is outside the desired requirement range of the utility. These fluctuations can cause harmonic distortions, which is associated with power quality that can be reduced by adequate PF control in the inverter output. The adjustment of the PF can provide improved stability and greater flexibility of the utility's grid and can assist in supplying loads connected to the grid with the required power quality (Taggart, et al., 2018).

2.4.2.1 Power factor control system architecture

A PF control strategy purpose is to implement communication capabilities of the inverters internal control, power quality metering equipment and electronic intelligent device (EID) of a SPP to integrate the required control signal to the active control system. This is required for the PPC to compare the SAREGC requirements with the common-point PF of the SPP of which the inverter output is adjusted according to the new calculated control signal. When the inverters internal control is integrated with an industrial computing architecture platform or a real-time automation processor the internal control can be utilized for the PF control system (Taggart, et al., 2018).

The proposed control strategy for the PF control of utility scale SPP applications are closed-loop feedback control, which utilizes a PI controller to retain the PF within the required range. Implementation of the cost effective close-loop feedback system of the SPP is accomplished by using equipment that is installed to ensure power quality measurements, inverter internal control and EIDs. The tariff metering by the utility is done at the POC, which uses auxiliary transformers for the power quality measurements. Protective relays in the form of EIDs protects the SPP and the utility grid from any abnormal conditions, the communication signals obtained from the power quality meters and EIDs will be sent to the inverter internal control to produce the required PF. By using the typical components found on a SPP site, it can be quite easy to implement an active PF control system, as shown in Figure 2.14. Through the supervisory control and data acquisition (SCADA/HMI) system. The SCADA/HMI system displays collected data and identifies alarm conditions in the system allowing the controller to send instructions to the inverters to control the PF (Taggart, et al., 2018).

Inverters can then be started and stopped with control commands or setpoints can be set during these commands, the power factor reference set point is one of the set points in the power factor reference set. Using the communication channels available to the controller, the SO may affect the power factor reference set point by sending a value between 0.975 lagging or 0.975 leading as per the SAREGC for Category B SPPs. A PI controller at a PV installation serves two purposes: it is a control device and a data concentrator. Using multiple data sources including a protective relay, a power quality meter as well as an inverter as a controller, calculations are performed to control signals based on the collected data along with the SCADA/HMI setting reference. Inverters can be adjusted by using their power factor set points to affect the output power. Thus, the power factor set point of each inverter can be utilized as the control signal for power factor control (Taggart, et al., 2018).

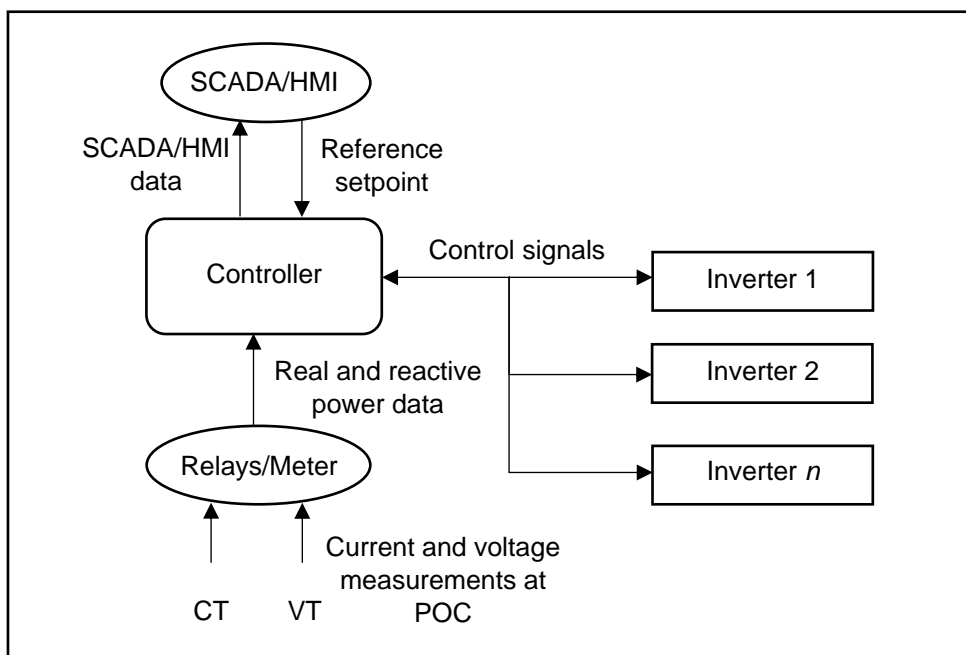


Figure 2.14: Simplified PF control strategy architecture (Taggart, et al., 2018)

The controller collects system data from each inverter, protective relay, or meter, then forwards the communication data to the SCADA/HMI. Information includes current and voltage values, power and energy values, as well as power factor information. Three-phase real and reactive power quantities are provided to the controller by the protective relay or power quality meter. This is achieved by a current transformer (CT) and voltage transformer (VT), which is used to measure circuit voltages and currents, and this data is used to calculate real and reactive power. The protective relays and power quality meters periodically feed calculated values to the controller. Besides these two data sources, the controller will periodically sample the system and send the data to the SCADA/HMI to possibly calculate new control signals for new setpoints for grid code compliance requirements (Taggart, et al., 2018).

2.4.2.2 Power factor control through solar irradiation

Another aspect of the control strategy implementation for PF control is reducing the switching of onload tap changers of transformers and voltage regulators, which can cause high switching frequencies in the network. The PF control capabilities of inverters can be used to solve frequent tap switching and voltage rise problems. According to literature, inverters are generally operated with fixed power factors to reduce overvoltage issues (absorbing reactive power). When the local generation exceeds the local demand, this control strategy could be used in PF control. Although, voltage rises are not always observed during the daytime, voltage drops are also possible, especially during periods of low irradiance. Considering these facts, inverters may be operated near the unity power factor during low generation times (low irradiance), and near the allowed limit of inductive power factor during high generation times (high irradiance), thus mitigating voltage drop and voltage rise issues. As illustrated in Figure 2.15, inverters can be adjusted dynamically to maintain a desirable power factor depending on the amount of solar irradiance that reaches the solar modules. For finding the power factor values associated with the variable total solar irradiance stated in Equation (2.20), a simple linear approximation method is described (Gokmen, et al., 2017).

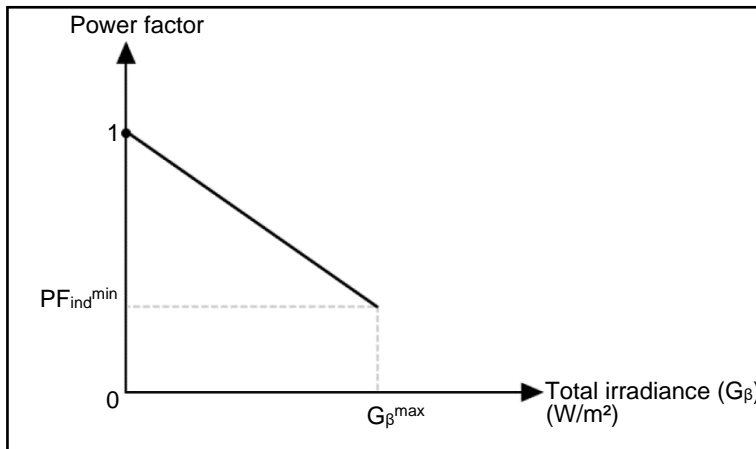


Figure 2.15: PF solar irradiance curve (Gokmen, et al., 2017)

$$PF = 1 - \frac{1 - PF_{ind}^{min}}{G_{\beta}^{max}} \cdot G_{\beta} \quad (2.20)$$

Where PF_{ind}^{min} indicates the inductive power factor limit, G_{β} denotes the total irradiance that has fallen onto the PV array surface in W/m^2 and β denotes the angle of tilt of the PV arrays. G_{β}^{max} is a parameter that allows you to set the maximum solar irradiation for a specific condition to be assumed as $1000 W/m^2$ (Gokmen, et al., 2017).

2.4.2.3 Power factor control through closed-loop control system

Based on a closed-loop control system, the PF control can be described and modelled as illustrated in Figure 2.16. The SCADA/HMI provides the desired power factor set point reference in this closed-loop system, using the protective relay or power quality meter at the POC, the system PF can be obtained. Whenever a process is used, the inverter will be used, and the control signals will be used to set the inverter. There can be either a set point for power factor or a set point for real power and reactive power, depending on the manufacturer. As part of implementing the closed-loop system at the POC, the controller sets up a control cycle and initiates the process by sampling the protective relay or power quality meter for the instantaneous real and reactive power. This is to determine how much power is available to the system in real time. A set of inverter data statistics is then viewed by sampling each inverter, to calculate the error between the reference and the inverter output values, the calculated power factor is compared to the SCADA/HMI power factor set point reference. A control signal is calculated based on the error calculation and the collected information and data from the inverters, and the signal is then sent to the inverters to change their output power. A control cycle is complete when the inverters change their output power to comply with the new control signal. This dynamic system is designed to adjust continuously until the SCADA/HMI reference setpoint is reached. To maintain the setpoint at the reference level, the controller continuously monitors the setpoint value and makes any needed adjustments as necessary (Taggart, et al., 2018) (Ghani, et al., 2021).

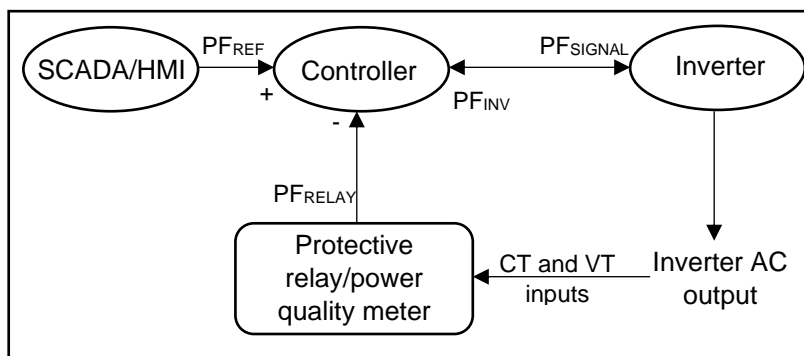


Figure 2.16: PF closed-loop system (Taggart, et al., 2018)

This control strategy is further explained as follows:

- The PF is defined as the ratio between real power and apparent power ($P_{\text{real}}/P_{\text{apparent}}$), the following conventions can be considered:
 - When current lags voltage the system comprises of inductive loads (positive PF);
 - When current leads voltage the system comprises of capacitive loads (negative PF).

- SCADA/HMI provides a PF reference as PF_{REF} ;
- Inverter output PF denotes PF_{INV} ;
- PF from the protection relay or EID is PF_{RELAY} ;
- PF_{REF} and PF_{RELAY} is differentiated by $PF_{ERROR} = PF_{REF} - PF_{RELAY}$;
- Control signal output from the controller is PF_{SIGNAL} .

Inverter data is processed by computing the PF_{SIGNAL} output from the PF_{REF} , PF_{RELAY} and PF_{INV} input values as well as inverter data to calculate what will be sent to the inverter of the SPP. Additionally, numerous limiting factors need to be considered when implementing the closed-loop system, specifically when the closed-loop system is the main component of the controller (Taggart, et al., 2018).

2.4.2.4 Power factor control utilizing PI control

PF control is controlled by the PI controller in normal conditions. The PI controller is implemented as shown in Figure 2.17 to control the PF.

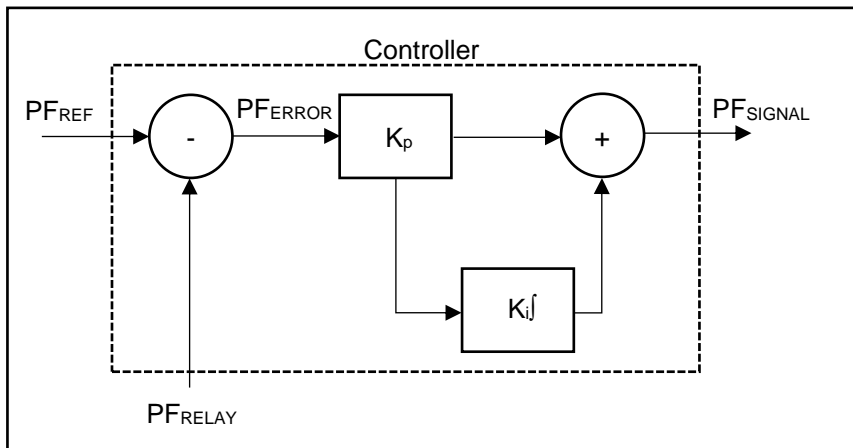


Figure 2.17: PI control algorithm for PF control (Taggart, et al., 2018)

Where the two constants K_i and K_p , which are the integral and proportional constants, respectively, can be determined in the testing phases of tuning and simulation. Using the integral constant $K_i = K_p / T_i$ which corresponds to the integration constant of T_i , the PF error in Equation (2.21) can be expressed as follows (Taggart, et al., 2018):

$$PF_{ERROR} = PF_{REF} - PF_{RELAY} \quad (2.21)$$

For the controller to calculate internal integral terms, a difference equation is used to approximate the integral term. As a result, for the integral term the following Equation (2.22) can be implemented in the PI control algorithm:

$$PF_{INTEGRAL_NEW} = PF_{INTEGRAL_OLD} + \frac{K_p}{T_i} \cdot CTRL_{CYCLE} \cdot PF_{ERROR_NEW} \quad (2.22)$$

Where the previous sampling instant is denoted as an integral term $PF_{INTEGRAL_OLD}$, a new sampling instant is shown as $PF_{INTEGRAL_NEW}$ and the sampling during the new and old integral term is the $CTRL_{CYCLE}$ period (Taggart, et al., 2018).

The signal at a new sampling instant can be expressed in Equation (2.23) as follows:

$$PF_{SIG_NEW} = K_p PF_{ERROR_NEW} + PF_{INTEGRAL_NEW} \quad (2.23)$$

Equation (2.23) can be expanded to express the new signal in recursive form by implementing the new Equation (2.24) derived as the following (Taggart, et al., 2018):

$$PF_{SIG_NEW} = PF_{SIG_OLD} + K_p (PF_{ERROR_NEW} - PF_{ERROR_OLD}) + \frac{K_p}{T_i} \cdot CTRL_{CYCLE} \cdot PF_{ERROR_NEW} \quad (2.24)$$

As soon as a new value of signal is obtained from (2.24), the output control signal is updated by the controller (Taggart, et al., 2018).

2.4.2.5 Power factor control logic function

An PF control logic function of a simplified control cycle loop is shown in Figure 2.18. During this loop, the controller will collect the control data, check the limiting factors, run the PI control algorithm to calculate the output signals, and then transmit the signal to the inverters. A repeating procedure is used to reach the SCADA/HMI reference setpoint.

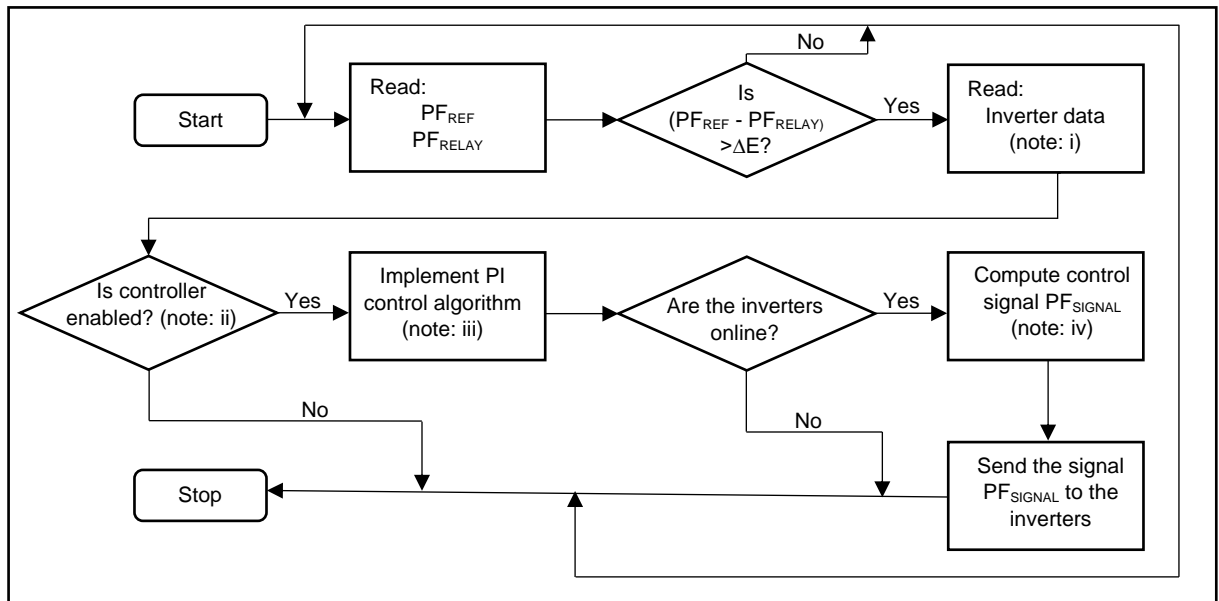


Figure 2.18: Simplified PF control cycle loop (Taggart, et al., 2018)

The following notes from (i) to (iv) needs to be adhered to in the specific PF control looped cycle for the SCADA/HMI reference setpoints to be achieved to achieve grid code compliance in terms of control as the SO will instruct the SPP to operate and perform (Taggart, et al., 2018):

- i) Power factor, ramp rates, output power and maximum output power limits are some of the data that can be stored as inverter data;
- ii) Depending on the data quality, the communication status and the out-of-range value, a decision is made;
- iii) PI control algorithm in section 2.4.3.4 implemented;
- iv) Calculation of the control signal initiation, considering the maximum output of the power limit and ramp rate (Taggart, et al., 2018).

2.4.3 Voltage control strategy

Utilizing the control capabilities of the SPP inverters, a three-level distributed voltage control strategy can be proposed to maintain the voltage control strategy. Three methods are implemented to stabilize the voltages, namely, the local voltage control (LVC), the flicker control (FC) and the coordinated voltage control (CVC). By using the grid information to formulate inverter setpoints in the SPP for reactive power support and real power curtailment, LVC responds robustly to voltage violations outside the dead band and improves voltage quality. FC eliminates the fast voltage fluctuations by leveraging the SPP power fluctuations and short-circuit impedance values as controlling inputs, during the SPP integration to the utility grid. Furthermore, CVC is initiated at the POC of the network if it detects a voltage violation or a SPP curtailment command. The CVC system uses a multi-agent system to systematically reduce curtailment, network losses and to coordinate the various droop control functions to enable the inverter to perform reactive power support. According to the methodology, there are three levels, each with a different operating time step. A brief description of each control level is as follows (Arshad & Lehtonen, 2019):

- Local Voltage Control: Maintaining voltages close to one per unit and implementing the grid information from the utility to determine the capability range of the voltage and reactive power at the POC, which is connected to the SPP;
- Flicker control: The inverters can provide fast local voltage control, which assists in the mitigation of the flickering caused by the variation in irradiation (100 ms operation cycle);

- Coordinated voltage control: The scheme works to lower the curtailment, and consequently, the losses from the SPP, while fully utilizing the reactive power capability of the inverters (60 s operation cycle) (Arshad & Lehtonen, 2019).

2.4.3.1 Local voltage control

In a voltage control strategy, FC is the innermost loop that attempts to eliminate fast voltage fluctuations and maintain stability. However, the FC doesn't attempt to maintain the voltage within the regulatory framework of the dead-band framework as defined in the SAREGC, the FC provides a previous setpoint in the voltage that the control attempts to maintain. The voltage will need to be stabilized by large amounts of P curtailment and Q support operations. Voltage standards include a margin of error to allow for voltage deviation. Therefore, stabilizing the voltage within limits, without considering the implications for the collector group losses and the P curtailment of the installed SPP, this is not a realistic option for the voltage control strategy. Hence, a Q(V) control strategy is suggested for the LVC algorithm, which implements a piecewise relationship function as illustrated in Figure 2.19 (Arshad & Lehtonen, 2019).

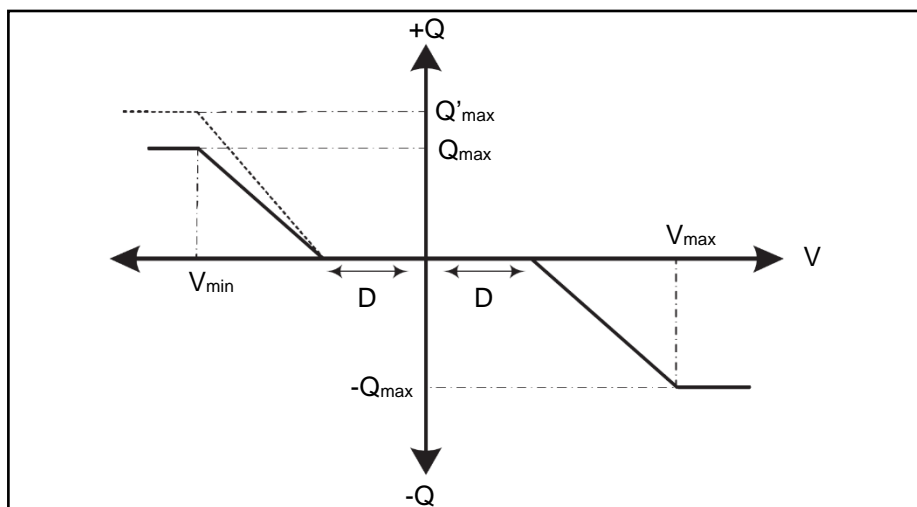


Figure 2.19: LVC – Q (V) droop characteristics (Arshad & Lehtonen, 2019)

The LVC algorithm will provide Q support, which is dependent on the voltage at the POC of the SPP. In a particular SPP location, the dead-band width 'D' is dependent on the short circuit impedance values, i.e. 'D' is smaller when the short circuit impedance values are large and vice versa. In the network further downstream, voltage fluctuations will be more pronounced due to intermittency, additionally, Q sensitivity increases as one gets farther from the transformer, as a result, the downstream SPP inverters will begin voltage regulation earlier. The power factor can be reduced in an undervoltage scenario (without SPP generation and large utility loads) so that the voltage remains within statutory limits (illustrated by the droop line in dots of Figure 2.19), because the inverter has large Q capacity. Q support, however, is

limited when large amounts of power or overvoltage's are being applied to the SPP. The SPP will be curtailed momentarily if Q_{max} is not enabled to keep the voltage within the limits of the dead band. As shown in Figure 2.20 (a), LVC provides limited Q support, V_{t-1} represents the voltage without drooping Q(V) and V_t represents the voltage after the drooping implementation.

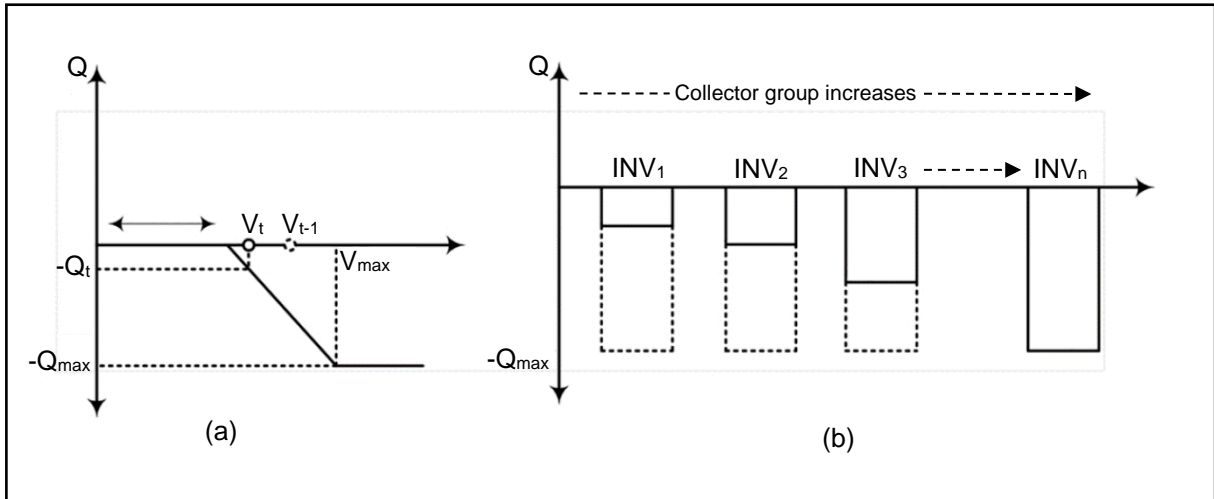


Figure 2.20: (a) Q (V) droop partial rectification on overvoltage conditions, (b) Q support by the inverters of the SPP relative to the collector group distance (Arshad & Lehtonen, 2019)

Due to the LVC's instantaneous nature and the use of data obtained at the time of the SPP integration to the utility grid, the real power requirements of the SPP will be curtailed to remove any voltage violations. It may be possible to use the reactive power of the SPPs inverters closer to the primary transformer to control the voltage, as shown in Figure 2.20 (b). Due to this, a voltage control algorithm with coordinated voltage control will be crucial to remove any voltage violations outside the dead band in the SPP, resulting in real power curtailments of a much lower magnitude than autonomous algorithms of FC and LVC control (Arshad & Lehtonen, 2019).

A control scheme for self-adaptive Q(V) droop is shown in Figure 2.21, where an extrapolation of maximum reactive power is based on terminal voltage, active power, and ambient temperature. The SPP inverters with excessive power are equipped with a temperature measurement system, which prevents the inverter from overheating. In this case, based on the SPP inverter's maximum reactive power exchange capability, the maximum reactive power exchange capacity given in a known condition of terminal voltage, temperature, and irradiance. In the SPP inverter, the reactive power reference is generated from the adaptive droop block using the terminal voltage measured as shown in Equation (2.25) in the SPP design (Arshad & Lehtonen, 2019).

$$Q = k_{QV} \cdot \Delta V \tag{2.25}$$

Where Q is the reactive power capability of the inverter and the predefined QV droop is denoted as k_{QV} , the deviation in voltage from the SPP inverter terminals setpoint is shown as ΔV .

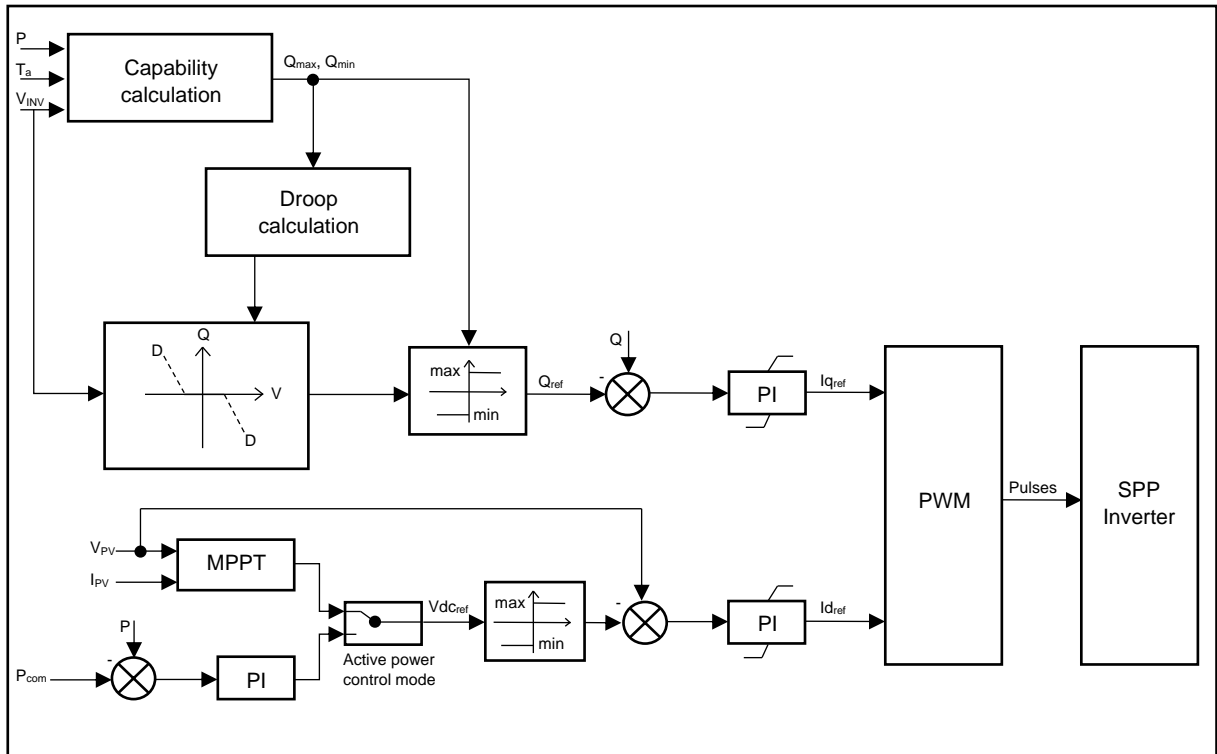


Figure 2.21: Adaptive Q(V) droop control for SPP (Karbouj, et al., 2021)

A SPP inverter's active power supply is set by the unit operator command (P_{com}) of the solar array, which is based on MPPT reference. The PI controller calculates a current command by comparing the reactive and active power commands coming from the inverter with the measured values. In order to control the inverter switches, the commands used in current command dq components are then converted into pulse-width modulator (PWM) pulses (Karbouj, et al., 2021).

2.4.3.2 Flicker voltage control

When a voltage angle difference exists between the nodes as well as the transformer in a distribution network, the X/R ratio is normally greater than one, which causes a small voltage angle difference. It can then be assumed in Equation (2.26) that the difference in voltage between the two nodes is approximately as follows (Arshad & Lehtonen, 2019):

$$\Delta V = V_1 - V_2 \approx \frac{PR+QX}{V_2} \quad (2.26)$$

In equation (26), if the voltage of the change in voltage is equal to zero, then equation (2.27) is implemented (Arshad & Lehtonen, 2019):

$$\Delta Q_{req}(t) \approx -\Delta P(t) \cdot \left(\frac{R_N}{X_N}\right) \quad (2.27)$$

Equation (2.28) and (2.29) is utilized to calculate R_N and X_N , which are the network's short-circuit resistance and reactance at the POC and N is the node number with which the SPP is attached (Arshad & Lehtonen, 2019).

$$R_N = \sum_{n=1}^N R_n \quad (2.28)$$

$$X_N = (X_t + \sum_{n=1}^N X_n) \quad (2.29)$$

Where, the two resistances are R_n and X_n , and the transformer reactance is X_t . Equation (2.27) indicates that, in the event of a change in the SPPs real power, that the change in real power that occurs to be matched by a change in the reactive power. This is done to keep the voltage remaining at a constant while flickering is reduced. However, if excessive reactive power cannot be supplied due to lack of capacity, real power curtailment will occur. According to the following Equations (2.30) to (2.34), the Q-capability of the inverter decreases during peak generation hours, resulting in a reduction in the amount of real power that is generated (Arshad & Lehtonen, 2019).

$$Q(t) = Q_{max}(t) \quad (2.30)$$

$$Q_{max}(t) = \sqrt{S_{max}^2 - P_{Gen}^2(t)} \quad (2.31)$$

$$\Delta Q_R(t) = \Delta Q_R(t) - Q_{max}(t) \quad (2.32)$$

$$\Delta P_R(t) = -\Delta Q_R(t) \cdot \left(\frac{X}{R}\right) \quad (2.33)$$

$$P_{SPP}(t) = P_{Gen}(t) - \Delta P_R(t) \quad (2.34)$$

The real and reactive power of the SPP at a time instant (t) is shown as $P_{SPP}(t)$ and $Q(t)$ respectively. Reactive power compensation that is exceeded is denoted as $\Delta Q_R(t)$, which will be used to control the flicker and the required curtailment is $\Delta P_R(t)$. Maximum reactive

capability of the SPP inverter is $Q_{\max}(t)$, generation of the real power is $P_{\text{Gen}}(t)$ and the SPP inverter's apparent power is S_{\max} in the equation (Arshad & Lehtonen, 2019).

2.4.3.3 Coordinated voltage control

As explained in the previous sections, the CVC strategy utilizes a token transversal methodology, which is augmented by a flat communication architecture, to remove voltage violations from the SPP. Based on the nodal voltage inputs, the autonomous LVC strategy changes inverter settings as outlined in section 2.4.4.1. However, sensitivity-based token transversal methodology can be used to deal with upstream SPP inverters without resorting to curtailment in the voltage control strategy. Also, until the required Q support is available, Reactive Power Control consisting of only Q(V) droop characteristics will be functional. If SPP inverters operate close to their maximum generation production, then the Q_{\max} for CVC will not suffice, and PF (V) droop will be utilized, which will reduce the PF from 1 to 0.9, depending on voltage level. For voltage control, when coordination between the two reactive power control strategies is insufficient, Active Power Curtailment (APC) is used, which includes P(V) droop control. The control logic function is implemented in the voltage control algorithm for the droop of the SPP to utilize the CVC strategy (Arshad & Lehtonen, 2019).

2.4.3.4 Voltage control logic function

Various steps of the proposed voltage control strategy repeat themselves on each time step, as illustrated in Figure 2.22. There is a brief description of the steps in each case (Arshad & Lehtonen, 2019):

- Step 1: Data consisting of power system loading and SPP inverter generation increase constantly, resulting in distinct values at every time step. The first step of the process initiates the time step counter to cover each instant of the time period.
- Step 2: In the beginning of each of the time steps, data on the SPP will be loaded. Moreover, for the purpose of determining SPP inverter generation data, irradiance data were used to obtain the data.
- Step 3: Upon reaching the minimum time interval after the last CVC control command has been invoked, the agent associated with each network node will check the network state for violations, that is whether the constraints are being met or not.
- Step 4: LVC algorithm is started if t_{LVC} is equal to one second, that is, if time since last LVC implementation is one second. Depending on the SPP location within the network and the nodal voltage value, SPP voltage nodes will check for dead band violations and provide the Q support.

Step 5: To provide an immediate response to the PV generation fluctuation, the FC algorithm is executed every time step.

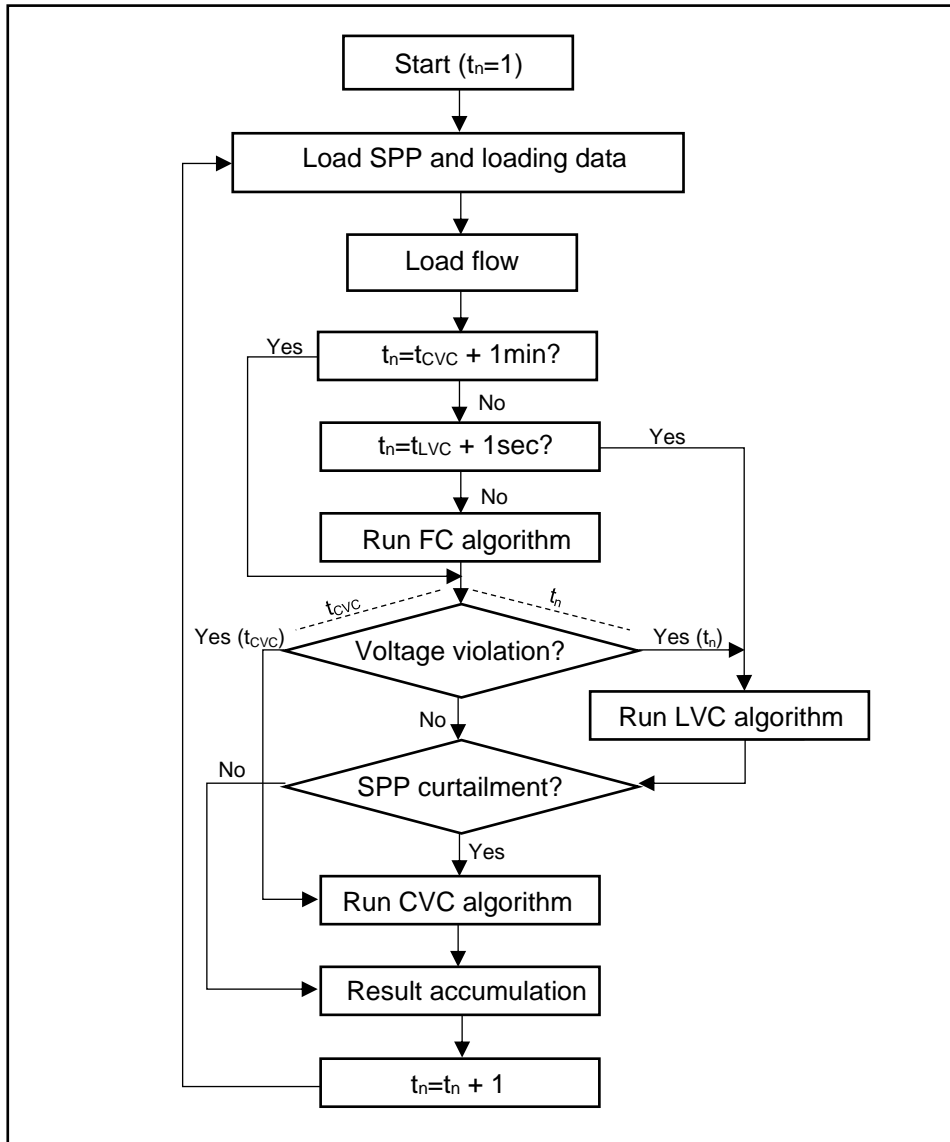


Figure 2.22: Adaptive Q(V) droop control for SPP (Arshad & Lehtonen, 2019)

Step 6: In order to analyse the results of the control strategy implementation, the network specifications and their results are stored.

Step 7: The time step increment t_n at the start for the next step is repeated, with steps 2 through 6 to complete the simulation.

2.5 Power Quality requirements for grid compliance

The power system experiences harmonics when there are non-linear loads, such as arc furnaces, power transformers, welders, switch-mode converters or reactors. Because the power system has a limited short-circuit capacity, the presence of harmonics will manifest itself in the supply voltage no matter what the harmonic emission source is. In addition, grid voltage

distortion can increase the harmonic content of inverter current. As a result, the inverter should be designed so that its effect on the voltage quality is minimized. A grid application such as the SPP integration can also firmly outline the permissible harmonic injection in the current and, when exceeded, denies permission for operation. In addition, an increasing number of nonlinear power sources and loads may cause higher losses in the system and higher heating i.e. insulation degradation, transformer overload, utility equipment distortion, etc. Control, modulation and topology can all be used to decrease harmonic emission when grid-connected SPP inverters are operational. Inverters' topology is crucial to reducing the potential for current and voltage harmonics (Chmielewski, et al., 2021).

Harmonics occur at multiples of the fundamental frequency that are odd or even. An example of a third harmonic would be $3 \times 50 \text{ Hz} = 150 \text{ Hz}$ for an electrical distribution network in SA. As opposed to momentary conditions such as sags and transients, harmonics are a relatively static. A harmonic distortion limit is expressed as a percentage of the magnitudes of the utility grid, as shown in Table 2.1 for Category B SPP. On a 22 kV grid, for example, the voltages associated with the 3rd harmonic magnitude should not be greater than 1.1 kV, representing 5 % of the nominal voltage. According to IEEE Guidelines, the allowable Total Harmonic Distortion (THD) for long-term harmonic effects is 8% and for short-term harmonic effects is 11 %. For long-term effects, weekly measurements are employed, whereas for short-term effects, daily measurements are utilized. As a result of non-linear loads in electrical systems, harmonics are caused by the current drawn by the loads which draws current which is non-sinusoidal from a sinusoidal voltage source. To suppress harmonic frequencies, harmonic filters can be added, either passively or actively. In passive filters, frequencies or a group of frequencies are tuned to be filtered, the benefit of a passive filter diminishes with increasing load, however, despite being a less expensive option. A power factor countermeasure may also be implemented to shift the natural frequency of the overall system (Nobela, et al., 2019).

Table 2.1: Inverter harmonic emission requirements for SPPs (Mchunu, 2020)

Harmonic order (h)*	$3 \leq h < 9$	$11 \leq h < 15$	$17 \leq h < 21$	$23 \leq h < 33$	$33 \leq h \leq 55$	Even	THD
Percentage of rated current (odd harmonics)	<4,0	<2,0	<1,5	<0,6	<0,3	25% of odd harmonics	<5,0

Inverters in the SPP shall not exceed the limits specified in the International Electromechanical Commission (IEC) IEC61727 for their individual harmonic currents and shall not exceed a THD of less than 5 % for their currents (up to the 50th harmonic). In the context of the growth in grid-connected renewable energy sources in South Africa. Below is the explanation of the

reasoning behind why it is important to improve the understanding of the impact of measurement on power quality simulations and the development of best practices for the assessment of grid code compliance. It is mandatory that a SPP be assigned a specific harmonic emission level in accordance with methods in IECs Technical Report (TR) 61000-3-6 in order to be eligible for the SAREGC compliance. In addition to site-specific emission values, SPP size and harmonic planning levels influence the emission values. Assuming that the SO will maintain harmonic distortion at the POC below the respective planning levels, this enables an equitable allotment of harmonic emissions to all loads connected to a SPP POC. IEC/TR 61000-3-6 has a method of allocating an emission value for a specific harmonic order based on the harmonic voltage emission value. As harmonic current signifies the concept of “emission,” the SO converts the harmonic voltage emission generated by the grid at the POC to a value that represents the harmonic current emission value (Marais, et al., 2018). Based on the assumption of a linear harmonic impedance profile, the following Equation (2.35) is performed:

$$Z_h = 3 \cdot \frac{V^2}{S} \cdot h \quad (2.35)$$

Where, the harmonic order of the linear harmonic impedance is Z_h , PCC line to line rms voltage level denoted by V and the kVA at the PCC 3-phase short-circuit capacity is S (Marais, et al., 2018) (Mchunu, 2020).

In the case of HV, application of the above may result in very low harmonic current emission levels, even milliamps. The SO network has low short-circuit capacities due to its high harmonic impedance. The South African SO therefore assigned harmonic currents of 0.1% of rated current at the SPPs of interest to account for the effect of harmonics. Under normal operating conditions, the SPP is required to provide evidence that it adheres to the harmonic emission regulations by recording voltages and currents that occur harmonically at the plant. It is normal to use a conventional metering circuit in order to obtain a scaled voltage and current input (110 V and 1 A nominal) into the measuring device that is being used. After the compliance assessment has been performed, the CIGRE/CIREN technical working group C4.109 outlines the use of the Harmonic Vector method to conclude the assessment. In addition to recording the harmonics of the voltage and current, we should also record the harmonics of the frequency. The SO’s network is assumed to be experiencing harmonic currents as a result of the SPP’s operation because of the harmonic currents flowing in the network. There is a possibility that harmonic currents can also flow from the grid into the SPP in some states of operation, but from the standpoint of the SO, the SPP would not have harmonic currents flowing into it in any direction regardless of how it is connected to the grid. As a result, the harmonic emission level allocated at the SPP is estimated by comparing the

top 95% percentile of maximum harmonic currents measured at the SPP. Achieving the required emission level is an absolute necessity, and if the SPP is not capable of achieving that, it will be required to mitigate the harmonic currents in order to obtain a commercial operation license. It is essential to perform the DigSILENT PowerFactory studies to indicate that the SPP is compliant to the SAREGC with the influence from the SO's utility grid (Marais, et al., 2018).

2.6 Control function requirements for grid compliance

When the SPP is in design phase, the compliance requirements with the utility's SOA will determine the control mode of the inverter at the POC. The PPC will regulate the requirements of the control mode at the POC and the inverters are required to provide support to the utility grid at the predetermined control mode, which is indicated in the SOA. Control methods will be applied to the inverters in order to provide the required control functions as and when needed by the PPC. The SAREGC document provides guidelines on the specific control modes, which the inverter requires to achieve to meet grid compliance in the utility network. The control methods will be discussed for the following control modes as required by the SAREGC compliance to the Electricity Regulation Act (Act 4 of 2006) as amended (Sewchurran & Davidson, 2017).

2.6.1 Reactive power (Q) control function requirement

Reactive power (Q) control – the grid code of south Africa indicates that the following conditions and responses shall be met when the SPP is controlled by the PPC in Q control mode. Q control is the function of controlling the reactive power absorption and supply at the POC and should be independent of the voltage and active power. The vertical purple line indicated in Figure 2.23 illustrates the Q control function requirement to be achieved when set by the transmission SO (Mchunu, 2020). The following functionality should be achieved by the IPP to prevent non-compliance:

- When the SO, NSP or their agents request for a new Q control setpoint value, the IPP should respond within two seconds from the initial echo analog set point value. The IPPs PPC has 30 seconds to reach the new setpoint from order to change the existing setpoint;
- Deviation in control and accuracy performed of not more than ± 2 % of the setpoint value, the maximum reactive power not to deviate by ± 5 %. The highest tolerance yields shall be the deciding factor on which value gets preference;

- Accuracy of the Q setpoint should be within 1 KiloVolt-ampere reactive (kVar) once received from the SO.

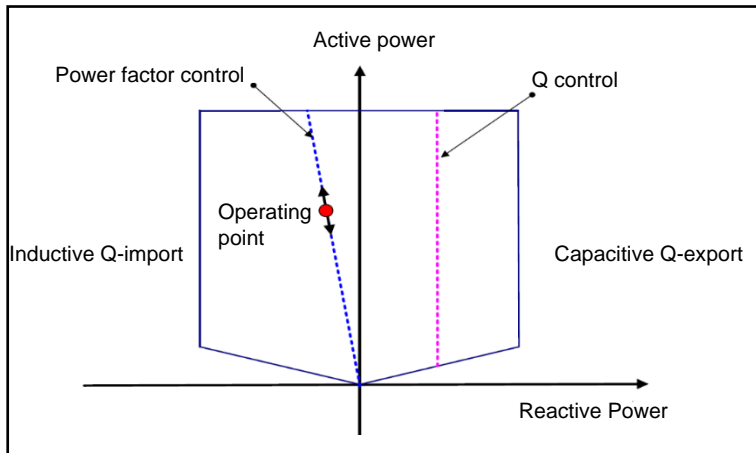


Figure 2.23: Q control for a SPP (Mchunu, 2020)

2.6.2 Power factor control function requirement

Power factor control is when the reactive power and active power is controlled proportionally to each other at the POC, which is shown in Figure 2.23 and illustrated as a constant gradient by a blue line (Mchunu, 2020). The following control and accuracy should be achieved:

- When the SO, NSP or their agents request for a new power factor control setpoint value, the IPP should respond within two seconds from the initial echo analog set point value.
- The IPPs PPC has 30 seconds to reach the new setpoint from order to change the existing setpoint;
- Deviation in control and accuracy performed of not more than ± 2 % of the setpoint value.

2.6.3 Voltage control function requirement

Voltage control is when the voltage is controlled at the POC from the SPP (Mchunu, 2020). Non-compliance should be avoided by achieving the following control and accuracy:

- Request for a new voltage control setpoint value should commence within two seconds from the initial echo analog set point value and will be completed by not later than 30 seconds;
- Voltage setpoint accuracy shall be within ± 0.5 % of the voltage at nominal level and deviation in control and accuracy performed of not more than ± 2 % of the required

absorption or injection of the reactive power. The droop characteristics are with the reactive power as illustrated and defined in Figure 2.24 for the voltage requirement capability compliance;

- Both the voltage limit and dynamic range of the SPP should be able to perform the control requirements as per the configuration of the droop shown in Figure 2.24. The voltage change per unit (p.u.) from the effect of reactive power (p.u.) change is conceptualise as the droop in this context;
- When the design limits have been reached by the voltage control function, the control function will expect the power transformer's on-load tap changer (OLTC) or other voltage control device to decrease or increase the voltage to ensure compliance;
- Voltage control coordination of the overall IPP will be requested by the NSP in co-operation with the SO.

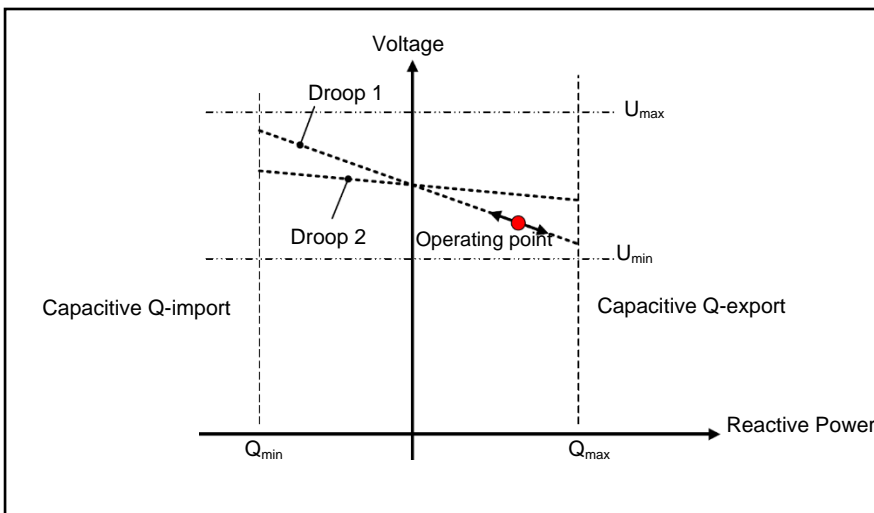


Figure 2.24: Voltage control for a SPP (Mchunu, 2020)

2.7 Steady-state compliance studies for a grid-connected SPP

Technical specifications governing the use of generation units connected to utility grids, including SPPs, are known as grid codes. In most developed countries, utility Sops publish standard grid codes for the SPP to comply with (Vrana, et al., 2021). Since renewable energy is increasingly being used on utility grids, many countries have created grid codes to regulate grid support for renewable energy sources during fault conditions and steady-state operation. In the past, grid codes were mainly for synchronous generators, but with the increase in SPP energy generation there was a need to adopt grid codes to avoid degradation of system reliability due to an increase in the number of renewable energy sources installed. Initially SPPs did not require to support the utility grid with ancillary services (Q support) for network stability, also the SPPs did not provide reactive power provision or voltage control participation in the grid. In South Africa, SPPs do not currently provide ancillary services, but could if the

SO requires the functionality to be activated. To support the grid and provide ancillary services, renewable energy plants must be able to mimic conventional power plants in normal and faulted conditions. The main requirements for renewable energy generation plants to maintain the network stability are frequency regulation, reactive power control, voltage regulation, and fault or low voltage ride-through capability. Faults in the system cause voltage drops that propagate widely, when this happens, SPP inverter units can trip and shut down. SPP inverters were previously allowed to disconnect from the grid in the event of a disruption in the power grid or low voltage. However, if large amounts of SPP generation are disconnected at the same time, the system voltage may drop and voltage collapse can occur. Additionally, SPP generation that is disconnected to a significant extent can result in an active imbalance, resulting in the utility grid instability (Nhlapo & Awodele, 2020). In cases of non-compliance with grid codes, the SO of utility grids can enforce disconnection from the grid and enforce subsidy curtailment after connection with the grid again. An objective and systematic standard about compliance simulation and assessment against the grid code is needed to unite the level of understanding and measurement of grid code compliance. A renewable power software program (i.e. DlgSILENT PowerFactory) aims to outline simulation methods for the evaluation of power generating units and plants utilizing modern technology. In addition, a specification needs to be given on the method for simulating the electrical behaviour of SPPs according to grid code requirements. Due to the technical requirements on grid-connected SPP generation units and plants outlined by grid codes or international/regional standards, it is useful to determine how grid code compliance should be simulated. It is beneficial for manufacturers to identify the performance of grid-connected SPP units, operators to determine whether or not the required characteristics are met and planners and regulators to determine how to connect renewable power plants to the grid (Yongning, et al., 2019). In the following sections the SAREGC for Category B renewable power producer (RPP) requirements will be discussed to focus on the simulations that will be done in order to identify non-compliance factors.

2.7.1 Reactive power requirements

Each SPP requires (according to the latest SAREGC) to comply with the specification and regulations as set out by the SO. According to section 2.6.2, RPPs of this category must be capable of operating in a voltage (V), reactive power (Mvar or Q) or power factor mode. With the NSP, the actual operating mode (Q, V or power factor control) as well as the operating setpoint shall be agreed upon before final grid integration. If the available reactive power at POC operates between 5 and 100% of rated power P_n (MW), the RPP of a Category B SPP shall be capable of providing reactive power (Mvar) support. In terms of the voltage dependent ranges defined by Figure 2.25, where Q_{min} and Q_{max} depend on the voltage. The reactive power capability required are based at nominal voltage as illustrated in Figure 2.26 (Mchunu, 2020).

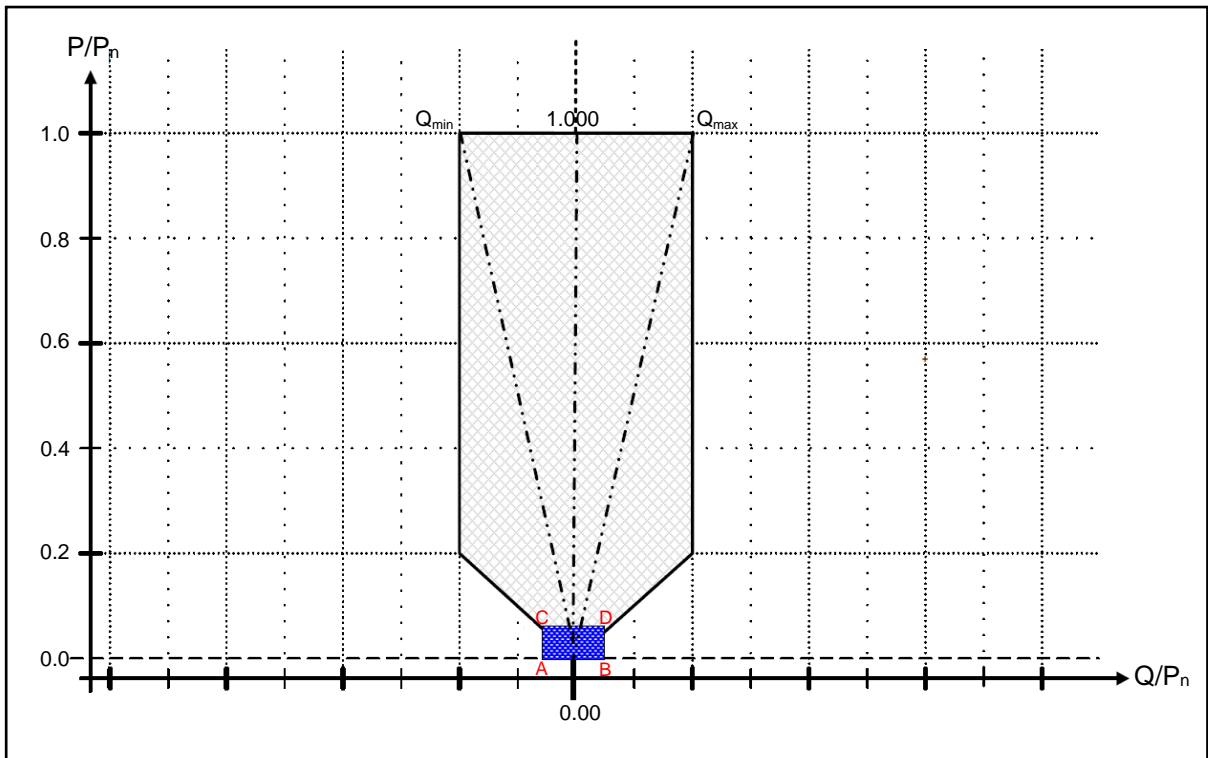


Figure 2.25: Reactive power capability requirements at the POC (Q_{min} and Q_{max} are voltage dependent) (Mchunu, 2020)

There is no prerequisite for reactive power capability below 5% of the rated power P_n (MW) but within the reactive power tolerance range not exceeding +5% of the rated power; that is Areas A,B,C and D indicated in Figure 2.26 (Mchunu, 2020).

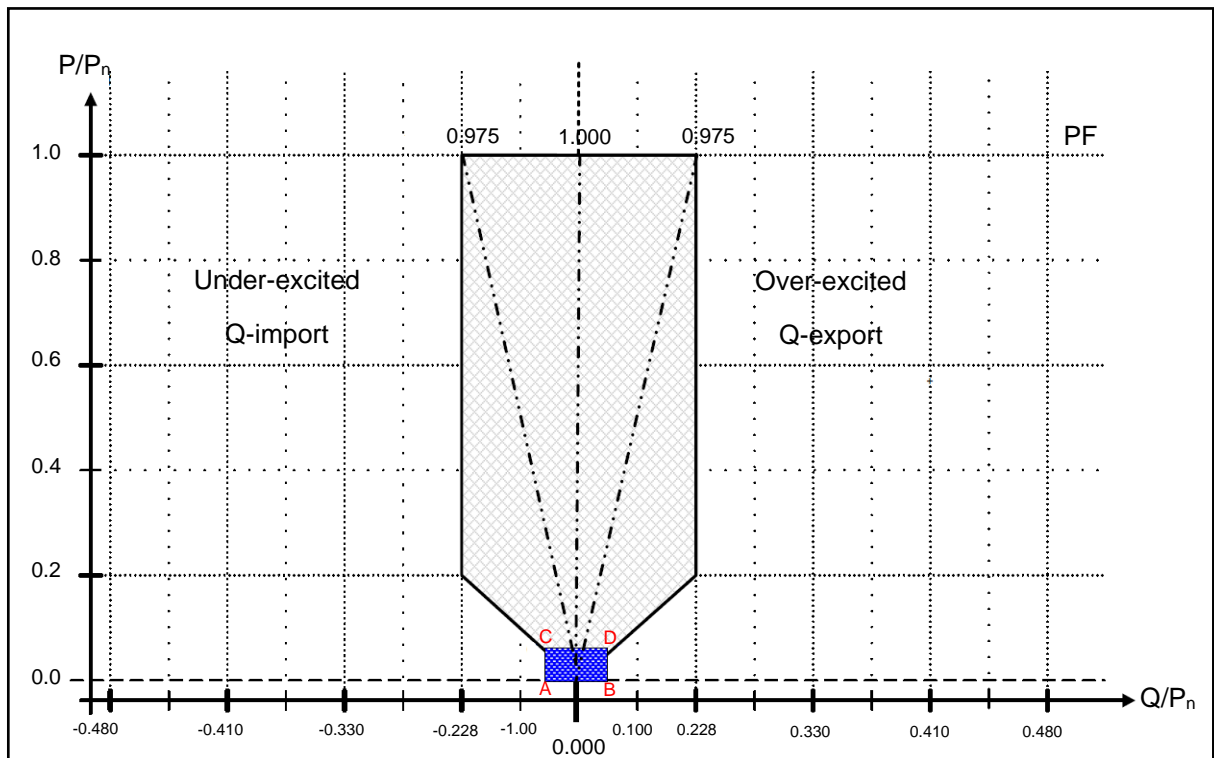


Figure 2.26: Reactive power capability requirements at the POC (for nominal voltage at POC) (Mchunu, 2020)

2.7.2 Voltage requirement capability

Category B SPP should have the following voltage compliance requirements when in operation:

- RPPs must be equipped with reactive power control functions that control the reactive power supplied by the SPP at the POC, as well as a voltage control function that controls the voltage at the POC via orders using gradients and setpoints as set out in Figure 2.27;
- It is mutually exclusive for reactive power and voltage control to operate at the same time and should comply with the functions that can be implemented at a time instant:
 - Voltage control;
 - Q control;
 - Power factor control.

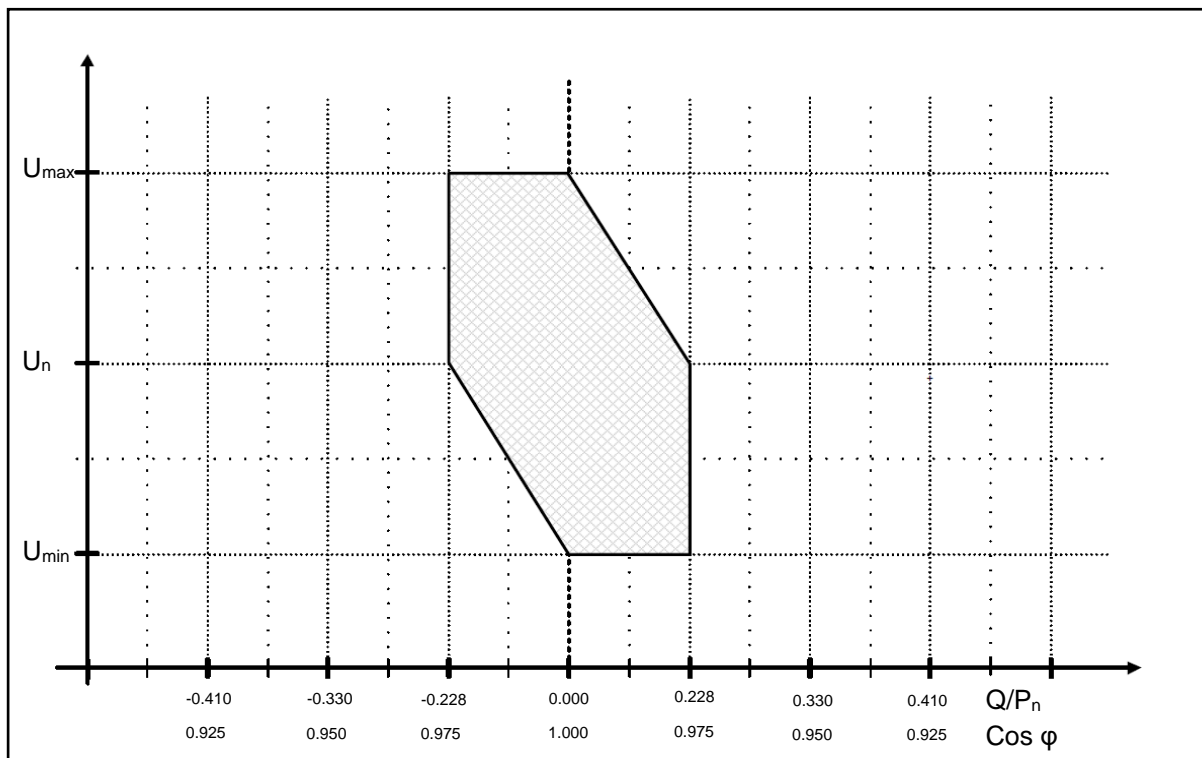


Figure 2.27: Reactive power capability requirements at the POC (for nominal voltage at POC) (Mchunu, 2020)

In addition to defining the control function and applied parameter settings for reactive power and voltage control functions in collaboration with the SO, the NSP shall implement the control function on the SPP inverter. The operating agreement is to document the control functions that have been agreed upon.

2.7.3 Power quality requirements

Power quality must be maintained at acceptable levels by the NSP. South Africa monitors and manages power quality in line with the NRS 048 series of specifications, which include input from the IEC 61000 series and EN 50160. In addition to the Grid Code and other regulations, such as the PQ Directive, NERSA determines the licensing conditions. There are entities that connect to the NSP network (e.g., RPP) that have a responsibility to limit their impact on the power quality levels as defined in relevant documents, such as the Grid Connection Code for Renewable Power Plants (GCRPP), or connection protocols or agreements (Mchunu, 2020).

A description of the simulation guidelines for the harmonic assessment of the SPP is provided, as well as how it contributes to the utility grid. This set of industry specifications identifies minimum guidelines for customers and utilities to coordinate power quality levels at the point of interface within the local distribution network. The NRS 048 document has three parts that specifically provide reference to this document and the coordination of total quality of supply levels: the first defines both compatible and characteristic levels, while the second outlines methods for measuring the power quality standards provided by an NSP in accordance with compatibility and characteristic levels. IEC 61000-4-30 and EN 50160 are included as references in this section. Part 4 addresses coordinating aspects, including apportioning parameters of power quality for simulation values, and evaluating the apportioned emission limits of SPPs, in addition to IEC 61000-3-6, it also links to IEC 61000-7. Part 7 of the specification deals with the SPP applications in relation to the power quality content expected in the background. As a result, the power quality of the existing power grid has to be considered as well as how it will impact the network when the equipment has to be planned. The three main power quality levels that are important for the purpose of this document are compatibility values, planning values, and emission values. In order to ensure that NRS 048-2 complies with international standards, it defines levels of compatibility. According to electromagnetic compatibility (EMC), compatibility levels are defined as: "Specified disturbance levels above which it would be expected that electrical compatibility will exist with a high probability." These are the standards by which the performance of a NSP is compared. Harmonic levels in the background should generally be lower than compatibility levels, the NRS 048-4 is in line with the planning levels, which are defined according to international standards (Mchunu, 2020).

The NSP should design their networks to comply with these levels in order to prevent present and future disturbances on their networks from exceeding their compatibility levels. According to NRS 048-4 (adopted from IEC 61000-3-6, -7, and -13) the emission limit is calculated for each customer and RPP, as detailed in the manual. In order to determine the specific emission limits, a SPP are allowed to contribute the maximum amount of power quality disturbances to

determine the magnitude of the individual power quality contribution at the POC. Background levels are generally much higher than emission limits. Compatibility levels, planning levels, and background levels should not be confused with emission limits. A background level is a level under which all emissions are combined to operate and generates for the purpose of representing the combined effect of all emissions at the POC at that point in time (Mchunu, 2020).

2.7.3.1 Definition of harmonic emission levels in SPPs

A harmonic emission quantity, defined as a vector of the magnitude of a vector that is caused by an installation in the power system at the point of evaluation (in the case of RPPs), is said to be expressed according to IEC 61000-3-6. An emission which is derived in relation to a post-connection vector having a smaller magnitude than the pre-connection vector is generally considered to be zero, i.e. a filter may not be considered as generating an emission with respect to a harmonic voltage (Mchunu, 2020).

Due to the system impedance being injected with current harmonic along with voltage amplification, the emission is the result of the combined voltage harmonic and voltage amplification, the IEC 61000-3-13 provides a similar definition for voltage unbalance. Despite the fact that the definition of voltage flicker in IEC 61000-3-7 is not quite as clear, the principle is the same, as voltage flicker does not add linearly between different installations. There is no direct relationship between the definition of rapid voltage changes (RVCs). Defining the voltage changes for rapid changes in voltage is separate from defining the voltage changes for background. By simultaneously simulating the voltage and current of the installed equipment in the SPP, the contribution of the installation can be confirmed (Mchunu, 2020).

2.8 Summary

An understanding of the main electrical equipment used in a grid-connected SPP installation is provided in this chapter, along with a summary of the components that are applicable in a SPP installation. Because the control strategies play an important role in identifying the mitigation in non-compliance factors, the focus of the paper is on different types and methods of control that can be implemented by the SO. The specific simulation requirements for SAREGC simulations were discussed and analysed so that a comprehensive set of requirements could be defined for grid-connected SPP grid code simulations in steady-state environments. In Chapter 3, the focus will be on simulation requirements in the DlgSILENT PowerFactory simulation software, the building of a model with all the required parameters to perform simulations.

CHAPTER THREE: MODELLING AND SIMULATION OF A SOLAR PHOTOVOLTAIC PLANT

3.1 Introduction

This chapter presents the case study designs combined with modelling and a simulation model that will be implemented in DigSILENT PowerFactory, which includes the SPP equipment and control strategies discussed in chapter 2. The simulation model will be explained in stages from the external grid (representing the utility) and proceeding to the LV terminals of the inverters. All components in the simulation model are available in the PowerFactory library and the components may be modified to operate according to the stability frame of the controllers of the inverters. The benchmarked typical data and the validation of the model and network will be achieved in accordance with the SAREGC, NRS, IEEE and the Western Electricity Coordinating Council (WECC) for solar PV power plant modelling and validation guideline.

PowerFactory is a power system simulation software package to use to simulate the network, the software has built-in dynamic inverter models that can be made use of in the study. The only acceptable software that is used to prove compliance and to indicate non-compliance for the South African utility Eskom is PowerFactory, the software is mandatory for the SAREGC simulations. Simulating and modelling systems can be used for studying networks and their compliance with grid codes, which are used as tools to represent them in a virtual setting. As a measure of individualism, this approach looks at autonomous entities that can interact with each other, which results in the disaggregated model of the network. It is possible to create models that represent specific components individually and then combine and integrate those models so that they can represent the SPP. Modularly assembling the models can represent the system by aggregating them like building blocks, in this thesis, a SPP is used as a modular network of how the generation plant is connected to the utility grid. Furthermore, the modelling and simulation are presented in a heterogeneous way, such as by parameterizing electrical and SPP components according to standards, requirements and specifications.

The modelling and simulation will represent a network that contains benchmarked values and reputable publishing professional association institute standards. That is based on design methodologies and certain assumptions, which is used to provide a model that can be used to derive compliance studies according to expected results at the POC. In the following sections, the outline will represent the implementation of the model used in this chapter, exploring and documenting the generation model that is integrated with the utility grid at the POC.

3.2 Network model

A network model consisting of features that enable the conducting of the steady-state studies in a grid-connected SPP, that includes the following: fault level analysis for fault contribution at the POC by the inverters, reactive power (Q) compensation studies, voltage compliance studies and harmonic load flow and frequency sweep studies. The studies listed will ensure that all compliance factors during steady-state studies will be addressed. This will allow the case study to present the compliance factors and/or non-compliance factor to be mitigated to achieve compliance. Grid code compliance studies will be conducted in line with the guidelines provided in the SAREGC document by Mchunu (2019).

Using the inverter data from PowerFactory and creating a SPP layout the model will be developed in a full DIgSILENT PowerFactory project (network model) for the proposed case study. At the POC, the model will be measured for compliance as per SAREGC requirements, the contribution by the utility and the SPP will contribute to the final modelling and simulations. Steady-state studies will be conducted to determine the voltages and power flows within the SPP and at the POC (an additional busbar will be created to act as the POC substation). The steady-state limits will be implemented with respect the voltage and thermal constraints under healthy system conditions for minimum and maximum SPP conditions in the network. With the fault level studies the three-phase and single-phase fault levels shall be conducted according to the IEC 60909 standard to determine the expected fault level rating at the POC and of the SPPs equipment. The fault rating will be used to determine any fault level exceedances in the network and on the fault rating violations of the electrical equipment in terms of SANS 60947-2 for the power plant equipment. Reactive power requirements will be simulated and modelled in PowerFactory to achieve acceptable voltage regulation at the POC according to the requirements of the SAREGC, NRS 097-2, NRS048-2 and IEEE standards. The location, sizing and steps required to achieve the reactive power capability specified in the SARGC will also be explained in the context of acceptable limits. A harmonic load flow study will be assessed and carried out only indicating the requirements for the SAREGC as specified in the NRS048-2 and NRS048-4 standard. The modelling and simulation will include a process to conduct and determine the resonant points of the network model contributed from the SPP to the utility grid. Voltage distortions can be expected at the POC, due to the contribution of voltage and current harmonics from the existing utility grid.

Intended for instructing decision-makers on how to integrate distributed renewable energy sources (RES) with the electric grid effectively, IEEE standard 1547 provides guidance. RES technologies have been integrated into this standard, assisting to modernize power grid infrastructure. According to the IEEE 1547 standard, all interoperability requirements,

operational conditions and maintenance requirements, as well as the operation details of the essential equipment and methods must meet the mandatory technical requirements. Among some of the most important standards, including those embodied in the IEEE 1547 standard, relating to the interconnection of the source of RES are the following (Oskouei & Mohammadi-Ivatloo, 2020):

- i) IEEE 1547-1: Standard specifies the test method for determining compliance with the IEEE 1547 standard when equipment is connected to power grids during distributed energy resource operations;
- ii) IEEE 1547-2: In addition to being used as a reference guide for IEEE 1547, this standard serves as an application guide;
- iii) IEEE 1547-3: Using this part of the IEEE 1547 standard, distributed energy resources interconnected with power grids can be monitored, controlled, and information exchanged;
- iv) IEEE 1547-4: Distributed energy resources with power grids in islanding mode can be operated, designed, and integrated using this standard;
- v) IEEE 1547-6: To interconnect the distribution secondary networks with distributed energy resources, the section of the IEEE 1547 standard specifies a recommended practice for communicating this part of the standard;
- vi) IEEE 1547-7: This section of the IEEE 1547 standard contains the following parts that are used to evaluate the impacts of distributed energy resources on electrical power grids through the lens of a practical guide;
- vii) IEEE 1547-8: A supplemental procedure and novel methods are included in this standard in order to extend the IEEE 1547 standard in a more efficient manner.

In summary, IEEE 1547 addresses the distribution-level distributed energy resources in the form of connected distributed energy resources. This includes items such as:

- Technologies for generating renewable energy;
- Intermittency and uncertainty of renewable energy sources;
- Components of the modern grid and renewable energy technologies have advanced characteristics;
- Improved simulation and modelling requirements as part of testing and assessment;
- Assessment of RES-grid interconnection resiliency and reliability requirements.

The following section will provide an overview of the base case model to be simulated to provide perspective in terms of how the SPP is modularly combined to function as a generation plant and providing energy in the form of electricity into the utility network.

3.3 Overview of SPP model in PowerFactory

The base case model will be analysed from the top section as a complete modular unit that will comprise of the utility network to indicate that the SPP is grid-connected on a common utility busbar, which is shared by the AC voltage source for harmonic studies. The SPP will have a MEC capacity of 9 MW at a voltage level of 11 kV. By implementing a separate busbar labelled as the POC, the simulation model can control the requirements by utilizing a PPC with all the defined controls destined at the specific busbar. A network model is illustrated in Figure 3.1 to indicate the overall network configurations that will be discussed.

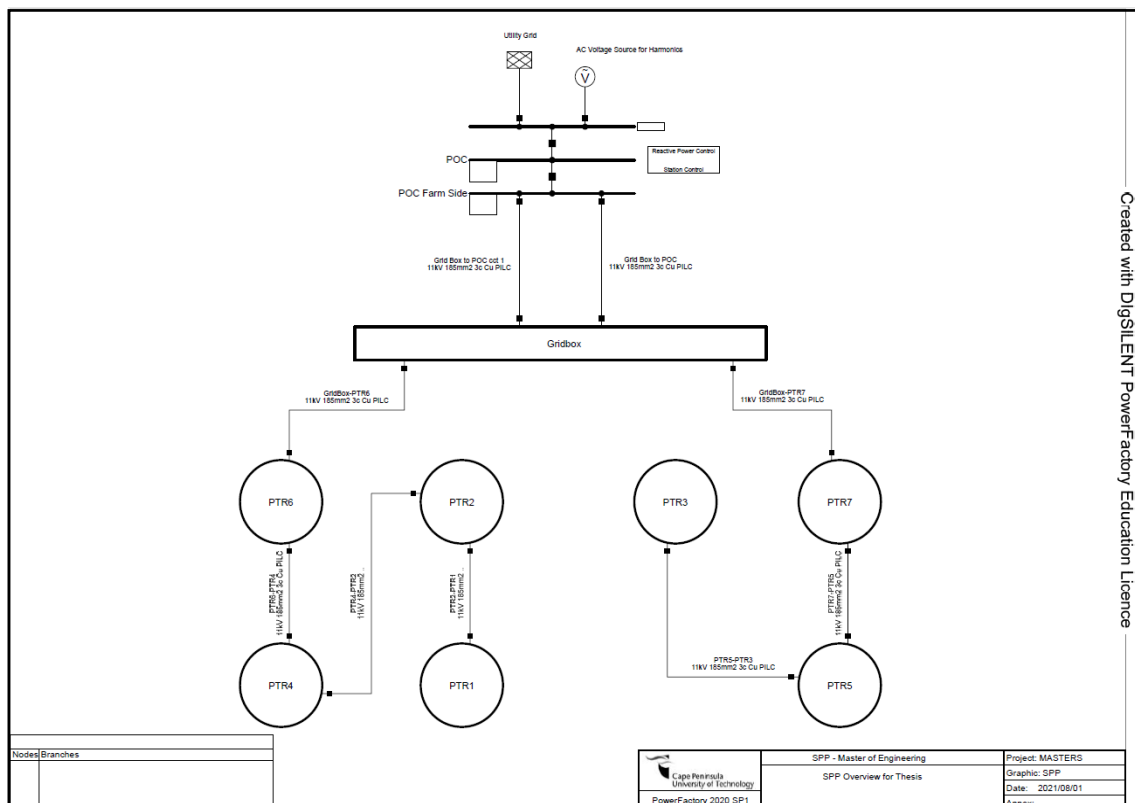


Figure 3.1: Overview of complete SPP model in PowerFactory

The POC is connected to the POC busbar with underground distribution primary incomer cables and is connected to a grid box, which indicates the collector group substation for the SPP. As the Grid box are connected to the PV and transformer stations (PTRs) by two feeder cables, the complete facility base case model is represented with 7 x PTRs connected to the grid box.

3.3.1 Utility network

An element can be defined as an external grid in PowerFactory to represent the complete network contributions at a specific point in the network. An AC circuit, in the context of the

external grid, is comprised of an inductive component (X) and a resistive component I as illustrated in Figure 3.2 as a simplified network model (de Beer & Rix, 2017).

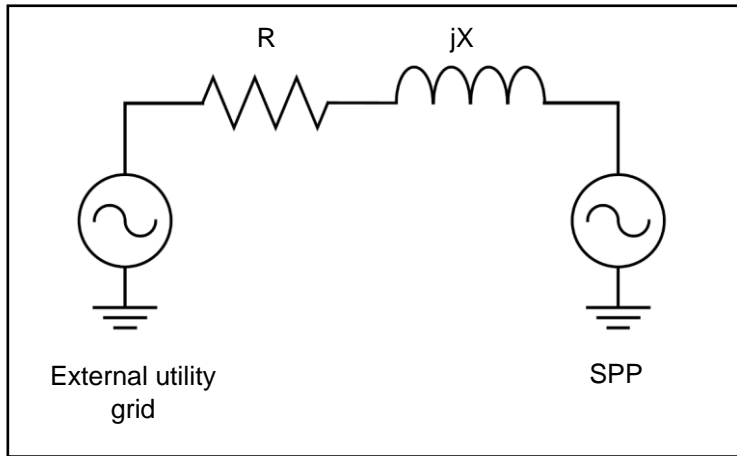


Figure 3.2: Network model simplified (de Beer & Rix, 2017)

When these components are added together, $Z_{\text{external grid}} = R + jX$, as subjected to the POC, the inductance over resistance corresponds to the ratio represented by X/R . By using Equations (3.1) and (3.2), it is possible to divide the grid impedance into its separate components. A weak external grid is classified as a grid that comprises of an ohmic character, which is a ratio of 0.5 for the X/R ratio (de Beer & Rix, 2017).

$$X = \frac{Z}{\sqrt{1 + \left(\frac{1}{X/R}\right)^2}} \quad (3.1)$$

$$R = \frac{Z}{\sqrt{1 + \left(\frac{X}{R}\right)^2}} \quad (3.2)$$

Where X and R is the inductance and resistance respectively and the Z denotes the impedance of the external grid with X/R as the ratio that represents the complete parameter of the external grid (Grunau & Fuchs, 2012).

Parameters that are required for the external grid is the X/R value at a minimum and maximum value for the base case model and is represented in Appendix B under Table B.1. The external grid is modelled as a slack bus with an active power rating of 9 MW and a voltage setpoint of 1 per unit (p.u.). By implementing the user defined X/R ratio for maximum and minimum values in PowerFactory, the other resulting values in Table B.1 will be added by the software program. Values that were not included is added by assumptions for the network model to function as per SAREGC requirements. The addition of the c-factor in the model for simulation represents the pre-fault conditions and is multiplied by the p.u. voltage at nominal level (DlG SILENT GmbH, 2020).

3.3.2 AC voltage source for harmonic simulations

The addition of an AC voltage source model for harmonic simulations are added to the 11 kV utility bus, the AC voltage source model is required for the external controller, which is the PPC to enable the harmonic emission performance and frequency sweep analysis at the utility bus. Simulation values are implemented based on the current and voltage distortions at the POC in the network model as per requirements from IEEE 519 as illustrated in Figure 3.3. This element (ElmVac) will not have a dynamic controller, due to the function of control at the utility grid being performed by each individual inverter's harmonic spectrum.

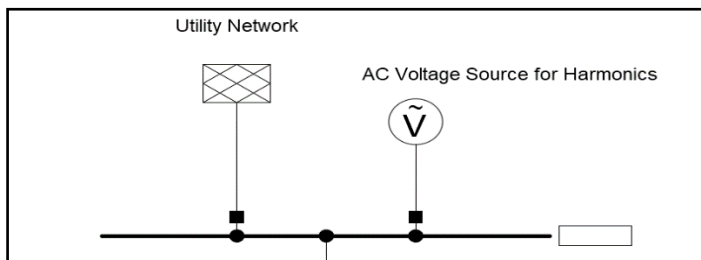


Figure 3.3: AC voltage source for harmonic simulations

Assessing the grid impact by the addition of an AC voltage source at the utility grid close to the POC can benefit the network model studies for the SAREGC compliance. Due to switching the element in and out of service to determine the impact on the network model. Element type will be a voltage source in the basic data and the remaining data is presented in Appendix B Table B.2 for the positive and negative sequence of the resistive and reactance values. Values for the positive and negative sequence will be the same as the simulation model is for steady-state conditions.

3.3.3 Power park controller

A direct link exists between producers (IPPs) and consumers (utility clients) in traditional electric power systems and the IPPs or generation facility requires to be controlled at a common point of measurement such as the POC (Vokony, et al., 2012). The PPC in Powerfactory will be added as the station controller for the controlling of all inverters in the SPP for the case study.

As the inverter controllers will be discussed later it is important to note that the inverter controllers will portray the role of the inner controllers of the network model and the PPC will have the functionality of the outer control. The outer controller will be responsible to task the inner controllers to perform certain tasks in active power control, reactive power control and power factor control discussed in chapter 2 (Gonzalez-Longatt, et al., 2014). In the network

model base case the PPC is added at the POC as per SAREGC requirements and is shown in Figure 3.4 for the application to control the inverter’s output functions.

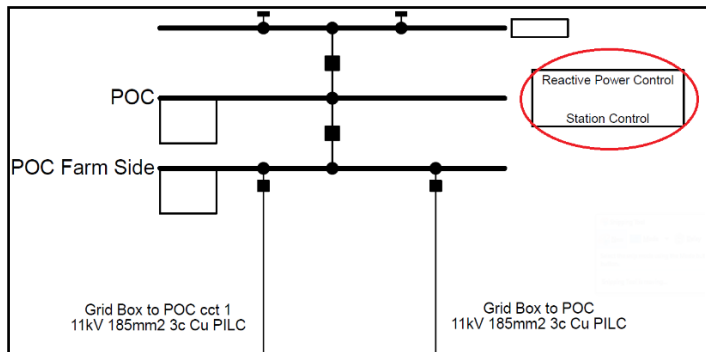


Figure 3.4: PPC in network model at the POC

The PPC requires a structure that allows the control of the inverter’s composite model architecture and composite frame (DIgSILENT GmbH, 2020). PowerFactory allows this option to be investigated by incorporating control conditions of the following elements in the composite model and frame as illustrated in Figure 3.5 from the base case network model.

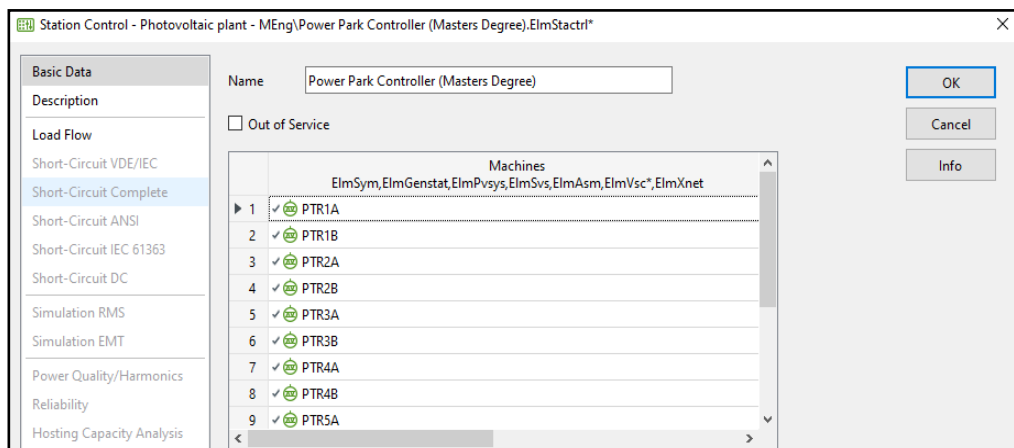


Figure 3.5: PPCs dialog within the base case PowerFactory model

By assigning control functions to each inverter represented as PTR1A – PT7A, the required output functions can be obtained in terms of the desired control by the SO. As per Figure 3.4 above, the following elements in is controlled (DIgSILENT GmbH, 2020):

- i) ElmSym – Synchronous machine;
- ii) ElmGenstat – Static generator;
- iii) ElmPvsys – PV system;
- iv) ElmAsm – Asynchronous machine;
- v) ElmVsc – Pulse-width modulation (PWM) converter;
- vi) ElmXnet – External grid;

All the above elements are implemented in the PPCs element namely the station controller (ElmStactrl). In the load flow section of the dialog, the PPC can be controlled in different control modes as seen below in Figure 3.6 as required by the SAREGC, the plant can be selected to be operated in voltage control, reactive power control and power factor control.

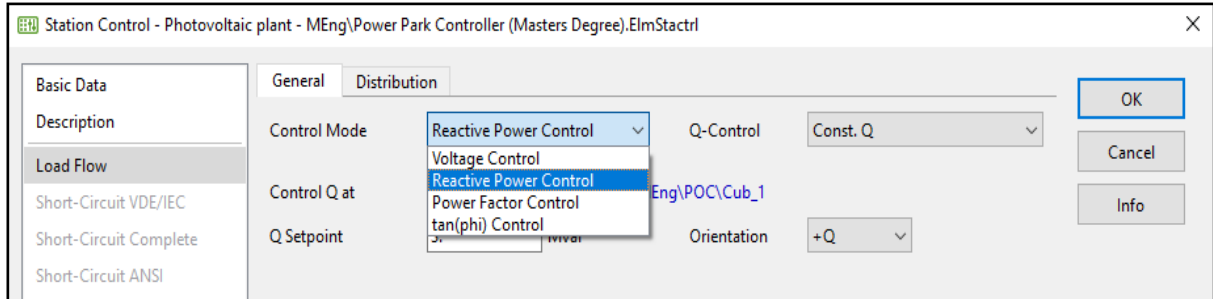


Figure 3.6: Different control modes of the PPC

The tan (phi) control mode will not be discussed in this thesis as the control mode is not required to be performed from a SAREGC perspective. For this specific base case model that will be used to identify compliance and non-compliance, the Q setpoint must still be calculated in the following chapter 4. In the base case network model, the example value will be set to 3 MVar at a positive Q support (overexcited) as illustrated in Figure 3.7, it is assumed for the SPP to provide Q support by injecting reactive power in the utility grid (Jiang, et al., 2021).

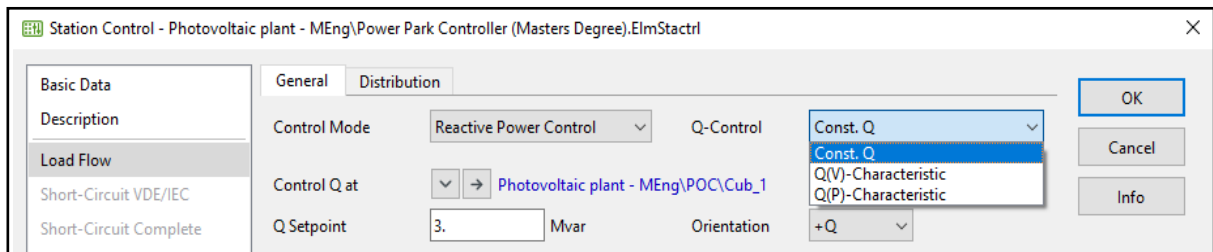


Figure 3.7: Setpoints, orientation and control characteristics in the network model

With the implementation of the constant Q control mode, the voltage dependency will be for a reactive power control mode. The Q(V) control will be for voltage and Q(P) is the voltage dependency on the real power (P), which is not required for the SAREGC compliance studies (DIgSILENT GmbH, 2020).

3.3.4 Primary incomer and secondary feeder cables

In order for the cable transmission line model to be implemented, the composition of the cable transmission line is firstly determined, which is shown in Equation (3.3) and (3.4). Voltage and current are represented by V and I , respectively, and impedance and admittance are represented by Z and γ , respectively. The conductance is denoted by G , whilst C is the capacitance of the distributed cable parameters and E is represented by the electromagnetic

field of the circuit. According to Equation (3.5) and (3.6), the V_F and I_F represent distributed voltage source and distributed current source, respectively, caused by external electromagnetic fields (Liu, et al., 2020).

$$\frac{\partial}{\partial y}V(y, \omega) + Z(\omega)I(y, \omega) = V_F(y, \omega) \quad (3.3)$$

$$\frac{\partial}{\partial y}I(y, \omega) + G(\omega)V(y, \omega) = I_F(y, \omega) \quad (3.4)$$

$$V_F(y, \omega) = -\frac{\partial}{\partial y}E_T(y, \omega) + E_L(y, \omega) \quad (3.5)$$

$$I_F(y, \omega) = -j\omega CE_T(y, \omega) \quad (3.6)$$

For the underground cable model to be considered reliable it must be subjected to the verification of numerical calculations accuracy as well as the confirmation of the underground cable model accuracy. As part of the analysis of the accuracy of numerical computation, a distributed cable parameter model is introduced in the PowerFactory simulation in terms of its theoretical value for the distributed parameter, this model is shown in Figure 3.8. To analyse the confidence in the cable distribution parameter model, it is crucial that a good confidence is established by the underground cable modelling (Liu, et al., 2020). The distribution parameters of a cable model can be done by implementing information from a recognized cable supplier.

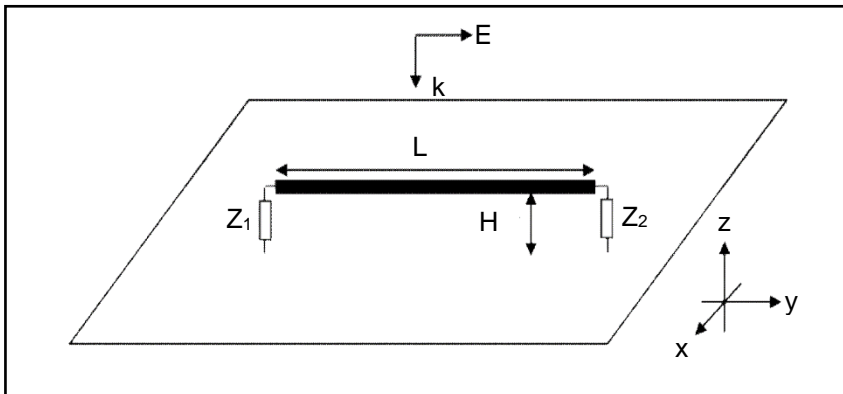


Figure 3.8: Distributed parameter model of a cable (Liu, et al., 2020)

In PowerFactory, cables and lines are treated the same way: both types are instances of the generalised line element ElmLne. A line may be modelled simply as a point-to-point connection between two nodes and will refer to a line (TypLne), tower (TypTow), a tower geometry (TypGeo), a line coupling (ElmTow), or a cable system coupling (TypCabsys, TypCabmult) type. As an alternative, lines may be divided into sections that refer to different types within them. In its simplest form, a line model consists of a point-to-point connection between two

nodes (DIgSILENT GmbH, 2020). The underground cable illustrated in Figure 3.9 for the primary incomers and secondary feeder will have equal parameters.

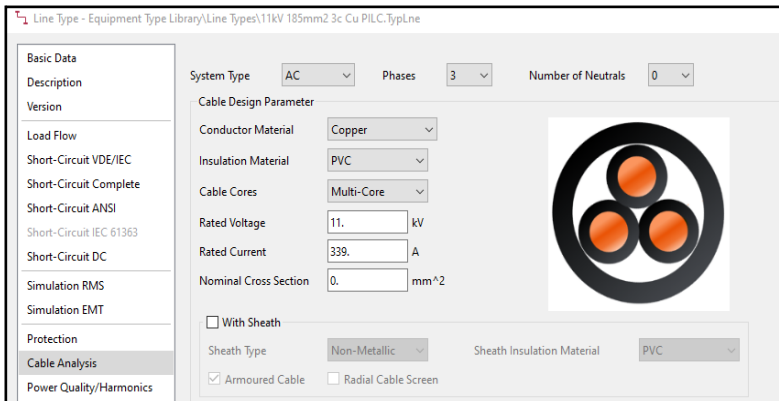


Figure 3.9: Cable analysis in PowerFactory for the SPP

Cable data represented in Appendix B in Table B.3 will be implemented in the network model between the POC farm side to the grid box and the grid box to PTR6 and PTR7, there will be two composite circuits 1 and 2 between the POC and grid box and single feeders to the PTRs. By implementing a well-known supplier cable parameters to the model, the validity of the underground cable distributed model is benchmarked with accredited values. The distances between the electrical equipment connections in meter (m) will provide a resulting value in PowerFactory and Table B.4 indicates the lengths of the circuits.

3.3.5 Grid box of a SPP

A grid box or a collector group bus is where the incoming primary cables and secondary feeder cables are continuously connected in order to transfer energy between each other as shown in Figure 3.10 in PowerFactory. Feeders that are distinguished as secondary feeders will be placed inside the SPP and the primary feeders will connect to the utility grid. The grid box also comprises of an auxiliary load that is usually used for lighting, protection equipment and cooling (air conditioners for inverters). The implementation of an auxiliary load for 7 x PTRs, it can be assumed that the apparent power drawn is 35 kVA with a power factor of 0.85 at a voltage of 1 p.u. at the busbar.

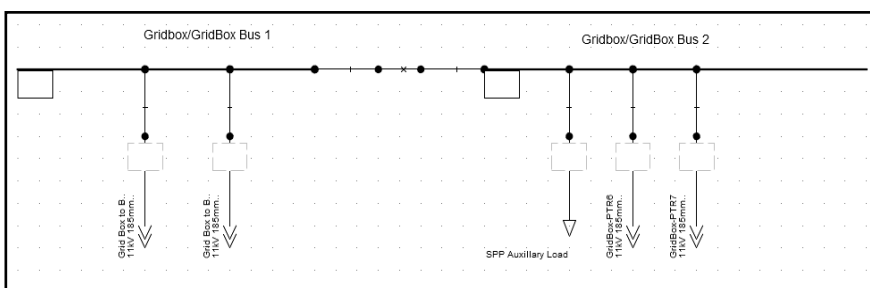


Figure 3.10: Grid box in PowerFactory as modelled in the network

3.1.6 Step-up transformers

For the conversion of voltage from 0.380 kV to 11 kV, the requirement of a transformer is necessary to perform the stepping up of the voltage. The inverter's will be connected to a three-winding transformer with a vector group of D0y11y11, which indicates that the transformer's medium voltage (MV) side is delta connected with a 0 ° rotation. On the star-connected LV side of the transformer the LV winding lags the MV winding by 30 ° and the rotation is 11 °, which will result in a -330 ° vector group notation (Rajput & Dheer, 2020).

As illustrated in Figure 3.11, the equivalent circuit of a three-winding autotransformer is exactly the same as the equivalent circuit of the three-winding transformer. It is possible to calculate the ratio between the primary voltage and the secondary voltage as from Equation (3.7) and Equation (3.8) shows the difference between the primary and secondary voltages (Volcko, et al., 2012).

$$P_{12} = \frac{U_1}{U_2} = \frac{N_C + N_S}{N_C} \quad (3.7)$$

$$P_{13} = \frac{U_1}{U_3} = \frac{N_C + N_S}{N_T} \quad (3.8)$$

The difference between primary and secondary voltage, and the difference between primary and tertiary voltage can therefore be used to measure the change in the number of turns of the common and serial winding (Volcko, et al., 2012).

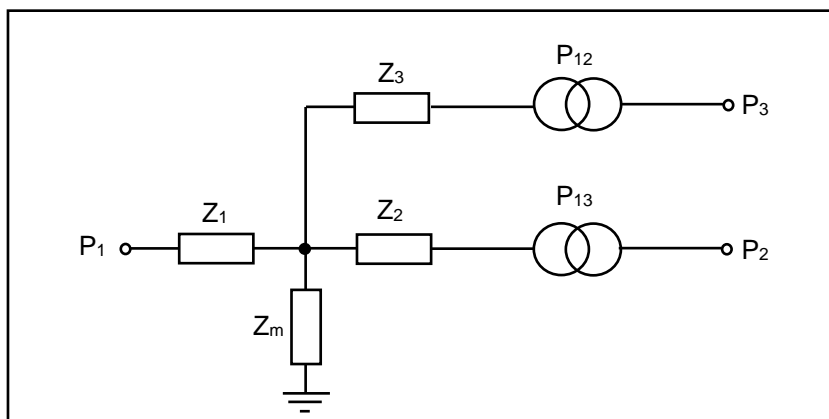


Figure 3.11: Three-winding equivalent circuit (Volcko, et al., 2012)

A substitute impedance of the primary, secondary, and tertiary windings, relating to the primary voltage, replaces the real impedances of the serial, common, and tertiary windings. In this case, there's no reason to derive the relationship between real impedances and substitute impedances. The system of three equations can be used to calculate the substitute

impedances of the transformer. Summarizing the two options Z_I and Z_J impedances, the following Equations (3.9) can be implemented for the calculations (Volcko, et al., 2012).

$$Z_I + Z_J = \frac{u_{kJ}}{100} \cdot \frac{U_{N1}^2}{S_N} \quad (3.9)$$

A circuit equivalent is formed by adding two optional resistances of its windings in Equation (3.10):

$$R_I + R_J = \Delta P_{KIJ} \cdot \frac{U_{N1}^2}{S_N^2} \quad (3.10)$$

Using the characteristics measured in the no-load test, it is possible to calculate the magnetizing impedance in Equation (3.11) and (3.12):

$$\frac{1}{Z_M} = \gamma_M = \frac{i_0}{100} \cdot \frac{S_N}{U_{N1}^2} \quad (3.11)$$

$$G_M = \frac{\Delta P_0}{U_{N1}^2} \quad (3.12)$$

Where, k is the constant primary voltage, U_{N1} represents the nominal terminal voltage, S_N denotes the nominal apparent power. γ_M represents the magnetizing admittance, Z_M is the magnetizing impedance and G_M is the magnetizing conductance (Volcko, et al., 2012).

In the same way as a delta-star-star connection, we can extend the analysis to all three-winding transformers including autotransformers, and to all transformers that have more than one winding regardless of how many circuits are considered. As an example, consider the case of a star-star-delta transformer with solidly earthed neutrals. According to Figure 3.12, the A, B, C, N and A' B' C' N' star primary winding (P and S) ends, and the T terminals on the delta tertiary winding (T) end are shown as a, b, c (Say & Laughton, 2003).

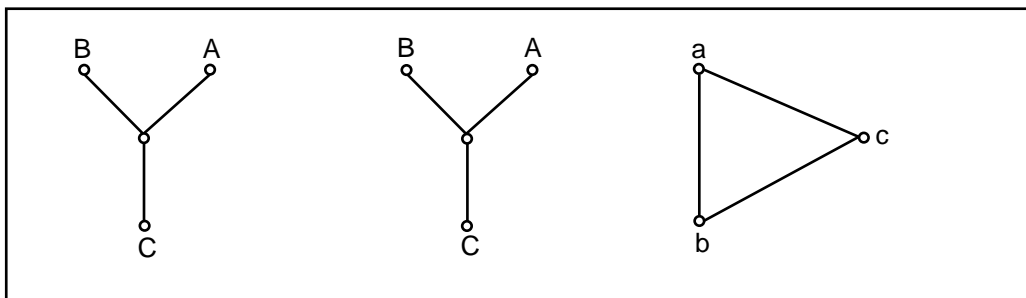


Figure 3.12: Three-winding transformer terminal markings (Say & Laughton, 2003)

From paralleling one star-star equivalent circuit and two star-delta equivalent circuits in turn, the assemble of a three-phase equivalent circuit can be achieved by implementing the short-circuit per unit admittances (γ_{PS} , γ_{PT} and γ_{ST}) of the two windings indicated by the subscripts. The circuit line diagram is complicated for convenient illustration, but the same convention will apply to identifying single-phase units by matching the parallel sides, $-A - N$ wit' $- ' N'$, $-A - N$ with $-c - b'$ $A' 'N'$ with $-c - b$, etc. In the connection Table 3.1 shown below the following Equations (3.13) – (3.15) will be used to calculate the corresponding admittance between the transformer winding (Say & Laughton, 2003).

$$\alpha = 1 + t_p \text{ p.u.} \quad (3.13)$$

$$\beta = 1 + t_s \text{ p.u.} \quad (3.14)$$

$$\gamma = \sqrt{(1 + t_T)} \text{ p.u.} \quad (3.15)$$

where, α represents the turns ratio of the winding P, β represents the turns ratio of the winding S, and γ represents the turns ratio of the winding T.

Table 3.1: Connection table for star-star-delta transformer (Say & Laughton, 2003)

Admittance	Between nodes
$(\gamma_{PS} + \gamma_{PT})/\alpha^2$	$N - A, N - B, -N - C$
$(\gamma_{PS} + \gamma_{ST})/\beta^2$	$N' - N', N' - B', N' - C'$
$\gamma_{PS}/\alpha/\beta$	$A - A', B - B', C - C'$
$-\gamma_{PS}/\alpha/\beta$	$N' - A, N' - B, N' - C, N' - A, N' - B, -' - C$
$(\gamma_{PT} + \gamma_{ST})/\gamma^2$	$a - b, b - c, -c - a$
$\gamma_{PT}/\alpha\gamma$	$A - c, B - a, -C - b$
$\gamma_{ST}/\beta\gamma$	$A' - c, B' - a, -' - b$
$-\gamma_{PT}/\alpha\gamma$	$A - b, B - c, -C - a$
$-\gamma_{ST}/\beta\gamma$	$A' - b, B' - c, -' - a$

There is a solid earth connection for the neutrals represented by N an' N'. In the case of two windings connected to two nodes on the same symmetrical lattice network, (e.g., a and b). The total admittance is the sum of the corresponding admittances between each of these two networks as shown in Equation (3.16) representing the nodes (Say & Laughton, 2003).

$$\frac{\gamma_{PT}}{\gamma^2} + \frac{\gamma_{ST}}{\gamma^2} = (\gamma_{PT} + \gamma_{ST})\gamma^2 \quad (3.16)$$

For the three-winding transformer in the network model, the utilization of a transformer to transform the voltage was selected in the “WECC Photovoltaic Templates” for solar PV power plant modelling and validation guideline. That is available in PowerFactory as seen in Appendix

B in Figure B.1 of the proposed base case model. As the inverters are connected to the three-winding transformers, the topology of the connection of the circuit is shown in Figure 3.13 for the simulation of the base case network model in PowerFactory. The PV arrays are connected to a central inverter station and the inverter stations are in return connected to the three-winding transformer.

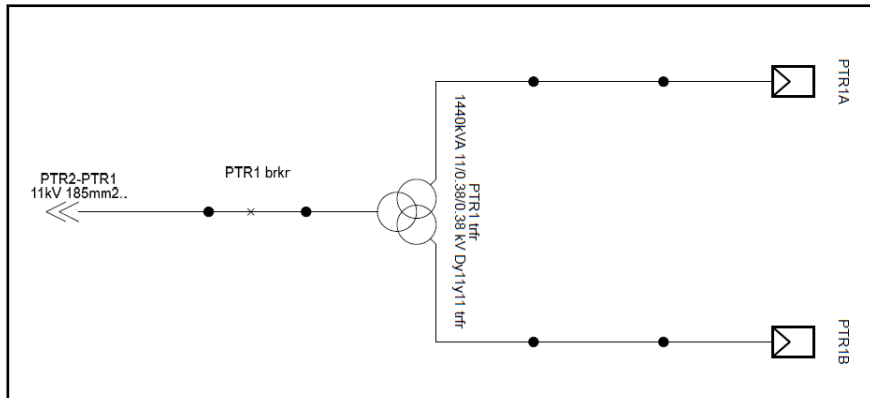


Figure 3.13: Three-winding transformer simulation in network model

To accommodate the 2 x 720 kVA inverters, the transformer windings shall be able to transfer a total apparent power rating of 1440 kVA at the PTR. The HV winding of PTR 6 and 7 will be terminated at the grid box and PTR 1 to 5 will have the primary sides connected between each other depending on what circuit the PTRs are connected to. The transformers are set to operate at a maximum loading of 100% and the nominal tap position that the tap changer is set on is tap position number 3. For the tap position of the SPP for the SAREGC requirements the POC busbar voltage can be set to 1.09 p.u. of the nominal voltage of 11000 V, the simple calculation of $V_1/V_2 = N_1/N_2$ is utilised. The V_1 value is assumed to be $1.035 \text{ p.u.} \times 11000 = 11385 \text{ V}$ at the three-winding transformer. Therefore, the reason for the assumption is that the SPP and POC are separated by an 815 m underground cable and the underground cable will be subjected to voltage drops. Due to the long distances of the utility and SPP a safe assumption would be to implement the second tap position as illustrated in Figure 3.14 (IEEE Std C57.159, 2016).

A step-up transformer modelling and later the selection in a SPP is generally a complex task, as several variables are involved, depending on the transformer size, such as the initial system cost, energy losses caused by the transformer, energy storage system efficiency, and any network instability. Specifically, the selection of the transformer identifies a general methodology for achieving a suitable sizing of step-up transformers for grid-connected SPPs, which may be directly connected to the utility grid or may be equipped with energy storage systems. Many transformer sizes for PV plants are selected using deterministic approaches, resulting in oversized designs (Testa, et al., 2012). Furthermore, the transformers are modelled

with the following parameters in PowerFactory as shown in Appendix B in Table B.5 according to the inverter sizing and requirements for specifically on voltage compliance requirements.

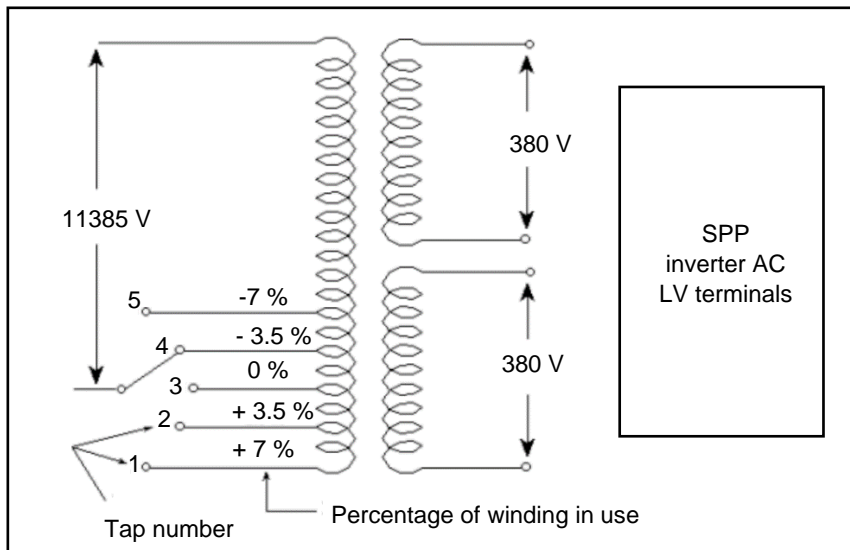


Figure 3.14: Tap positions for the SPP modelling

The values are obtained from the generic WECC for solar PV power plant modelling and validation guideline in PowerFactory. The rest of the values are obtained from IEEE Std C159-2016 and as per relevant SAREGC requirements for the compliance studies in a SPP. The element used in the base case of the model for the simulation is the Elm.Tr, which can be set up for steady-state analysis for grid code compliance studies.

3.1.7 Inverter model

The inverter control strategies, as mentioned in chapter 2, should control the active and reactive power generation to support and provide remedial action schemes that improve system stability since the SPP is subjected to the SAREGC compliance requirements. An inverter controller has been developed specifically for this purpose and implemented in the PowerFactory software DIgSILENT simulation language (DSL) environment.

Under the following sub-sections, the explanations will follow on how the PowerFactory inverter control is implemented in a composite frame and composite model (ElmComp), which includes several components as illustrated in Figure 3.15. The composite frame and composite model had modifications done in the DSL and DPL and is documented in Appendix B from Figure B.2 – B.7 to perform the SAREGC requirements. It is important to mention that for the steady-state modelling and simulation of the SPP inverter in PowerFactory, the element defined as ElmGenstat, which is a static generator defined as a 720 kVA “Photovoltaic” in the plant

category as illustrated in Appendix B in Figure B.8. The reason for this selection is to implement control functionalities for SAREGC requirements.

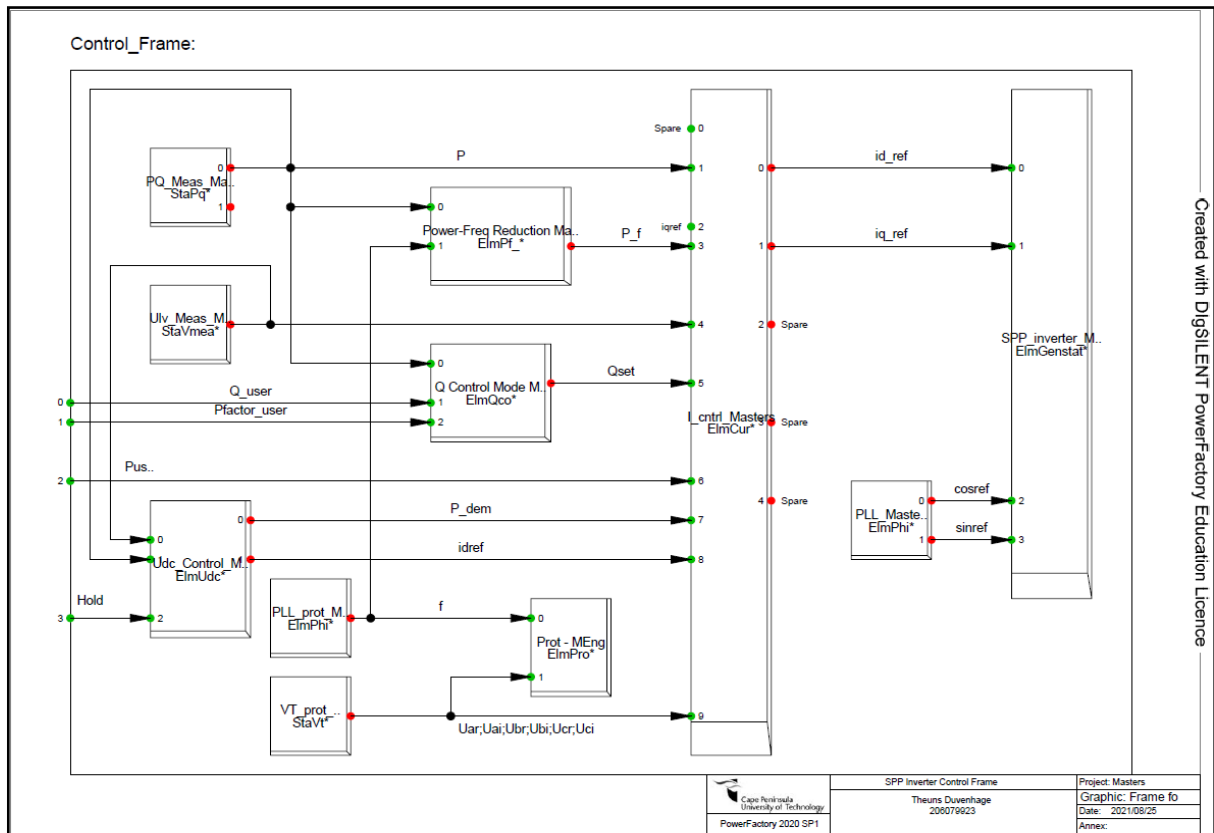


Figure 3.15: Composite control frame of a SPP modelled in PowerFactory

In PowerFactory the control frame will be discussed in further detail to document the measurement of the PQ measurements and LV voltage measurement with the control elements represented by voltage control, Q control and cos phi control (Chmielewski, et al., 2021).

The phase-locked loops will be used for protection of the inverter by means of frequency measurement and control by phase shift inputs of the inverter in terms of the voltage to be supplied as illustrated in Appendix B in Figure B.9 (Gonzalez-Longatt, et al., 2021)

3.3.7.1 PQ measurement

A PQ measurement is used in Figure 3.16 to measure the amount of active and reactive power (P, Q) traveling through the power supply system. The measured power is compared with reference values (P_{ref} and Q_{ref}) to control the P_{md} and P_{mq} values.

The following Equations (3.17) and (3.18) are defined to determine the P_{md} and P_{mq} for the control values (Khoshkhoo, et al., 2021)

$$P_{md} = \frac{2}{V_{dc}}(u_d - L\omega(t)i_q + V_{sd}) \quad (3.17)$$

$$P_{mq} = \frac{2}{V_{dc}}(u_q - L\omega(t)i_d + V_{sq}) \quad (3.18)$$

Where L is the equivalent inductance [H] of the transformer and reactor, which the inverter is connected to the utility with. The AC system voltage at the utility side is represented by V_s and the specific voltage is transformed into dq-frame components shown as V_{sd} and V_{sq} of the network model. V_{dc} is denoted as the DC-side voltage on the inverter LV terminal connections and P_m is the pulse width modulation indications of the DC-side of the inverters that is also transformed into dq-frame components P_{md} and P_{mq} of the control frame. P_m is controlled by i_d and i_q references between the current controller and inverter, u_d and u_q are the new inputs for control to ensure compliance (Khoshkhoo, et al., 2021).

3.3.7.2 Phase-locked loop

According to Figure 3.15, in the AC portion of the inverter control frame, the PLL element (ElmPhi) of the SPP inverters voltage and current requires to be transformed to a dq-frame from the standard abc-frame. The PLL element is utilised to perform the measurement of the AC portion to calculate the voltage angle that is linked to $\sin(\varphi)$ reference and $\cos(\varphi)$ reference and the system frequency (F_{meas}). The F_{meas} is calculated by implementing Equation (3.19) in the network model (Khoshkhoo, et al., 2021).

$$F_{meas} = \omega/2\pi \quad (3.19)$$

3.3.7.3 Current measurement

A model for measuring the current that passes through an inverter's AC side is known as a current measurement model. As a result of this model, there are two outputs namely, i_r and i_i , which indicate the real and imaginary parts of the current measured in the network model of the SPP.

3.3.7.4 AC bus voltage measurement

This voltage measurement model illustrates the voltage measurement of the AC bus according to Figure 3.15, which shows the voltage measurement of the AC bus. There are two outputs for this model u_r and u_i which are the real and imaginary parts of the voltage generated by this AC bus. When a system exhibits voltage instability, at least one feeder or bus has increase in Q and a V magnitude that declines with the at the same bus or feeder. It is usually the power

flow equations or their modifications that are used to analyse voltage the AC bus voltage measurement in a network model for base case scenarios. A frame controller is presented in the literature for calculating voltage at different buses/feeders in a SPP network.

3.3.7.5 dq transformation

In this component, voltage and current are transformed from abc- to dq-frame using the angle of the AC bus voltage (i.e. $\cos(\varphi)$ and $\sin(\varphi)$) as shown in Figure 3.16. As a result of initializing and implementing this model, the following DSL code is used:

```
inc(vsd)=(ur*cosphi+ui*sinphi)*sqrt(2/3)      !1
inc(vsq)=(-ur*sinphi+ui*cosphi)*sqrt(2/3)     !2
inc(id)=- (ir*cosphi+ii*sinphi)*sqrt(2)       !3
inc(iq)=- (-ir*sinphi+ii*cosphi)*sqrt(2)      !4
vsd=(ur*cosphi+ui*sinphi)*sqrt(2/3)          !5
vsq=(-ur*sinphi+ui*cosphi)*sqrt(2/3)         !6
id=- (ir*cosphi+ii*sinphi)*sqrt(2)           !7
iq=- (-ir*sinphi+ii*cosphi)*sqrt(2)         !8
```

Figure 3.16: DSL for dq-transformation of voltage and current

The voltage measurement is based on the RMS value of line-to-line voltage (u_r, u_i). Therefore, in line 5 and 6 the coefficient of $\sqrt{2/3}$ is used to calculate the line-to-ground voltage amplitude and then the script is used to perform the V_{sd} and V_{sq} calculations. In the Equation (3.20) the line-to-ground voltage amplitude can be calculated and is represented by V_{sm} . Similarly, the coefficient of $\sqrt{2}$ in line 7 and 8 can be used to calculate i_d and i_q from the RMS current measurement of i_r and i_i (Khoshkhoo, et al., 2021).

$$V_{sm}e^{j\omega} = \vec{V}_s(t) = \begin{bmatrix} V_{sa} \\ V_{sb} \\ V_{sc} \end{bmatrix} = \begin{bmatrix} V_{sm}\cos(\omega) \\ V_{sm}\cos(\omega - 120) \\ V_{sm}\cos(\omega + 120) \end{bmatrix} \quad (3.20)$$

Where, V_s is the abc-transform values of the AC system voltage from the inverter of the network model and $\varphi = \omega t + \varphi_0$.

3.3.7.6 Q control

There are several factors that determine how much reactive power can be injected into the utility grid, such as the control approach used, the amount of active power generated and the size of the SPP inverter. Therefore, the capacity of reactive power is constrained by the power production of active power. An inverter's reactive power capacity can be seen as a result of both the inverter's property and the impact of the subsystems of the SPP. Therefore, the inverter's-Q trait corresponds to the same for the inverters, but it focuses on the capacitive side.

Since the SPP needs to be capable of acquiring reactive power from the utility grid, the maximum amount of reactive power resources can be utilized while operating the SPP. Various equipment like static Var compensator (STATCOM) or capacitor banks can be utilized for optimizing the reactive power requirements among inverters within the SPP (Marzbali, et al., 2017). As illustrated in Figure 3.17, in Q control mode, the activation of Q is represented, which differentiates between the reactive power measurement and the reactive input. The values are compared in an ideal delay function with a summation point to average out the discrepancy between the two components. When the Q control frame receives a $Q_{activate}$ input from Q_a, Q_{in} and Q_{meas_in} , the additional equations in the DSL script for the measurement is provided as $Q_{set2} = \text{select}(Q_{act} = 1, Q_{in}, Q_{meas_in})$ and $Q_{set} = \text{delay}(Q_{set2}, 0.0)$.

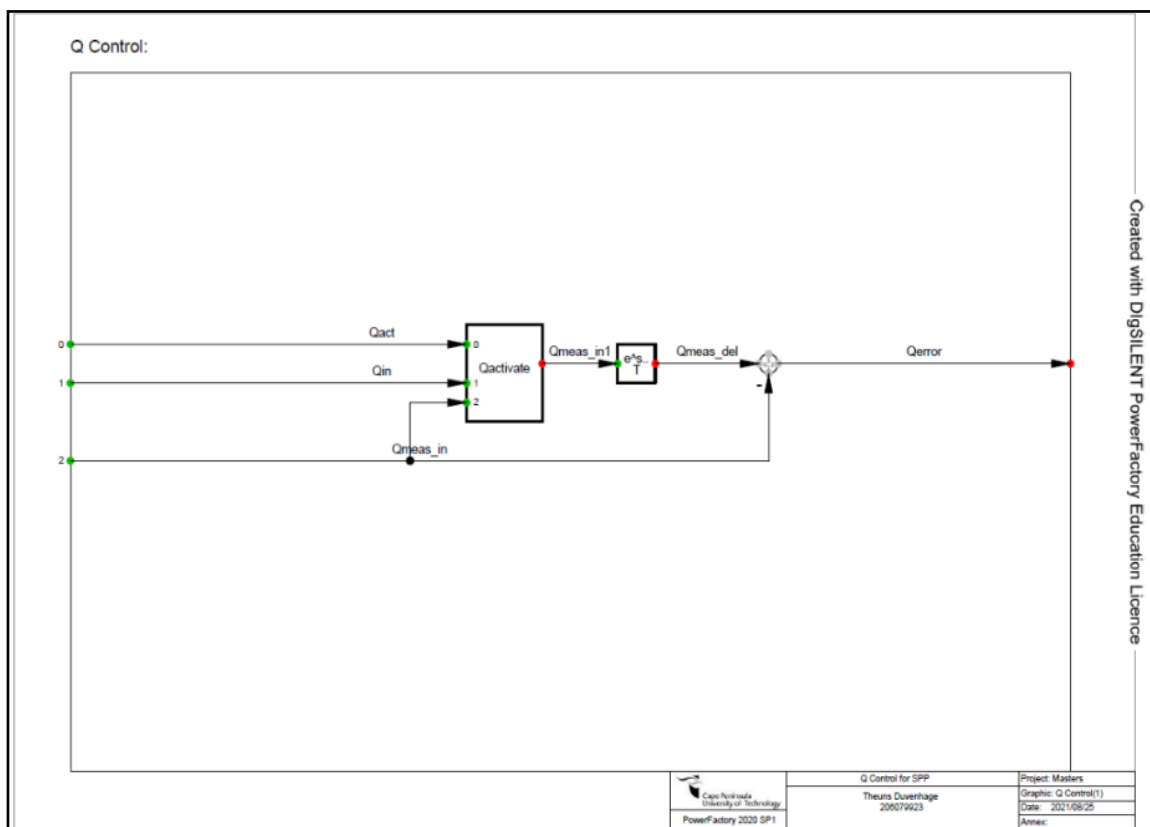


Figure 3.17: Control frame for Q control functions

For the simulations in PowerFactory, the complete SPP will be sit in Q control with the inverter's control mode also set in Q control mode as illustrated in Figure 3.18. On the energy source side, the inverter determines the maximum power extraction function, while on the grid side, the inverter carries out the control function for the grid interface.

Inverters on the grid can control both the active and reactive voltage according to the supervision that is given by the SO. In the case of grid connection, the SPP has both PV- and PQ-mode inverters that can work as per configuration. In the PQ mode, the PV system reactive

power is controlled at a fixed value or using a demand that comes from PPC, whereas the active power continues to be produced in accordance with the extraction of maximum power rule. In PV mode, the SPP system maintains the voltage of the inverter at a desired value by providing voltage control. There is a limit to the controllability of voltage of the SPP, because the allowed reactive power or the reactive power of a SPP, is determined by the active power output and the power factor of the grid-tied inverters in the SPP. Calculating the reactive power can be done by applying Equation (3.21).

$$Q_{SPP} = P_{SPP} \times \tan(\cos^{-1} PF_{SPP}) \quad (3.21)$$

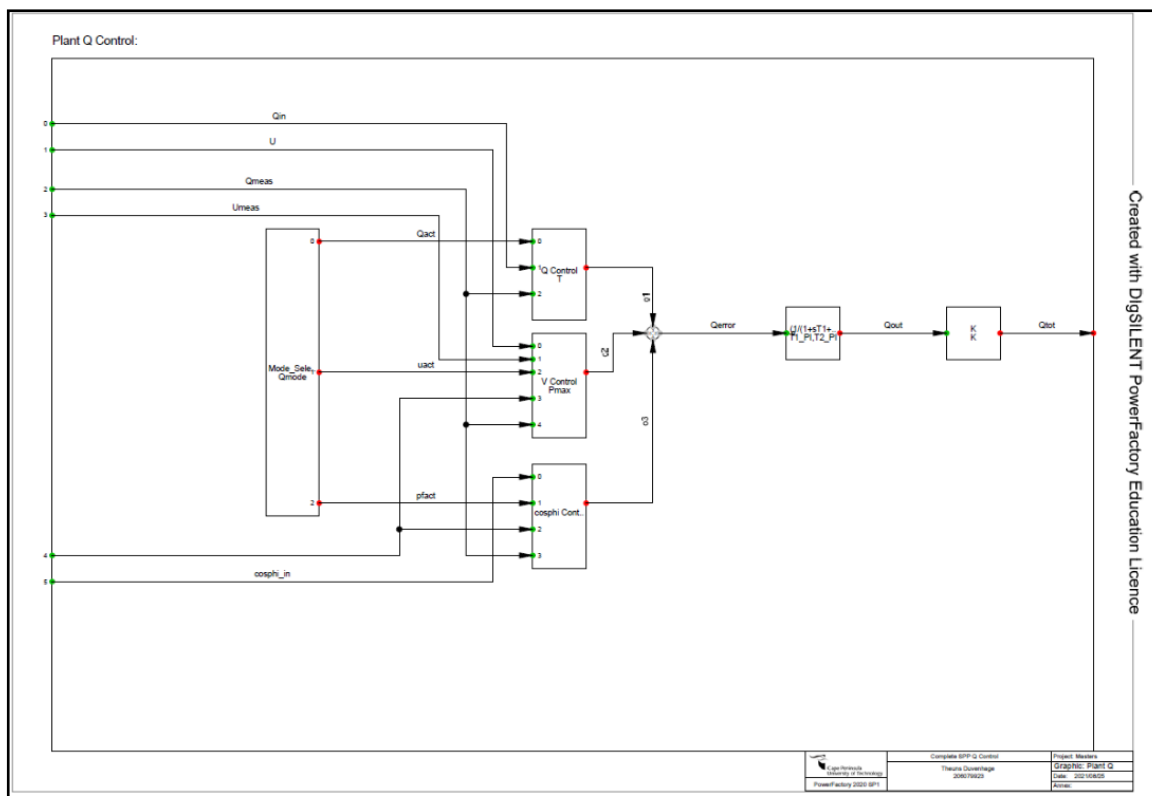


Figure 3.18: Q control for a SPP

3.3.7.7 Voltage control

During automatic voltage control, the measured voltage and reference voltage are compared, and reactive power is generated according to the difference. Signals U_{meas} , P_{meas} and Q_{meas} is introduced as a compensation for the transformer impedance because the voltage is measured on the MV side of the transformer. With the slope coefficient, the maximum permissible error between the reference voltage and the voltage measured is determined.

In addition to compensating for the reactive power that is generated by the SPP system, the compensation block also makes it possible to share the reactive power equally among other

voltage support elements that are connected in parallel (synchronous machine, wind turbine, etc.).

As a result, we get the following voltage error in Equation (3.22) (Pachanapan, 2021).

$$\Delta V = V_{ref} - V_{meas} - U_{meas} P_{meas} Q_{meas} \quad (3.22)$$

The voltage at the POC can be controlled and regulated by the capability of the voltage control of the SPP inverter. This feature is especially useful for a weak grid, in which there is a significant amount of resistance and inductance in the line, causing significant voltage fluctuations with changes in the power flow. By altering I_d , this controller modulates the AC voltage level (V_{ac}) at the common bus to achieve the reference value. Accordingly, what this means is that the controller is taking steps to control the converter so that it generates a sufficient amount of reactive power to match the given reference voltage ($V_{ac,ref}$). With the SPP, the voltage needs to be well controlled to maintain a balance of power between all nodes connected in the network. As illustrated in Figure 3.19, the framework for implementing the voltage controller is determined by control function inputs from the measured voltage and actual voltages (Gonzalez-Longatt, et al., 2014). The input in the composite frame Qf(U) terminal number 3 is where the reactive power input measurement is added to produce Quset.

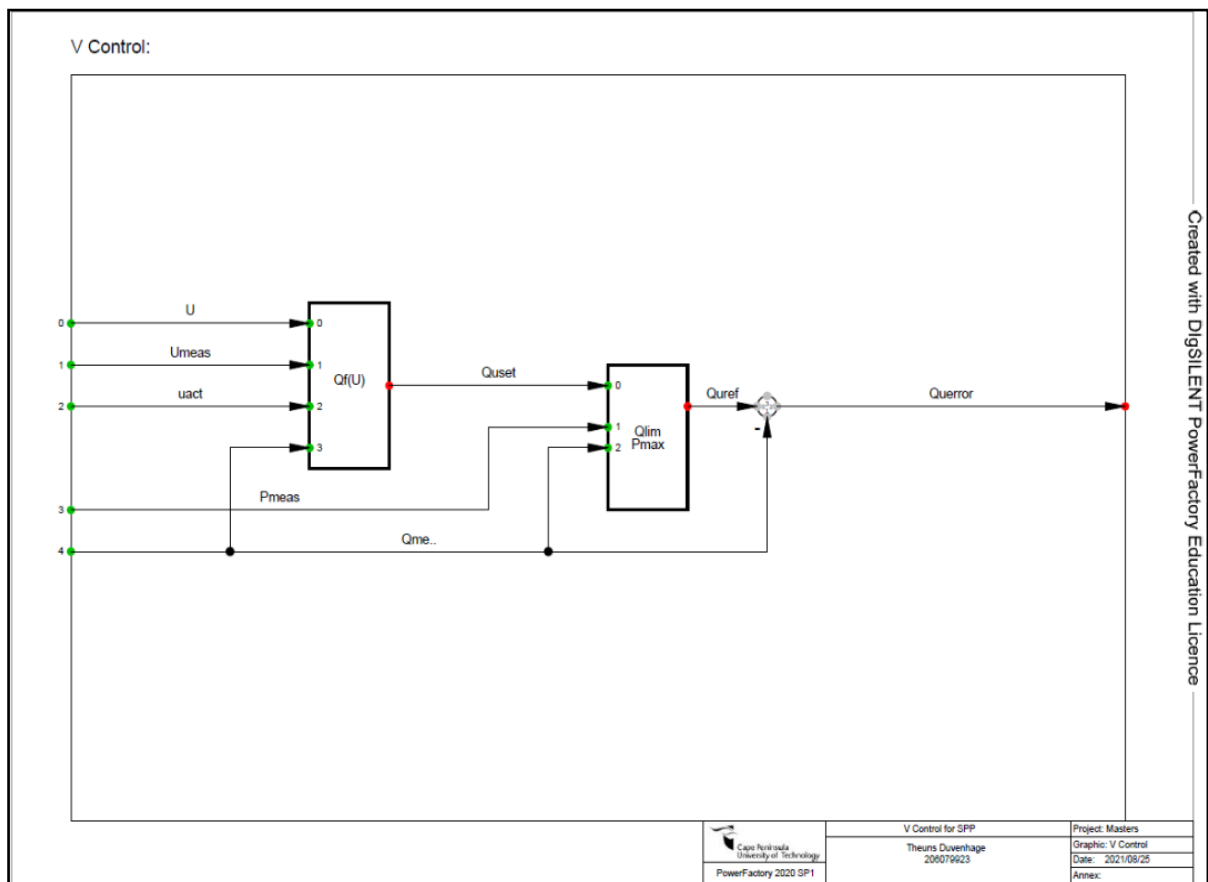


Figure 3.19: V control for a SPP

3.4 Studies to be conducted in steady-state analysis

For the steady-state requirements, the SAREGC compliance studies will be followed as set out in the previous chapters. The explanation will seek deeper explanations on how the model is created and specifically on how the simulations are carried out for the desired results to be shown for a grid-connected SPP.

An electromechanical, control, and thermal device is considered as a dynamic device in a time domain when the balanced RMS simulation is performed. Some components require dynamic capabilities to perform the required steady-state simulations. It allows for the simulation of transmission lines and other networks from a midterm and long-term perspective under balanced network conditions, using a continuous-state symmetrical representation of the voltages and currents that is considered only for the fundamental components of voltage and currents. Using PowerFactory, to implement a SPP for transient research using RMS data.

The following steps need to be followed when using the PowerFactory software (Pachanapan, 2021):

- Step 1: Build a test system, which includes generators, transformers, lines, inverters, and loads for testing the network model, moreover, the objecting type of each element of the network needs to be assigned along with input parameters;
- Step 2: Dynamic models should be created for SPP grid-tied inverters that are controllable devices, for example composite models and common models;
- Step 3: The dynamic models can be enhanced by adding network elements, common models, measurement devices, etc;
- Step 4: Identify the initial values of all internal variables in the network model for the base case and the initial conditions of all connected SPP inverters and controllers as well as any other transient models after the system has been started;
- Step 5: Determining the events that will be part of the simulation;
- Step 6: Defining the variables to be used to determine the result;
- Step 7: Run the simulation and create the plots based on the simulation results.

Dynamic simulation of the frequency and voltage controllers in the SPP inverters is required to demonstrate how they respond dynamically as described in steps 2 and 3, respectively. Using the PowerFactory tool set, Dynamic modelling is made flexible by the fact that any model of any type can be built with the same set of tools. A set of nested blocks is automatically converted to a set of DSL equations based on the model equations written in the DSL. Following the DSL equations, the RMS equations are parsed and interpreted during the simulation. Dynamic modelling works through an object-oriented approach that enforces strict

distinctions between libraries (types) and grids (elements). The library contains type objects (e.g. composite frame and model definitions) the elements of which are referenced (i.e. composite models and common models). An illustration of the dynamic modelling block diagram is given in Figure 3.20 (Pachanapan, 2021).

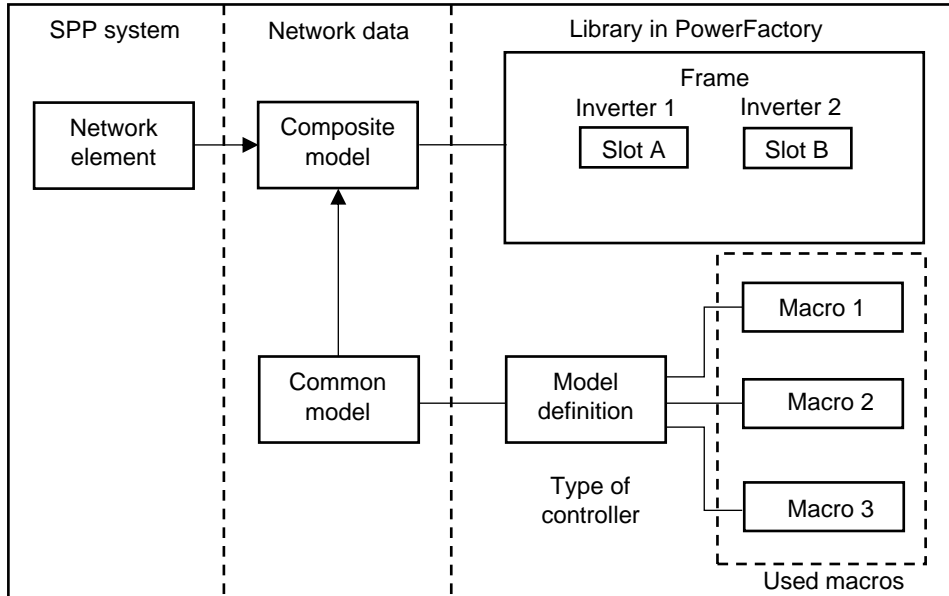


Figure 3.20: Modelling block diagram for PowerFactory (Pachanapan, 2021)

There are various types of composite models, which are grid objects that represent the complete dynamics of a system. It enables the composite frame to link up to actual network components, measurement devices, and system models that are common to all DSL systems. An overview of the composite frame shows the interconnections between the slots. There are different types of slots that are indicated by the type of objects that should be assigned to each slot.

Model definitions consist of equations and/or diagrams to define the transfer function in a dynamic model. Additionally, block diagrams are also capable of being built in the form of equations, which can be constructed in the form of objects, which is the block definition (BlkDef). In addition, the DSL common model will enable the SPP inverter with specific properties to be linked to the definition of the model representing the operating procedures and capabilities of the inverter. An example of this is shown as described in Figure 3.22, where an electric frame represents the connection of PWM converters (Slot A) to an electric controller (Slot B). The frame is used to house two inverters used in a SPP (e.g. network elements 1 and 2), these inverters can also be used as grid-tied inverters in a SPP system. The controllers for the different inverters are programmed so that each inverter has the same local parameter settings, but if the inverters are made to use the same controller type (that is, the same model definition), then two different types of common models are created (Pachanapan, 2021).

Choosing a dynamic model in PowerFactory is described in the DSL advanced tutorial of the user manual as follows (DlG SILENT GmbH, 2020):

- i) Modelling a system requires examining its structure and how various components can be separated and modelled separately;
- ii) Identify the slots that are interconnected with a composite frame;
- iii) Assign appropriate initial conditions to each model definition;
- iv) Using the composite model, fill the grid slots with the relevant grid elements, including the common model, an existing model, and a measurement device;
- v) Check that the model is accurate and complete.

The flowchart for SAREGC studies and setting up a network model is illustrated in Figure 3.21 on the grid code compliance studies and requirements. Modelling and simulation processes in the flow chart is for steady-state analysis for a network model assigned for SPP performance connected to a utility grid.

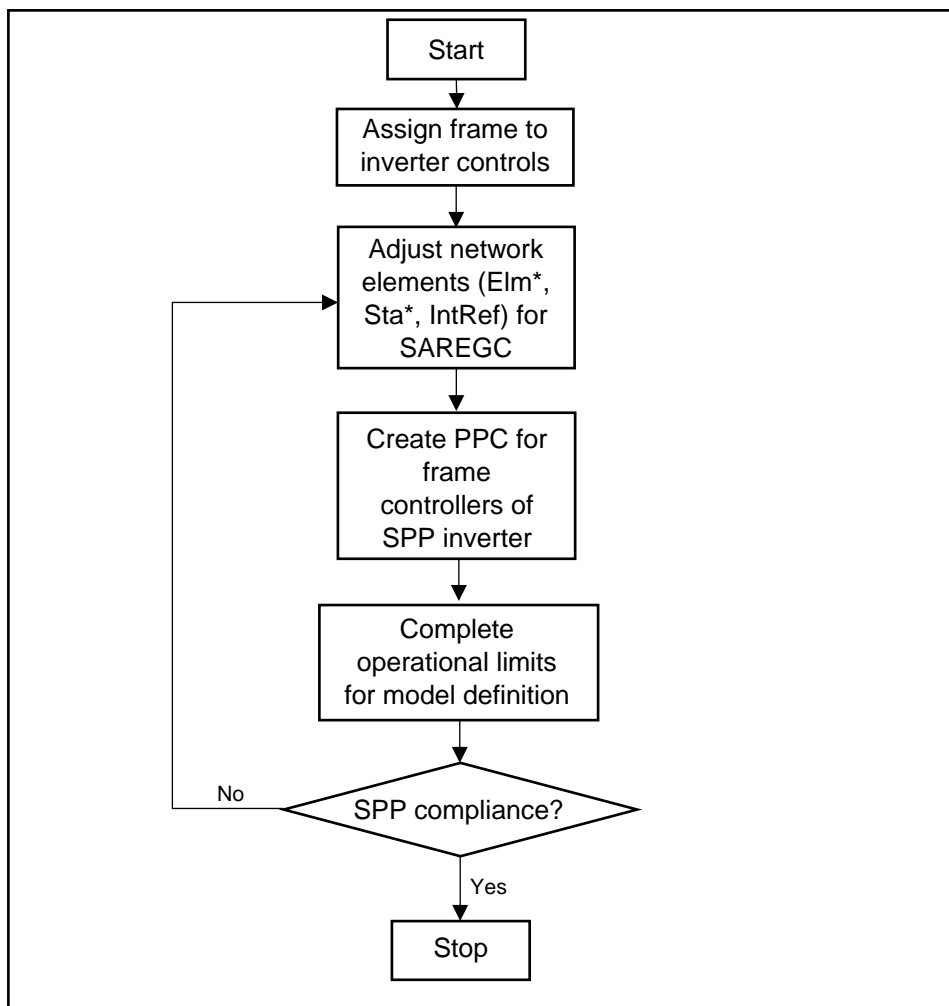


Figure 3.21: Flowchart overview of creating a steady-state network model

3.4.1 Reactive capability simulation

Besides determining the strength of the grid in the joint connection point of the place where the inverters are installed, the reactive power of inverters in SPPs (generation or consumption) is also important and necessary. Measurements related to the output of the inverter can be used to determine the reactive power (or power factor). Reactive power consumption is determined by a function of active power generation in prevailing types of inverters. In nominal generation, their coefficient of power differs from a lagging to a leading value based on the size and type of inverter design. Through the connection of a capacitor bank to the SPP, it is possible to reach the coefficient of unity power factor in the event of non-compliance (Effatnejad, et al., 2017).

By assigning each inverter in the SPP network model a reactive power capability as illustrated in Appendix B in Figure B.10, the study can continue with the illustration of the reactive power curve shown in the SAREGC and in chapter 2. The inverters are setup to provide a nominal apparent power of 720 kVA (as shown in sections 3.3.6 and 3.3.7) with a power factor of 0.95. These values will have an impact on the Q capability as the values are interdependent in terms of generation from the SPP. By applying the power factor to the nominal apparent power, the active operational limits and active power rating of the SPP inverters have changed to 684 kW as shown in Appendix B in Figure B.10. Furthermore, the configuration of the Q capability was achieved by assigning a voltage level p.u. and a setpoint for the apparent power as described by the SAREGC and is shown in Appendix B in Table B.6. The setpoints limits in Table B.6 will be used to provide the Q capability curve for the matrix of the Q_{\max} p.u. and Q_{\min} p.u. as in Appendix B shown in Table B.7A, Table B.7B, B.8A and B.8B for the assigned SPP inverters of the network model reactive capability curve. In Appendix B in Figure B.11 the Q capability curve is shown with the values implemented to perform according to IEEE, NRS and WECC standards. Once all the SPPs inverter spectrum of capability in reactive power are implemented and assigned to each inverter in the software, there should be a way to measure the compliance of the 9 MW SPP. A graph is created in PowerFactory through the utilisation of a script function with DSL to determine if the SPP has not contributed to any non-compliance factors in reactive power capability. This can be done by creating a new frame diagram in the software and assigning the input parameters to the SAREGC and defining the external objects values to be executed in the scripts. For this study the objects that is going to be defined is the POC as the point where the required reactive power should be measured, the PPC as the external controller to the inverters of the SPP.

Lastly the script is inserter in the object functionality to implement the requirements as shown in Table B.6. The illustration in Figure 3.22 of a reactive power capability graph is created and

is shown in blue for a category B plant. For the reactive power requirement of the 9 MW SPP, the Q/P_n is required to have an operating value between 0.228 (leading and lagging) at a PF range between 0.975 (leading and lagging) as per SAREGC guidance and as shown in chapter 2. Further the reactive power requirement can be calculated from instituting the values previously described and is concluded by implementing Equation (3.23).

$$Q_{capability\ requirement} = P \times Q/P_n \quad (3.23)$$

Where, P is the MEC of the SPP and for this study will have a value equal to 9 MW and Q/P_n is provided in the SAREGC as the value 0.228. By implement Equation (3.23), the reactive power capability requirement can be calculated as below:

$$Q_{capability\ requirement} = 9\ MW \times 0.228 = 2.052\ MVar$$

Confirmation in Figure 3.22 is obtained from PowerFactory that the value of $Q = 2.052\ MVar$ matches the requirements as per the calculation above.

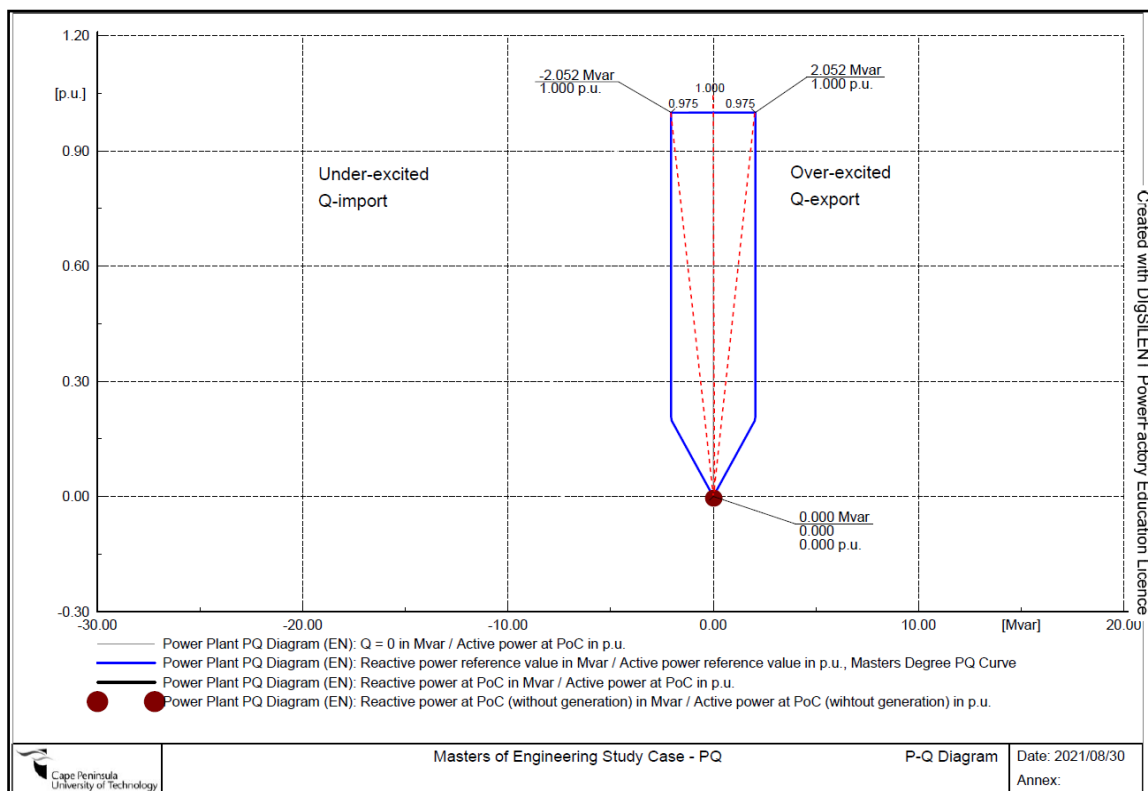


Figure 3.22: Q capability curve in PowerFactory according to the SAREGC

Therefore, the simulation will have to prove that the SPP is grid code compliance at the POC by providing a 100% MEC of 9 MW at a PF of 0.975 leading (inductive) and a 100% MEC of 9 MW at a PF of 0.975 lagging (capacitive) as shown in Figure 3.22. For the specific plant, the

studies to be performed will require P at the POC to be set to 5 %, 20% and 100%, whilst Q to 5 % and 22.8% for Q export (inject) and Q import (absorb). In the flowchart illustrated in Figure 3.23, the main processes are implemented to indicate the accurate procedure in PowerFactory to perform studies to indicate if non-compliance issues might arise if the SPP does not have the ability to perform within SAREGC specifications.

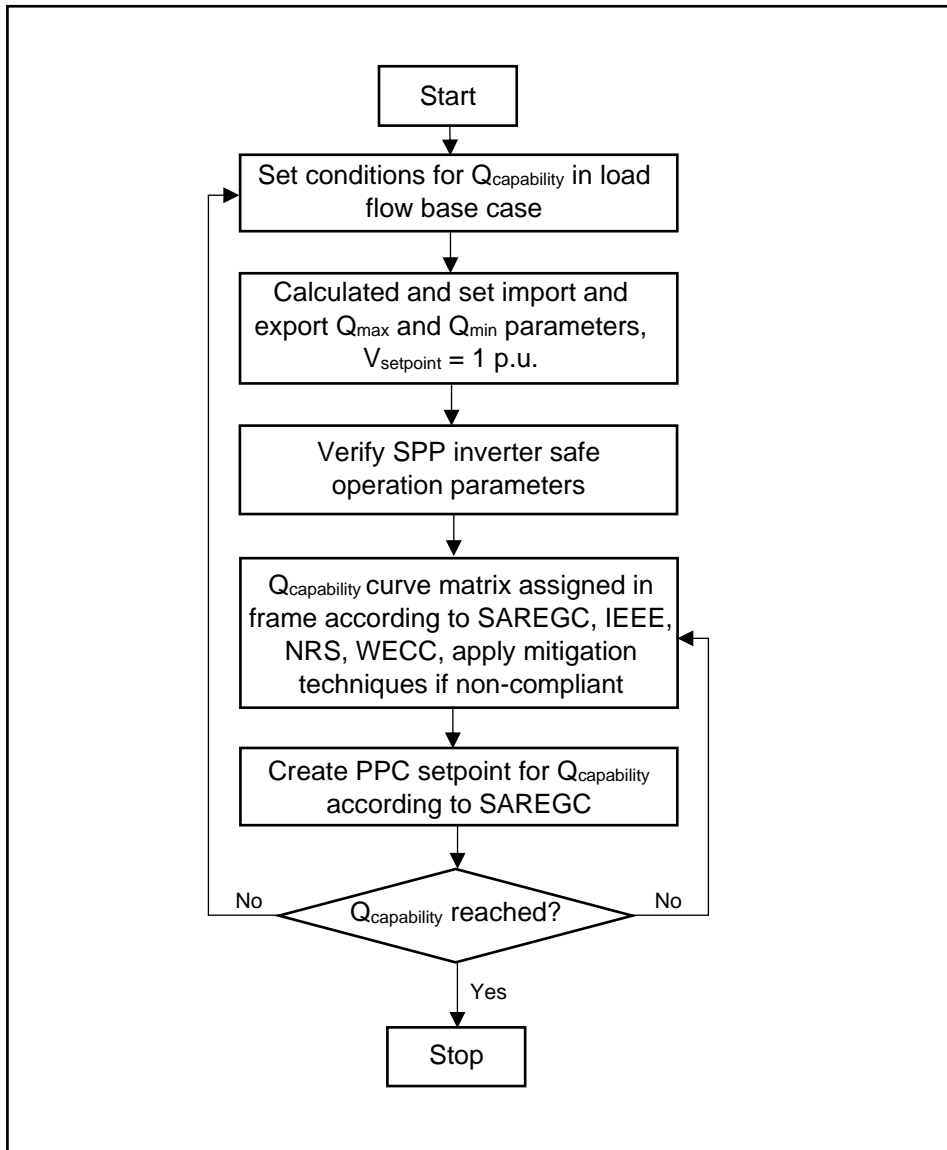


Figure 3.23: $Q_{\text{capability}}$ assessment flowchart

3.4.2 Voltage capability requirements simulation

When determining the behaviour of the voltage at the POC, reactive power requirements can assist and enhance the quality of power delivered to the utility network. Reactive power is absorbed by or produced by the inverters that is represented in the network model starting from the SPP subsystems. Grid-connected utilities have a relationship with the reactive power injections or absorptions in terms of voltage compliance with the grid. Maintaining the voltage capability requirements at the POC and distributing active power throughout the utility network

require reactive power, the voltage will drop when the level of reactive power is below the level that is considered acceptable in the network performance. If the voltage at the POC is not sufficient to supply the necessary power to the loads, the power system can become unstable and will provide non-compliance issues to the SO and IPP. In a power system, it is essential to study reactive power flow in the network model since some SPP equipment is dependent on these factors. It is imperative to understand that the amount of reactive power consumed by the electrical equipment will depend on the phase angle between current and voltage. A voltage adjustment can be performed by using reactive power flow control on a continuous basis, which is used as a primary way to regulate voltage, or it can be done in two steps, which is used as a secondary method of adjustment. Within the PQ availability diagram, voltage adjustment is based on the capability of the SPP inverter units to absorb and inject reactive power (Iorgulescu & Ursu, 2017).

For the voltage capability study, the voltage at the POC was adjusted between 1.1 p.u. to 0.9 p.u., whilst maintaining maximum farm output (9 MW). The inverters were set to voltage control, to check the power factor at the POC. The power factor was then checked against the requirements as illustrated in Figure 2.27 in chapter 2, this is to ensure the SPP can operate at all voltages and power factors as required. The 0.38 kV to 11 kV step-up transformers were on fixed nominal tap. Conditions of the SPP will be checked as per requirements from the SAREGC and Table 3.2 generated for the simulations to prove compliance or indicate non-compliance in the network.

Table 3.2: Voltage capability requirements in PowerFactory

Study point	Real Power (% of Pmax)	Voltage at the POC (p.u.)	Required Q at POC (% of Pmax)	Required Q at POC (MVar)
1	P = 100%	1.1	Q = 22.8% import	2.052
2	P = 100%	1.0	Q = 22.8% import	2.052
3	P = 100%	0.9	Q = 0%	0
4	P = 100%	1.1	Q = 0%	0
5	P = 100%	1.0	Q = 22.8% export	2.052
6	P = 100%	0.9	Q = 22.8% export	2.052

As per the benchmarked SPP inverter network model, the SPP inverters can operate between 0.8 p.u. and 1.2 p.u. in the power system model. Once all the operational requirements are implemented in the PowerFactory software according to the SAREGC, the V-Q diagram can be created by implementing DSL script for the performance at the POC. Objects to be defined for this study include the POC, the point at which the reactive power requirement will be determined as the voltage p.u. value is raised or lowered and the controllers external to the SPP inverters such as the PPC. The voltage compliance graph shown in Figure 3.24 indicates the six points that the simulation will focus on and the most important compliance will be the

setup for a 1.1 p.u. and 0.9 p.u. voltage value. The SPP should import a Q value of 2.052MVar and export a Q value of 2.052MVar for 1.1 p.u and 0.9 p.u., respectively.

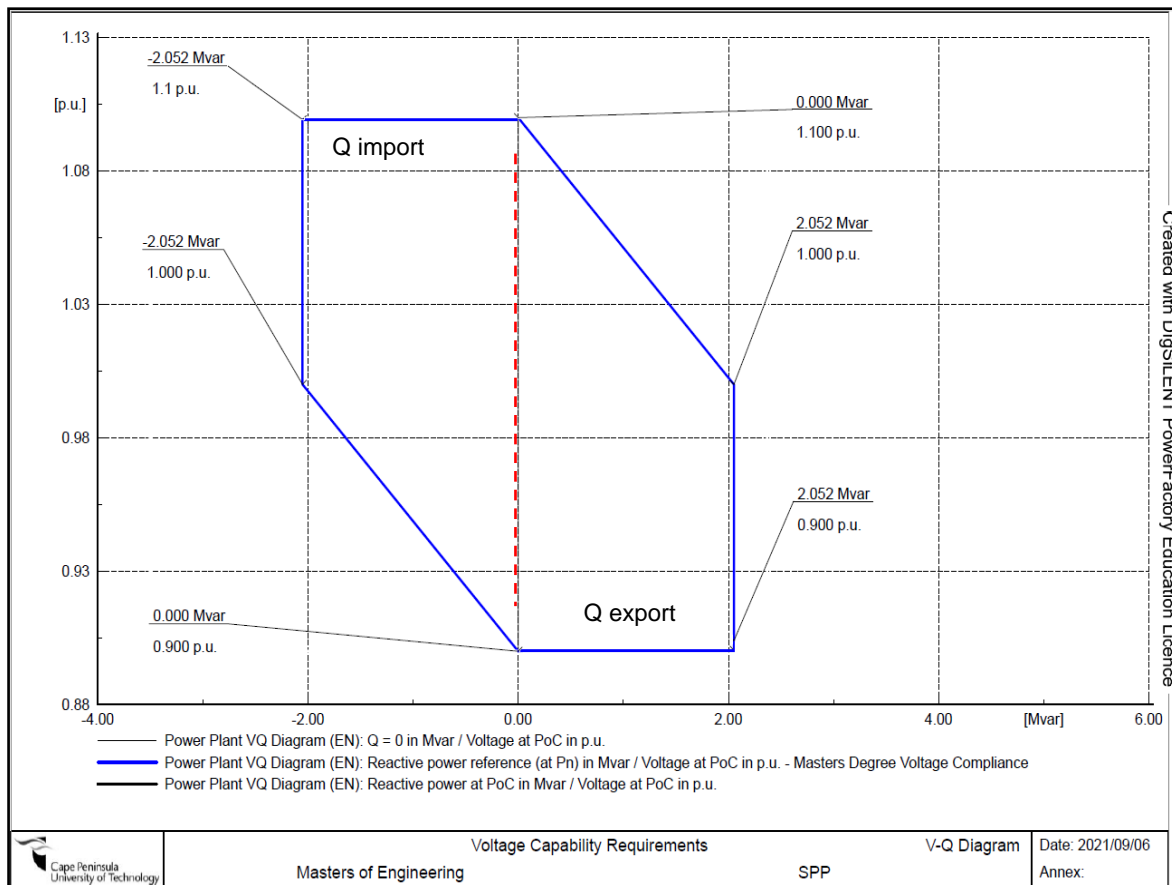


Figure 3.24: Voltage capability diagram in PowerFactory according to the SAREGC

In the voltage capability diagram indicated as a blue diagram as illustrated in the above Figure 3.24, the requirements of a known Q import value and a known Q export value related to the voltage p.u. of the SPP should not create any voltage violations at the POC. The matrix for the voltage capability diagram is provided in the element (IntMat) of PowerFactory and is shown in Appendix B in Table B.9, which comprise of the voltage p.u., Q_{min} in MVar and Q_{max} in MVar.

3.4.3 Fault level study simulation

As the fault levels and information at the POC is represented by the 11 kV busbar in the simulation network model, the information was discussed in section 3.3.1 where details of the user defined values were implemented. The values to be inserted in PowerFactory that is utilised for the fault level study is the maximum- fault level and X/R ratio, also the minimum-fault level and X/R ratio. The SAREGC does not explicitly specify any guidelines as to what acceptable fault level contribution from the SPP to the utility network is. Furthermore, there is still ongoing research into calculating the fault level current contributions from SPP inverters, using different technologies (Barnes, et al., 2021). As a simplification of the superposition

method (Complete Method) in PowerFactory, IEC 60909 uses an equivalent voltage source at the faulted bus to apply the equivalent voltage source at the faulted bus. By using this method, it is possible to compute an almost real-world short-circuit calculation without having to perform the preceding load-flow calculations or the associated definition of actual operational conditions. In Figure 3.25 the method of deriving equivalent voltage sources from the superposition method is shown. These are the main simplifications that have been made in PowerFactory (DIgSILENT GmbH, 2020):

- i) The network is assumed to have nominal conditions, i.e. parameters $U_i = U_{n,i}$
- ii) Current load is neglected, i.e. parameters $I_{Op} = 0$
- iii) Positive and negative sequence networks are simplified, i.e. loads are excluded;
- iv) The voltage at the busbar with a fault is corrected by c , ensuring that the results are representative and conservative. During the calculation of a network's maximum and minimum short-circuit currents, this factor differs.

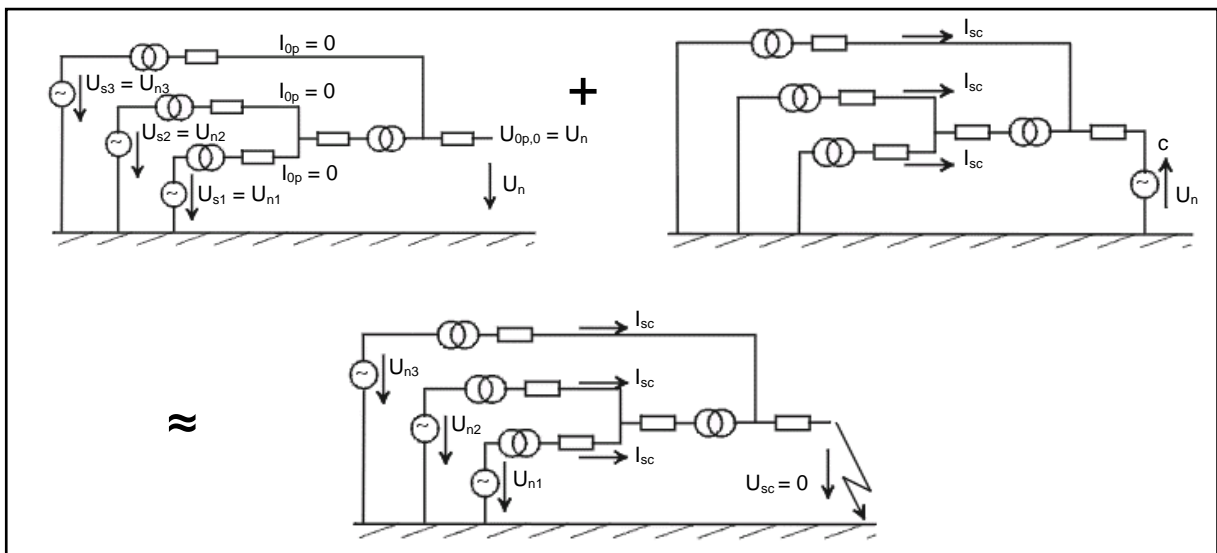


Figure 3.25: IEC 60909 method illustration used for PowerFactory fault level simulations (DIgSILENT GmbH, 2020)

These simplifications may not provide sufficient short-circuit calculations for some applications. As a result, the physical impedances of the network elements are corrected with additional impedance correction factors. Additionally, IEC 60909 does not address single-phase elements (except for neutral conductors with single-phase elements) (Aljarrah, et al., 2019). Based on the Thevenin equivalent method, the IEC 60909 standard calculates the fault current in power systems. By comparing a voltage source connected to the faulty point with the equivalent impedance seen by the point during the fault condition, I_{sc} represent the system during this situation. It should be noted that in such calculations, the impact of SPPs is not taken into consideration. The fault contribution of SPPs will, however, be calculated based on the current source model, and then the sum of the fault contribution of the utility grid and the

SPPs will be computed as the total fault current. Using Equation (3.24) as the basis for calculating the final symmetrical fault current, it should be noted that the calculation follows the IEC 60909 requirements (Aljarrah, et al., 2019):

$$I_{K_Total} = I_{K_Utility_Grid} + I_{K_SPP} \quad (3.24)$$

Where, I_{K_Total} is denoted by the total fault current contribution at the POC, $I_{K_Utility_Grid}$ represents the existing fault current and I_{K_SPP} is the fault current contribution from the SPP at the POC.

Based on the IEC 60909 standard, only rated parameters of network elements are used, in this manner, short-circuit calculations can be performed with very little information. Assuming, however, that the short-circuit contribution of an excitation voltage and a tap changer position play an important role in a synchronous generator, we considered the worst-case value of this impedance by applying a correction factor (< 1). A good illustration of this idea is shown in Figure 3.26, where the correction factor c is set to equal $I_K = I_{IEC}$, each element type has a calculation method defined by the IEC 60909 standard. Several PowerFactory elements require additional data due to the IEC 60909 stand'rd's provision for worst-case short-circuit current estimation. As a result, a fault level element is defined by an actual current source running in the positive sequence. The software allows the user defined values to be entered in the current value that varies based on the type of short circuit. The IEC 60909, at the time of this thesis being published, have not finalised any method to conclusively calculate fault level contributions from the SPPs, using steady-state calculation methods. This is primarily due to the quick controller actions within the SPP inverters control elements within the inverters control frame when the simulation of the network model is executed in PowerFactory.

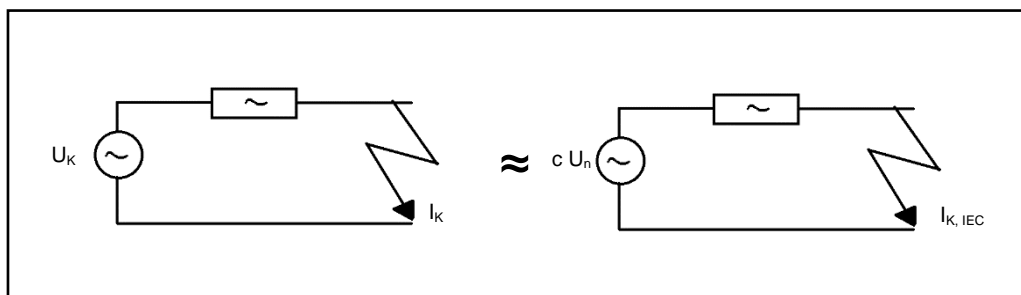


Figure 3.26: IEC 60909 impedance correction principles (DlgSILENT GmbH, 2020)

This being identified will result in some dynamic modelling of the fault level contribution behaviour of the SPP, as such, the fault level results simulated using steady-state analysis methods, will only serve as a guide. The intention is for the utility grid SO to identify if there are any significant increases in the fault levels that may cause breakers and other subsystem equipment to fail or any violations towards the contribution of non-compliance factors (Aljarrah, et al., 2019).

The fault level study flowchart is shown in Figure 3.27 and examines individual fault level contribution from the utility grid and the SPP inverters to identify any violations on excessive fault current that may damage electrical equipment when a fault condition is encountered.

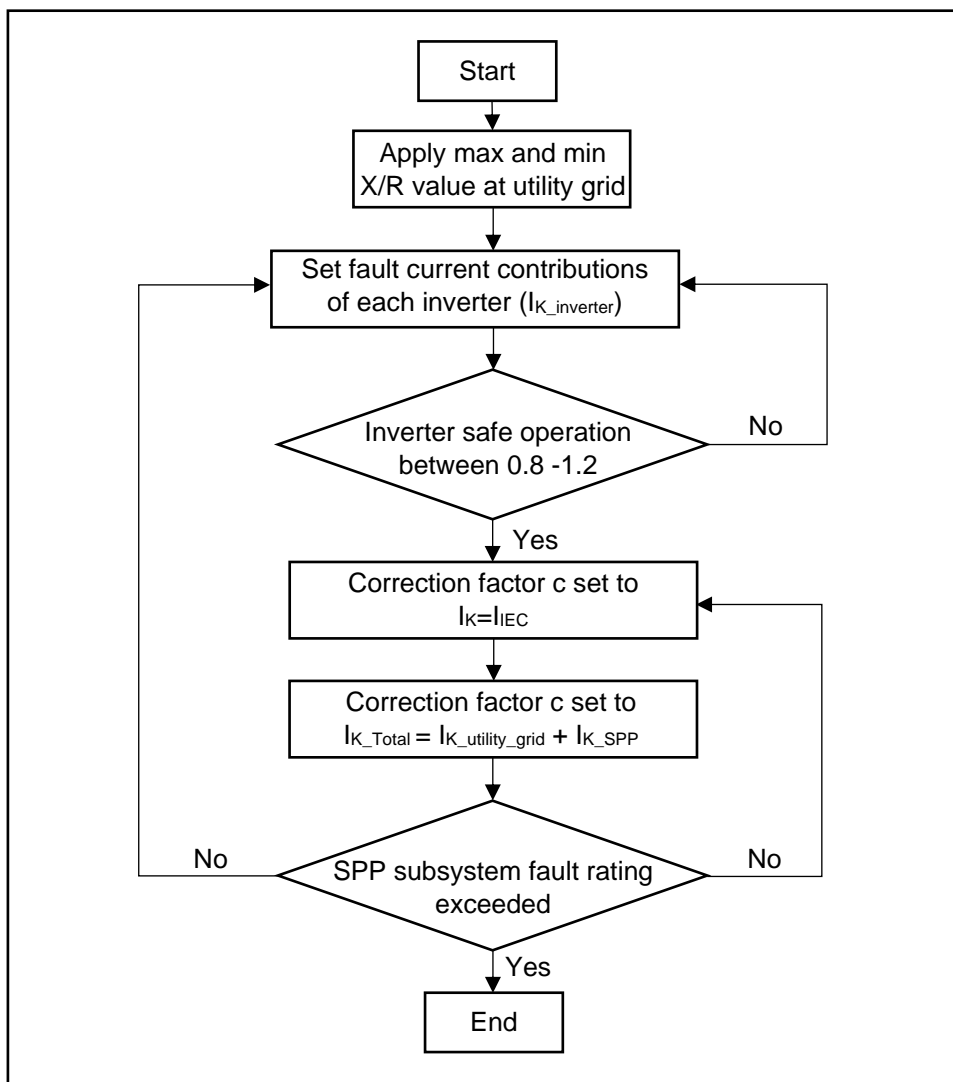


Figure 3.27: Flowchart for fault level compliance

3.4.4 Power quality studies simulation

In terms of power quality issues, harmonic content is one of the many aspects of the power system that needs to be considered. A harmonic analysis can be performed in either the time or frequency domains, using Fourier Analysis and post-processing. PowerFactory harmonic tools can perform harmonic analysis at the frequency level of the SPP and the contributions of the utility grid at the POC. Among the functions required to be performed for steady-state analysis to prove compliance according to the SAREGC, the following power quality studies will be performed (DIgSILENT GmbH, 2020):

- i) Harmonic load flow (according to IEC 61000-3-6);

- ii) Flicker analysis (according to IEC 61400-21);
- iii) Frequency sweep

Harmonic loads are calculated by PowerFactory's harmonic load flow, including distortion and harmonic losses from the non-linear loads (such as current converters). It is possible to define harmonic sources by either a harmonic current spectrum or a harmonic voltage spectrum. Whenever harmonic loads are defined at a frequency, PowerFactory performs a steady-state network analysis. Analysis of ripple-control signals is a special application of harmonic load flow, in addition to harmonic load flows, ripple-control signals can also be analysed with harmonic load flows. For this application, it is possible to calculate a harmonic load flow only at one frequency. It is also possible to calculate flicker disturbance factors introduced by SPP inverters using the harmonic load flow command, which also offers the option of working on long- and short-term periods. Although the IEC 61400-21 is specifically for wind turbine generators, the standard will be implemented for the SPP inverter flicker study, during continuous operations and switching operations.

A frequency sweep by PowerFactory compares harmonic loads in a continuous frequency domain to a harmonic load flow. It should be noted that one of the common applications of the frequency sweep function is the calculation of network impedances. This calculation allows the simulation network study to obtain the series and parallel resonances at minimum- and maximum fault level contributions in the network model implementing the results of the calculation. This type of resonance point can be used to locate the frequencies at which low and high harmonic voltages are produced due to low and high harmonic currents. In applications such as the design of filters, network impedances play an important role (DIgSILENT GmbH, 2020).

Adding a load type to the load element will allow you to assign a spectrum to the load element, and then setting the model to current source will enable you to assign the spectrum. It is necessary to define and assign the spectrum in the Load Element's Harmonics tab to be able to use it. The harmonic voltage distortion from a SPP can be simulated in two ways:

- i) Entering harmonics on the Harmonics tab and modelling the infeed as a voltage source.
- ii) Modelling the infeed as an external grid and entering the harmonics under the Harmonic Voltages tab on the Harmonics page.

The model has been setup in PowerFactory for the impedance scan at the POC to enable the frequency sweep analysis with a minimum and maximum fault current contribution and is

illustrated in Appendix B in Figure B.15. In the flowchart illustrated in Figure 3.28, the main power quality simulations are addressed as per SAREGC requirements.

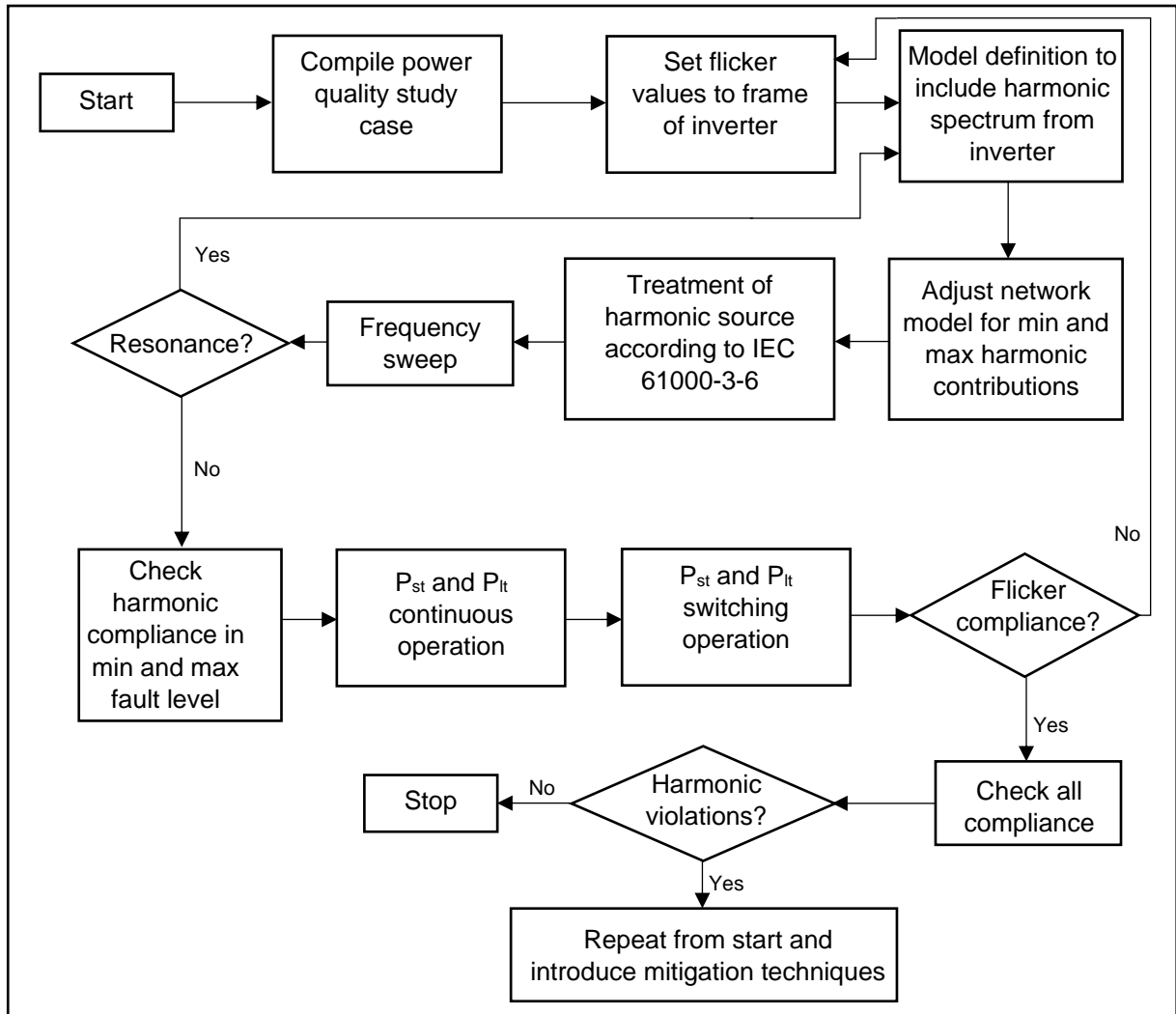


Figure 3.28: Power quality flowchart to determine non-compliance factors

3.4.4.1 Harmonic load flow

Setting up the network model as a study case for harmonics is a function that can be set in PowerFactory to perform power quality studies as per SAREGC requirements. The addition of harmonic current injections in the SPP inverter element ElmGenstat under the current spectrum object (TypHMccur) according to IEC 61000 as illustrated in Appendix B in Figure B.12. It is therefore appropriate to model every switched device as a harmonic source, the harmonic sources in PowerFactory can either be current sources or voltage sources.

In the Harmonic Sources type that is set to the option IEC 61000, harmonic current magnitude injections are allowed to be defined for integer and non-integer harmonics. As part of the above balancing and unbalancing of harmonic load flows, injecting zero-order harmonics and non-integer harmonics in the 'positive sequence' is considered. It is also possible to model

background harmonics with PowerFactory, power quality/harmonics pages are tailored to use the external AC voltage source element (ElmVac) as described in section 3.3.2. In situations where only the harmonic voltage amplitude (and not the angle) is known, the option of the IEC 61000 can be opted for. Whether a harmonic source is a voltage source or a current source is irrelevant to the harmonic source object. A harmonic source object consists of a single characteristic that determines whether harmonic voltages or harmonic currents are fed into the system. According to the spectrum type, the quantities are calculated as a percentage based on a reference value. The element's linked harmonic spectrum can be used to select a current (or voltage) reference value. The fundamental frequency of the element or its rated value can serve as a reference value for phase-correct spectra, as the fundamental frequency can be determined by performing a load flow calculation preceding the initial simulation of the SPP network model (McGranaghan & Beaulieu, 2006).

Spectra submitted according to IEC 61000 in the SPP network model will always have the rated value as a reference, the reference value is always the rated value for spectra according to IEC 61000. Accordingly, the injected current at frequency f_h of the IEC 61000 source is defined by Equation (3.25) (DIgSILENT GmbH, 2020):

$$I_h = k_h \cdot I_r \quad (3.25)$$

Where, $k_h = I_h/I_r$ indicates the harmonic content marked out in the spectrum, and where I_r signifies the supply current of the source.

3.4.4.2 Flicker analysis

Inverters connected to the grid have their power quality characteristics measured and assessed by methods described in the IEC 61400-21. In terms of power quality characteristics, voltage fluctuations are one of the characteristics. There can be negative effects on the consumer side for voltage fluctuations, for example, flicker (visible flickering caused by light sources), and voltage changes (excessive or inadequate voltage). The inverter operation can be divided into two modes based on voltage fluctuations when evaluating a SPP inverter's power quality. In PowerFactory, flicker disturbance factors are calculated by considering both continuous- and switching operation modes of operation whilst calculating the short-term and long-term flicker disturbance factors. In the harmonic load flow command, flicker can also be calculated optionally as part of the harmonic load flow process and is added to the network model as illustrated in Appendix B in Figure B.13.

There are six parameters that can be specified under the Flicker Coefficients type of input (each of these parameters is specified in IEC standard 61400-21) (DIgSILENT GmbH, 2020):

- Network Angle, ψ (degrees): An angle of network impedance must be entered either in the range $[-180,180]$ (default) or $[0,360]$. It is not permissible to mix these ranges in any way, the angles of the network must be entered in ascending order;
- Coefficient, $c(\psi)$: Using the network impedance angle as a function of the flicker coefficient, the total flicker coefficient can be obtained.
- Step Factor, $k_f(\psi)$: The flicker step factor is based on the network impedance angle as a function of flicker step factor;
- Voltage Change Factor, $k_u(\psi)$: The voltage change factor is determined by the network impedance angle;
- Maximum Switching Operations - N10: This is the maximum number of times that the switching of the inverter can be used in a span of 10 minutes;
- Maximum Switching Operations - N120: This is the maximum number of times that the switching of the inverter can be used in a span of 120 minutes.

A separate tab or section of the Harmonics page of the dialogs for these elements allows the assignments of Flicker Coefficients. In the case of unassigned flicker coefficients, the generator will be considered an ideal source for the flicker calculation. In addition, PowerFactory calculates flicker disturbance factors and relative voltage changes with impedance angles for lines with 20-degree Celsius temperatures and maximum operating temperatures. Using the temperature range as a guide, the following results variables represent the worst-case scenarios (DIgSILENT GmbH, 2020):

- P_{st_cont} ; P_{lt_cont} : There are both short-term and long-term factors affecting flicker disturbance of the SPP inverter/s over a continuous period of operation;
- P_{st_sw} ; P_{lt_sw} : There are both short-term and long-term factors affecting flicker disturbance of the SPP inverter/s over a switching period of operation;
- d_{sw} : Change in relative voltage (in percentage).

The different operation scenarios are explained further below (DIgSILENT GmbH, 2020).

i) Continuous operations

In the IEC standard 61400-21, continuous operation is defined as the normal operation of the SPP inverter, excluding start-ups and shutdowns.

In Equation (3.26), the following factors are defined for flicker disturbances in continuous operation:

$$P_{st} = P_{lt} = c(\psi_k, v_a) \cdot \frac{S_n}{S_k} \quad (3.26)$$

In this case, P_{st} represents the short-term flicker disturbance factor, the flicker disturbance factor, P_{lt} , is the long-term flicker disturbance factor, if continuous operation is used, c is the flicker coefficient, a network impedance angle (degrees) is determined by ψ_k . The average annual solar irradiation (W/m²) is determined by the factor v_a , in this context, S_n refers to the apparent power (VA) of the inverter and S_k is the apparent short-circuit power of the grid (VA) during the short-circuit condition (DIgSILENT GmbH, 2020). The flicker disturbance factors for continuous operation summed across more than one inverter are given by Equation (3.27) as follows:

$$P_{st\Sigma} = P_{lt\Sigma} = \frac{1}{S_k} \sqrt{\sum_{i=1}^{N_{inv}} c(\psi_k, v_a) \cdot S_{n,i}^2} \quad (3.27)$$

Where in this case, N_{inv} is the number of SPPs (each SPP with a specific number of inverters) that are to be installed at the PCC.

ii) Switching operations

In the IEC standard 61400-21, switching operations are defined as starting up or switching between SPP inverters. The flicker disturbance factors used in Equation (3.28 and 3.29), which describe the short-term and long-term flicker factors occurring during switching operations during this mode, are (DIgSILENT GmbH, 2020):

$$P_{st} = 18 \cdot N_{10}^{0.31} \cdot k_f(\psi_k) \cdot \frac{S_n}{S_k} \quad (3.28)$$

Where a time interval of ten minutes is defined as N_{10} switching operations, k_f stands for flicker step factor, a network impedance angle (degrees) is determined by ψ_k . The inverter's rated apparent power (VA) is S_n and S_k is the apparent short-circuit power of the grid (VA) during the short-circuit condition.

$$P_{lt} = 8 \cdot N_{120}^{0.31} \cdot k_f(\psi_k) \cdot \frac{S_n}{S_k} \quad (3.29)$$

Where a time interval of ten minutes is defined as N_{120} switching operations, k_f stands for flicker step factor, a network impedance angle (degrees) is determined by ψ_k . The inverter's rated apparent power (VA) is S_n and S_k is the apparent short-circuit power of the grid (VA) during the short-circuit condition.

The flicker disturbance factor is defined by Equation (3.30) as: In the case where there is more than one WTG at the PCC, this is calculated as follows (DIgSILENT GmbH, 2020):

$$P_{st\Sigma} = \frac{18}{S_k} \left[\sum_{i=1}^{N_{inv}} N_{10,i} \cdot (k_{f,i}(\psi_k) \cdot S_{n,i})^{3.2} \right]^{0.31} \quad (3.30)$$

Similarly, the long-term flicker disturbance factor under switching operations is defined in Equation (3.31) as follows:

$$P_{lt\Sigma} = \frac{8}{S_k} \left[\sum_{i=1}^{N_{inv}} N_{120,i} \cdot (k_{f,i}(\psi_k) \cdot S_{n,i})^{3.2} \right]^{0.31} \quad (3.31)$$

Where in this case, N_{inv} is the number of SPPs (each SPP with a specific number of inverters) that are to be installed at the PCC.

According to Equation (3.32), the relative voltage change (in units of %) for a single inverter switching operation is computed (DIgSILENT GmbH, 2020).

$$d = 100 \cdot (k_u(\psi_k) \cdot \frac{S_n}{S_k}) \quad (3.32)$$

In PowerFactory the long-term and short-term factors are included in the result columns for a harmonic load flow study as illustrated in Appendix B in Figure B.14 for the SPP network model during continuous and switching operations.

3.4.4.3 Frequency sweep

With the Frequency Sweep command (ComFsweep), it is possible to compute frequency dependent impedances. Frequency sweep harmonic analyses are normally used for analysing network impedances, both self and mutual. In addition to self-and mutual impedances, other impedances can also be shown and analysed. In PowerFactory, each voltage source model (ElmVac, ElmVacbi) can be defined with any spectral density function. As a result, impulse and step responses can be calculated for any variable in the frequency domain in the network model for the SPP. Analysis of power quality problems and oscillations is the most common application of parallel and series resonances when performing frequency sweep analysis.

Considering a resistive/inductive network without any capacitive components in the SPP, additional impedance result variables may be used to investigate the impact of capacitances on the network impedance. Considering a resistive/inductive network without any capacitive components, additional impedance result variables may be used to investigate the impact of capacitances on the network impedance. Step size can be automatically adjusted with the Automatic Step Size Adaptation option in the network model for steady-state analysis with the frequency sweep configuration. The calculation will normally be faster once this option is enabled and the results will be more detailed if the steps are smaller when required (DIgSILENT GmbH, 2020).

3.5 Summary

In this chapter, the relevant standards was discussed to determine specifically how a SPP is modelled as a network element and the SPP subsystem equipment formed part of the network data and how the library data in PowerFactory was utilised for the compliance studies. Some DSL was applied to the execution scripts and the DPL modifications to perform the studies according to the SAREGC and international standards such as the IEEE, NRS and WECC.

Furthermore, the subsystem components were also discussed and values are well documented in Appendix B to complete the network model and perform the required simulations and the contributions of the SPP subsystem is also considered a priority. Studies, which will be included in chapter 4 was discussed according to the requirements of standards and specifications, also this chapter dealt with important settings to be applied in PowerFactory to obtain a model that can perform the required SAREGC studies. The network model was discussed to show how a reactive compliance simulation is performed and the necessary steps to be undertaken to execute the type of study. Voltage capability requirements were also in the category of steady-state performance simulations to scrutinize for possible compliance issues. This chapter also included the stand-alone SPP fault level contribution to the utility grid and how the study's will be performed in a manner of which an easy comparable compliance can be made from graphical and informational judgement. Focus on the power quality requirements and studies to be done were discussed and presented in terms of power system modelling in PowerFactory for steady-state requirements. Power quality challenges found in SPPs can contribute to non-compliance with the SAREGC, such as harmonic distortion.

In Chapter 4, the modelled network will be simulated to determine any violations at the POC according to the SAREGC. All requirements will be simulated in the PowerFactory network model and the parameters and network elements combined with the SPP inverter control performance will be discussed and analysed.

CHAPTER FOUR: NON-COMPLIANCE IDENTIFICATION OF A SOLAR PHOTOVOLTAIC PLANT

4.1 Introduction

In this chapter the benchmarked model that was created and introduced for the SAREGC studies in chapter 3 will be executed according to the requirements that is set out in the context of grid compliance of a SPP connected to the utility grid. The network model will be analysed for any violations and non-compliance issues that may arise in the simulations and modelling of the network element setup including the composite inverter frame with controllers.

These studies' primary objective is to determine if the SPP is grid code compliant, to perform these studies, an accurate simulation model of the SPP was created in chapter 3 in a power system analysis software called DIgSILENT PowerFactory software, version 2020. Additional explanations will be provided with the simulations for the model, which will confirm the similarity in values expected at the POC and contributions to the utility grid. The network model was created in PowerFactory software with different operation scenarios implemented as required by the SAREGC. Results obtained from the data included in PowerFactory guided by standards obtained from IEEE, NRS and WECC will be benchmarked against the expectations of the SAREGC. These simulations that will only consist of steady-state analysis will provide results in the required framework for reactive power requirements in terms of capability and compliance. The other dependent study will comprise of voltage requirements for any violations that may be created from increasing or decreasing the voltage setpoints at the utility grid. This chapter will include fault level contribution studies from the SPP and from an islanded perspective. Lastly the investigation will also include the power quality studies that consists of harmonic emissions, frequency sweeps and voltage flicker. Any non-compliance aspects for the simulations will be identified and discussed for further investigation in terms of grid code compliance for a SPP.

For any utility size SPP these studies will be mandatory to carry out and perform for the SO at the utility grid, the studies will indicate whether the plant is performing within operational limits for the subsystem equipment of the SPP protection. Though, the impact on the utility grid shall be documented in order to present a safe and compliant grid-connected SPP that will not appallingly effect the utility grid. The SPP should provide support to a certain extend at the POC to the grid in terms of electrical performance. The focus of this chapter will be to provide results that are simulated according to the data from chapter 3, with the inclusion of indicating any non-compliance factors in the SPP that is contributed to the existing POC.

4.2 Grid code compliance studies

Simulation of the network elements are performed in steady-state analysis with the SPP comprising of fourteen central inverters, which delivers an apparent power of 720 kVA each, totalled installed capacity is 10 080 kVA. The SPP consist of seven three-winding transformers that can transform the two LV windings from 0.38 kV to the 11 kV MV winding, the LV windings each has a rated power of 720 kVA and the MV windings rated power is 1 440 kV. Each PTR is connected with 11 kV cables with different distances as the layout of the plant would require the PTRs to be at a certain distance to allow for equipment placement at the SPP. From the gridbox each collector group is connected to a common 11 kV busbar allowing the evacuation of power generated from the SPP to be injected in the utility grid. Between the gridbox and the utility grid a POC is provided, which constitutes the statutory point where all simulation results should be obtained.

4.2.1 SPP reactive power capability

To verify the reactive capability of the solar plant, with no additional reactive compensation, a station controller is defined at the POC. This station controller is used to adjust the power factor of the solar plant, at the POC. This controls the SPP to either supply or absorb reactive power as required in terms of the grid code. The utility grid network is represented by an external grid object at the POC. The load flow calculation is set to “distributed slack by loads” to limit the real power at the POC to perform the simulation with the required real power as shown in Table 4.1. For this study the voltage at the POC is regulated to 1.0 p.u. by the external grid, but the real power is adjusted at the POC as per SAREGC requirements.

Table 4.1: Reactive power requirements and results of the SPP

Requirements			Results from simulation						
Real Power (% of Pmax)	Required Q at POC (%)	Required Q at POC (MVar)	Inverter reactive limit (Y/N)	Voltage at POC (p.u.)	Overloading/voltage violations in the SPP (Y/N)	P at POC (MW)	Q at POC (MVar)	Power Factor at POC	SAREGC requirement compliant (Y/N)
P=5 %	5 % export	0.45	N	1.0	N	0.45	-0.450	0.707	Y
P=5 %	5 % import	0.45	N	1.0	N	0.45	0.450	0.707	Y
P=20 %	22.8 % export	2.052	N	1.0	N	1.80	-2.052	0.659	Y
P=20 %	22.8 % import	2.052	N	1.0	N	1.80	2.052	0.659	Y
P=100 %	22.8 % export	2.052	N	1.0	N	9.00	-2.052	0.975	Y
P=100 %	22.8 % import	2.052	N	1.0	N	9.00	2.052	0.975	Y

For the purpose of testing the SPP capability, the station controller is set up so that a specific Q value for a specific P output for the SPP is assigned to the reactive power at the POC. In order to begin, six key points are assessed. These include P = 5 %, 20 %, and 100 % while

adjusting Q to be 5 % and 22.8 % (for imports and exports) respectively. According to the results obtained in the power flow of the SPP base case for the network model, all conditions are met and is within normal operational requirements. None of the SPP subsystem equipment is overloaded when the reactive power capability is done, even the inverters are normally loaded for the operation and simulation requirements. The initial results are illustrated in Figure 4.1 where the reactive power flow can be seen at the POC and the import and export are achieved in the simulation with the indication given by the direction of reactive power flow in the network model. The remaining results are documented in Appendix C in Figure C.1 to C.5 for the reactive power requirements.

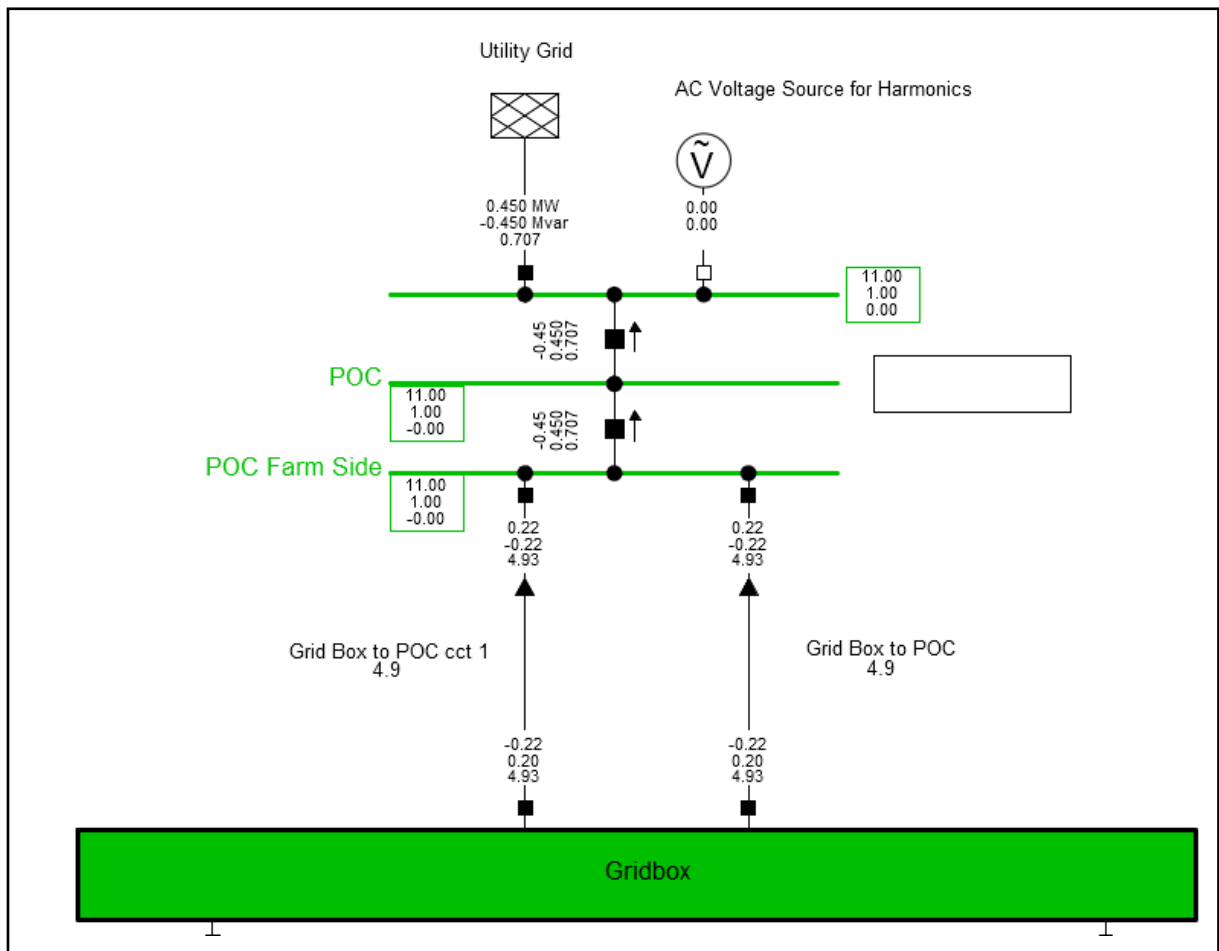


Figure 4.1: Reactive power requirements for Q = -0.450 MVar & P = 0.450 MW at POC

The plant is fully compliant during the export of 0.450 MVar to the utility grid with the real power adjusted to 0.450 MW as per grid code requirements in the SAREGC. The rest of the studies as tabulated in Table 4.1 has all been proven compliant and the next step in the network model simulation will be to perform the reactive power capability for the complete plant. This will determine if the plant can absorb or inject the specified reactive power as set out by the SO for the control of the SPP.

According to the results for the key operating points that were studied, the SPP does not meet the requirements for full reactive capability of the SAREGC requirements for the six key operating points. A second study was performed in order to further quantify the compliance with the requirements, where the SPPs real power output was increased from 0% to 100%, and the firm's maximum import and export reactive power capabilities were calculated. The full reactive power capability of the SPP is shown in Figure 4.2 and the SPP is not capable of providing Q support during requirements as set by the SO.

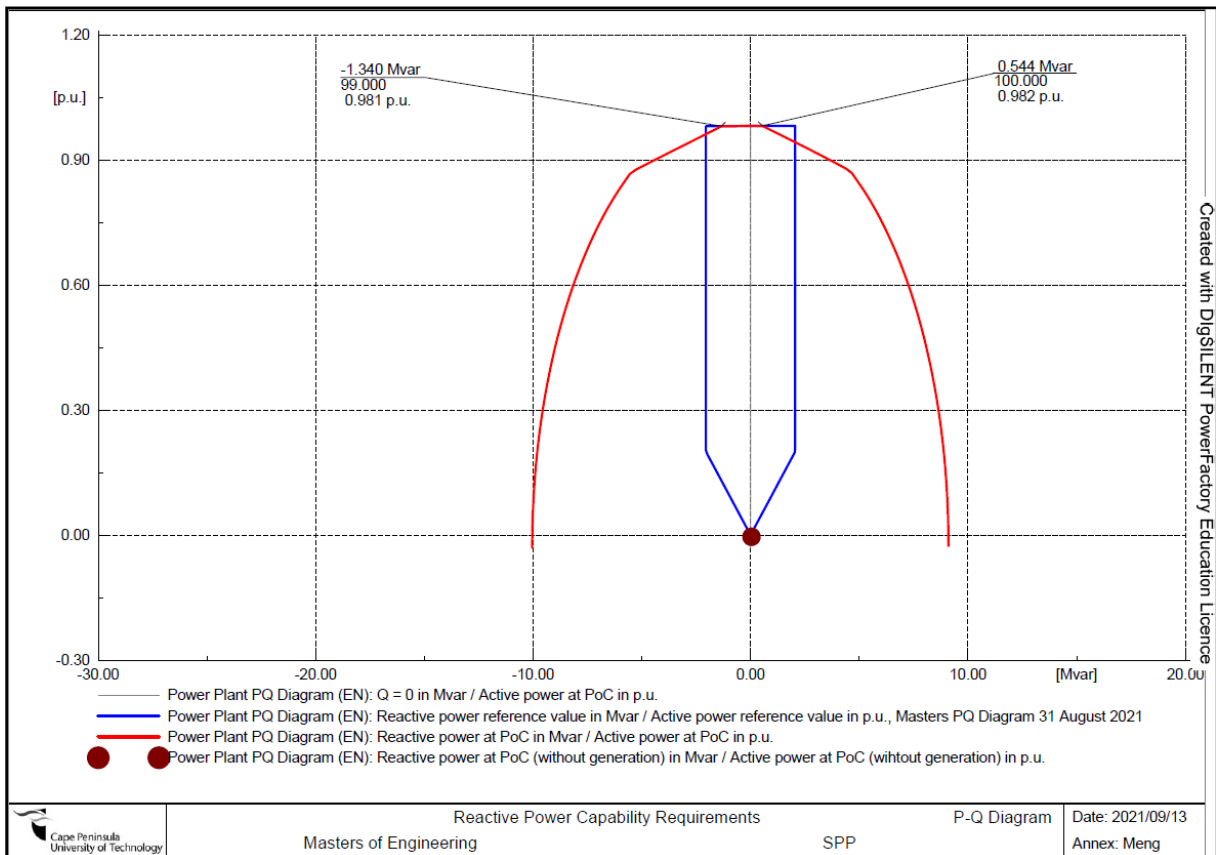


Figure 4.2: Full reactive power capability of the SPP

At the point taken in Figure 4.2 above for the maximum capacitive Q export the SPP can only inject a maximum of 0.544 MVar at a 0.982 p.u. voltage. From the import of the inductive reactive power, the SPP is only capable of absorbing a Q import of -1,340 MVar at a 0.981 p.u. voltage. This indicates that the plant has failed the full reactive power capability requirements, though the plant passes the reactive power requirements at the six key simulation points. This may be attributed to inverters not being sized correctly with the operational limits reached or the cable distances between the gridbox and the POC being too long. Another factor that might play a role is the absence of a compensation device to support reactive power requirements. To further investigate the different reactive power capability, the simulations should be done for voltage capability requirements, which goes together with the reactive power capability simulation and requirement of the plant.

4.2.2 SPP voltage capability

For this study the voltage was adjusted at the POC between 1.1 p.u. to 0.9 p.u. while maintaining maximum farm output (9 MW). Inverters were configured with voltage control at the POC for power factor verification as illustrated in Figure 4.2. The PPC was also adjusted to accommodate the droop to perform the studies, which PowerFactory provides a droop % according to the user selection of the required reactive power. The setpoint to control the SPP at the POC is at the station controller (PPC) and the phase control is set to positive sequence studies for the requirements to simulate the network model as per SAREGC specifications for voltage capability (Sewchurran & Davidson, 2016).

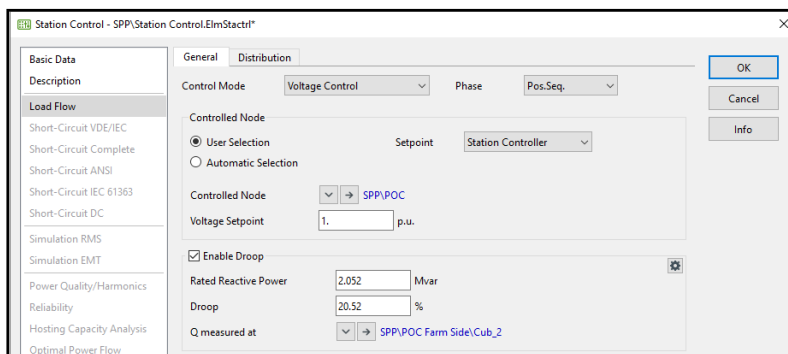


Figure 4.2: PPC set to voltage control for SPP inverters

It is always important to design the SPP with a complete balance in the gridbox from collector group feeders as this will increase compliance when the system is balanced. Keeping voltage within acceptable limits is accomplished by means of voltage regulation. The SO is responsible for voltage regulation and for setting the voltage for each SPP connected to the utility grid according to their equipment design limitations. An application is made to the SPP on behalf of the SO to supply or absorb reactive power in an area that demands it, such as the substation where consumption of reactive power is governed by power factor requirements or other utility related requirements. A definite terminal voltage is specified for all SPP subsystem equipment in the network model for SAREGC studies. As a result of the voltage drop in the network elements of the SPP, the transformer tap dependent impedance was selected in the network model in for compliance studies in the simulation model. The step-up transformers are not equipped with OLTCs to regulate the voltage automatically and this would be a manual process that will have to be implemented in the network model. The power factor of the SPP was also checked against the requirement in Figure 4.3, making sure that it was able to operate at all voltages and power factors as required. The six study points will be done under different reactive power and settings for import and export, while the real power remains the same at a different voltage p.u. value, which is user defined in the network model for compliance (Sewchurran & Davidson, 2016).

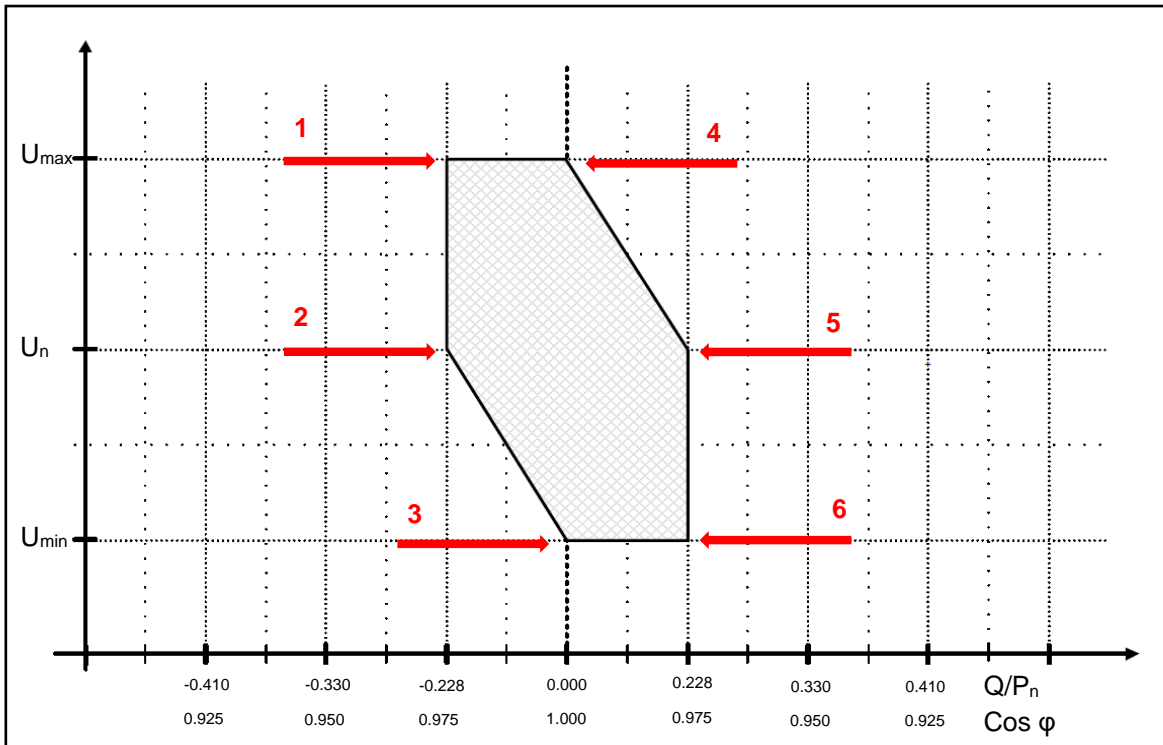


Figure 4.3: Study points to confirm SPP voltage capability (Mchunu, 2020)

As shown in Table 4.2, the results are from the study where the voltages at the POC are manually adjusted by user defined value as per the SAREGC and the inverter were automatically adjusted according to safe operational limits. General inverter data indicates that the inverters can operate at 0.8 p.u. to 1.2 p.u. values. In essence, if the SPP is able to reach the six study points, then it can meet the criteria set forth in the grid code.

Table 4.2: Requirements and results of voltage capability at the POC

Requirements				Results from simulation						
Study Point	Real Power (% of Pmax)	Required Q at POC (%)	Required Q at POC (MVar)	Inverter reactive limit (Y/N)	Voltage at POC (p.u.)	Overloading/voltage violations in the SPP (Y/N)	P at POC (MW)	Q at POC (MVar)	Power Factor at POC	SAREGC requirement compliant (Y/N)
1	P=100 %	22.8 % import	2.052	N	1.1	Y	9.0	2.052	0.975	Y
2	P=100 %	22.8 % import	2.052	N	1.0	N	9.0	2.052	0.975	Y
3	P=100 %	0 % import	0	N	0.9	N	9.0	0.000	1.000	Y
4	P=100 %	0 % export	0	N	1.1	Y	9.0	0.000	1.000	Y
5	P=100 %	22.8 % export	2.052	N	1.0	N	9.0	-2.052	0.975	Y
6	P=100 %	22.8 % export	2.052	N	0.9	N	9.0	-2.052	0.975	Y

The simulation results are shown in Figure 4.4 for study point 1 and from study point 2 to 6, the results are illustrated in Appendix C in Figure C.6 to Figure C.10 and the inverters overloading conditions are shown in Appendix C in Figure C.11 and Figure C.12. At study points 1 and 4, the inverters are overloaded and are operating above 1.2 p.u of the voltage in

order to provide the required reactive power at the specific p.u. voltage level. In these conditions the SPP will remain compliant, but the IPP is at risk of losing the SPP inverters at certain voltage operational levels. Although the 1.1 p.u voltage level is seen as a temporary occurrence, the SPP inverter for that specific period will be subjected to an environment where the lifespan of the inverter may be reduced significantly.

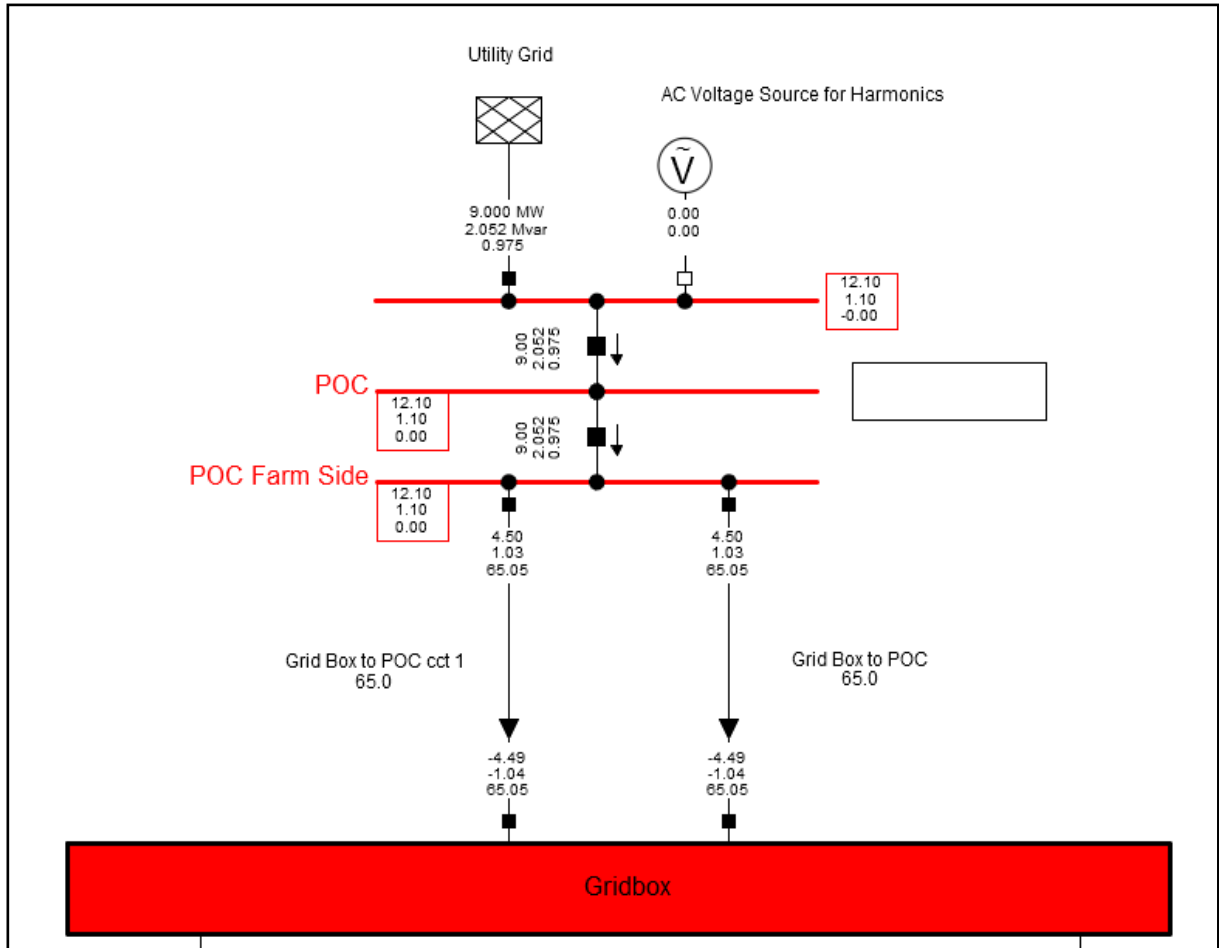


Figure 4.4: Voltage capability at 1.1 p.u. for Q = 2.052 MVar & P = 9.000 MW at POC

Each of the voltage level simulations that was done under different p.u. voltages in steady-state provide a different colour output to the results i.e. green is 1.0 p.u. (normal condition), blue is 0.9 p.u. (abnormal condition) and red is 1.1 p.u. (abnormal condition). Furthermore, the simulations of the modelled network are within the requirements of the SAREGC indicating that the benchmarked network model information provides accurate information and data. The model in PowerFactory was further expanded to determine if the overall voltage capability will be met with no conditions instituted by the SO. In PowerFactory, the simulation index is provided with red lines (results), which indicates the reactive power at the POC in MVar divided by the voltage at the POC in a p.u. value. The blues lines (user defined) are shown as the reactive power reference at nominal real power (P_n) in MVar divided by voltage at the POC in p.u. value. The x-axis represents the MVar divided by the voltage at the POC in a p.u. value,

while the y-axis is the actual MVar requirement at the POC. As per the network model setup of the SPP, the V-Q script was executed with the parameters of the SAREGC to show compliance. Furthermore, the results can be seen in Figure 4.5 at the six key study points as discussed in chapter 3.

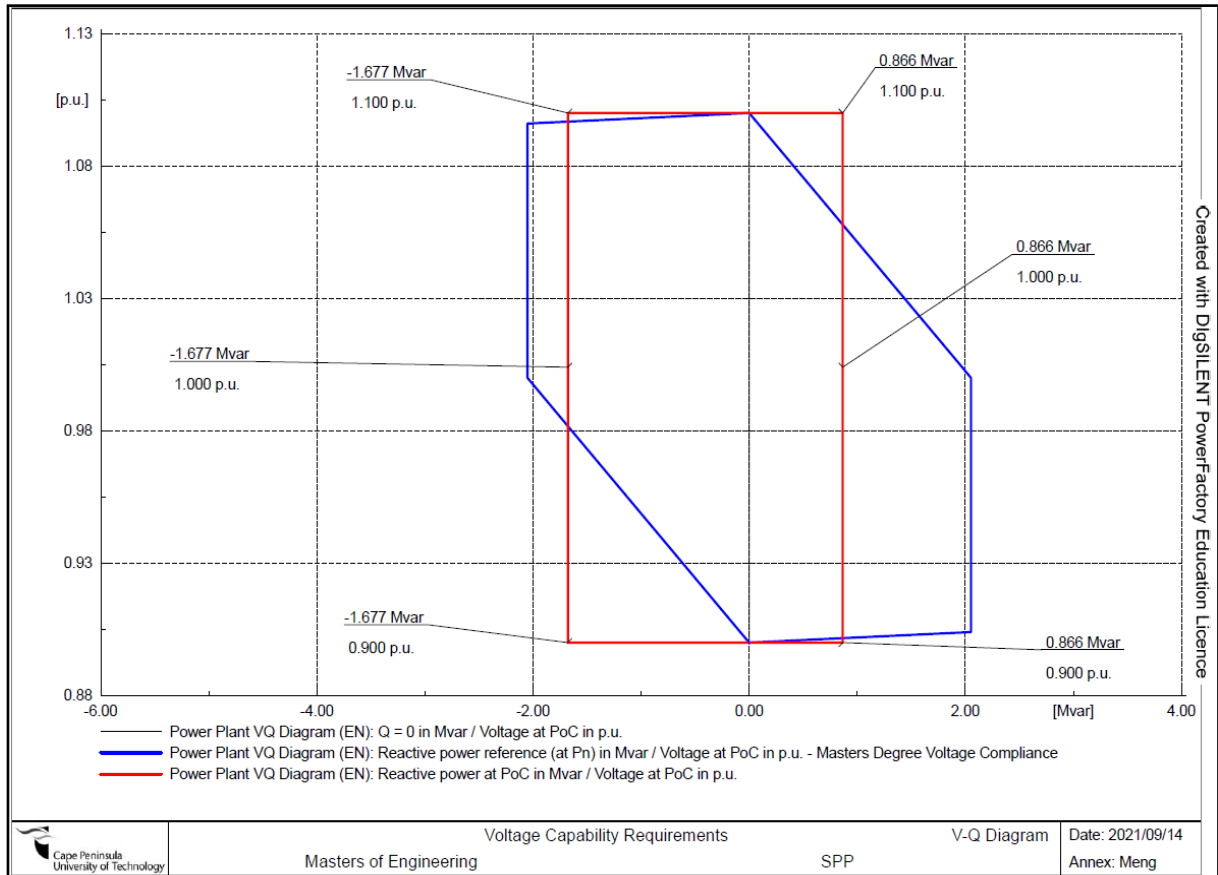


Figure 4.5: Full voltage requirement capability of the SPP

For each of the six study points in Figure 4.5, none of the areas studied was grid code compliant and will not be able to support the utility grid in reactive power requirements, without imposing an operational risk on the SPP subsystem equipment, due to overvoltage conditions at the SPP. Additional simulations have been performed to confirm whether the voltage / power factor has been achieved in the voltage capability requirement study and as per previous findings non-compliance has been identified. In Appendix C in Figure C.13, where the under excited condition is simulated and represents the available power factor ($\cos(\phi)$) at the POC (redline) and at the SAREGC requirement (blueline), which is then divided by the voltage requirement at the POC. The overexcited condition for the simulation results includes the available power factor at the POC (redline) divided by the voltage requirement at the POC in p.u. value to obtain the results. The SPP has non-compliance issues in respect to the voltage capability requirements in the SAREGC context.

4.2.3 SPP fault level study

In this section, the fault level results have been calculated using the 'IEC60'09' method presented in Powerfactory. This network model has the option 'Static Converter Fed Drive' selected to perform the fault level studies in steady-state conditions. The three-phase fault level is shown in Appendix C in Figure C.14 and the fault level values at the POC = 5.741 kA with a 0.541 kA contribution from the SPP during short-circuit conditions. Furthermore, a dynamic study was included by implementing the maximum and minimum X/R values to investigate the SPP performance when a time domain is applied.

4.2.3.1 Dynamic fault level contributions

This dynamic study involved applying a three-phase fault to the POC and clearing it, so that the fault levels calculated using steady-state methods could be verified. As displayed in Figure 4.6, the SPPs fault current contribution to the utility grid at the POC can be identified.

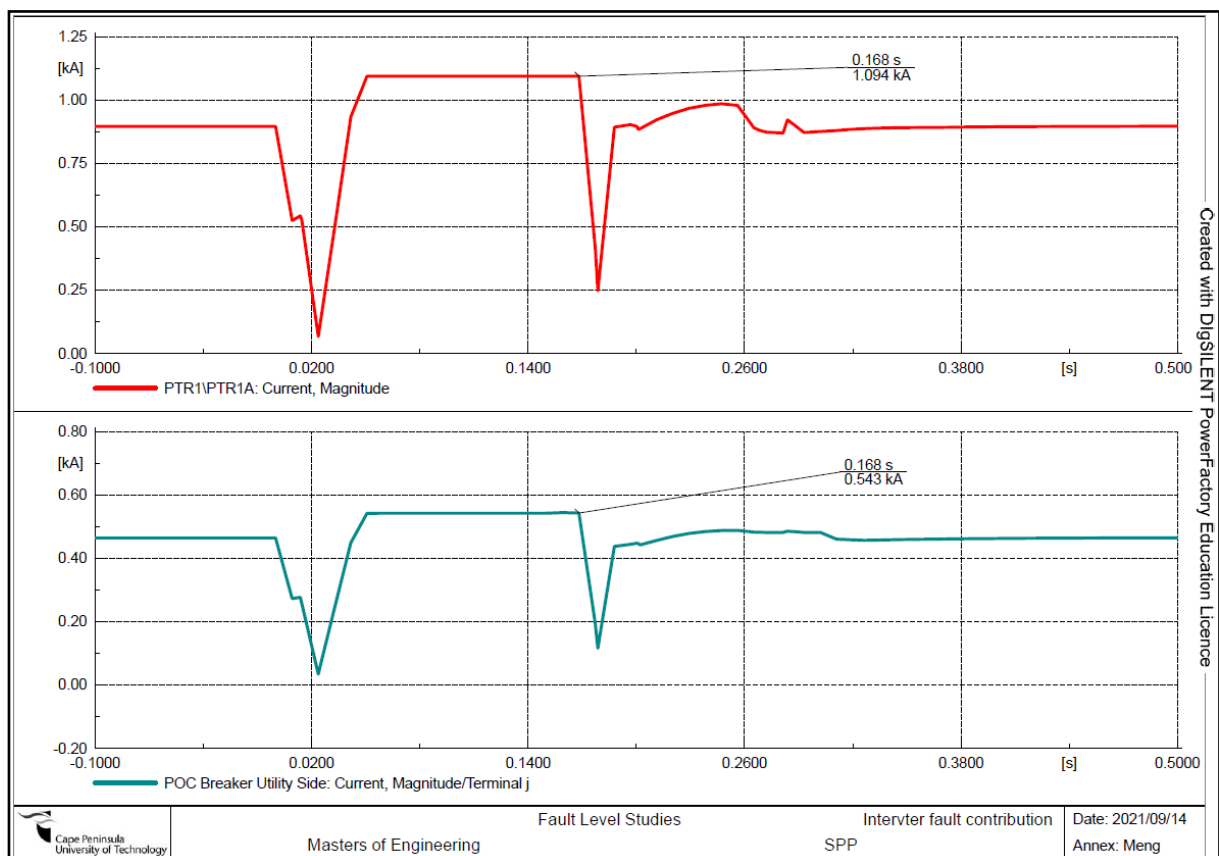


Figure 4.6: Fault current contributions from the SPP to the POC

At dynamic studies performed the total fault current contributions from the SPP is 1.094 kA and the fault current at the POC = 0.543 kA. The noticeable difference is the SPP fault current increasing by 100 % and the fault current at the POC decreasing to only 10 % of the

contributions. According to the SAREGC, the SPP is grid code compliant in terms of fault level studies and contributions to the utility grid and pose no risk to the SPP subsystem or inverters as the SPP is rated at 25 kA at 11 kV. The fault current contributions comply to the SAREGC and will not be checked again for compliance.

4.2.4 Power quality

Based on the SAREGC utility grid requirements, the IPP need to ensure that the SPP has met the following power quality requirements:

- i) In accordance with the NRS 048-4, the SPP will be required to meet the quality of supply limits, which are detailed in Annexure B (Quality of supply specification);
- ii) To perform the study and compare against benchmarked required results, Table 4.3 was compiled using generic values contained in the NRS 048-4;
- iii) A SPP shall ensure that the harmonic voltage emissions from the connected utility grid are kept within the limits as set out.

Table 4.3: Harmonic emission limits for compliance of the SPP (NRS 048-4, 2004)

Harmonic order	2	3	4	5	7	9	11	13	23	25
Voltage (%)	0.5	1.5	0.3	2.8	2.2	0.6	2.1	1.7	0.8	0.7

According to the NRS 048-2, the IPP shall ensure that all other harmonic voltage emission levels caused by the CUSTOMER at the PCC shall be less than 30 % of the individual voltage harmonic limits (NRS 048-2, 2007). If the network model harmonic impedance at the PCC for the range of reference fault levels specified in section 4.2.3 does not exceed a harmonic impedance of Equation (2.35) as described in chapter 2.

4.2.4.1 Harmonic analysis

As indicated by Table 4.4, the NRS 048-2 specifies the complete compatibility levels for harmonic distortion for utility networks. Although the utility grid specifies the allowable limits at the POC, all other limits must be applied at 30 % of the NRS levels. As per NRS048-4, the maximum interharmonic distortion is 0.2 %, when calculating harmonic distortion at the POC, the harmonic contribution as provided by the generic SPP inverter model should be included in the network model (NRS 048-4, 2004). It should be noted that the harmonic contribution reached the 100th harmonic, which is quite high, in the PowerFactory model, this distortion was

added to each inverter. A harmonic load flow was calculated based up to the 50th harmonic order and on all frequencies up to the 100th order for the inverter model in the network model.

Table 4.4: Compatibility levels for harmonic voltages for HV and EHV networks (expressed as a percentage of the reference voltage) (NRS 048-2, 2007)

1	2
Harmonic order (h)	HV and EHV harmonic voltage (%)
3	2.5
5	3.0
7	2.5
11	1.7
13	1.7
17	1.2
19	1.2
23	0.8
25	0.8

Note: The compatibility levels are those recommended by Cigré TB261, which contains recommendations derived from international data collected. Data for even harmonics and higher-order harmonics was not available and has therefore not been included. Reference values for these harmonic orders may be based on the planning levels give in NRS 048-4.

The NRS 048-2 also indicates that if any reference values are not given, the values may be based on the planning levels in the NRS 048-4 as per Table 4.5.

Table 4.5: Recommended planning levels for harmonic voltages (as a percentage of the rated voltage of the power system) (NRS 048-4, 2004)

1		2		3		4		5		6		7		8		9	
Odd harmonics (non-multiples of 3)			Odd harmonics (multiples of 3)			Even harmonics											
Order h	Harmonic voltage %		Order h	Harmonic voltage %		Order h	Harmonic voltage %		Order h	Harmonic voltage %		Order h	Harmonic voltage %				
	MV	HV/EHV		MV	HV/EHV		MV	HV/EHV		MV	HV/EHV		MV	HV/EHV			
5	5.0	2.0	3	4.0	2.0	2	1.6	1.5									
7	4.0	2.0	9	2.0	2.0	4	1.0	1.0									
11	3.0	1.5	15	0.3	0.3	6	0.5	0.5									
13	2.5	1.5	21	0.2	0.2	8	0.4	0.4									
17	1.6	1.0				10	0.4	0.4									
19	1.2	1.0	>21	0.2	0.2	12	0.2	0.2									
23	1.2	0.7															
25	1.2	0.7				>12	0.2	0.2									
>25	0.2+	0.2+															
	$0.5\frac{25}{h}$	$0.5\frac{25}{h}$															

Note: Total harmonic distortion (THD): ≤3% in HV networks

At the POC, harmonic distortion is measured in the SPP, and the results are plotted against the allowable maximum limits for the SPP. In the simulation the network model was expanded to produce a plot diagram indicating the allowable harmonic distortion (in red hatched bars). Using the simulation, the results are shown in Figure 4.7 and Figure 4.8, for maximum and minimum fault levels respectively, with a X/R value of 8.354 (max) and 9.14 (min) for the utility grid.

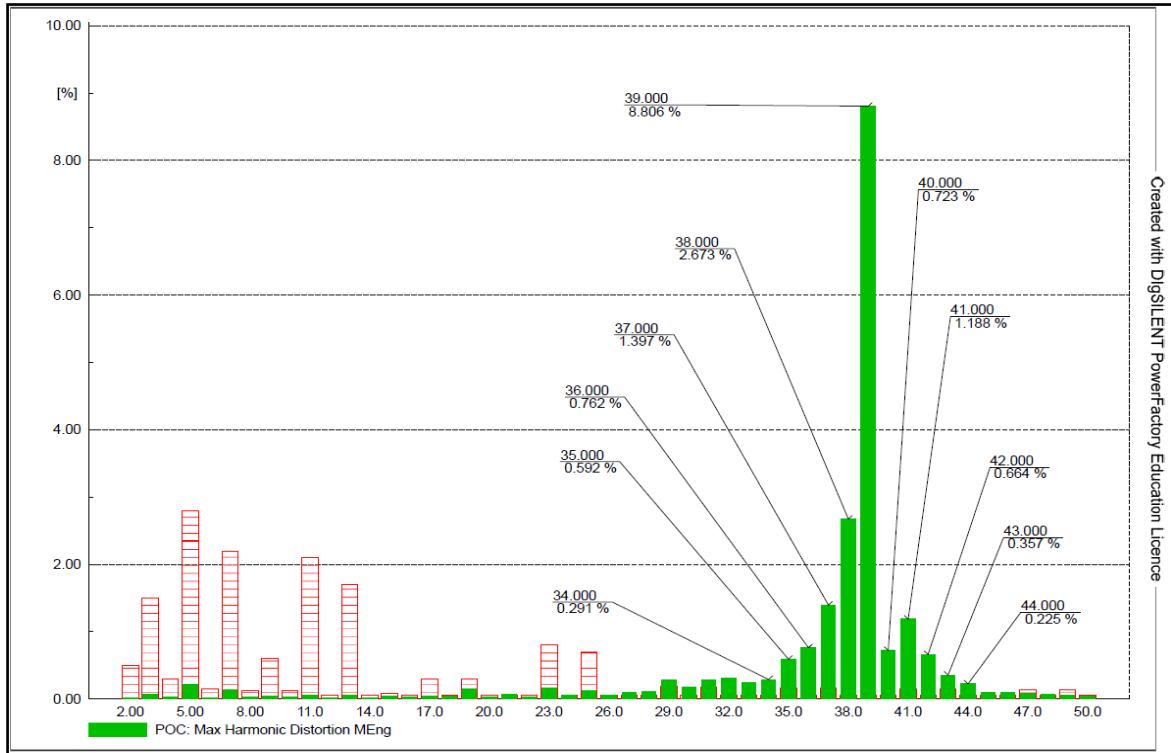


Figure 4.7: Harmonic distortion at the POC for maximum fault level

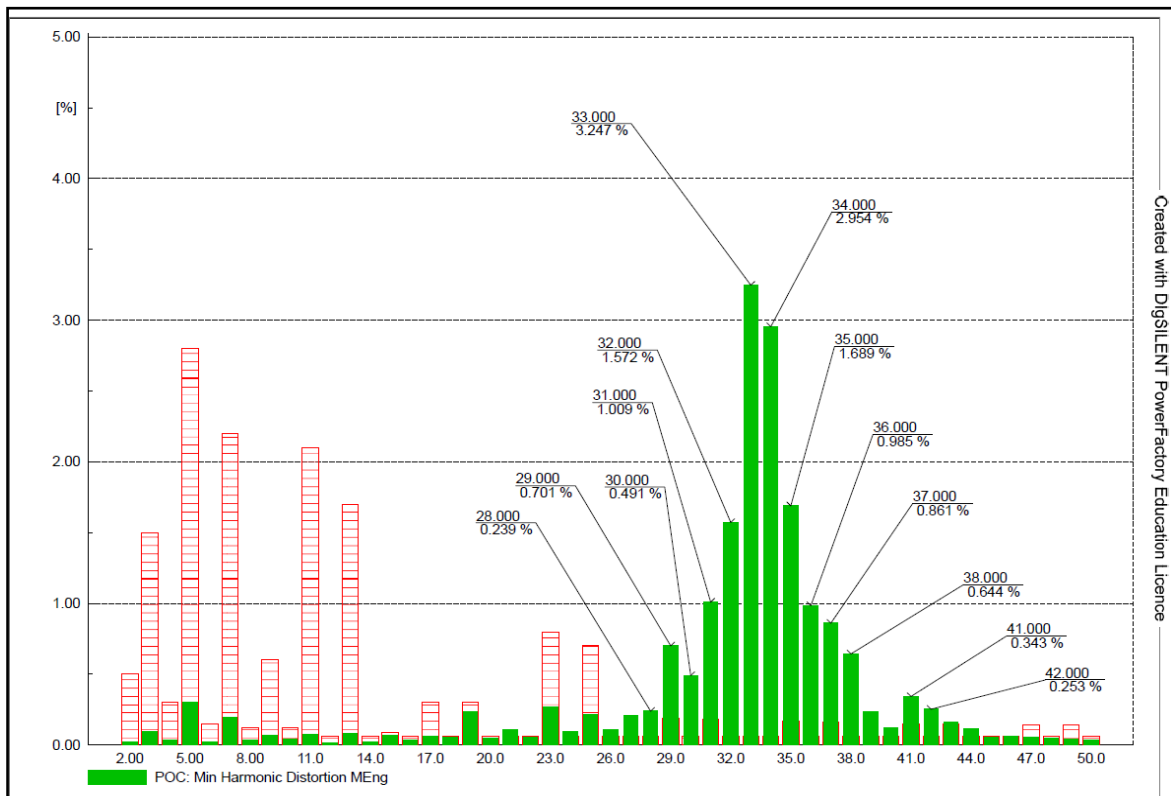


Figure 4.8: Harmonic distortion at the POC for minimum fault level

According to Figure 4.7 and Figure 4.8, integer and non-integer harmonic orders exceeds the allowable limits at maximum and minimum fault levels. The results were exported and is detailed in Appendix C in Table C.1, highlighting the harmonic orders that fail to meet the

harmonic order requirements in red as per NRS 048-2 and NRS 048-4. Furthermore, a harmonic load flow was carried out for maximum and minimum fault levels at the POC and the results are as follow: THD at the POC: 9.53 % (maximum fault level at POC) and 4.05 % (minimum fault level at POC). Also, the result of the simulations is illustrated for maximum and minimum fault currents at the POC in Appendix C in Figure C.15 and Figure C.16, respectively.

4.2.4.2 Frequency sweep

A frequency sweep has been performed at the POC to determine if any resonance points are created in the network model. The following parameters were implemented as previously mentioned: Maximum and minimum fault levels from the utility and SPP contributions at the POC, X/R ratio for 9.14 maximum and 8.354 minimum fault conditions at the POC. As can be seen from Figure 4.9, the results from the simulation are as follow.

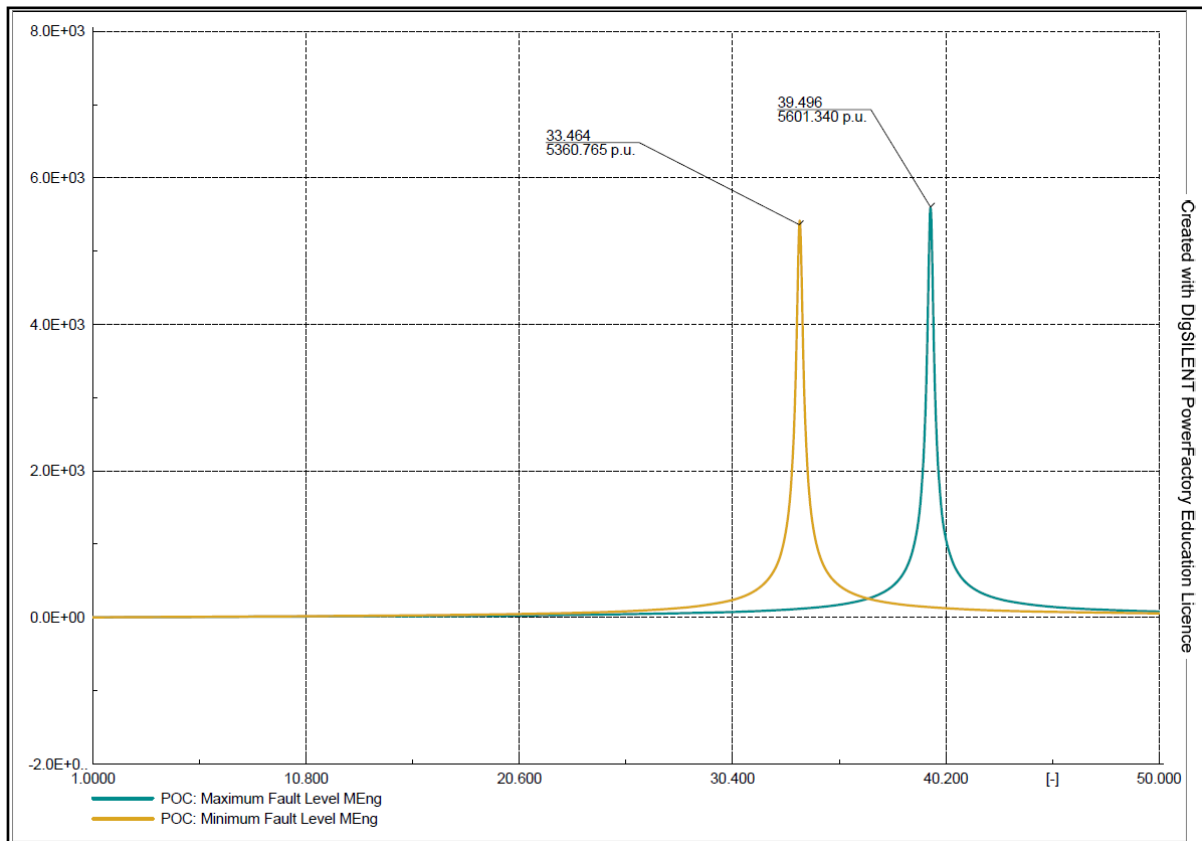


Figure 4.9: Frequency sweep from the POC

At the POC, a parallel resonance can be detected based on the results of the frequency scan. This resonance is sensitive to the impedance ratio X/R of the utility grid. Furthermore, since the impedance of the utility grid network is assumed to be linear (3x), the results do not consider any parallel resonances that may occur within the utility grid network, which may negatively affect the SPP. Moreover, a parallel resonance may cause the maximum network

impedance to not necessarily give the biggest harmonic distortion and, if there is a parallel resonance, the assumption of 3x linear 50Hz impedance may not be correct. Based on the results and the non-compliance identified, there is a need for mitigation techniques at the SPP to provide compliance at the POC to the SAREGC requirements. However, the range of fault levels and the network impedance (3x and lower) result in parallel resonances that occur over a wide frequency range, resulting in harmonics whose frequency exceeds the allowed level of distortion.

4.2.4.3 Flicker

According to contract NRS 048-4 and SAREGC, the utility grid requirements for flicker are: In the case of a range of references fault levels specified in the simulated network model, the IPP shall ensure that the contribution to voltage flicker at the PCC by the SPP always shall be less than the following amounts:

- i) In the case of short-term voltage flicker of 0.6;
- ii) In the case of long-term voltage flicker of 0.5.

The results are obtained from the network model and is presented in Table 4.6 for the flicker disturbance factors for long-term and short-term continuous operation and for long-term and short-term switching operation.

Table 4.6: Flicker disturbance factors at the POC

Description	Maximum fault levels	Minimum fault levels
Short-term, continuous operation	0.08	0.07
Short-term, switching operation	0.04	0.04
Long-term, continuous operation	0.08	0.07
Long-term, switching operation	0.04	0.07
Change in relative voltage (in percentage)	0.1	0.1

According to the simulations all the conditions are met with the requirements of flicker disturbance factors and no violations was detected according to the NRS 048-4 and SAREGC. In Appendix C in Figure C.17 to Figure C.20. As the SPP complies to the relative standards the compliance will not be checked again for flicker as this section complies to the SAREGC.

4.3 Summary

The aim of chapter 4 was to provide a full steady-state simulation requirement as per the SAREGC with user defined values as illustrated in the previous chapter. In this chapter the network model was analysed for any non-compliance challenges. All the compliances to the grid code were highlighted and will not be further investigated as the studies proved compliance and any changes to the network will not affect the results to cause violations in the network.

The primary objective of these studies is to determine whether the SPP is grid code compliant. The simulations were based on steady-state analyses which provided results for the requirements on reactive power from a capability and compliance standpoint. During reactive power requirement studies, it was found that all conditions in the SPP inverters LV terminals had no overloading or overvoltage conditions, due to performance requirements. Furthermore, all conditions on the reactive power requirements were met when the individual setting of the SPP was performed on the six key points. The SPP failed compliance when the full reactive power capability simulation was done and additional compensation will be required to be compliant according to the SAREGC. Voltage capability studies indicated compliance to the SAREGC, but the SPP inverters experienced overvoltage conditions at the terminals to provide the required power factor at the POC. Additional simulations were carried out to confirm the voltage compliance and none of the six key points studied in the full voltage requirement capability was compliant. Since the SPP was subjected to maximum and minimum fault levels a fault level study was done in steady-state conditions and in dynamic conditions to confirm whether there would be any violations, all conditions were compliant in the fault level study. Power quality studies were performed and the harmonic emissions contributed at the PCC and POC are problematic and does not provide compliance to the SAREGC. After, the harmonic emission simulation a frequency sweep was done during maximum and minimum fault level conditions to determine if any resonance points are created. This study indicated that the SPP has resonance present in the network model and should be mitigated to comply with the grid code. Lastly, the flicker disturbance in the network model was simulated and all conditions were satisfactory and according to the SAREGC.

Chapter 5 will focus on the proposed mitigation techniques and the results will be compared with the results obtained in this chapter. The results will be illustrated and analysed with different proposed mitigation techniques for compliance strategies implemented to provide solutions to the grid-connected SPP.

CHAPTER FIVE: MITIGATION TECHNIQUES FOR NON-COMPLIANCE FACTORS

5.1 Introduction

This chapter will review and discuss the application of mitigation techniques to the network model that was simulated. After the simulations in PowerFactory in chapter 4, there were non-compliance challenges that was identified and discussed. When the proposed mitigation techniques are applied to the network model, a comparative analysis of the new results and the previous chapter results where non-compliance was identified in the network model.

According to the grid code, a SPP asset must meet certain electrical performance requirements before it can be connected to a utility grid. An increasing number of individual generating SPP inverters composed of renewable generation plants presents the SO with challenges in terms of technical singularities, connection processes, and management of plant models. To address these issues, specific compliance procedures have been established by the SAREGC for SPPs based on simulation. Providing documentation of the type tested equipment, simulation assumptions and results of a simulation to prove that a network model meets grid code requirements will prevent misinterpretations on grid code compliance studies. The network model will be simulated with the proposed mitigation techniques for reactive power capability requirements to determine the supply and absorb of reactive power on the function of the POC voltage, with the focus on inverter overloading. Voltage capability compliance will also form part of this chapter to ensure that all conditions according to the grid code is met. Furthermore, the power quality studies on the network model will be implemented with the proposed changes to the network model to determine the effect on the harmonic emissions, frequency sweeps and voltage flicker disturbances. When SPPS don't comply with the SAREGC, the MEC may be curtailed, even after they are disconnected from the grid (Yongning, et al., 2019). To illustrate compliance the proposed mitigation techniques will be implemented for safe operation of equipment and to achieve support to the utility grid by enhancing the performance of the grid.

The same strategy and network model will be used in this chapter to prove that the network model is compliant to the SAREGC. Firstly, the proposed investigation will be to identify all the non-compliance challenges and introduce previous research solutions to the network model. Steady-state studies that will not be further investigated will comprise of the studies that complied to the grid code. As the proposed mitigation techniques requires to be added to the network model, the results will be documented for compliance assurance.

5.2 Mitigation techniques for grid code compliance

By keeping the MEC at 9 MW, the SPP network model will be subjected to the proposed mitigation techniques. According to literature available on grid code compliance techniques, once a violation is detected in the SPP, there are comprehensive amounts of research available on power quality enhancement. One application is the implementation of shunt capacitor filter bank for steady-state conditions that will enhance the performance of a SPP in terms of power quality requirements (Kunte, et al., 2012). Sizing and the application of the capacitor bank will be determined by the previous simulation requirements that were not achieved or caused non-compliance violations in the network model. Another proposed mitigation technique will be to add a dynamic response to reactive power compliance capabilities and voltage capability requirements with the implementation of STATCOM (Elshahed, 2017). However, this will not be done as the studies will be for steady-state analysis. To avoid expensive rework and costly remedial actions, SAREGC conducts a power system simulation assessment during the design stage, when designing the RPP, there are opportunities for performance and cost optimization. The following case studies represented from 1 to 3 for the proposed mitigation techniques can be implemented for grid code compliance (Yuill & Carter-Brown, 2016):

- 1) Assembling the reactive power capability requirements as efficient as possible by optimizing the number of SPP inverters;
- 2) Optimizing the reactive power capability of the SPP inverter will minimize or eliminate the additional requirement of installing reactive compensators such as capacitor banks, which are used to generate a reactive power;
- 3) Aiming to reduce the amount of harmonic emissions injected or absorbed by the SPP by implementing a shunt filter bank.

5.3 Grid code compliance studies including the proposed mitigation techniques

Based on simulations of the network elements in the previous chapter, case studies 1 (reactive power capability) and case study 2 (voltage compliance capability) will be implemented with the proposed mitigation technique. For case study 1, the SPP will be made up of fifteen central inverters delivering a total of 720 kVA each, with an aggregate installed capacity of 10 800 kVA. In addition to the three-winding transformers, each of which is rated at 720 kVA, the total installed capacity of transformers will also reach 10 800 kVA in the SPP. As the layout of the plant may result in the new PTR 8 consisting of inverters 8A and 8B being placed at a specific distance. In the gridbox, each collector group is still connected to an 11 kV busbar which allows the generated electricity to be routed into the utility grid. Gridboxes are connected to utility grids

by POCs, which are still the statutory points from which simulation results have to be obtained. Case study 2 will be implemented with the base case study as provided in chapter 4, the only difference would be that the SPP inverter will be configured to perform at the maximum optimisation allowable limit to provide the required compliance as set out by the SAREGC. The comparative analysis will be done to determine which mitigation technique will be implemented for the power quality case study.

5.3.1 Case study–1 - SPP reactive power capability and voltage capability requirement mitigation techniques

For case study 1A, the additional inverter will be added to the SPP for the proposed reactive power capability compliance to avoid any violations. The mitigation technique will also be applied with case study 1B, which will investigate the voltage capability requirement compliance.

5.3.1.1 Case study –A - SPP inverter for reactive power capability

As shown in Figure 5.1, an additional inverter (PTR 8) is added to the network model in case study 1 to verify the reactive capability of the solar plant. The outcome of this mitigation technique is for the inverter to provide additional reactive compensation.

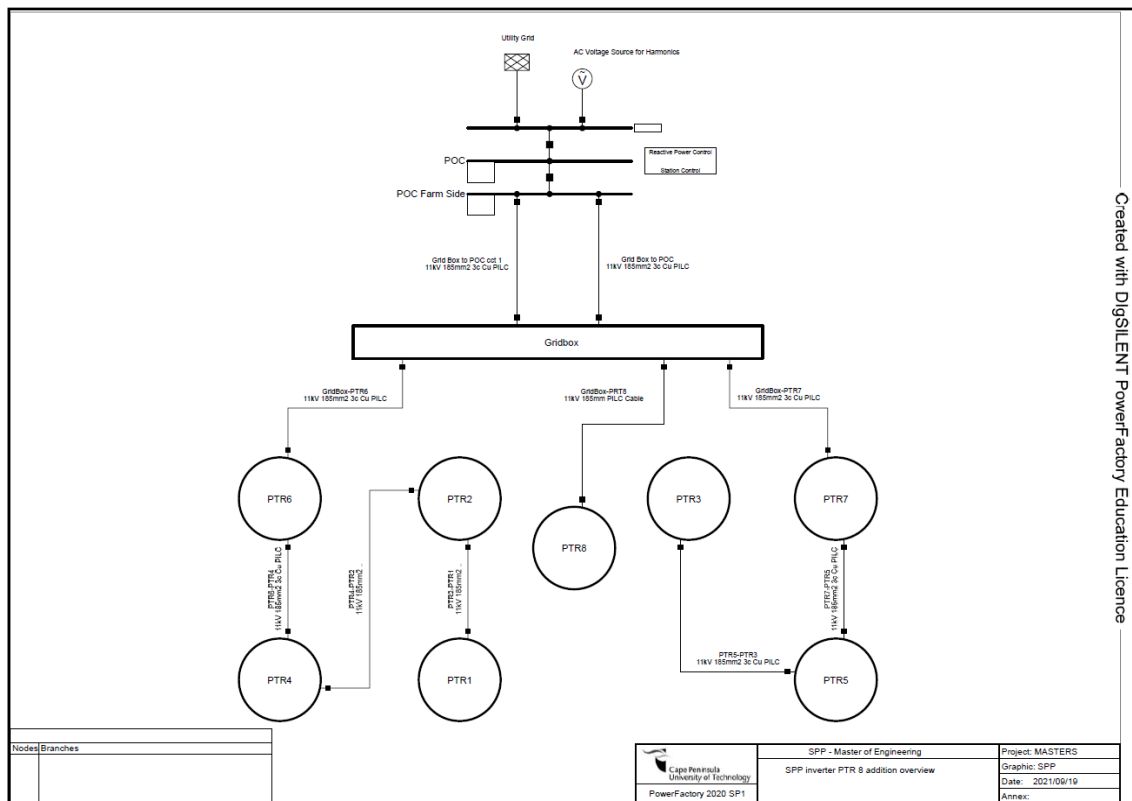


Figure 5.1: SPP inverter PTR 8 addition overview

As per chapter 4, none of the SPP subsystem equipment is overloaded when the reactive power capability is done for an additional inverter (PTR 8). All simulation methodologies are as per chapter 4 as the station controller (PPC) is still defined at the POC. The simulation results with the additional inverter are illustrated in Table 5.1, which is the same as the base case results as all conditions are compliant. The results are shown in Appendix C in Figure C.21 to Figure C.26, where the reactive power flow and the power factor can be seen at the POC.

Table 5.1: Case study –A - reactive power requirements and results of the SPP

Requirements			Results from simulation						
Real Power (% of Pmax)	Required Q at POC (%)	Required Q at POC (MVar)	Inverter reactive limit (Y/N)	Voltage at POC (p.u.)	Overloading/voltage violations in the SPP (Y/N)	P at POC (MW)	Q at POC (MVar)	Power Factor at POC	SAREGC requirement compliant (Y/N)
P=5%	5% export	0.45	N	1.0	N	0.45	-0.450	0.707	Y
P=5%	5% import	0.45	N	1.0	N	0.45	0.450	0.707	Y
P=20%	22.8% export	2.052	N	1.0	N	1.8	-2.052	0.659	Y
P=20%	22.8% import	2.052	N	1.0	N	1.8	2.052	0.659	Y
P=100%	22.8% export	2.052	N	1.0	N	9.0	-2.052	0.975	Y
P=100%	22.8% import	2.052	N	1.0	N	9.0	2.052	0.975	Y

Furthermore, a complete reactive power capability curve was simulated for the additional SPP inverter PTR 8. The reactive power capability curve is illustrated in Figure 5.2, all conditions of the SPP operation relating to reactive power capability are covered in the curve.

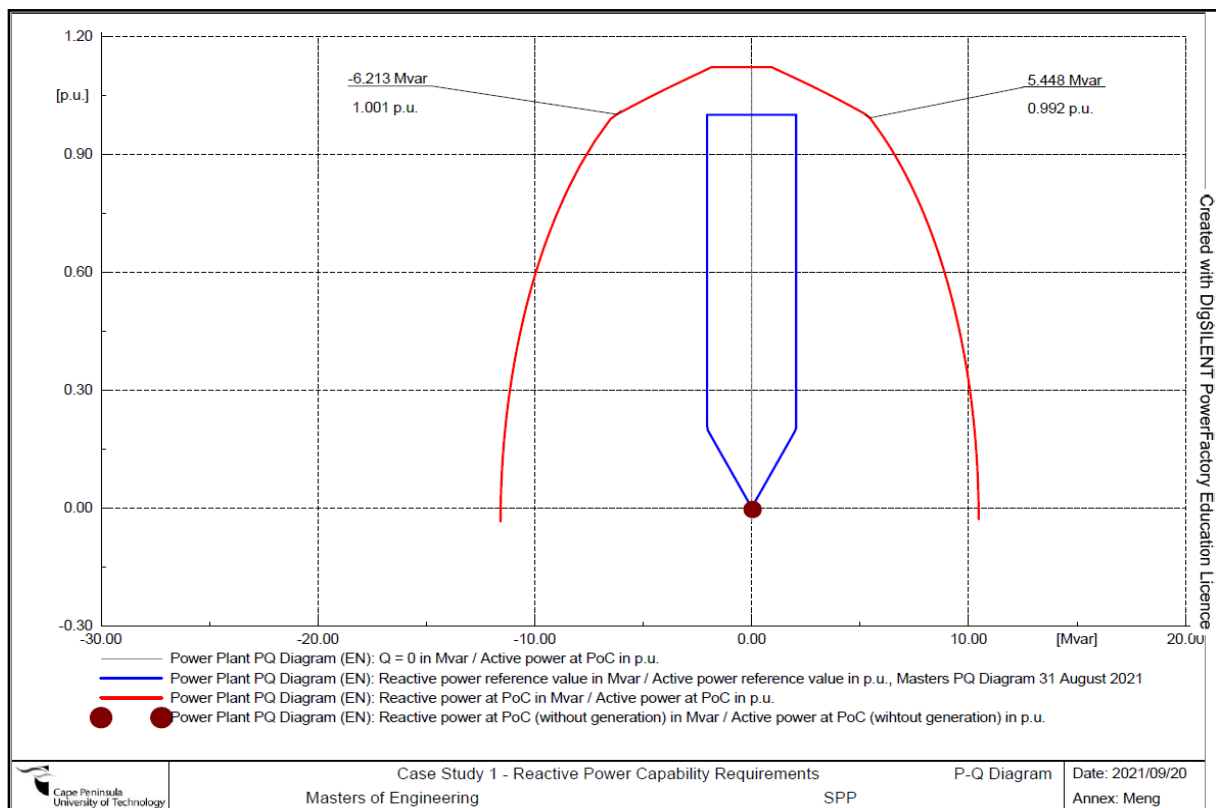


Figure 5.2: Case study –A - full reactive power capability of the SPP

With the full reactive power capability, the SPP is compliant and covers the complete spectrum of capability. The maximum import capability of the SPP is now 6.213 MVar and the export capability is 5.448 MVar, which is well above the SAREGC requirement of 2.052 MVar for import and export of a 9 MW SPP.

5.3.1.2 Case study –B - additional SPP inverter for voltage capability

This study used a manual adjustment of the voltages at the POC, as per SAREGC, and an automatic adjustment of the inverter based on safe operational limits, as shown in Table 5.2. Inverters can be safely operated at 0.8 p.u. to 1.2 p.u. for general inverter data as per generic inverter model in PowerFactory and WECC suggestions. SPPs should be capable of reaching six study points in order to meet the criteria of the grid code.

Table 5.2: Case study –B - requirements and results of voltage capability at the POC

Requirements				Results from simulation						
Study Point	Real Power (% of Pmax)	Required Q at POC (%)	Required Q at POC (MVar)	Inverter reactive limit (Y/N)	Voltage at POC (p.u.)	Overloading/voltage violations in the SPP (Y/N)	P at POC (MW)	Q at POC (MVar)	Power Factor at POC	SAREGC requirement compliant (Y/N)
1	P=100 %	22.8% import	2.052	N	1.1	N	9.0	2.052	0.975	Y
2	P=100 %	22.8% import	2.052	N	1.0	N	9.0	2.052	0.975	Y
3	P=100 %	0% import	0	N	0.9	N	9.0	0.000	1.000	Y
4	P=100 %	0% export	0	N	1.1	N	9.0	0.000	1.000	Y
5	P=100 %	22.8% export	2.052	N	1.0	N	9.0	-2.052	0.975	Y
6	P=100 %	22.8% export	2.052	N	0.9	N	9.0	-2.052	0.975	Y

As per results obtained from the simulation of the network model with the addition of PTR 8 in case study 1, all conditions are satisfactory according to the SAREGC. The findings are illustrated in Appendix C in Figure C.27 to C.32 and the inverter operation at 1.1 p.u. voltage at the POC for study point 1 and 4 is shown in Appendix C in Figure C.33 and C.34. All operation conditions were simulated at the POC for the SPP and no overloading or voltage violations was seen at the inverter LV terminals.

For each of the six study points in Table 5.2, all the study areas were grid code compliant and will be able to support the utility grid in reactive power requirements. Additional simulations have been performed to confirm whether the voltage / power factor has been achieved in the voltage capability requirement study and the results is shown in Appendix C in Figure C.35. Where the under excited condition is simulated and represents the available power factor of -3.917 MVar at the POC and for overexcited conditions the results indicated 2.865 MVar. In Figure 5.3 the full voltage capability requirement is illustrated and appose no violation to the utility grid of the SO.

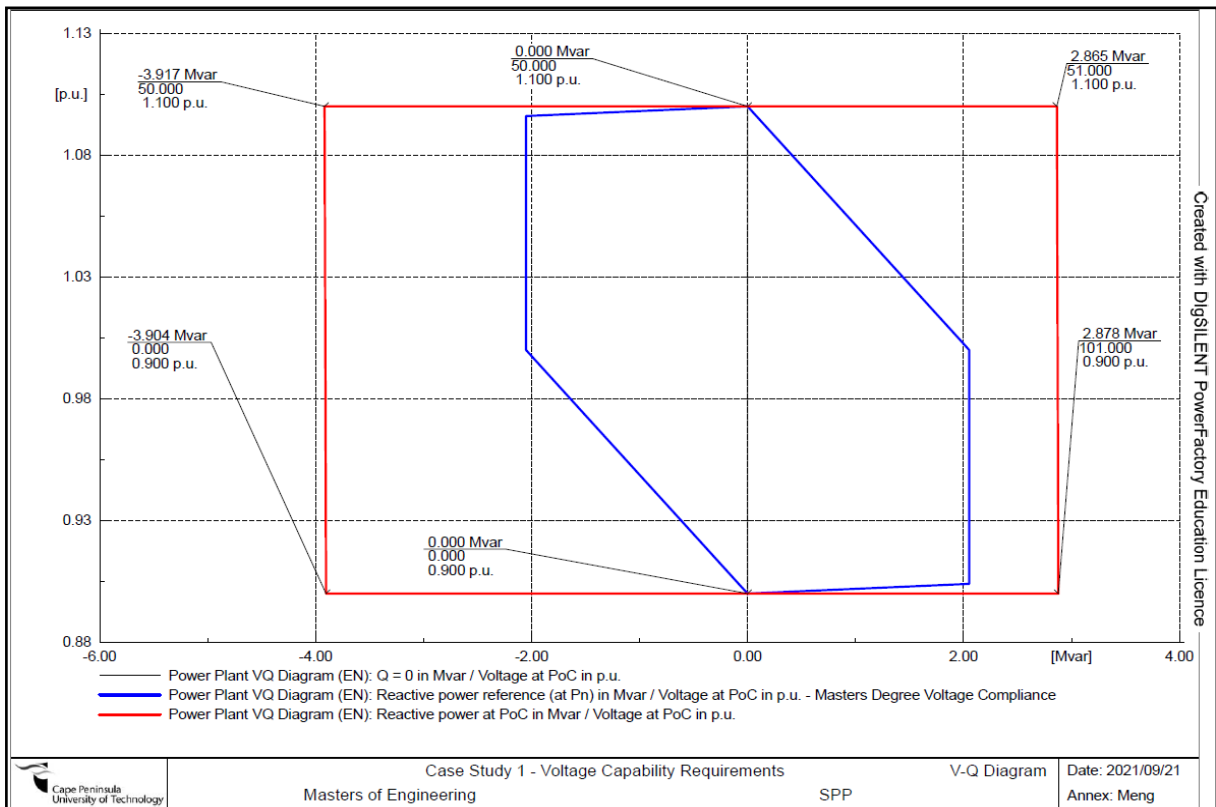


Figure 5.3: Case study –B - full voltage requirement capability of the SPP

The voltage requirement is represented by the blue line diagram and indicates the operational requirements for the SPP. By simulating the SPP and the voltage requirement the red line diagram indicates the operational performance of the SPP with an additional inverter.

5.3.2 Case study–2 - SPP reactive power capability and voltage capability requirement mitigation techniques

For case study 2A, the optimisation of the inverters within safe operational scenarios will be done to perform the required reactive power capability. The study will implement the base case as reference and only the modification to the inverters operational performance will be made to determine a viable mitigation technique for the SPP. Additionally, the mitigation technique will be applied to case study 2B, which examines the compliance of voltage capability requirements.

5.3.2.1 Case study –A - optimization of SPP inverter for reactive power capability

The setpoints limits in Table B.6 will be used to provide the Q capability curve for the matrix of the Q_{max} p.u. and Q_{min} p.u. as in Appendix B shown in Table B.10A, Table B.10B, B.11A and B.11B for the assigned SPP inverters of the network model reactive capability curve. All results

are shown in Table 5.3 and for case study 2A, the SPP will undergo the same simulation procedures as previous applied.

Table 5.3: Case study –A - reactive power requirements and results of the SPP

Requirements			Results from simulation						
Real Power (% of Pmax)	Required Q at POC (%)	Required Q at POC (MVar)	Inverter reactive limit (Y/N)	Voltage at POC (p.u.)	Overloading/voltage violations in the SPP (Y/N)	P at POC (MW)	Q at POC (MVar)	Power Factor at POC	SAREGC requirement compliant (Y/N)
P=5%	5% export	0.45	N	1.0	N	0.45	-0.450	0.707	Y
P=5%	5% import	0.45	N	1.0	N	0.45	0.450	0.707	Y
P=20%	22.8% export	2.052	N	1.0	N	1.8	-2.052	0.659	Y
P=20%	22.8% import	2.052	N	1.0	N	1.8	2.052	0.659	Y
P=100%	22.8% export	2.052	N	1.0	N	9.0	-2.052	0.975	Y
P=100%	22.8% import	2.052	N	1.0	N	9.0	2.052	0.975	Y

Detailed simulation results are illustrated from PowerFactory in Appendix C in Figure C.36 to C.41, which indicates all the desired outcome as per SAREGC requirements. Furthermore, a full reactive power study was also conducted as per previous simulations and the results is shown in Figure 5.4 for case study 2.

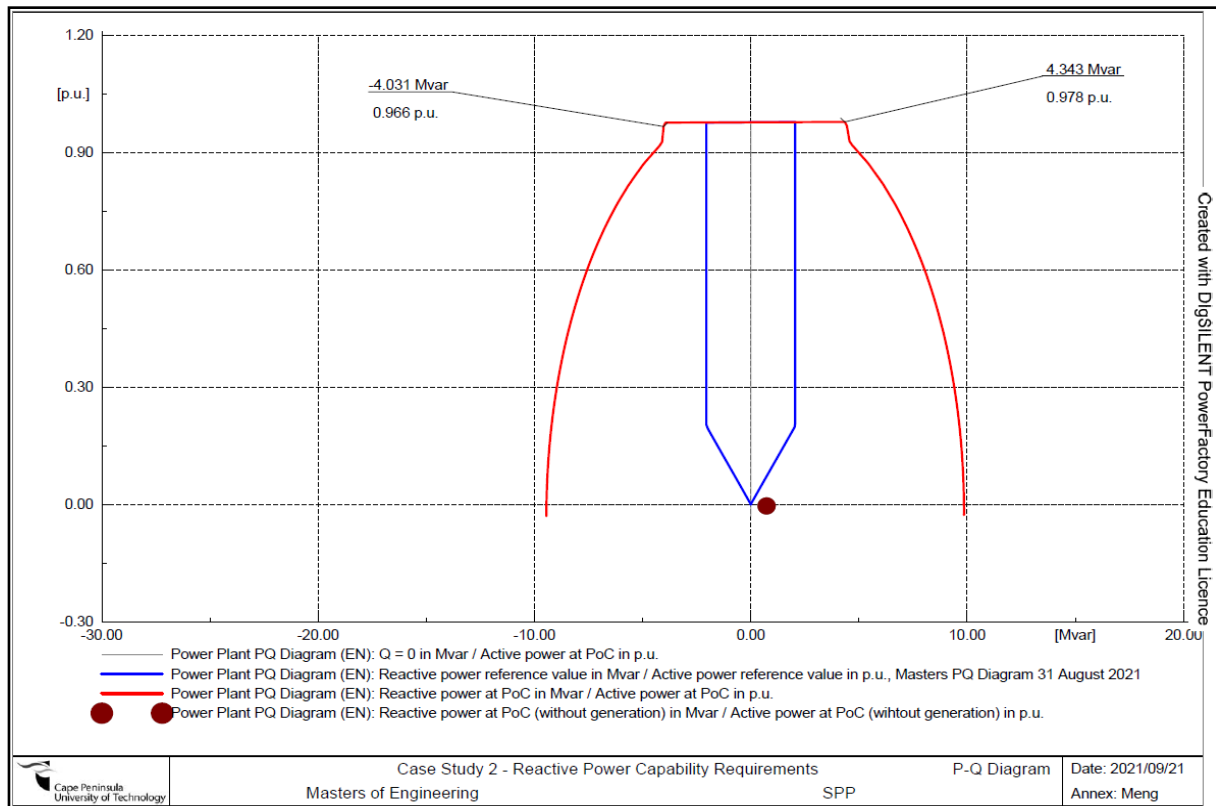


Figure 5.4: Case study–2 - full reactive power capability of the SPP

All conditions of the base case for case study 2 have been carried out for the reactive power capability and no concerns have been identified. In Figure 5.4, the SPP inverter capabilities

are sufficient for the requirements of the SAREGC with regards to the full reactive power capability requirements. The SPP can import reactive power during under exciting conditions to a maximum of -4.031 MVar and overexciting conditions resulting in a maximum export condition of 4.343 MVar.

5.3.2.2 Case study –B - optimization of SPP inverter for voltage capability

Continuing with the simulation methodology of the base case with optimized SPP inverter parameters, the results for voltage capability in study case 2 will indicate any violations indicated in the SAREGC. Table 5.4 indicates the results for the simulation in the network model and the results are documented in Appendix C in Figure C.42 to C.47

Table 5.4: Case study –B - requirements and results of voltage capability at the POC

Study Point	Requirements			Results from simulation						
	Real Power (% of Pmax)	Required Q at POC (%)	Required Q at POC (MVar)	Inverter reactive limit (Y/N)	Voltage at POC (p.u.)	Overloading/voltage violations in the SPP (Y/N)	P at POC (MW)	Q at POC (MVar)	Power Factor at POC	SAREGC requirement compliant (Y/N)
1	P=100 %	22.8 % import	2.052	N	1.1	N	9.0	2.052	0.975	Y
2	P=100 %	22.8 % import	2.052	N	1.0	N	9.0	2.052	0.975	Y
3	P=100 %	0 % import	0	N	0.9	N	9.0	0.000	1.000	Y
4	P=100 %	0 % export	0	N	1.1	N	9.0	0.000	1.000	Y
5	P=100 %	22.8 % export	2.052	N	1.0	N	9.0	-2.052	0.975	Y
6	P=100 %	22.8 % export	2.052	N	0.9	N	9.0	-2.052	0.975	Y

All conditions have been simulated for the voltage capability and the inverter overloading / voltage violations in the SPP is illustrated in Appendix C in Figure C.48 and C.49 for the study points 1 to 6 of the requirements. Although the 1.1 p.u. voltage level is seen as a temporary occurrence, the SPP inverter for that specific period will be subjected to an environment where the lifespan of the inverter will not be affected in terms of overloading in both study points. There were six different areas studied in Table 5.4 as per previous simulations, and all the study areas were compliant. The SPP are expected to support the utility grid in regard to the reactive power requirements. The study results of the voltage capability requirements were verified by additional simulations to determine if the voltage capability has been achieved. The results are shown in Figure C.50 of Appendix C. Both conditions are modelled and represent available a under excited reactive power capability of -3.834 MVar for import at the POC, whereas for overexcited conditions, the results indicate available reactive power capability of 4.358 MVar for export. The full voltage capability requirement of Figure 5.5 is illustrated, and it is not showing any violations to the utility grid of the SO.

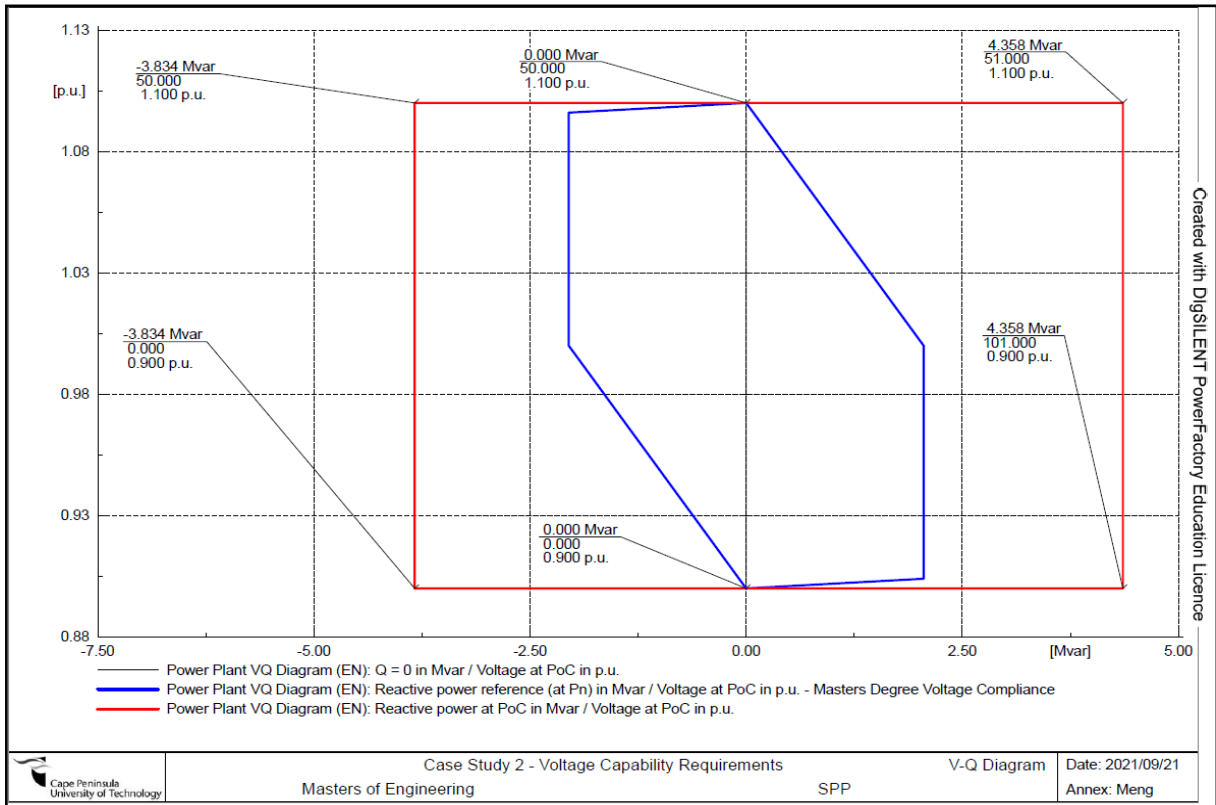


Figure 5.5: Case study-2 - full voltage requirement capability of the SPP

Under different p.u. voltages in steady-state condition simulations, each voltage level simulation in the network model produced a different result and is within acceptable limits for compliance.

5.3.3 Comparative analysis between case study 1 and case study 2

Both case studies with each mitigation technique identified have been proven to have no violations and is grid code compliant according to the SAREGC. The addition of an SPP inverter and the optimization of the inverter performance prove to be measures that can be implemented if a grid-connected SPP is subjected to any non-compliance challenges. All results obtained between case study 1 and 2 were very similar, but case study 1 had the overall best performance in terms of reactive power capability and voltage requirement capability in the full SPP spectrum as indicated in Table 5.5. When the case studies were compared to perform according to each individual requirement as per the SAREGC, the case studies did not introduce any violation or non-compliance.

Table 5.5: Case study 1 versus case study 2 – reactive power and voltage capability

Case Study	Full reactive power capability (MVar)	Full voltage requirement capability
1	-6.213 import and 5.448 export	-3.917 import and 2.865 export
2	-4.031 import and 4.343 export	-3.834 import and 4.358 export

According to Table 5.5 the capability of case study 1 is more desirable for performance and results, the only capability that case study 2 outperforms case study 1 is the export of reactive power during voltage requirement capability. During design stage the IPP should investigate the option of increasing the number of SPP inverters in the generation facility, if cost is not a concern and the LCOE is within normal electricity tariffs. Further investigation will be conducted by implementing the case study 1 mitigation technique for the power quality investigation.

5.3.4 SPP power quality mitigation techniques

For this case study scenario, the network model for case study 1 will be utilised as the benchmark. The IEEE standard association was implemented to provide design selection specifications and guidelines on the shunt filters for the user input in the PowerFactory network model of the SPP. Only the non-compliant studies that was identified in the previous chapter will be further investigated in this case study, thus only the harmonic load flow and the frequency sweep will be addressed to mitigate the non-compliance. In the previous chapter the harmonic analysis indicated a violation in the THD, which is a non-compliance according to the SAREGC. To mitigate the violation and not to negatively impact the utility grid in terms of power quality, the implementation of a shunt filter will be done at the gridbox of the SPP. The measurement of the harmonic load flow and frequency sweep will still be done at the POC during steady-state analysis.

5.3.4.1 Case study–3 - implementation of shunt filter for harmonic emission violations

As per the previous results illustrated in Figure 4.7 and Figure 4.8 the harmonic order violation occurred for the maximum fault current at the 39th harmonic order and for the minimum fault current, the highest harmonic distortion at the POC transpired at the 33rd order. According to the IEEE standard 18-2012, the applicable capacitor size for voltages ranging between 6350 V and 14 400 V is between 0.05 MVar and 0.8 MVar. The selection of the shunt filter was based on the highest rating available according to the application guide of the IEEE and is shown in Table 5.6 (IEEE Std 18, 2012). For the resonant frequency value, the selection was based on the average of the highest value of the maximum fault current and the highest value of the minimum fault current harmonic order, which is the 36th order. Furthermore, the resonant frequency was calculated by 36×50 Hz, which equals 1800 Hz and the quality factor at the resonant frequency is the harmonic order with the highest value. The quality factor of the shunt filter is the harmonic order that produces the greater than average voltage distortion, which in this case study would be the 36th harmonic order (IEEE Std 519, 2014) (IEEE Std 1036, 2020) (IEEE Std 1531, 2020). The technology of the shunt type filter is a R-L-C three-phase delta connection complete with a series resistor, inductor and capacitor with a fixed number of steps

in the network model. In Appendix B in Figure B.16, the illustration of the PowerFactory parameters including the terminal of the shunt filter implemented in the network model for SAREGC studies.

Table 5.6: Case study 3 – shunt filter 1 data

Shunt filter 1 – user selection			
Description	Values	Description	Values
Nominal voltage	11 kV	Rated reactive power	0.8 MVar
Technology	3PH-D	Resonant frequency	1800 Hz
Shunt type	RLC	Quality factor	36
Shunt filter 1 – resulting values			
Description	Values	Description	Values
Rated current	41.98911 A	Reactance	0.3503861 Ω
Susceptance	2202.156 uS	Inductance	1.115314 mH
Capacitance	7.009681 uF	Resistance	0.3503861 Ω

By implementing the shunt filter configuration as per Table 5.6, the results are shown in Figure 5.6 for the harmonic distortion for the maximum fault current at the POC.

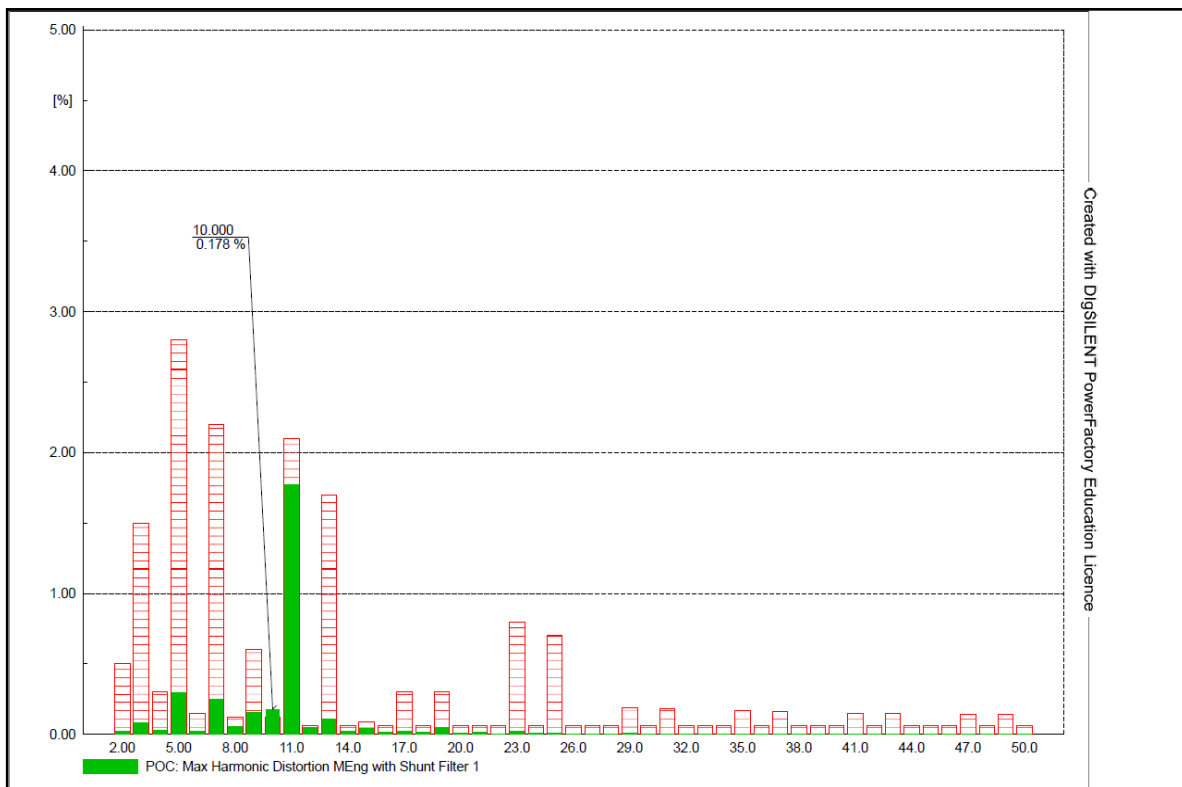


Figure 5.6: Case study–3 - harmonic distortion at the POC for maximum fault level with shunt filter 1 installed

According to Figure 5.6, the 11th harmonic orders exceed the allowable limits at maximum fault levels. The results were exported and is detailed in Appendix C in Table C.2, highlighting the harmonic orders that fail to meet the harmonic order requirements in red as per NRS 048-2

and NRS 048-4. Furthermore, a similar study was implemented for the minimum fault levels and is shown in Figure 5.6 with the detailed results also exported to Table C.2. Also, a harmonic load flow was carried out for maximum and minimum fault levels at the POC and the results are as follow: THD at the POC: 1.8 % (maximum fault level at POC) and 2.5 % (minimum fault level at POC). The result of the simulations is illustrated for maximum and minimum fault currents at the POC in Appendix C in Figure C.51 and Figure C.52, respectively.

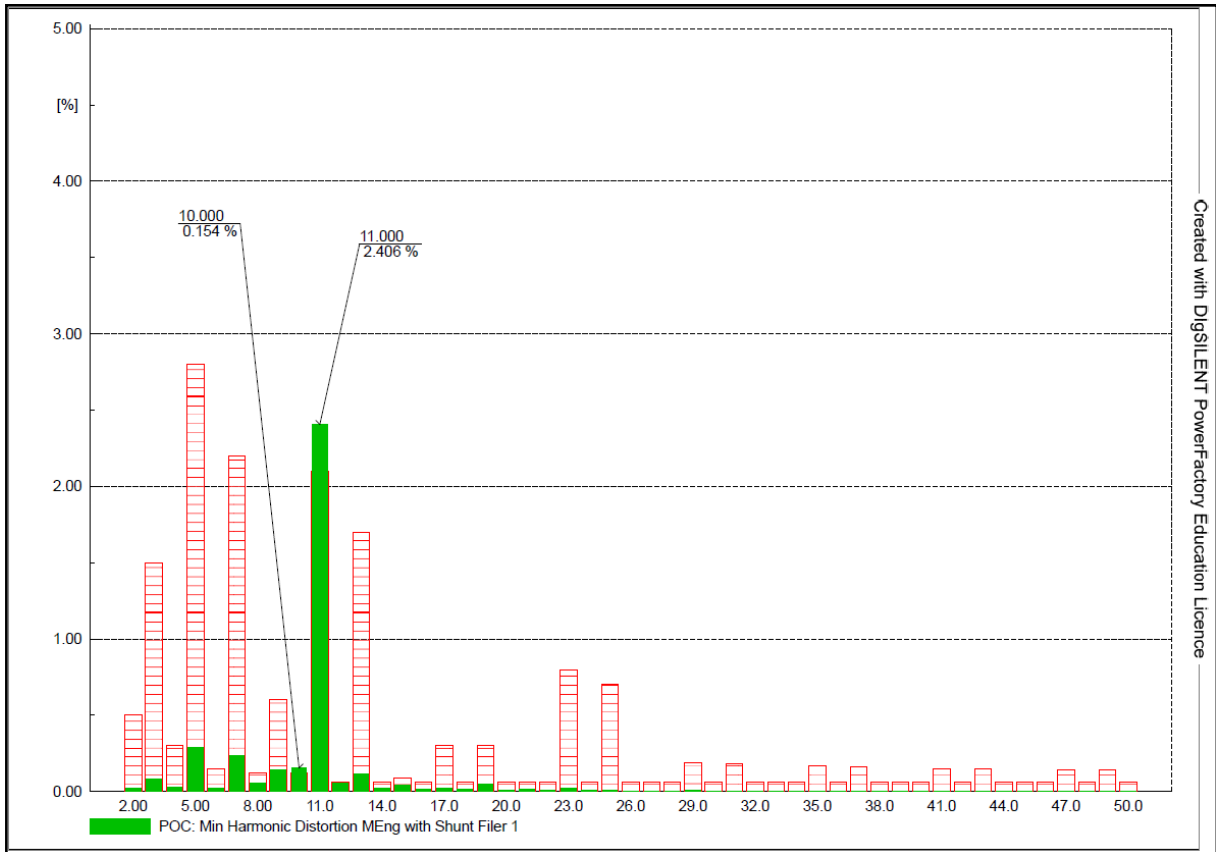


Figure 5.7: Case study–3 - harmonic distortion at the POC for minimum fault level with shunt filter 1 installed

By implementing the shunt filter 1, the violations occurred for both the maximum fault level and minimum fault level. Further investigation of the network model led to the installation of an additional shunt filter for an iterative approach to mitigate the non-compliance as shown in Figure 5.8.

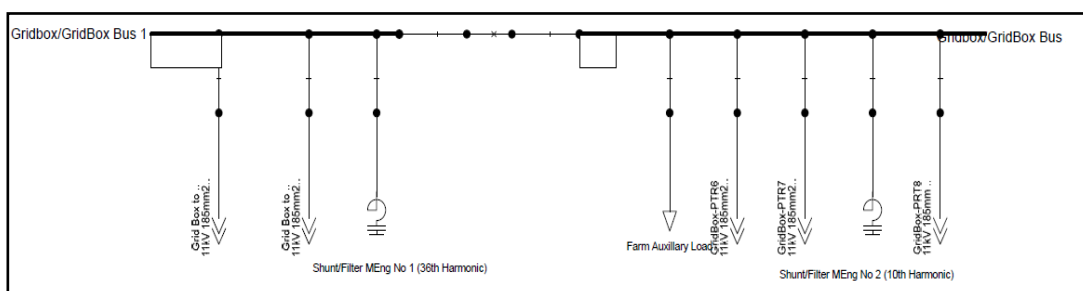


Figure 5.8: Case study 3 – Gridbox with shunt filter 1 and shunt filter 2 installed

By adding an additional shunt filter the possibility of eliminating any violations are increased, due to the enhancement in power quality. From the previous simulation results, the harmonic distortions shifted from higher harmonic orders to lower harmonic orders. The shift from between the 3rd-9th to the 10th and 11th harmonic order by adding shunt filter 1, triggered a requirement for an additional shunt filter. For the user selection values of the implementation of the shunt filter 2, the data of Figure 5.7 and Table C.2 is utilised. According to previous discussion the size of the capacitor will remain 0.8 MVar, but for this simulation compliance requirement, the capacitor had a fixed step switching for two capacitors, totalling the installed capacity as 1.6 MVar. The resonant frequency will be calculated as 10×50 Hz, which equals 500 Hz. The quality factor to be achieved should be on the 10th harmonic order as the specific harmonic order provides non-compliance at maximum and minimum fault level studies.

Table 5.7: Case study 3 – shunt filter 2 data

Shunt filter 1 – user selection			
Description	Values	Description	Values
Nominal voltage	11 kV	Rated reactive power	1.6 MVar
Technology	3PH-D	Resonant frequency	500 Hz
Shunt type	RLC	Quality factor	10
Shunt filter 1 – resulting values			
Description	Values	Description	Values
Rated current	83.97823 A	Reactance	2.291667 Ω
Susceptance	4363.637 uS	Inductance	7.294601 mH
Capacitance	13.88989 uF	Resistance	2.291667 Ω

Once the additional shunt filter 2 has been added to the network model, the simulations and results can be obtained for the SPP to verify compliance to the grid code. With the addition of the second shunt filter, the compliance was achieved of the SPP during maximum and minimum fault conditions. According to Figure 5.8 and Figure 5.9, both simulations for the harmonic distortions are within the allowable limits for the SAREGC compliance. The simulation results were exported from PowerFactory and is detailed in Appendix C in Table C.3, the harmonic orders are all within the limits of the NRS 048-2 and NRS 048-4.

The THD of the SPP was also verified again at the POC with the addition of the shunt filter 2 electrical components. A harmonic load flow carried out for compliance requirements is illustrated in Appendix C in Figure C.53 and Figure C.54 for the maximum and minimum fault currents, respectively. As per the simulation of the network model for the SPP the THD at the POC during maximum fault conditions are simulated as 0.8 % and for the minimum fault level contribution the THD at the POC is 0.7 %, which are all within acceptable voltage distortion limits. Values from the simulation indicated compliance to the SAREGC and the study case

can be further evaluated for the remaining power quality violations that occurred in the previous chapter.

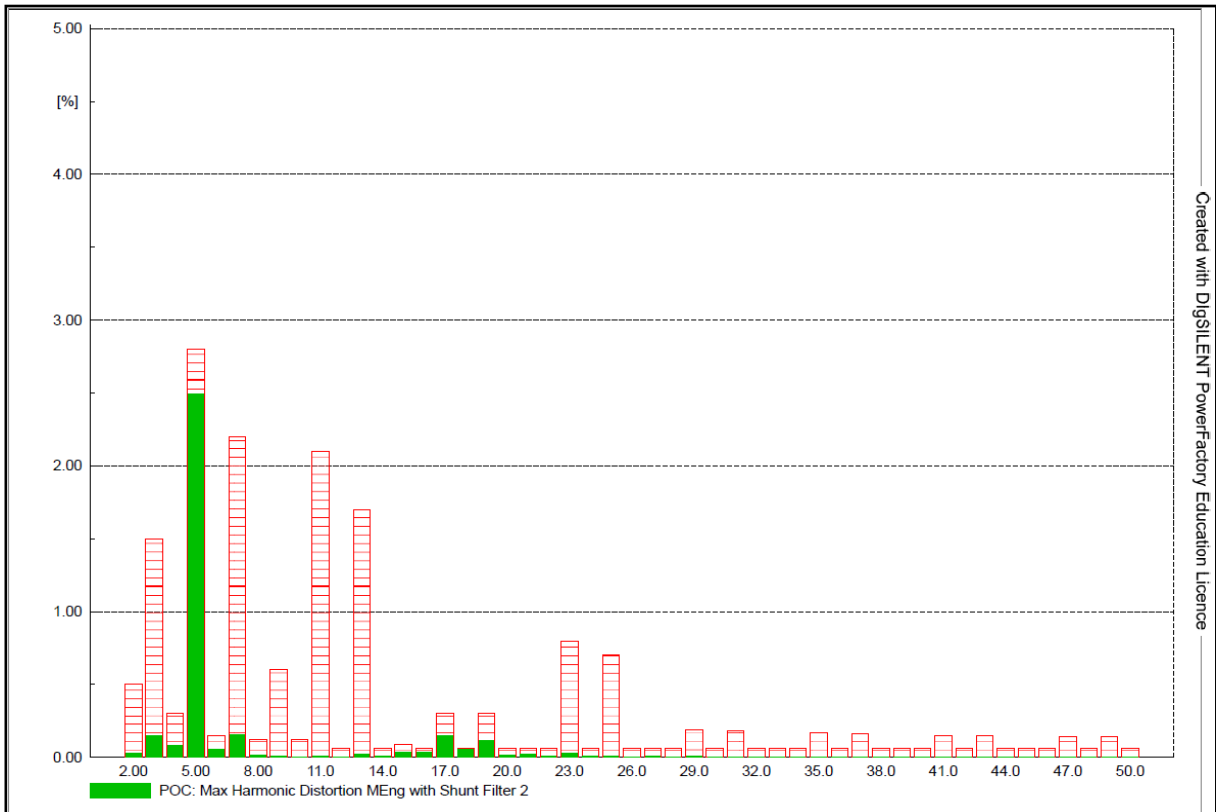


Figure 5.8: Case study–3 - harmonic distortion at the POC for maximum fault level with shunt filter 2 installed

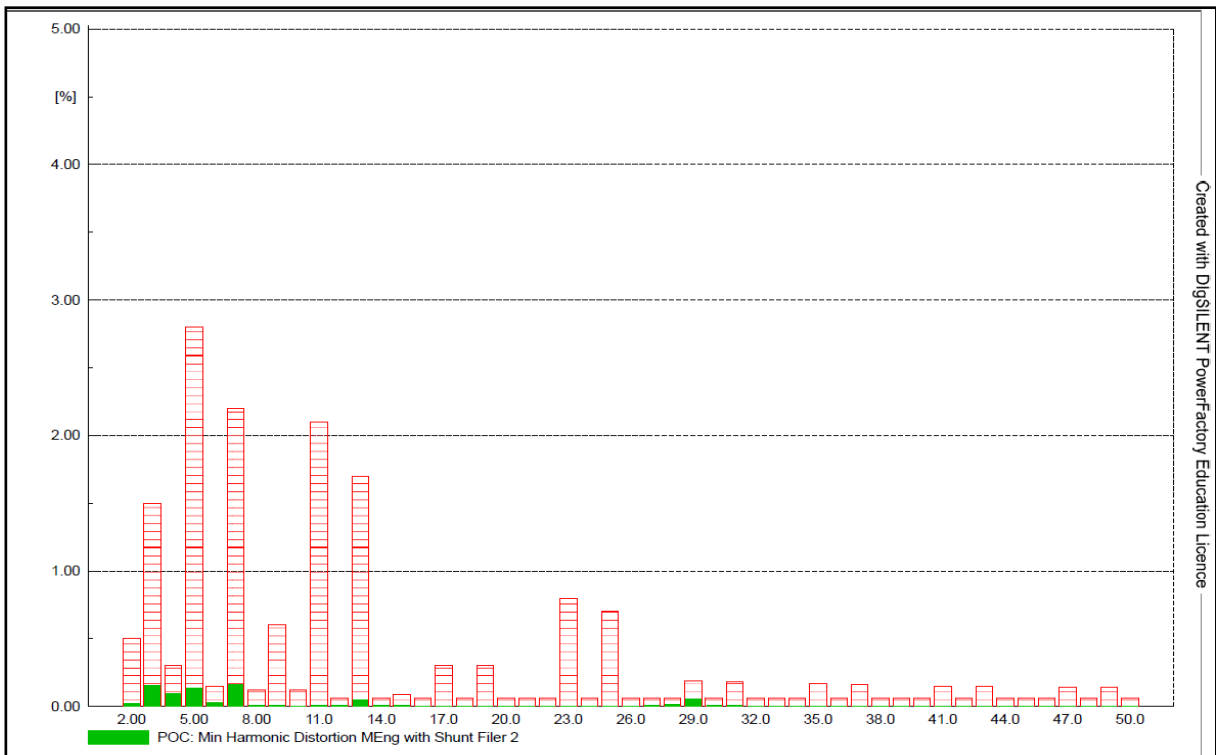


Figure 5.9: Case study–3 - harmonic distortion at the POC for minimum fault level with shunt filter 2 installed

5.3.4.2 Case study 3 – Frequency sweep with shunt filter 2

At the POC, a frequency sweep has been carried out to determine if any resonance points exist in the network model. Based on the results from the frequency scan in Figure 5.10, it is noted that a small parallel resonance can be detected at the POC, which is within the harmonic distortion limits of the SAREGC and NRS 048 requirements.

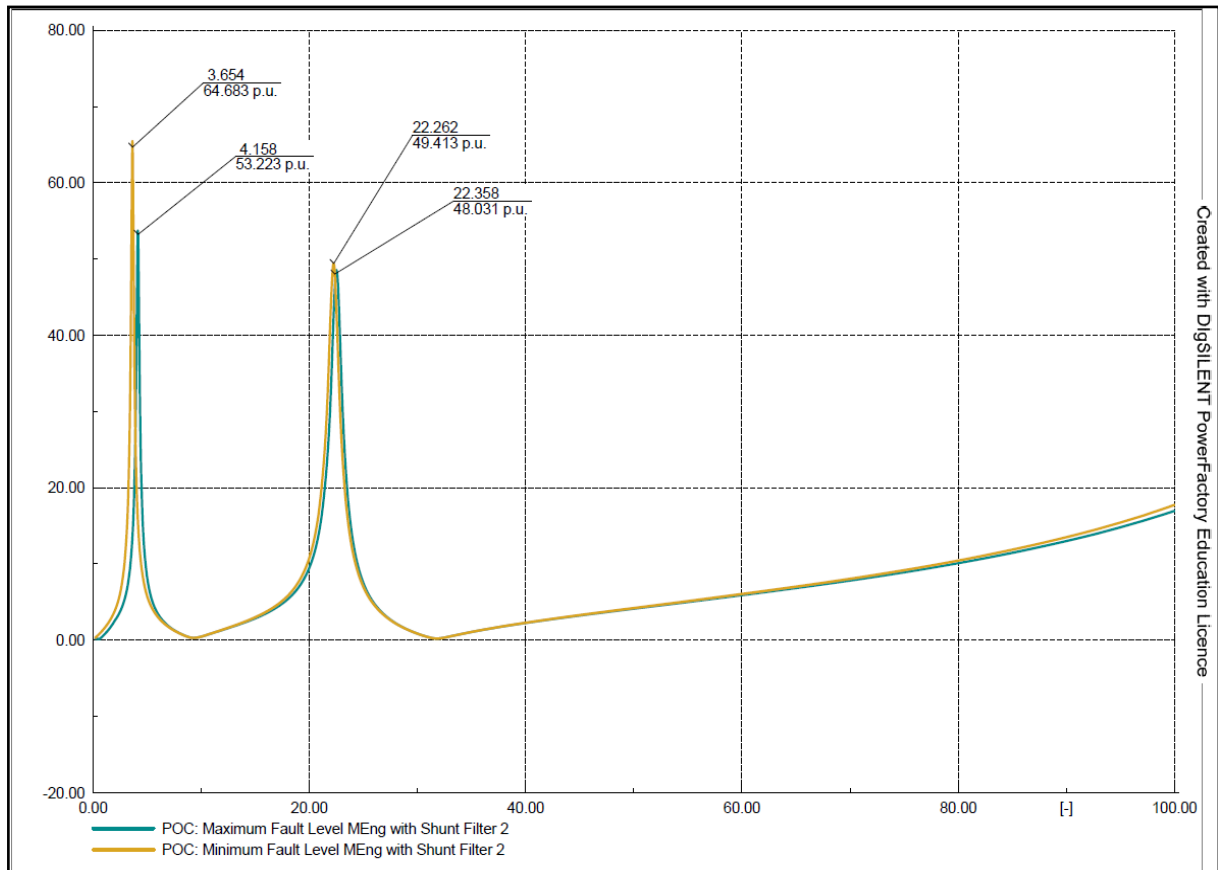


Figure 5.10: Frequency sweep from the POC with shunt filter 2

The impedance ratio X/R used by the power grid dictates how sensitive the resonance is to this impedance ratio. There may also be parallel resonances that may cause the maximum network impedance to not necessarily give the biggest harmonic distortion, thus, the assumption of 3x linear 50Hz impedance may not be accurate. Considering the results and compliance achieved at the SPP, it is no longer necessary to apply mitigation techniques to ensure compliance at the POC with the requirements of SAREGC.

5.4 Summary

An understanding of the main grid compliance challenges with electrical equipment were presented by studies in steady-state conditions to produce mitigation techniques when violations and non-compliance were present. The three case studies that was implemented

indicated all to be successful in enhancing the performance of the utility grid and contributes positively to compliance aspects to the requirements.

The first study case that was implemented was to ensure that the plant equipment namely the SPP inverters could perform within the reactive power capability of the requirements of the 9 MW SPP. Case study 1 proved to be successful with all the non-compliance factors being eliminated during the analysis, especially the overloading in the inverters LV terminals and the full reactive power capability of the SPP compliance. Also, in terms of the voltage capability requirements, the plant performance was within desirable limits for case study 1 during steady-state conditions. The second case study performed was the optimization of the SPP inverters reactive power capability. This was achieved by accordingly implementing safe operational parameters for the generic inverter model within PowerFactory with guidance from the WECC, IEEE, NRS and the SAREGC, which is all documented in the Appendix B in Table B.10A to Table B.11B. With all the compliance also achieved for case study 2, the next step was to provide a comparative analysis between the two case studies to determine which case study provides the best performance for the SPP grid code compliance. The results documented indicated that although both case studies are grid code compliant and enhances the utility grid performance in terms of reactive power capability and voltage capability requirements, the case study that performed the most favorable were case study 1 in the comparative analysis. Furthermore, case study 1 was implemented to further investigate the compliance requirements for power quality in terms of harmonic emissions and frequency sweeps. For the first initial case study 1 network model a shunt filter was introduced to eliminate the harmonic emissions and the parallel resonance points that was present in the network model. The study found that the addition of one shunt filter reduced the harmonic emission in the higher order but caused a violation in the lower order harmonics. To increase the power quality a second shunt filter was introduced in the gridbox to reduce the voltage distortion due to the harmonic emissions. The second shunt filter proved to be successful in reducing the harmonic distortion to an acceptable level and within the compliance requirement of the SAREGC, however the second shunt filter created two resonant points in the frequency sweep analysis. The two resonant point are well within the required limits of the NRS 048 requirements and propose no risk to the electrical equipment life expectancy and performance.

Studies in steady-state conditions are now used to develop mitigation techniques when violations and non-compliances with grid codes are encountered. This makes it possible to acquire a deeper understanding of the main challenges associated with grid code compliance. The mitigation techniques implemented was successful in obtaining compliance during the studies and is proven to change outcomes in the equipment performance as a SPP operating as a grid-connected generation facility connected to the utility grid.

CHAPTER SIX: CONCLUSIONS AND FUTURE WORKS

6.1 Conclusions

In this dissertation, the primary objective was to identify specific non-compliance factors, which become evident during the steady-state condition simulation and may hinder the successful connection of a SPP to a utility grid. As a second objective, the investigated mitigation techniques were applied to the identified non-compliance factors, enabling IPPs to successfully connect to the grid and achieve significant cost and time savings. At the POC, the utility grid information was implemented to imitate the performance of the specific SPP connection. Analysing the full SPP model as a steady-state operation case highlighted the potential non-compliance factors. A steady-state study was done for the integration of SPP into the utility grid, which included an analysis of the reactive power capabilities of the inverters when compared with the grid parameters. The SPP was able to absorb- or inject reactive power within the power factor range required by the existing regulations, which varied with plant size and maximum export capacity. The compliance simulations involved the reactive power capability of the SPP inverter and having the inverter alleviate the power factor. Keeping the desired parameters within the threshold, while delivering either an under excitation or an over excitation condition to the grid. In addition to studying the reactive power capability, steady-state studies had to look at the voltage requirements of the SPP. For the SPP, power quality studies were also conducted at the POC and documented according to the power quality requirements in South Africa as set forth in the NRS 048. The contributing factor to the harmonic spectrum at the POC from the utility grid has an impact on the ability of the SPP inverter to reduce the harmonic emissions in the utility grid and SPP network. The dissertation continued to focus on the steady-state simulations of GCC factors that might obstruct the pl'nt's connection to the national grid of South Africa and provide possible mitigation techniques. In addition, the GCC studies indicated the methods to use in the SPP design to ensure compliance with the SAREGC and RETEC to help avoid delays in the design process. In this dissertation, the framework focuses on the steady-state SAREGC requirements and simulation studies for one SPP within the utility grid of SA. Simulations and identification of non-compliance factors were done only for Category B SPPs. As a result of simulations and modelling of the network model, beneficial factors were identified that may lead to easier grid integration. Standards and specifications from NRS, SANS, IEEE, and WECC were used to consider the factors contributing to GCC. The SPP was evaluated for its reactive power capabilities to determine if the SPP can inject or absorb the reactive power required when it must comply with certain control modes required by the SAREGC. While performing the reactive power analysis, the 'PP's voltage requirements were covered as well. Based on the conditions to be met in steady-state simulations of the network model, power quality studies

were also conducted to determine if any violations have occurred. The first case study for the mitigation techniques that was implemented was for the addition of an additional 720 kVA SPP inverter to increase plant size but keep the MEC at 9 MEC. This was to ensure that the SPP can provide the reactive power capability and voltage capability requirements. Both non-compliance factors were resolved during case study 1 and the SPP performance enhanced the utility grid's parameters. For case study 2, the reactive power capability of the SPP inverter was adjusted to within maximum allowable safe operation range when the SPP was instructed by the PPC to perform within the ranges of the power factor at the POC. Both case studies were found to be adequate for the non-compliance risk reduction to the SPP and both scenarios can be implemented for remedial action requirements. A comparative analysis between case study 1 and case study 2 resulted in case study 1 to be further investigated with power quality studies. The power quality studies that was carried out included the harmonic emissions at the POC, voltage flicker disturbance factors for short-term and long-term switching during continuous and switching conditions in the network model. Frequency scans was also conducted at the POC to determine if any resonance and violations was present during maximum and minimum fault conditions. It was found that two shunt filters had to be implemented at the gridbox to adhere to the SAREGC for category B SPPs. Once all mitigation techniques were applied to the network model, the overall assessment was presented with detail findings and indicated that all non-compliance factors were mitigated.

6.2 Future works

As a part of the network model study, which included both the SPP and utility grid as two components that have an impact on each other's performance, several researchable aspects were identified that may be pursued further by IPPs, power system engineers, and solar PV engineers. According to the results of the three case studies, mitigation techniques are readily available before the SPP project has been finalized if the utility grid parameters are known to prevent grid code violations. There is therefore a need to address the non-compliance factors that may possibly impose a connection risk to the utility grid by introducing methods to elevate the performance of the SPP. As a result of this research, which goes beyond the steady-state analysis, it will be possible to conduct more intensive analyses of dynamic power system modelling. Especially on the detailed design of a tuned shunt filter for power quality during dynamic studies. Further research on how dynamic analysis is performed in a network simulation model can be investigated by introducing the renewable energy technology to utility grid parameters, which may contribute to non-compliance and techniques can be research on how to obtain compliance. It is a natural follow-up of this research to proceed in the simulation of the dynamic environment of a SPP or any other renewable energy technology, which presents new challenges to be investigated and solved in a category B or category C plant.

REFERENCES

- Aberdare, 2008. *Aberdare*. [Online]
Available at: <https://www.aberdare.co.za/product-categories/intermediate-voltage/>
[Accessed 18 August 2021].
- Alhussainy, A. & Alquthamni, T., 2020. Power quality analysis of a large grid-tied solar photovoltaic system. *Sage Publishing transactions on Advances in Mechanical Engineering*, 12(7), pp. 1-14.
- Aljarrah, R., Marzooghi, H., Terzija, V. & Yu, J., 2019. Modifying IEC 60909 Standard to Consider Fault Contribution from Renewable Energy Resources Utilizing Fully-Rated Converters. *IEEE*, pp. 1-6.
- Andrew Craib, 2013. *Standard for The Interconnection of Embedded Generation*. [Online]
Available at: <https://www.sseg.org.za/wp-content/uploads/2019/03/Standard-for-Interconnection-of-Embedded-Generation-Eskom-doc.pdf>
[Accessed 01 May 2021].
- Arshad, A. & Lehtonen, M., 2019. A comprehensive voltage control strategy with voltage flicker compensation for highly PV penetrated distribution networks. *Elsevier transaction on Electric Power System Research*, Volume 172, pp. 105-113.
- Barnes, A. K., Tabarez, J. E., Mate, A. & Bent, R. W., 2021. Optimization-Based Formulations for Short-Circuit Studies with Inverter-Interfaced Generation in PowerModelsProtection.jl. *Energies*, 2160(14), pp. 1-27.
- Bassam, N. E., 2021. *Distributed Renewable Energies for Off-Grid Communities*: 2nd ed. Amsterdam: Elsevier.
- Bullich-Massague, E. et al., 2015. Power Plant Control in Large-scale Photovoltaic Plants: Design, Implementation and Validation in a 9.4MW Photovoltaic Plant. *IET transactions on Renewable Power Generation*, 10(1), pp. 50-62.
- Cabrera-Tobar, A., Bullich-Massague, E., Aragues-Penalba, M. & Gomis-Bellmunt, O., 2019. Active and Reactive Power Control of a PV Generator for Grid Code Compliance. *Energies*, 12(3872), pp. 1-25.
- Castro, L. M., Rodriguez-Rodriguez, J. & Martin-del-Campo, C., 2020. Modelling of PV systems as distributed energy resources for steady-state power flow studies. *Elsevier transactions on Electrical Power and Energy Systems*, Issue 115, pp. 1-9.
- Chmielewski, T. et al., 2021. Modified repetitive control based on comb filters for harmonic control in grid-connected applications. *Elsevier transaction on Electric Power System Research*, 200(107412), pp. 1-11.
- de Beer, B. & Rix, A., 2017. *Network Strengthening Using Storage Support: A Case for Increasing Remote Generation*. Stellenbosch, IEEE Africon 2017.
- Department of Mineral Resources and Energy, 2019. *Energy.gov.za*. [Online]
Available at: <http://www.energy.gov.za/IRP/2019/IRP-2019.pdf>
[Accessed 01 May 2021].
- Diaz-Araujo, M. H., Medina-Rios, A., Madrigal-Martinez, M. & Cleary-Balderas, L. A., 2019. Analysis of Grid-Connected Photovoltaic Generation Systems in the Harmonic Domain. *Energies*, 12(4785), pp. 1-14.

- DigSILENT GmbH, 2020. *DigSILENT Power System Solutions*. [Online]
Available at:
https://www.digsilent.de/en/downloads.html?folder=files%2Fdownloads%2Fpublic%2F10_PowerFactory#navigation573
[Accessed 15 July 2021].
- Dinu, E.-D. et al., 2016. *Voltage - Reactive Power Control in Renewable Power Plants: Technical requirements applied in the Romanian power grid*. Cluj-Napoca, IEEE transactions on International Conference on Automation, Quality and Testing, Robotics (AQTR).
- DoE, 2019. *Integrated Resource Plan (IRP2019)*, Pretoria: Department of Energy: Republic of South Africa.
- Dunlop, J. P., 2010. *Photovoltaic Systems* 2nd ed. Illinois: American Technical Publishers, INC.
- Dursun, M. & Dosoglu, M. K., 2018. *LCL Filter Design for Grid Connected Three-Phase Inverter*. Duzee, IEEE, pp. 1-4.
- Eberhard, A., 2014. *Realise that Eskom Alone Cannot Solve Our Power Crisis*. [Online]
Available at: <http://www.gsb.uct.ac.za/files/RealiseEskomAloneCannotSolvePowerProblem.pdf>
[Accessed 01 May 2021].
- Eberhard, A., Gratwick, K., Morella, E. & Antmann, P., 2017. Independent Power Projects in Sub-Saharan Africa: Investment trends policy lessons. *Elsevier transactions on Energy Policy*, Volume 108, pp. 390-424.
- Eberhard, A. & Naude, R., 2016. The South African Renewable Energy Independent Power Producer Procurement Programme: A review and lessons learned. *SciELO transactions on the Journal of Energy in Southern Africa*, 27(43), pp. 1-14.
- Effatnejad, R. et al., 2017. Reactive Power Control in Wind Power Plants. In: N. M. Tabatabaei, A. J. Aghbolghi, N. Bizon & F. Baabjerg, eds. *Reactive Power Control in AC Power Systems*. Cham: Springer, pp. 191-225.
- Elshahed, M., 2017. *Complying Grid-Connected Wind Farm According to the Requirements of Utility Grid Code Using STATCOM*. Manama, IEEE transaction on .
- Eskom, 2018. *Eskom Transmission Development Plan 2019 to 2028*. [Online]
Available at:
https://www.eskom.co.za/Whatweredoing/TransmissionDevelopmentPlan/Pages/Transmission_Development_Plans.aspx
[Accessed 01 May 2021].
- Eskom, 2021. *Eskom*. [Online]
Available at: <https://www.eskom.co.za/CustomerCare/NewSupply/Pages/SelfBuild.aspx>
[Accessed 02 May 2021].
- Feldman, D. & Vasques de Oliveira, R., 2021. Operational and control approach for PV power plants to provide inertial response and primary frequency control support to power system black-start. *Elsevier transaction on International Journal of Electrical Power and Energy Systems*, 127(106645), pp. 1-13.
- Ghani, A., Ramachandramurthy, V. & Ying Yong, J., 2021. *Design of a master power factor controller for an industrial plant with solar photovoltaic and electric vehicle chargers*. Selangor, Springer, pp. 1-13.

- Gokmen, N., Hu, W. & Chen, Z., 2017. *A Simple PV Inverter Power Factor Control Method Based on Solar Irradiance Variation*. Manchester, IEEE.
- Gonzalez-Longatt, F. M., Acosta, M. N., Chamorro, H. R. & Torres, J. L. R., 2021. Power Converters Dominated Power Systems. In: F. Gonzalez-Longatt, ed. *Modelling and Simulations of Power Electronic Converter Dominated Power Systems in PowerFactory*. Zurich: Springer, pp. 1-35.
- Gonzalez-Longatt, F. M. et al., 2014. Implementation of Simplified Models of Local Controller for Multi-terminal HVDC Systems in DigSILENT PowerFactory. In: F. Gonzalez-Longatt & J. Rueda, eds. *PowerFactory Applications for Power System Analysis*. Zurich: Springer, pp. 447-472.
- Grunau, S. & Fuchs, 2012. *Effect of Wind-Energy Power Injection into Weak Grids*. Kiel, EWEA - European Wind Energy Association Conference.
- Hussain, M. W. & Qureshi, M. A., 2021. *Analysis and Design of Passive Filters for Power Quality Improvement in 3 ϕ Grid-Tied PV Systems*. Lahore, IEEE.
- IEEE Std 1036, 2020. IEEE Guide for the Application of Shunt Power Capacitors. *IEEE Power and Energy Society*.
- IEEE Std 1531, 2020. IEEE Guide for the Application and Specification of Harmonic Filters. *IEEE Power and Energy Society*.
- IEEE Std 18, 2012. IEEE Standard for Shunt Power Capacitors. *IEEE Power and Energy Society*.
- IEEE Std 519, 2014. IEEE Recommended Practice and Requirements for Harmonic Control in Electric Power Systems. *IEEE Power and Energy Society*.
- IEEE Std C57.159, 2016. IEEE Guide on Transformers for Application in Distributed Photovoltaic (DPV) Power Generation Systems. *IEEE Power and Energy Society*.
- IEEE, 2000. The Authoritative Dictionary of IEEE Standard Terms: 7th Edition. *IEEE*, December, pp. 1-1363.
- Iorgulescu, M. & Ursu, D., 2017. Reactive Power Control and Voltage Stability. In: N. M. Tabatabaei, A. J. Aghbolghi, N. Bizon & F. Baabjerg, eds. *Reactive Power Control in AC Power Systems*. Cham: Springer, pp. 227-248.
- Irazabal, I. et al., 2017. *Grid Code Compliant Controllers for Multi-terminal HVDC Grids Aimed to Integrate Wind Power: Assessing their Impact on the Operational Security of a Real-world System*. Cardiff, Elsevier transactions on the 9th International Conference on Applied Energy, ICAE2017, pp. 2165-2170.
- Jiang, M. et al., 2021. Reactive power characteristics and vibration properties under SISC in synchronous condensers. *Elsevier transaction on International Journal of Electrical Power and Energy Systems*, 133(107318), pp. 1-12.
- Kabalci, E., 2020. Review on novel single-phase grid-connected solar inverters: Circuits and control methods. *Elsevier transaction on Solar Energy*, Issue 198, pp. 247-274.
- Karbouj, H., Rather, Z. H. & Pal, B., 2021. Adaptive voltage control for large scale solar PV power plant considering real life factors. *IEEE transactions on Sustainable Energy*, 2(12), pp. 990-998.
- Khoshkhoo, H., Bourachalou, R. R. & Pouryetka, A., 2021. Integratoin of Large-Scale Photovoltaic Power Plants into Power Networks to Maintain System Stability. In: F. Gonzalez-Longatt, ed. *Modelling and Simulation of Power Electronic Converter Dominated Power Systems in PowerFactory*. Zurich: Springer, pp. 37-66.

Kunte, R., Pallem, C. & Mueller, D., 2012. *Wind Plant Reactive Power and Voltage Compliance with Grid Codes*. Knoxville, IEEE transactions on Power Electronics and Machines in Wind Applications, pp. 1-4.

Liu, Q. et al., 2020. *Confidence Analysis Method for Cable Distributed Parameter Model based on Verification and Validation*. Beijing, IEEE MTT-S International Conference on Numerical Electromagnetic and Multiphysics and Optimization.

Lund, H., 2010. *Renewable Energy Systems: The Choice and Modeling of 100% Renewable Solutions*: 1st ed. London: Academic Press (Imprint of Elsevier).

Maharjan, M. et al., 2021. Overvoltage Prevention and Curtailment Reduction Adaptive Droop-Based Supplementary Control in Using Smart Inverters. *MDPI transactions on Applied Sciences* , 11(7900), pp. 1-16.

Marais, Z., Rens, J., Peterson, B. & Botha, G., 2018. *Measurement uncertainty of current harmonics during the assessment of compliance to grid code requirements*. Potchefstroom, IEEE.

Marzbali, A. G. et al., 2017. Optimal Reactive Power Control to Improve Stability of Voltage in Power Systems. In: N. M. Tabatabaei, A. J. Aghbolghi, N. Bizon & F. Baabjerg, eds. *Reactive Power Control in AC Power Systems*. Cham: Springer, pp. 251-273.

McGranaghan, M. & Beaulieu, G., 2006. *Update on IEC 61000-3-6: Harmonic Emission Limits for Customers Connected to MV, HV, and EHV*. Montreal, IEEE transaction on Transmission and Distribution Conference and Exhibition.

Mchunu, T., 2020. *NERSA - Electricity Grid Code*. [Online]
Available at: <https://www.nersa.org.za/electricity-overview/electricity-grid-code/>
[Accessed 01 July 2021].

Meral, M. E. & Celik, D., 2021. Mitigation of DC-link voltage oscillations to reduce size of DC-side capacitor and improve lifetime of power converter. *Elsevier transaction on Electric Power Systems Research*, 194(107048), pp. 1-14.

Meteo Control, 2021. *Meteo Control*. [Online]
Available at: <https://www.meteocontrol.com/en/scada-plant-control/solutions/power-plant-controller-ppc>
[Accessed 31 May 2021].

Minnaar, U. et al., 2018. Power Quality Grid Code Compliance for Renewable Power Plants in South Africa. *IET transaction on Generation, Transmission and Distribution*, Volume 13, pp. 137-144.

Monyei, C., Jenkins, K., Viriri, S. & Adewumi, A., 2018. Policy discussion for sustainable integrated electricity expansion in South Africa. *Elsevier transaction on Energy Policy*, Volume 120, pp. 132-143.

Nhlapo, B. & Awodele, K., 2020. *Review and comparison of the South African grid code requirements for wind generation with the European countries' grid codes*. s.l., IEEE.

Nobela, O. N., Bansal, R. C. & Justo, J. J., 2019. A review of power quality compatibility of wind energy conversion systems with the South African utility grid. *Elsevier transaction on Renewable Energy Focus*, Volume 31, pp. 63-72.

NRS 048-2, 2007. *Part 2: Voltage Characteristics, Compatibility Levels, Limits and Assessment Methods*, Pretoria: NRS.

NRS 048-4, 2004. *Part 4: Application Guidelines for Utilities*, Pretoria: NRS.

- Nwagwe, K., Mutabilwa, P. & Dintwa, E., 2019. An overview of solar power (PV systems) integration into electricity grids. *Elsevier transaction on Materials Science for Energy Technologies*, Volume 2, pp. 629-633.
- Oskouei, M. & Mohammadi-Ivatloo, B., 2020. Introduction to Techno-Economic Assessment of Renewable Energy Source. In: *Integration of Renewable Energy Sources Into the Power Grid Through PowerFactory*. Cham: Springer, pp. 1-19.
- Pachanapan, P., 2021. Dynamic Modelling and Simulation of Power Electronic Converter in DigSILENT Simulation Language (DSL): Islanding Operation of Microgrid System with Multi-energy Sources. In: F. Gonzalez-Longatt & J. Torres, eds. *Modelling and Simulation of Power Electronic Converter Dominated Power Systems in PowerFactory*. Zurich: Springer, pp. 67-89.
- Raikar, S. & Adamson, S., 2020. *Renewable Energy Finance - Theory of Practice* 1st ed. London: Academic Press (Imprint of Elsevier).
- Rajput, S. K. & Dheer, D. K., 2020. Mathematical modelling and experimental validation for impact of high solar cell temperature on transformer loading and life. *Elsevier transactions on Renewable Energy Focus*, pp. 1-28.
- Rakhshani, E. et al., 2019. Integration of Large Scale PV-Based Generation into Power Systems: A Survey. *Energies*, 12(1425), pp. 1-19.
- Rodrigues, E. et al., 2016. Grid Code Reinforcements for Deeper Renewable Generation in Insular Energy Systems. *Elsevier transaction on Renewable and Sustainable Energy Reviews*, Volume 53, pp. 163-177.
- Rohmat, N. et al., 2019. *Design and Implementation of Three-Phase Grid-Connected Inverter for PV System*. Surabaya, IEEE.
- Say, M. & Laughton, M., 2003. Network Analysis. In: *Electrical Engineer's reference book*. s.l.:Elsevier, pp. 1-43.
- Sewchurran, S. & Davidson, I., 2016. Guiding Principles for Grid Code Compliance of Large Utility Scale Renewable Power Plant Integration onto South Africa's Transmission/Distribution Networks: *5th International Conference on Renewable Energy Research and Application (IEEE)*, pp. 528-537.
- Sewchurran, S. & Davidson, I., 2017. Introduction to the South African Renewable Energy (Part I - Introduction). *IEEE*, Volume IEEE Africon 2017 Proceedings, pp. 1220-1224.
- Sewchurran, S. & Davidson, I., 2017. Introduction to the South African Renewable Energy (Part II – Grid Code Technical Requirements). *IEEE*, Volume IEEE Africon 2017 Proceedings, pp. 1225-1230.
- Shi, Y., Sun, Y., Liu, J. & Du, X., 2021. Model and stability analysis of grid-connected PV system considering the variation of solar irradiance and cell temperature. *Elsevier transaction on Electrical Power and Energy Systems*, 132(107155), pp. 1-13.
- Smit, R., 2015. *EE Publishers*. [Online]
Available at: <https://www.ee.co.za/article/holistic-view-grid-integration-renewable-energy-generation.html>
[Accessed 02 May 2021].
- Taggart, D., Hao, K., Jenkins, R. & van Hatten, R., 2018. *Power Factor Control for Grid-Tied Photovoltaic Solar Farms*. Gangtok, CIGRE-AORC.

- Testa, A., Caro, S. D., Torre, R. L. & Scimone, T., 2012. A probabilistic approach to size step-up transformers for grid connected PV plants. *Elsevier transaction on Renewable Energy*, Volume 48, pp. 42-51.
- Turksoy, A., Hames, Y., Teke, A. & Latran, M. B., 2018. A novel adaptive switching method to reduce DC-Link capacitor ripple in PV based grid-connected inverter. *Elsevier transaction on Solar Energy*, Volume 173, pp. 702-714.
- Vokony, I., Hartmann, B. & Dan, A., 2012. *Developing a Dynamic Smart Grid Model*. Santiago de Compostela, Elsevier transactions on European Association for the Development of Renewable Energies, Environment and Power Quality (EA4EPQ).
- Volcko, V., Eleschova, Z., Bealn, A. & Janiga, P., 2012. *Mathematical Model of Three Winding Autotransformer*. Tatranske Matliare, Elsevier transactions on The 11th International Scientific Conference on Control of Power Systems.
- Vrana, T. K., Attya, A. & Trilla, L., 2021. Future-oriented generic grid code regarding wind power plants in Europe. *Elsevier transaction on Electrical Power and Energy Systems*, 106490(125), pp. 1-13.
- Yilmaz, S. & Dincer, F., 2017. Impact of inverter capacity on the performance in large-scale photovoltaic power plants – A case study for Gainesville, Florida. *Elsevier transaction on Renewable and Sustainable Energy Reviews*, Volume 79, pp. 15-23.
- Yongning, C. et al., 2019. *Study on Grid-connected renewable energy grid code compliance*. Beijing, IEEE transactions on Sustainable Power and Energy Conference (iSPEC).
- Yuill, W. & Carter-Brown, C., 2016. Enhancing Grid Code Compliance Assessment of Renewable Power Plants. *Energize Renewable Energy*, March, pp. 35-37.
- Zheng, T., Zhao, J., Zhao, F. & Litvinov, E., 2012. *Operational flexibility and system dispatch*. San Diego, IEEE transaction on Power and Energy Society.

APPENDICES

APPENDIX A: PUBLICATION SELECTION WITH THE ABSTRACTS

Paper A.1

Duvenhage, T.J., Abo-Al-Ez. 2021, December. Mitigation Techniques for Non-Compliance Challenges of a Grid-Connected Photovoltaic Plant. In 2021 4th International Symposium on Advance Electrical and Communication Technologies (ISAECT) (pp. 01-05). IEEE.

<https://ieeexplore.ieee.org/document/9668415>

Abstract — This paper presents information regarding the requirements for connecting a solar photovoltaic plant (SPP) to the South African (SA) utility grid according to the South African renewable energy grid code (SAREGC). A network model will be presented in DIgSILENT PowerFactory, which includes the utility grid and the connection of a grid-connected SPP. An objective will be to confirm the performance parameters of an inverter model within a designed network for possible non-compliance factors of a Category B SPP that may arise during grid code compliance (GCC) simulations in a steady-state environment. The mitigation techniques that will be implemented could provide insight to independent power producers (IPPs) to overcome any non-compliance challenges. These non-compliances may be detected from steady-state power system analysis studies performed for reactive power capability, voltage capability requirements or power quality, which might affect the normal operating conditions of the utility grid.

Keywords — grid code compliance, mitigation techniques, non-compliance challenges, solar photovoltaic plant, steady-state studies.

APPENDIX B: POWERFACTORY NETWORK MODEL DATA

Equipment data obtained from the SAREGC, NRS, IEEE and WECC for solar PV power plant modelling and validation guidelines. The information of the simulation elements is provided in Table B.1 and B.2

Table B.1: External grid parameters for a SPP in PowerFactory

Maximum values		Minimum values	
Description	Values	Description	Values
Short-circuit power $S_{k''}$ max	99.0733 MVA	Short-circuit power $S_{k''}$ max	85.73651 MVA
Short-circuit current $I_{k''}$ max	5.2 kA	Short-circuit current $I_{k''}$ max	4.5 kA
c-factor	1.1	c-factor	1
X/R ratio	8.353742	X/R ratio	9.140174
Maximum impedance ratios		Minimum impedance ratios	
Z2/Z1	1	Z2/Z1	1
X0/X1	19.48	X0/X1	17.018
R0/X0	1.998	R0/X0	1.998

Table B.2: AC voltage source values for steady-state simulations

Positive sequence		Negative sequence	
Description	Values	Description	Values
Voltage magnitude	1 p.u.	Voltage magnitude	1 p.u.
Resistance, R1	0.154 Ω	Resistance, R2	0.154 Ω
Reactance, X1	1.285 Ω	Reactance, X2	1.285 Ω
Voltage level	11 kV	Voltage level	11 kV
External control	PPC	External control	PPC

Information of the electrical equipment is provided in Table B.3 and B.5

Table B.3: Cable data used in the network model (Aberdare, 2008)

Description of cable: 11kV, 185mm ² , 3-core, Copper, PILC			
Description	Values	Description	Values
Rated current ground	339 A	Rated current air	378 A
AC resistance at 20 °C, R1&R2	0.1203 Ω	AC resistance at 20 °C, R0	1.4001 Ω
Reactance, X1&X2	0.093 Ω	Reactance, X0	0.0383 Ω
Voltage level	11 kV	Voltage level	11 kV
Maximum operating temperature	70 °C	External control	PPC
Capacitance, C1&C2	716 nF/km	Earth-fault current, I_{f0}	1.43 A/km
Conductance, G1&G2	0 uS/km	Conductance, G0	0 uS/km
Inductance, L1&L2	0.296 mH/km	Inductance, L0	0.121 mH/km

Table B.4: Cable lengths in the network model

Destination	Distance
Grid box circuit 1 - POC	775 m
Grid box circuit 2 - POC	775 m
Grid box – PTR 6	507.03 m
PTR 6 – PTR 4	94.3 m
PTR 4 – PTR 2	94.3 m
PTR 2 – PTR 1	94.3 m
Grid box – PTR 7	178.34 m
PTR 7 – PTR 5	94.3 m
PTR 5 – PTR 3	94.3 m

Table B.5: Transformer data for SPP

1440kVA 11/0.38/0.38 kV D0y11y11 transformer			
Description	Values	Description	Values
Rated power:			
MV-side	1.44 MVA	Copper losses	5.93 kW
LV-side	0.72 MVA	Neutral tap position	3
LV-side	0.72 MVA	Voltage per tap position	3.5 %
Vector group:			
MV-side	Delta	Phase shift	0*30 °
LV-side	Star	Phase shift	11*30 °
LV-side	Star	Phase shift	11*30 °
Short-circuit impedance uk1&2:		Short-circuit impedance uk0:	
MV-LV	6 %	MV-LV	3 %
LV-LV	10 %	LV-LV	3 %
LV-MV	6 %	LV-MV	3 %
No load current	0.2 %	Minimum tap position	1
No load losses	1.45 kW	Maximum tap position	5

Table B.6: Q capability limits of the SPP inverters provided in p.u. in PowerFactory

Rows	Voltage level p.u.	Columns	P-setpoints p.u.	Columns	P-setpoints p.u.	Columns	P-setpoints p.u.
1	0.800	1	0	9	0.400	17	0.800
2	0.850	2	0.050	10	0.450	18	0.850
3	0.900	3	0.100	11	0.500	19	0.900
4	0.950	4	0.150	12	0.550	20	0.950
5	1.000	5	0.200	13	0.600	21	1.000
6	1.050	6	0.250	14	0.650		
7	1.150	7	0.300	15	0.700		
8	1.200	8	0.350	16	0.750		

Table B.7A: Q capability curve matrix for Qmax (export)

Matrix for Q capability curve										
Q _{max} p.u.	0.000	0.050	0.100	0.150	0.200	0.250	0.300	0.350	0.400	0.450
0.800	0.800	0.798436	0.7937254	0.7858117	0.7745967	0.7599342	0.741619	0.7193747	0.6928203	0.661437
0.850	0.850	0.848528	0.8440972	0.8366600	0.8261356	0.8124038	0.795298	0.7745967	0.7500000	0.721110
0.900	0.900	0.898610	0.8944272	0.8874120	0.8774964	0.8645808	0.848528	0.8291562	0.8062258	0.779422
0.950	0.950	0.948683	0.9447222	0.9380832	0.9287088	0.9165151	0.901387	0.8831761	0.8616844	0.836660
1.000	1.000	0.998749	0.9949874	0.9886860	0.9797959	0.9682458	0.953939	0.9367497	0.9165151	0.893286
1.050	1.000	0.998749	0.9949874	0.9886860	0.9797959	0.9682458	0.953939	0.9367497	0.9165151	0.893028
1.150	1.000	0.998749	0.9949874	0.9886860	0.9797959	0.9682458	0.953939	0.9367497	0.9165151	0.893028
1.200	1.000	0.998749	0.9949874	0.9886860	0.9797959	0.9682458	0.953939	0.9367497	0.9165151	0.893028

Table B.7B: Q capability curve matrix for Qmax continued (export)

Matrix for Q capability curve											
Q _{max} p.u.	0.500	0.550	0.600	0.650	0.700	0.750	0.800	0.850	0.900	0.950	0.1000
0.800	0.6244998	0.5809475	0.5291503	0.466369	0.3872983	0.2783882	0	0	0	0	0
0.850	0.6873864	0.6480741	0.6020797	0.5477226	0.4821825	0.4000000	0.2872281	0	0	0	0
0.900	0.7483315	0.7123903	0.6708204	0.6224950	0.5656854	0.4974937	0.4123106	0.2958040	0	0	0
0.950	0.8077747	0.7745967	0.7365460	0.6928203	0.6422616	0.5830952	0.5123475	0.4242641	0.2785500	0	0
1.000	0.8660254	0.8351647	0.8000000	0.7599342	0.7141428	0.6614378	0.6000000	0.5267827	0.3125550	0.1000000	0
1.050	0.8660254	0.8351647	0.8000000	0.7599342	0.7141428	0.6614378	0.6000000	0.5267827	0.3125550	0.1000000	0
1.150	0.8660254	0.8351647	0.8000000	0.7599342	0.7141428	0.6614378	0.6000000	0.5267827	0.3125550	0.1000000	0
1.200	0.8660254	0.8351647	0.8000000	0.7599342	0.7141428	0.6614378	0.6000000	0.5267827	0.3125550	0.1000000	0

Table B.8A: Q capability curve matrix for Qmin (import)

Matrix for Q capability curve										
Q _{max} p.u.	0.000	0.050	0.100	0.150	0.200	0.250	0.300	0.350	0.400	0.450
0.800	-0.800	-0.798436	-0.7937254	-0.7858117	-0.7745967	-0.7599342	-0.741619	-0.7193747	-0.6928203	-0.661437
0.850	-0.850	-0.848528	-0.8440972	-0.83666	-0.8261356	-0.8124038	-0.795298	-0.7745967	-0.75	-0.721110
0.900	-0.900	-0.89861	-0.8944272	-0.887412	-0.8774964	-0.8645808	-0.848528	-0.8291562	-0.8062258	-0.779422
0.950	-0.950	-0.948683	-0.9447222	-0.9380832	-0.9287088	-0.9165151	-0.901387	-0.8831761	-0.8616844	-0.83666
1.000	-1.000	-0.998749	-0.9949874	-0.988686	-0.9797959	-0.9682458	-0.953939	-0.9367497	-0.9165151	-0.893286
1.050	-1.000	-0.998749	-0.9949874	-0.988686	-0.9797959	-0.9682458	-0.953939	-0.9367497	-0.9165151	-0.893028
1.150	-1.000	-0.998749	-0.9949874	-0.988686	-0.9797959	-0.9682458	-0.953939	-0.9367497	-0.9165151	-0.893028
1.200	-1.000	-0.998749	-0.9949874	-0.988686	-0.9797959	-0.9682458	-0.953939	-0.9367497	-0.9165151	-0.893028

Table B.8B: Q capability curve matrix for Qmin continued (import)

Matrix for Q capability curve											
Q _{max} p.u.	0.500	0.550	0.600	0.650	0.700	0.750	0.800	0.850	0.900	0.950	0.1000
0.800	-0.6244998	-0.5809475	-0.5291503	-0.466369	-0.3872983	-0.2783882	0	0	0	0	0
0.850	-0.6873864	-0.6480741	-0.6020797	-0.5477226	-0.4821825	-0.4	-0.2872281	0	0	0	0
0.900	-0.7483315	-0.7123903	-0.6708204	-0.622495	-0.5656854	-0.4974937	-0.4123106	-0.295804	0	0	0
0.950	-0.8077747	-0.7745967	-0.736546	-0.6928203	-0.6422616	-0.5830952	-0.5123475	-0.4242641	-0.2785500	0	0
1.000	-0.8660254	-0.8351647	-0.8	-0.7599342	-0.7141428	-0.6614378	-0.6	-0.5267827	-0.3125550	-0.1000000	0
1.050	-0.8660254	-0.8351647	-0.8	-0.7599342	-0.7141428	-0.6614378	-0.6	-0.5267827	-0.3125550	-0.1000000	0
1.150	-0.8660254	-0.8351647	-0.8	-0.7599342	-0.7141428	-0.6614378	-0.6	-0.5267827	-0.3125550	-0.1000000	0
1.200	-0.8660254	-0.8351647	-0.8	-0.7599342	-0.7141428	-0.6614378	-0.6	-0.5267827	-0.3125550	-0.1000000	0

Table B.9: Voltage capability matrix for the requirements of the SPP in PowerFactory

Point on graph	Voltage level p.u.	Qmin (MVar)	Qmax (MVar)
1	0.000	1.000	0.000
2	0.900	0.000	0.000
3	0.900	0.000	2.052
4	1.000	-2.052	2.052
5	1.000	-2.052	2.052
6	1.100	-2.052	0.000
7	1.100	0.000	0.000

Table B.10A: Case study 2 - Q capability curve matrix for Qmax (export)

Matrix for Q capability curve										
Q _{max} p.u.	0.000	0.050	0.100	0.150	0.200	0.250	0.300	0.350	0.400	0.450
0.800	0.800	0.798436	0.7937254	0.7858117	0.7745967	0.7599342	0.741619	0.7193747	0.6928203	0.661437
0.850	0.850	0.848528	0.8440972	0.83666	0.8261356	0.8124038	0.795298	0.7745967	0.7500000	0.721110
0.900	0.900	0.89861	0.8944272	0.887412	0.8774964	0.8645808	0.848528	0.8291562	0.8062258	0.779422
0.950	0.950	0.948683	0.9447222	0.9380832	0.9287088	0.9165151	0.901387	0.8831761	0.8616844	0.83666
1.000	1.000	0.998749	0.9949874	0.988686	0.9797959	0.9682458	0.953939	0.9367497	0.9165151	0.893286
1.050	1.000	0.998749	0.9949874	0.988686	0.9797959	0.9682458	0.953939	0.9367497	0.9165151	0.893028
1.150	1.000	0.998749	0.9949874	0.988686	0.9797959	0.9682458	0.953939	0.9367497	0.9165151	0.893028
1.200	1.000	0.998749	0.9949874	0.988686	0.9797959	0.9682458	0.953939	0.9367497	0.9165151	0.893028

Table B.10B: Case study 2 - Q capability curve matrix for Qmax continued (export)

Matrix for Q capability curve											
Q _{max} p.u.	0.500	0.550	0.600	0.650	0.700	0.750	0.800	0.850	0.900	0.950	0.1000
0.800	0.6244998	0.5809475	0.5291503	0.466369	0.3872983	0.2783882	0	0	0	0	0
0.850	0.6873864	0.6480741	0.6020797	0.5477226	0.4821825	0.4000000	0.2872281	0	0	0	0
0.900	0.7483315	0.7123903	0.6708204	0.6224950	0.5656854	0.4974937	0.4123106	0.2958040	0	0	0
0.950	0.8077747	0.7745967	0.7365460	0.6928203	0.6422616	0.5830952	0.5123475	0.4242641	0.3041381	0	0
1.000	0.8660254	0.8351647	0.8000000	0.7599342	0.7141428	0.6614378	0.6000000	0.5267827	0.4358899	0	0
1.050	0.8660254	0.8351647	0.8000000	0.7599342	0.7141428	0.6614378	0.6000000	0.5267827	0.4358899	0	0
1.150	0.8660254	0.8351647	0.8000000	0.7599342	0.7141428	0.6614378	0.6000000	0.5267827	0.4358899	0	0
1.200	0.8660254	0.8351647	0.8000000	0.7599342	0.7141428	0.6614378	0.6000000	0.5267827	0.4358899	0	0

Table B.11A: Case study 2 - Q capability curve matrix for Qmin (import)

Matrix for Q capability curve										
Q _{max} p.u.	0.000	0.050	0.100	0.150	0.200	0.250	0.300	0.350	0.400	0.450
0.800	-0.800	-0.798436	-0.7937254	-0.7858117	-0.7745967	-0.7599342	-0.741619	-0.7193747	-0.6928203	-0.661437
0.850	-0.850	-0.848528	-0.8440972	-0.8366600	-0.8261356	-0.8124038	-0.795298	-0.7745967	-0.7500000	-0.721110
0.900	-0.900	-0.89861	-0.8944272	-0.8874120	-0.8774964	-0.8645808	-0.848528	-0.8291562	-0.8062258	-0.779422
0.950	-0.950	-0.948683	-0.9447222	-0.9380832	-0.9287088	-0.9165151	-0.901387	-0.8831761	-0.8616844	-0.83666
1.000	-1.000	-0.998749	-0.9949874	-0.9886860	-0.9797959	-0.9682458	-0.953939	-0.9367497	-0.9165151	-0.893286
1.050	-1.000	-0.998749	-0.9949874	-0.9886860	-0.9797959	-0.9682458	-0.953939	-0.9367497	-0.9165151	-0.893028
1.150	-1.000	-0.998749	-0.9949874	-0.9886860	-0.9797959	-0.9682458	-0.953939	-0.9367497	-0.9165151	-0.893028
1.200	-1.000	-0.998749	-0.9949874	-0.9886860	-0.9797959	-0.9682458	-0.953939	-0.9367497	-0.9165151	-0.893028

Table B.11B: Case study 2 - Q capability curve matrix for Qmin continued (import)

Matrix for Q capability curve											
Q _{max} p.u.	0.500	0.550	0.600	0.650	0.700	0.750	0.800	0.850	0.900	0.950	0.1000
0.800	-0.6244998	-0.5809475	-0.5291503	-0.466369	-0.3872983	-0.2783882	0	0	0	0	0
0.850	-0.6873864	-0.6480741	-0.6020797	-0.5477226	-0.4821825	-0.4000000	-0.2872281	0	0	0	0
0.900	-0.7483315	-0.7123903	-0.6708204	-0.622495	-0.5656854	-0.4974937	-0.4123106	-0.295804	0	0	0
0.950	-0.8077747	-0.7745967	-0.7365460	-0.6928203	-0.6422616	-0.5830952	-0.5123475	-0.4242641	-0.3041381	0	0
1.000	-0.8660254	-0.8351647	-0.8000000	-0.7599342	-0.7141428	-0.6614378	-0.6000000	-0.5267827	-0.4358899	0	0
1.050	-0.8660254	-0.8351647	-0.8000000	-0.7599342	-0.7141428	-0.6614378	-0.6000000	-0.5267827	-0.4358899	0	0
1.150	-0.8660254	-0.8351647	-0.8000000	-0.7599342	-0.7141428	-0.6614378	-0.6000000	-0.5267827	-0.4358899	0	0
1.200	-0.8660254	-0.8351647	-0.8000000	-0.7599342	-0.7141428	-0.6614378	-0.6000000	-0.5267827	-0.4358899	-0.3122499	0

Three-winding transformer figure shown as per configuration in Powerfactory under the settings tab for the values of the transformer.

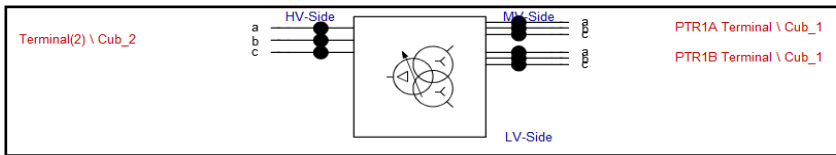


Figure B.1: Three-winding transformer modelling in PowerFactory

DlgSILENT simulation language (DSL) scripts used for the control frames in the SPP inverters model in the network model used for steady-state conditions as shown in Figures B.2 – B.7.

```

Block Definition - Equipment Type Library\Masters degree model\Qcontrol.BlkDef

Basic Options
Equations
Description
Version

Additional equations
Qset = select(Qcontrol_mode, Qset_pf, Q_user)

inc(Q_user) = Qset

Qset_pf = select(abs(Theta_user)<89.9999 .or. abs(Theta_user)>90.0001,
                & ptrack*tan(Theta_user*pi()/180), Q_user)

Theta_user = Theta_user_rad * 180/pi()
Theta_user_rad = select(Pfactor_user>=0, acos(Pfactor_user),
                       -acos(abs(Pfactor_user)))

inc(Theta_user_rad) = select(S>0, select(Qset>=0, acos(p/S), -acos(p/S)), 0)
inc(Theta_user) = Theta_user_rad*180/pi()
inc(argS) = max(abs((P*p)+(Qset*Qset)),0)
inc(S) = sqrt(argS)
inc(Pfactor_user) = select(sin(Theta_user_rad)>=0, cos(Theta_user_rad), -cos(Theta_user_rad))

xpw. = (p-xpw)/Tpw
ptrack = xpw
inc(xpw) = p

vardef(Qcontrol_mode) = '0/1' ; '0: Q control / 1: cosphi control'
vardef(Tpw) = 's' ; 'Active power time constant'

```

Figure B.2: Script for Q control

```

Block Definition - Equipment Type Library\Masters degree model\Current_Control.BlkDef

Basic Options
Equations
Description
Version

Additional equations
inc(Quser) = -iqr*u+Qcap
inc(Qpv) = -iqr*u
inc(Qcap) = 0
inc(P_dem) = idr*u
inc(P_f) = 2
inc(Puser) = 2
inc(Flt) = 0

inc(Uai) = 0
inc(Uar) = 0
inc(Ubi) = 0
inc(Ubr) = 0
inc(Uci) = 0
inc(Ucr) = 0

vardef(Tpick) = 's'; 'Fault mode, delay on start'
vardef(Tdro) = 's'; 'Fault mode, delay on exit'
vardef(Umin) = 'p.u.'; 'Voltage for dip detection'
vardef(Umax) = 'p.u.'; 'Voltage for swell detection'
vardef(Qmax) = 'p.u.'; 'Reactive power limit'
vardef(Dip) = '1/0'; 'Activate capacitive voltage support'
vardef(Swell) = '1/0'; 'Activate inductive voltage support'
vardef(Tcc) = 's'; 'Equiv. converter reaction time'
vardef(Imax) = 'p.u.'; 'Current limit'
vardef(Ramp_Id) = 'p.u.'; 'Post-fault active current ramp rate'
vardef(PostFlt_time) = 's'; 'Unused (=0)'
vardef(umin_FLL) = 'p.u.'; 'Min voltage for PLL blocking'
vardef(Tm) = 's'; 'Voltage filter time constant'

```

Figure B.3: Script for current control

```

Block Definition - Equipment Type Library\Masters degree model\Pf_Reduction.BlkDef

Basic Options
Equations
Description
Version

Additional equations
P_f = xP
xF. = (FHz-xf)/0.05
xP. = select(OF, lim((Pnew-xP)/0.01, -99, 0), (2-xP)/0.1)
xPini. = select(OF, 0, (P-xPini)/0.5)

OF = flipflop(set, res)
set = xf > f_enable
res = xf < f_reset

Pnew = xPini - Pf_slope*xPini*(xf-f_enable)

inc(xf) = FHz
inc(xP) = 2
inc(xPini) = P
inc(OF) = 0

!event(1, xf-f_enable, 'Create=EvtParam target=this name=Overfrequency dtime=0 val
vardef(f_enable) = 'Hz'; 'Begin power reduction'
vardef(f_reset) = 'Hz'; 'Return to normal operation'
vardef(Pf_slope) = 'p.u./Hz'; 'Power reduction slope'

```

Figure B.4: Script for power frequency reduction

```

Block Definition - Equipment Type Library\Masters degree model\Pf_non_hyst.BlkDef

Basic Options
Equations
Description
Version

Additional equations
vardef(Fa) = 'Hz'; 'frequency A'
vardef(Pa) = 'p.u.'; 'power A'
vardef(Fb) = 'Hz'; 'frequency B'
vardef(Pb) = 'p.u.'; 'power B'
vardef(Fc) = 'Hz'; 'frequency C'
vardef(Pc) = 'p.u.'; 'power C'
vardef(Fd) = 'Hz'; 'frequency D'
vardef(Pd) = 'p.u.'; 'power D'

!Fab=lim(Fb-Fa,0.001,100)
!Fbc=lim(Fc-Fb,0.001,100)
!Fcd=lim(Fd-Fc,0.001,100)

Fab=Fb-Fa
Fbc=Fc-Fb
Fcd=Fd-Fc

Sab=(Pb-Pa)/Fab
Sbc=(Pc-Pb)/Fbc
Scd=(Pd-Pc)/Fcd

Fab=Pa+Sab*(xf-Fa)
Fbc=Pb+Sbc*(xf-Fb)
Fcd=Pc+Scd*(xf-Fc)

!inc(xf) = FHz
!xf = (FHz-xf)/0.05

```

Figure B.5: Script for power frequency non-hysteresis

```

Block Definition - Equipment Type Library\Masters degree model\Protection.BlkDef

Basic Options
Equations
Description
Version

Additional equations
inc0(Uai) = 0
inc0(Uar) = 0
inc0(Ubi) = 0
inc0(Ubr) = 0
inc0(Uci) = 0
inc0(Ucr) = 0

argUAB=max(abs((sqrt(Uar-Ubr)+sqrt(Uai-Ubi))),0)
UAB=sqrt(argUAB)/Unom

argUBC=max(abs((sqrt(Ubr-Ucr)+sqrt(Ubi-Uci))),0)
UBC=sqrt(argUBC)/Unom

argUCA=max(abs((sqrt(Ucr-Uar)+sqrt(Uci-Uai))),0)
UCA=sqrt(argUCA)/Unom

High_V = max(UAB,max(UBC,UCA))
VHVset = picdro(High_V > vHV_threshold/100, 0, 0)
VHVtrip= picdro(VHVset, vHV_delay, 0.1)

HVset = picdro(High_V > HV_threshold/100, 0, 0)
HVtrip= picdro(HVset, HV_delay, 0.1)

Low_V = min(UAB,min(UBC,UCA))
VLVset = picdro(Low_V < vLV_threshold/100, 0, 0)
VLVtrip= picdro(VLVset, vLV_delay, 0.1)

```

Figure B.6: Script for protection of SPP inverter

Block Definition - Equipment Type Library\Masters degree model\Udc_Control.BlkDef

Basic Options

Equations

Description

Version

Additional equations

```

inc(ucap) = Udcn
inc(xd) = F_dem/u
inc(udc_ref) = udc
inc(Psun) = Pout

inc(Hold) = 0
inc(xum) = u

C_energy = C*udc*Udcn*udc*Udcn/2

vardef(Kd) = '-'; 'Proportional gain DC voltg. controller'
vardef(Td) = 's'; 'Integral time constant DC voltg. controller'
vardef(C) = 'F'; 'DC capacitance'
vardef(Pn) = 'W'; 'Rated power in Watt'
vardef(Udcn) = 'V'; 'Rated DC voltage'
vardef(MaxI) = 'p.u.'; 'Max active current value'

```

Figure B.7: Script for voltage control

Static Generator - Photovoltaic plant - MEng\PTR1\PTR1A.ElmGenstat*

Basic Data

Description

Load Flow

Short-Circuit VDE/IEC

Short-Circuit Complete

Short-Circuit ANSI

Short-Circuit IEC 61363

Short-Circuit DC

Quasi-Dynamic Simulation

Simulation RMS

Simulation EMT

Power Quality/Harmonics

Reliability

Generation Adequacy

Hosting Capacity Analysis

Optimal Power Flow

Unit Commitment

State Estimation

General Zero Sequence/Neutral Conductor

Name PTR1A

Terminal ... plant - MEng\PTR1\PTR1A Terminal\Cub_2 PTR1A Terminal

Zone

Area

Out of Service

Technology 3PH

Plant Category Photovoltaic

Subcategory

Number of parallel units

Ratings

Nominal Apparent P

Power Factor 0.95

Model ...Itaic plant - MEng\PTR1\PTR1A Controls

OK

Cancel

Figure

Jump to ...

Figure B.8: SPP inverter defined as static generator in PowerFactory

Data Manager - Equipment Type Library\Masters degree model\Control_Frame:

Name	Object modified	Sequence	Block Definition	Class Name
SPP_inverter_Masters	2021/08/25 12:...	0.		ElmGenstat*
Udc_Control_Masters	2021/08/25 12:...	0.		ElmUdc*
VT_prot_Masters	2021/08/25 12:...	0.		StaVt*
I_cntrl_Masters	2021/08/25 12:...	2.		ElmCur*
Prot - MEng	2021/08/25 12:...	3.		ElmPro*
PLL_Masters	2021/08/25 12:...	3.		ElmPhi*
Uiv_Meas_Masters	2021/08/25 12:...	4.		StaVmea*
PQ_Meas_Masters	2021/08/25 12:...	5.		StaPq*
PLL_prot_Masters	2021/08/25 12:...	10.		ElmPhi*
Power-Freq Reduction Masters	2021/08/25 12:...	11.		ElmPf_*
Q Control Mode Masters	2021/08/25 12:...	12.		ElmQco*

Figure B.9: Control frame of inverter measurements and control

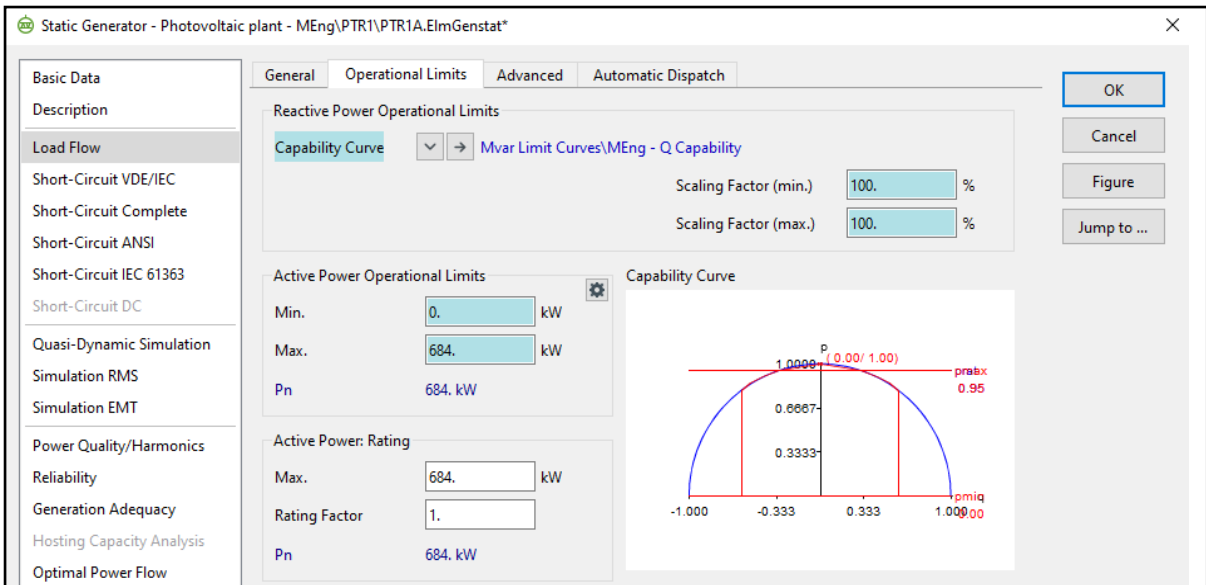


Figure B.10: Q capability operational limits of the SPP inverters

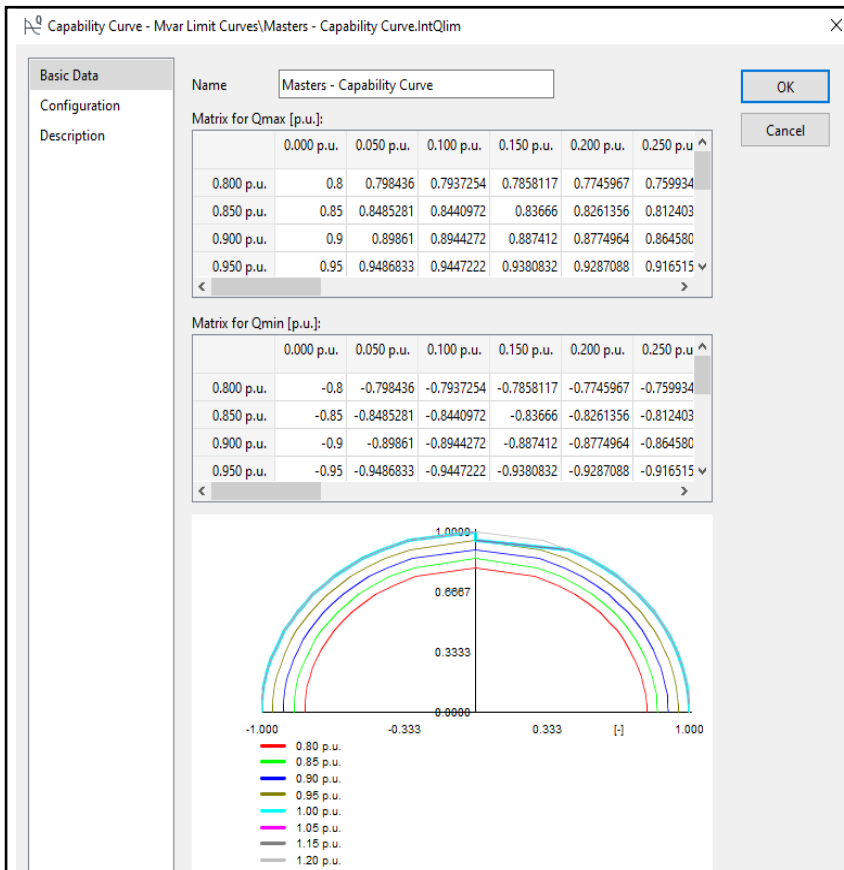


Figure B.11: Q capability curve of the SPP inverters

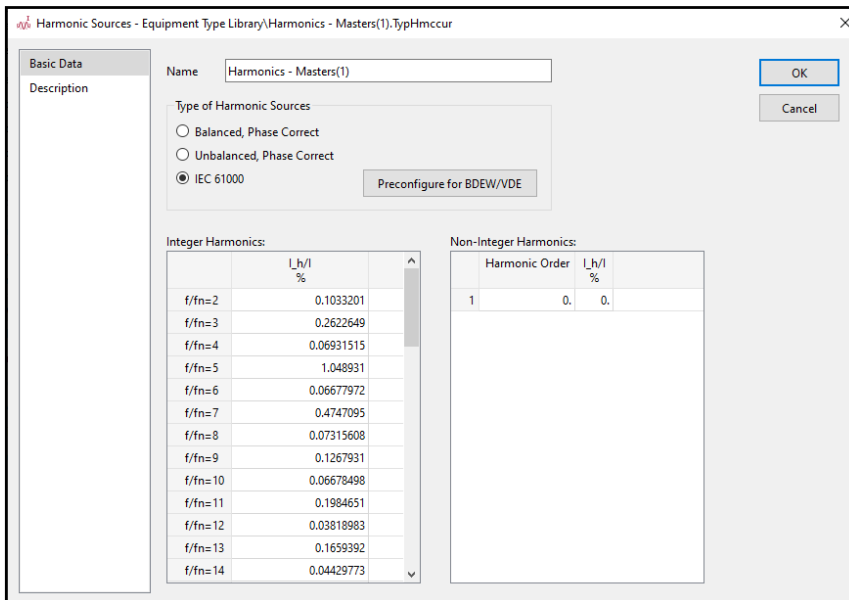


Figure B.12: Harmonic source type IEC 61000

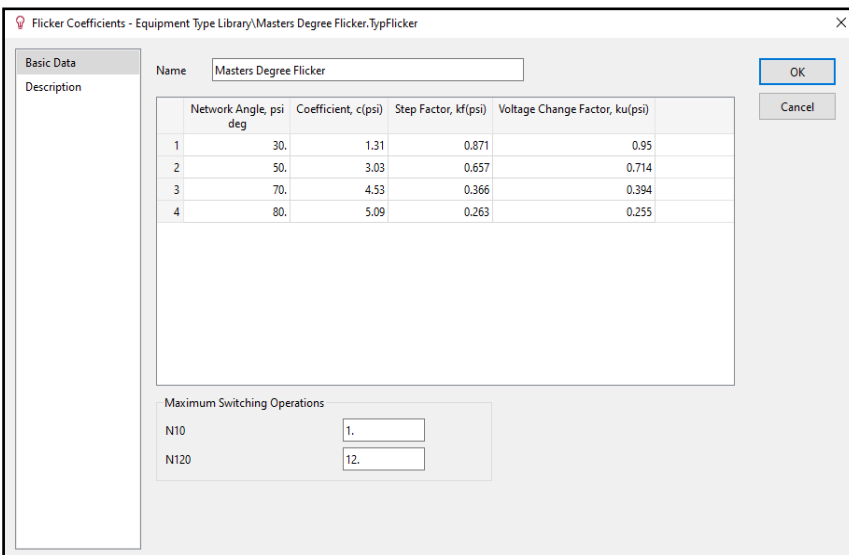


Figure B.13: Flicker data applied in SPP inverter controls

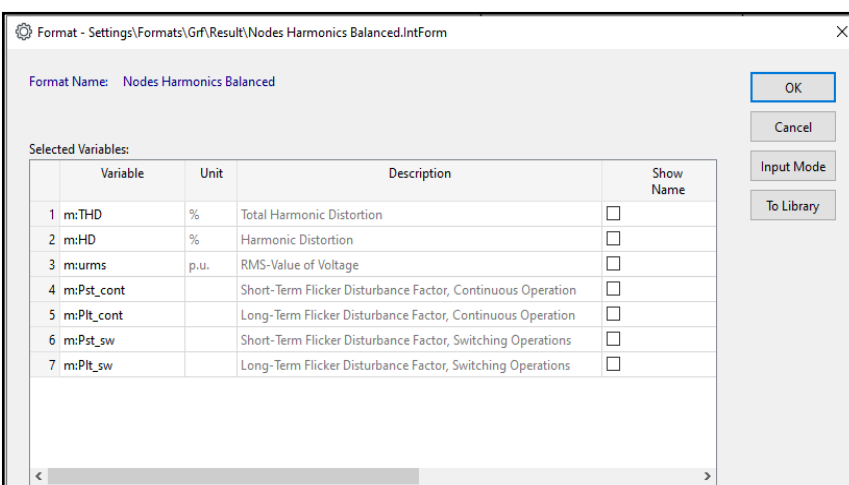


Figure B.14: Continuous and switching operations in PowerFactory

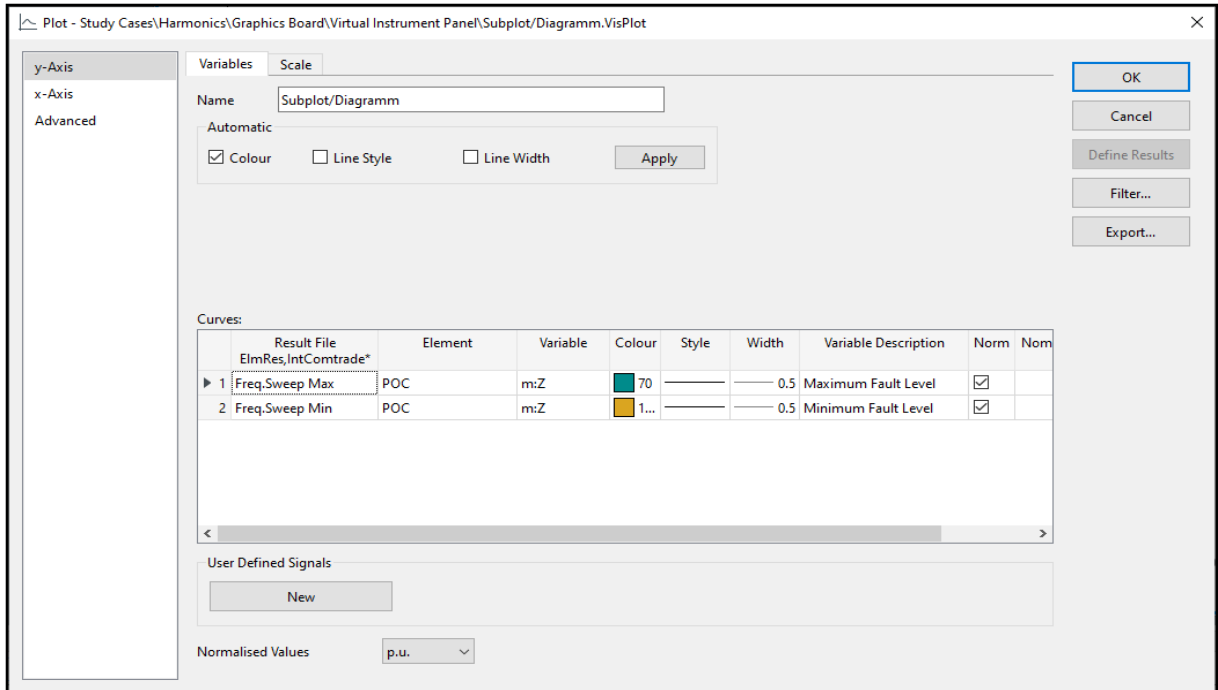


Figure B.15: Frequency sweep for minimum- and maximum fault current setup

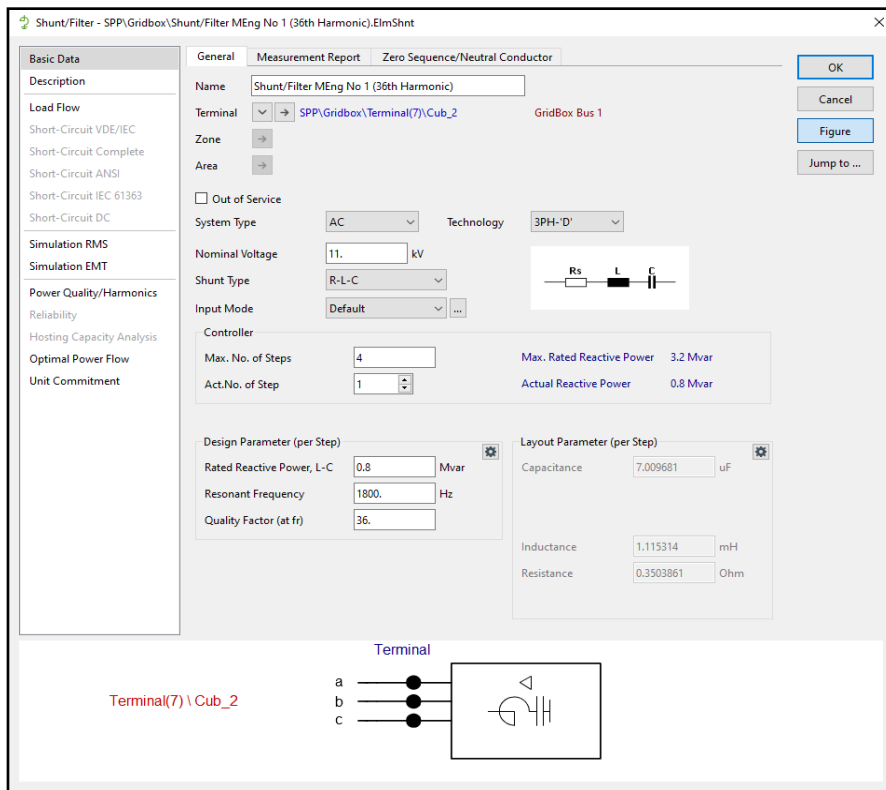


Figure B.16: Case study 3 – shunt filter 1 design parameters

APPENDIX C: POWERFACTORY NETWORK MODEL RESULTS

Table C.1: Harmonic Distortion at maximum and minimum fault level at POC

Harmonic order	Harmonic distortion allowable limits in %	Maximum fault level at POC	Minimum fault level at POC
		Harmonic distortion in %	Harmonic distortion in %
2	0.50	0.018194	0.017723
3	1.50	0.069451	0.067650
4	0.30	0.024582	0.023942
5	2.80	0.220087	0.214323
6	0.15	0.016939	0.016492
7	2.20	0.141728	0.137959
8	0.12	0.025221	0.024543
9	0.60	0.049762	0.048411
10	0.12	0.029517	0.028705
11	2.10	0.055649	0.054096
12	0.06	0.011879	0.011542
13	1.70	0.056961	0.055318
14	0.06	0.016713	0.016221
15	0.09	0.046466	0.045071
16	0.06	0.025660	0.024871
17	0.30	0.042414	0.041077
18	0.06	0.038827	0.037570
19	0.30	0.153996	0.148857
20	0.06	0.032784	0.031653
21	0.06	0.070094	0.067590
22	0.06	0.033643	0.032394
23	0.80	0.158319	0.152189
24	0.06	0.053151	0.050996
25	0.70	0.119712	0.114607
26	0.06	0.055894	0.053375
27	0.06	0.103559	0.098598
28	0.06	0.108886	0.103304
29	0.19	0.287518	0.271621
30	0.06	0.174267	0.163780
31	0.18	0.287824	0.268756
32	0.06	0.307493	0.284749
33	0.06	0.251403	0.230262
34	0.06	0.290592	0.262134
35	0.17	0.591918	0.52210
36	0.06	0.762426	0.648496
37	0.16	1.396707	1.109002
38	0.06	2.673149	1.773701
39	0.06	8.805660	2.332593
40	0.06	0.722608	1.395981
41	0.15	1.187986	1.571026
42	0.06	0.663716	0.791079
43	0.15	0.356944	0.405301
44	0.06	0.225107	0.248532
45	0.06	0.102610	0.111236
46	0.06	0.099707	0.106710
47	0.14	0.088174	0.093473
48	0.06	0.068491	0.072077
49	0.14	0.059015	0.061745
50	0.06	0.049995	0.052061

Table C.2: Harmonic Distortion at maximum and minimum fault level at POC with shunt filter 1

Harmonic order	Harmonic distortion allowable limits in %	Maximum fault level at POC	Minimum fault level at POC
		Harmonic distortion in %	Harmonic distortion in %
2	0.50	0.021378	0.02081
3	1.50	0.084743	0.082404
4	0.30	0.031731	0.030804
5	2.80	0.296004	0.286631
6	0.15	0.025418	0.024519
7	2.20	0.247735	0.237546
8	0.12	0.054975	0.052168
9	0.60	0.153458	0.142546
10	0.12	0.177585	0.154449
11	2.10	1.774600	2.406094
12	0.06	0.048046	0.053699
13	1.70	0.111949	0.118073
14	0.06	0.020500	0.021194
15	0.09	0.039560	0.04049
16	0.06	0.016067	0.016346
17	0.30	0.020238	0.020508
18	0.06	0.014447	0.014599
19	0.30	0.045371	0.045752
20	0.06	0.007725	0.007777
21	0.06	0.013290	0.013363
22	0.06	0.005147	0.00517
23	0.80	0.019546	0.019617
24	0.06	0.005282	0.005297
25	0.70	0.009527	0.009549
26	0.06	0.003534	0.003541
27	0.06	0.005145	0.005152
28	0.06	0.004187	0.004191
29	0.19	0.008386	0.008391
30	0.06	0.003753	0.003754
31	0.18	0.004411	0.004411
32	0.06	0.003181	0.00318
33	0.06	0.001621	0.001621
34	0.06	0.001023	0.001022
35	0.17	0.000875	0.000874
36	0.06	0.000368	0.000367
37	0.16	0.000980	0.000979
38	0.06	0.001690	0.001687
39	0.06	0.001095	0.001094
40	0.06	0.000859	0.000858
41	0.15	0.003414	0.003408
42	0.06	0.003351	0.003345
43	0.15	0.002745	0.00274
44	0.06	0.002426	0.002421
45	0.06	0.001467	0.001464
46	0.06	0.001818	0.001814
47	0.14	0.001991	0.001986
48	0.06	0.001871	0.001867
49	0.14	0.001916	0.001911
50	0.06	0.001899	0.001895

Table C.3: Harmonic Distortion at maximum and minimum fault level at POC with shunt filter 2

Harmonic order	Harmonic distortion allowable limits in %	Maximum fault level at POC	Minimum fault level at POC
		Harmonic distortion in %	Harmonic distortion in %
2	0.50	0.032114	0.025346
3	1.50	0.149300	0.154259
4	0.30	0.079687	0.095277
5	2.80	2.493184	0.135378
6	0.15	0.054600	0.028855
7	2.20	0.154102	0.164773
8	0.12	0.012138	0.010740
9	0.60	0.009839	0.008717
10	0.12	0.002190	0.002142
11	2.10	0.008026	0.009783
12	0.06	0.002949	0.005821
13	1.70	0.020703	0.050998
14	0.06	0.008612	0.005946
15	0.09	0.035779	0.009016
16	0.06	0.035541	0.003102
17	0.30	0.150572	0.003317
18	0.06	0.058625	0.001933
19	0.30	0.112308	0.004524
20	0.06	0.014774	0.000465
21	0.06	0.021691	0.000407
22	0.06	0.007547	0.000409
23	0.80	0.026532	0.003371
24	0.06	0.006766	0.001634
25	0.70	0.011666	0.004973
26	0.06	0.004175	0.003150
27	0.06	0.005903	0.008616
28	0.06	0.004689	0.017250
29	0.19	0.009202	0.054052
30	0.06	0.004048	0.011451
31	0.18	0.004686	0.008952
32	0.06	0.003336	0.005041
33	0.06	0.001682	0.002170
34	0.06	0.001050	0.001210
35	0.17	0.000890	0.000941
36	0.06	0.000371	0.000367
37	0.16	0.000982	0.000918
38	0.06	0.001682	0.001504
39	0.06	0.001084	0.000933
40	0.06	0.000846	0.000705
41	0.15	0.003344	0.002708
42	0.06	0.003267	0.003351
43	0.15	0.002665	0.002745
44	0.06	0.002346	0.002426
45	0.06	0.001413	0.001467
46	0.06	0.001745	0.001818
47	0.14	0.001905	0.001991
48	0.06	0.001785	0.001871
49	0.14	0.001822	0.001916
50	0.06	0.001801	0.001899

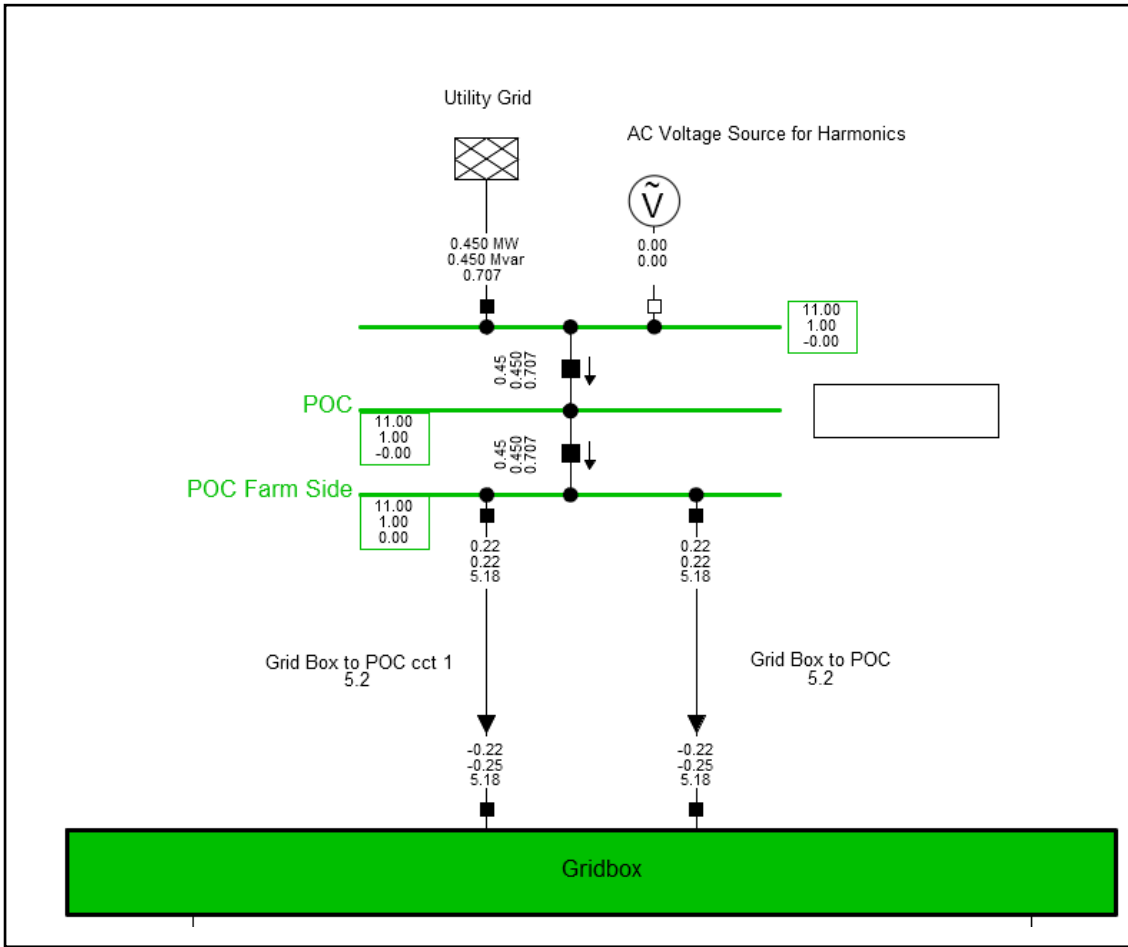


Figure C.1: Reactive power requirements for $Q = 0.450$ MVar & $P = 0.450$ MW at POC

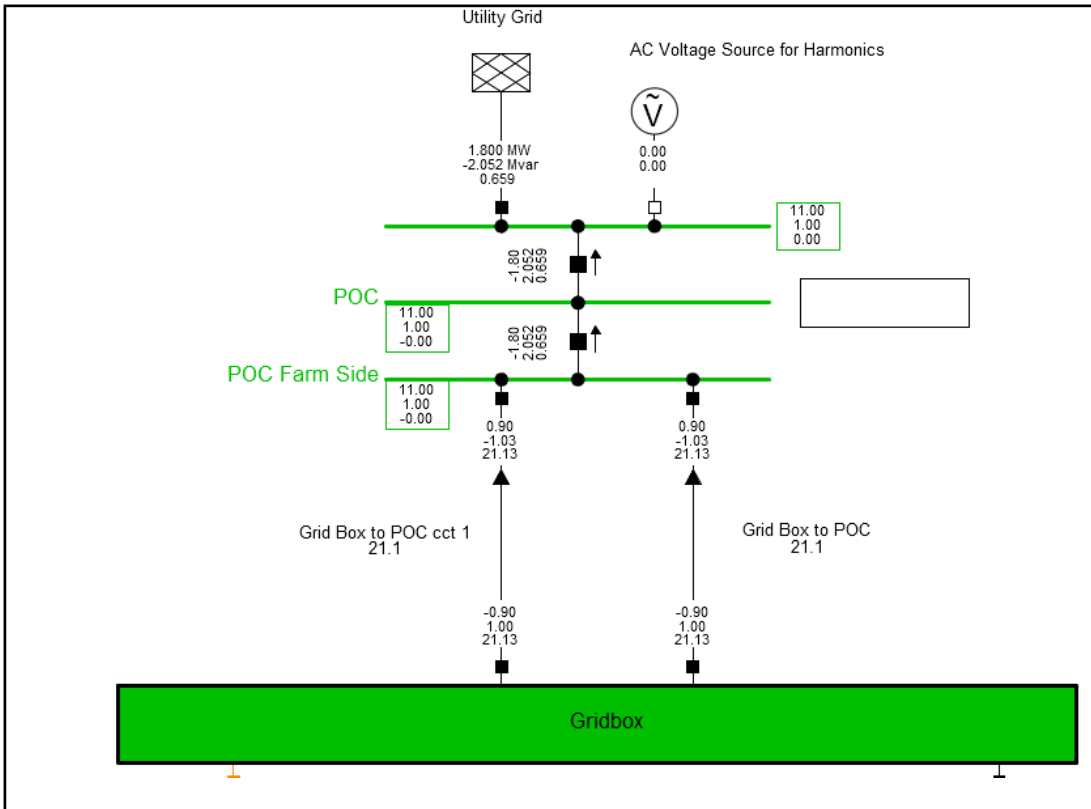


Figure C.2: Reactive power requirements for $Q = -2.052$ MVar & $P = 1.800$ MW at POC

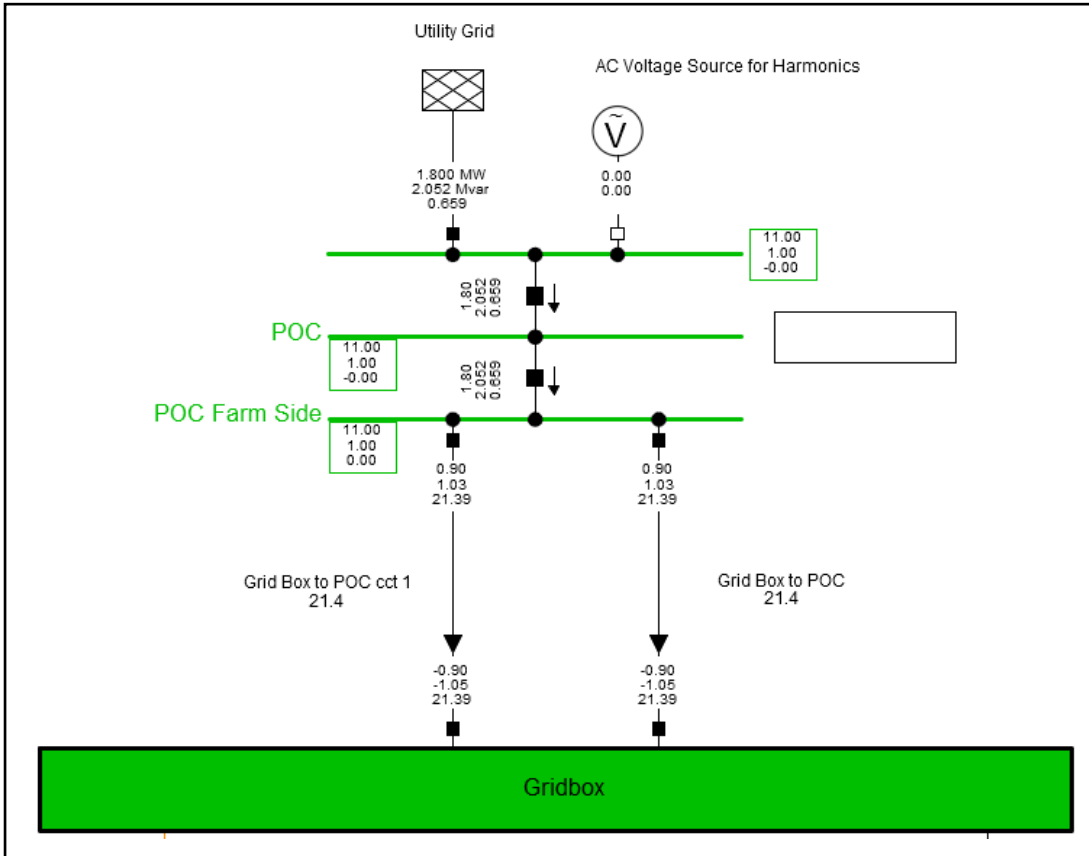


Figure C.3: Reactive power requirements for $Q = 2.052$ MVar & $P = 1.800$ MW at POC

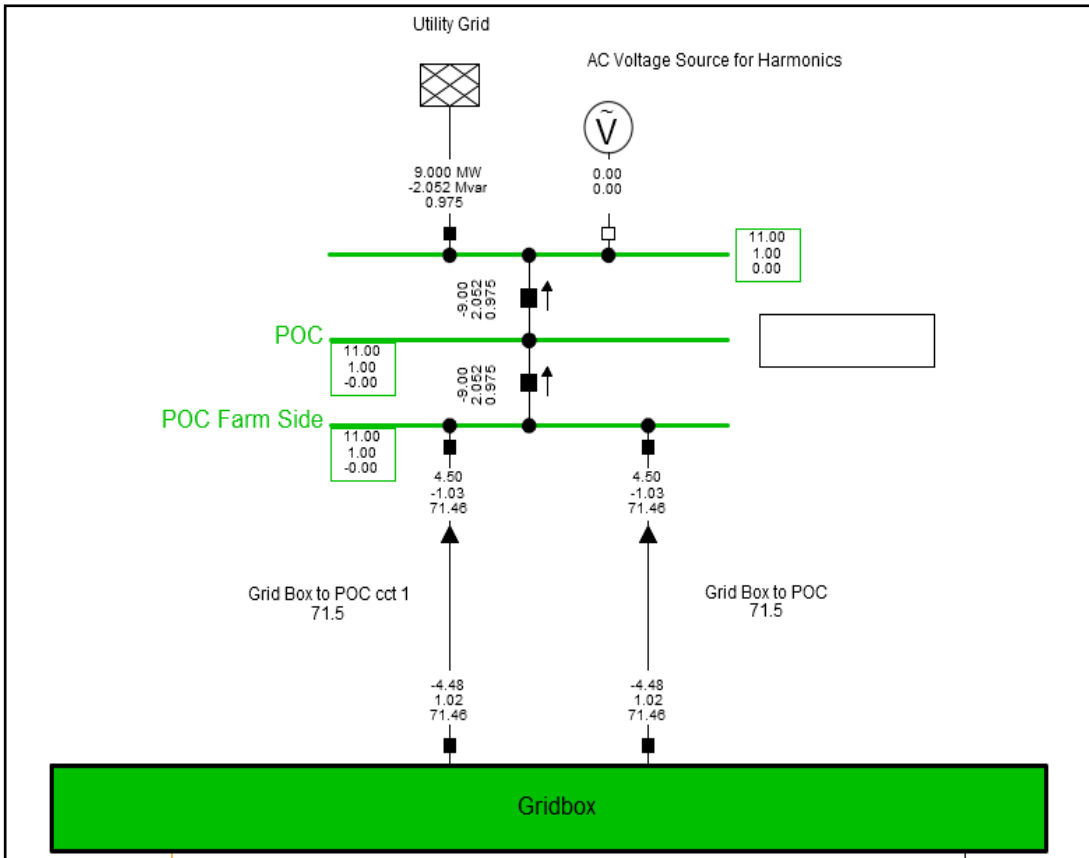


Figure C.4: Reactive power requirements for $Q = -2.052$ MVar & $P = 9.000$ MW at POC

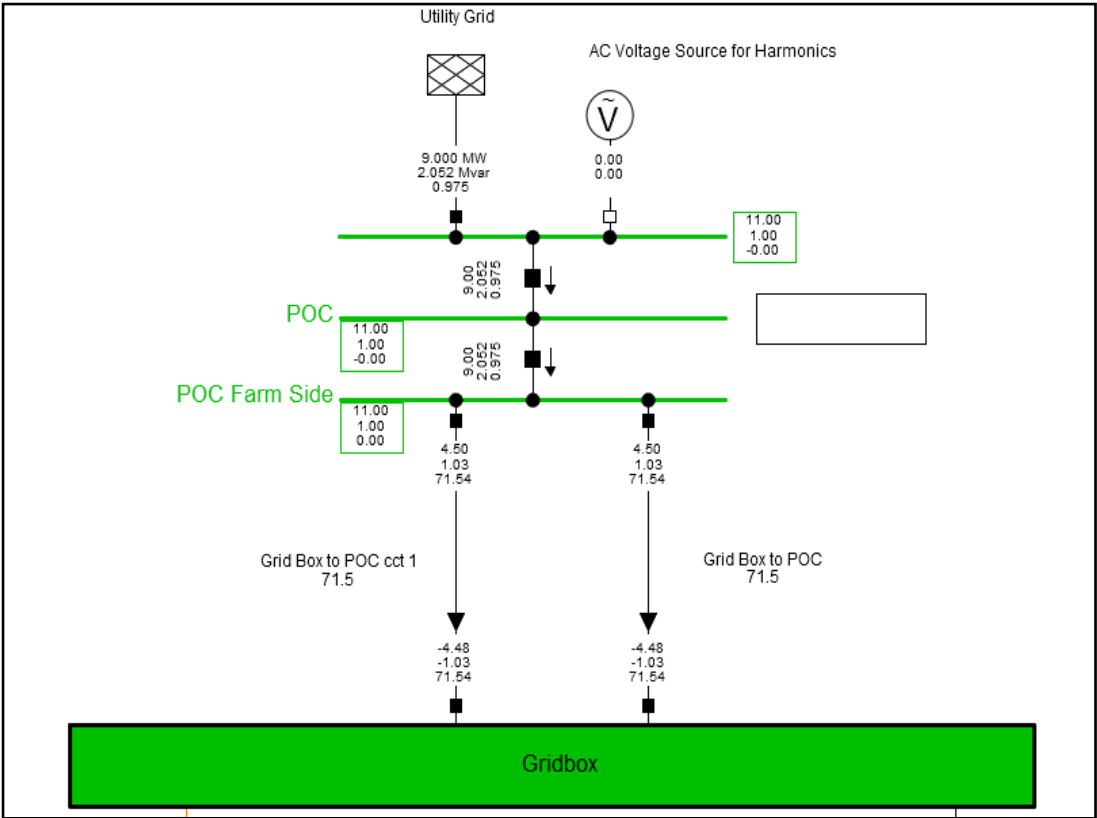


Figure C.5: Reactive power requirements for $Q = 2.052 \text{ MVar}$ & $P = 9.000 \text{ MW}$ at POC

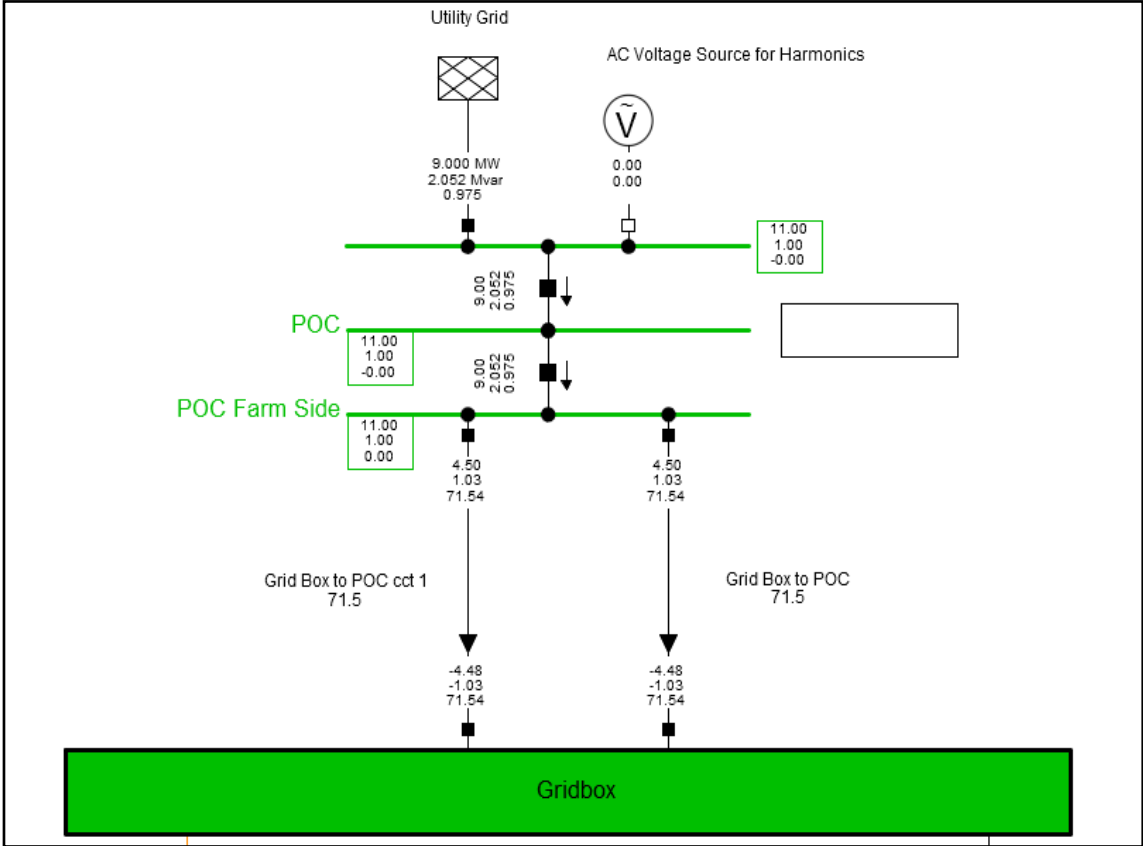


Figure C.6: Voltage capability at 1.0 p.u. for $Q = 2.052 \text{ MVar}$ & $P = 9.000 \text{ MW}$ at POC

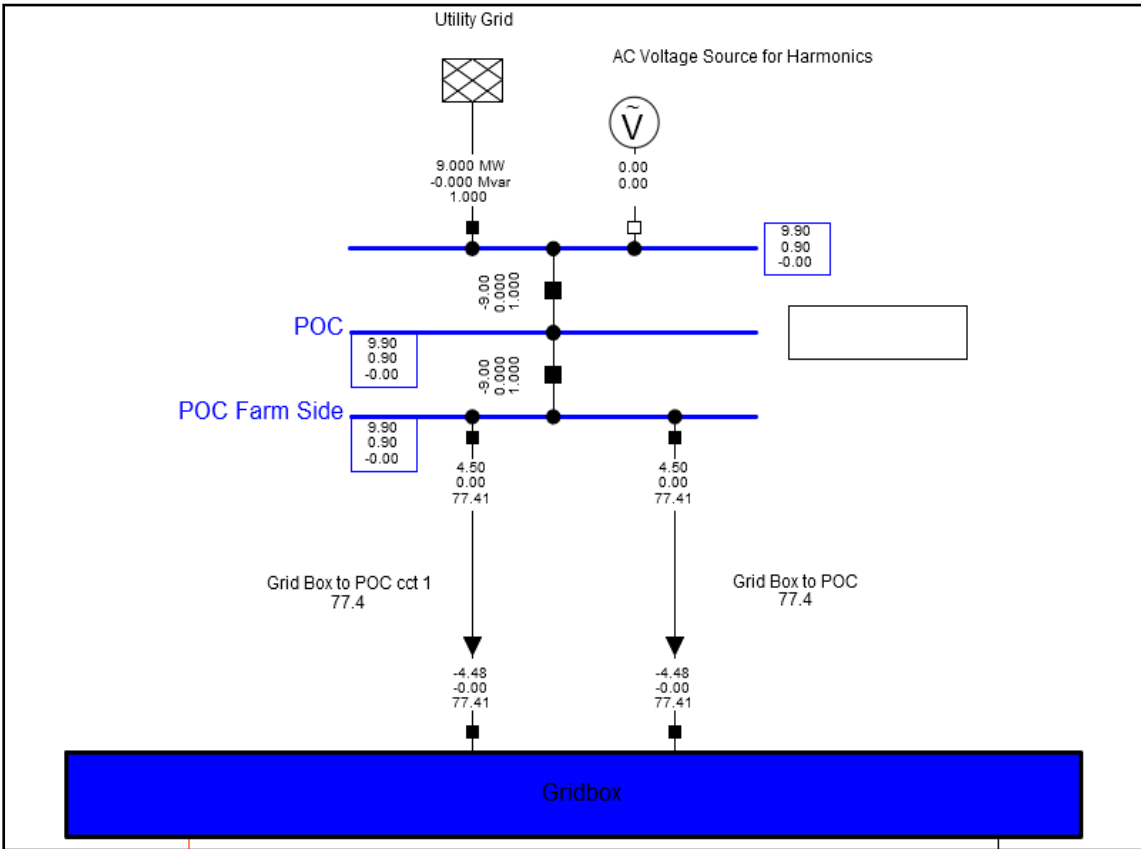


Figure C.7: Voltage capability at 0.9 p.u. for Q = -0.000 MVar & P = 9.000 MW at POC

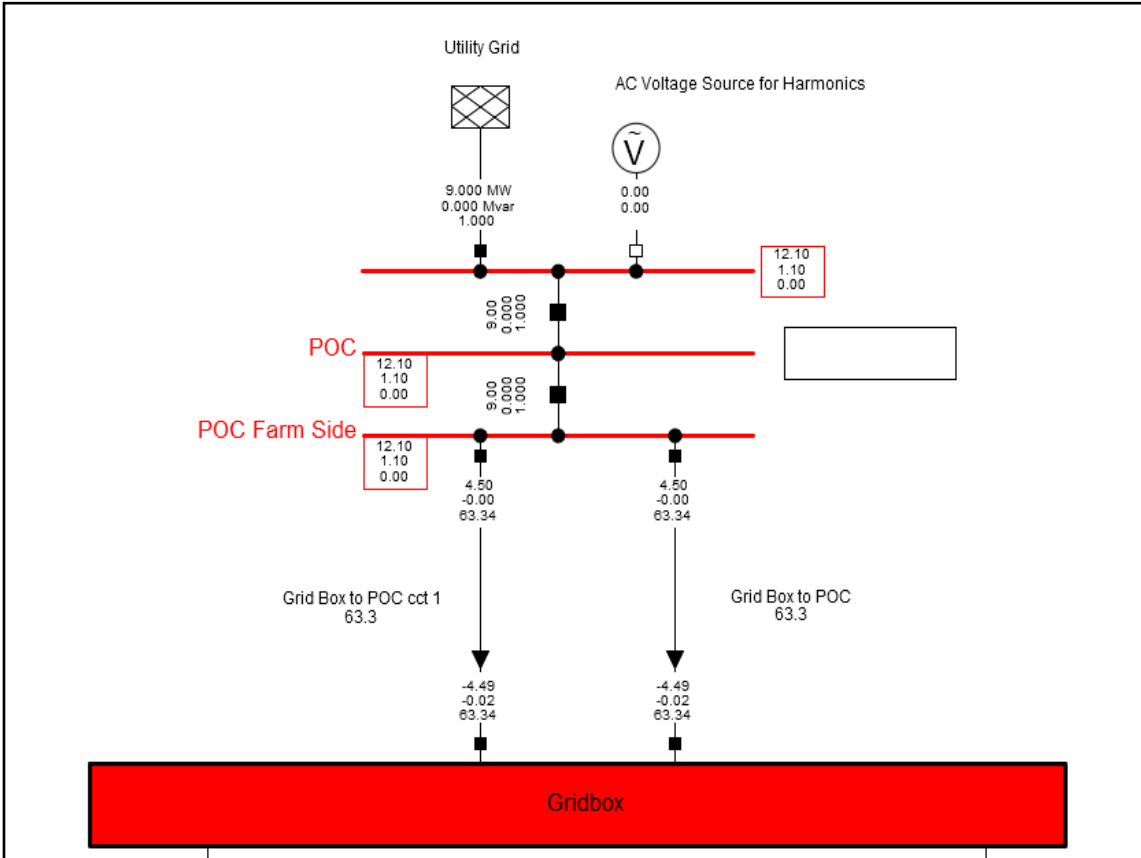


Figure C.8: Voltage capability at 1.1 p.u. for Q = 0.000 MVar & P = 9.000 MW at POC

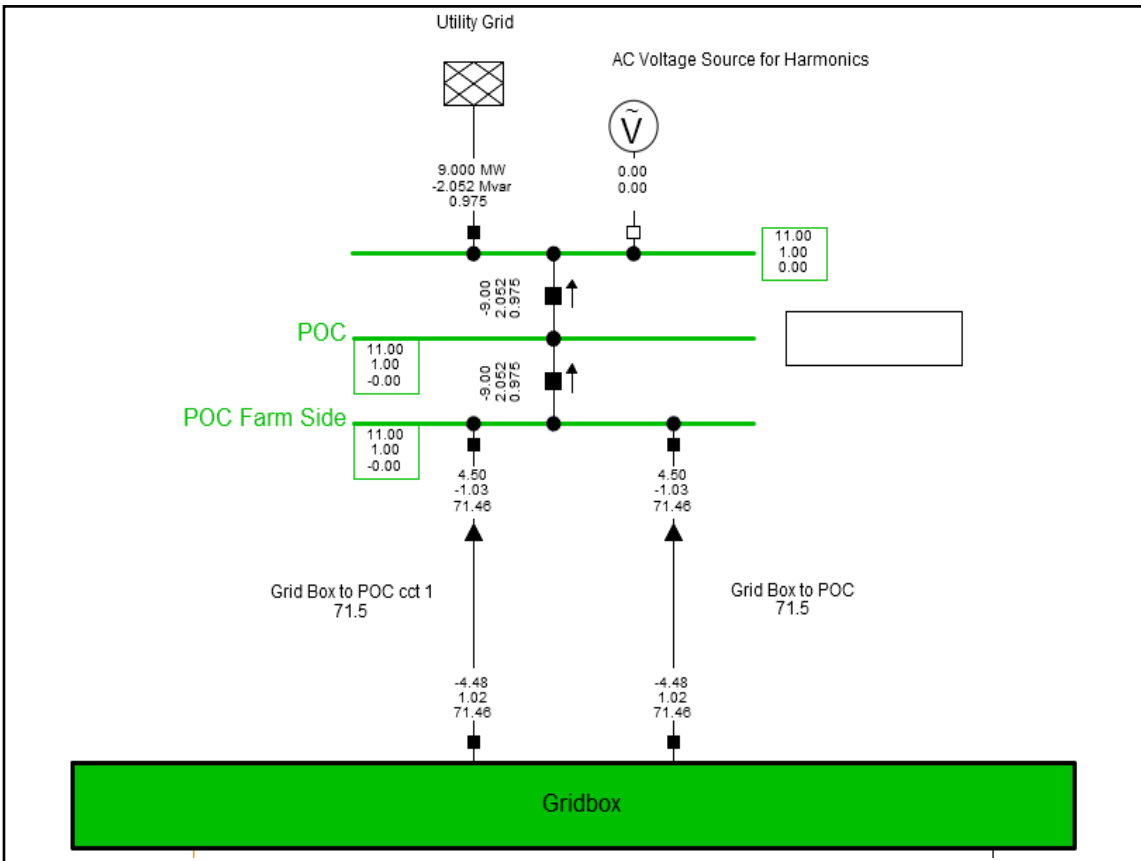


Figure C.9: Voltage capability at 1.0 p.u. for Q = -2.052 MVar & P = 9.000 MW at POC

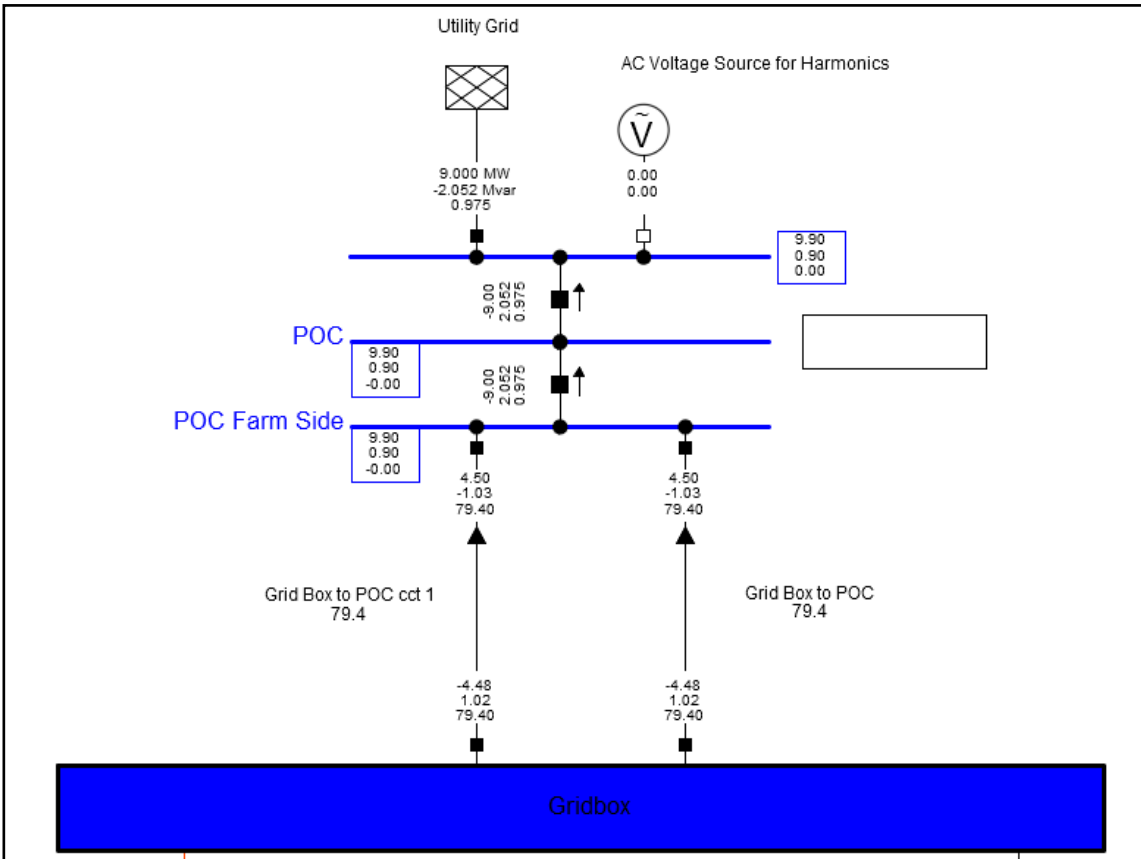


Figure C.10: Voltage capability at 0.9 p.u. for Q = -2.052 MVar & P = 9.000 MW at POC

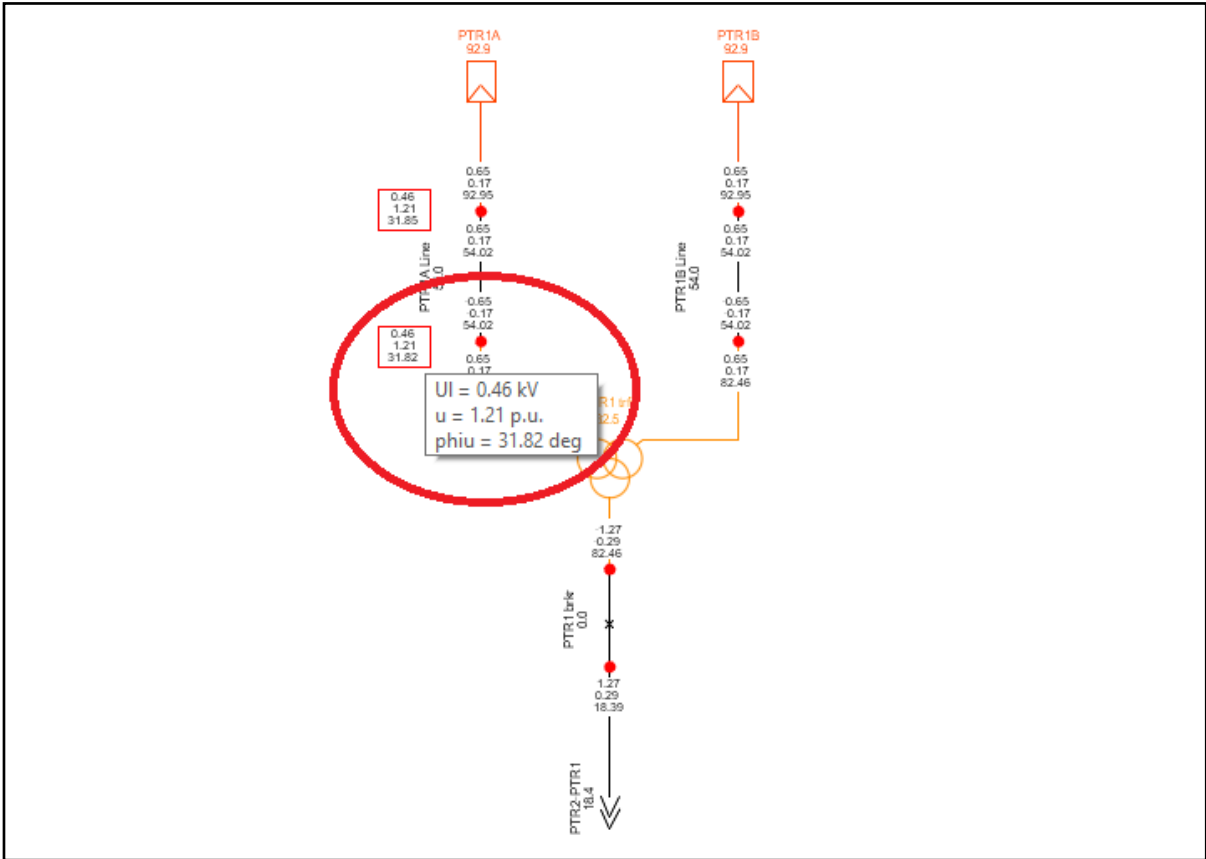


Figure C.11: Study point 1 during a voltage of 1.1 p.u. at the POC – inverter voltage overloaded

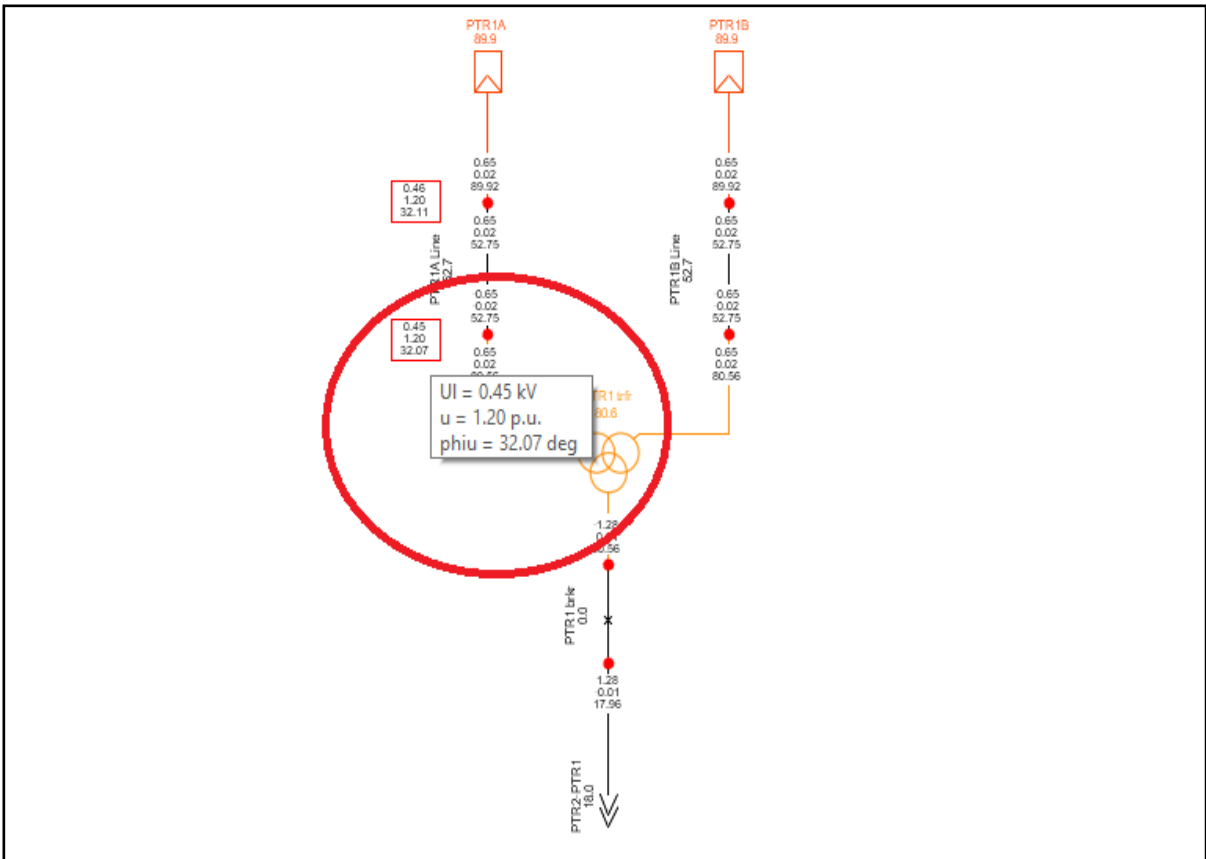


Figure C.12: Study point 4 during a voltage of 1.1 p.u. at the POC – inverter voltage overloaded

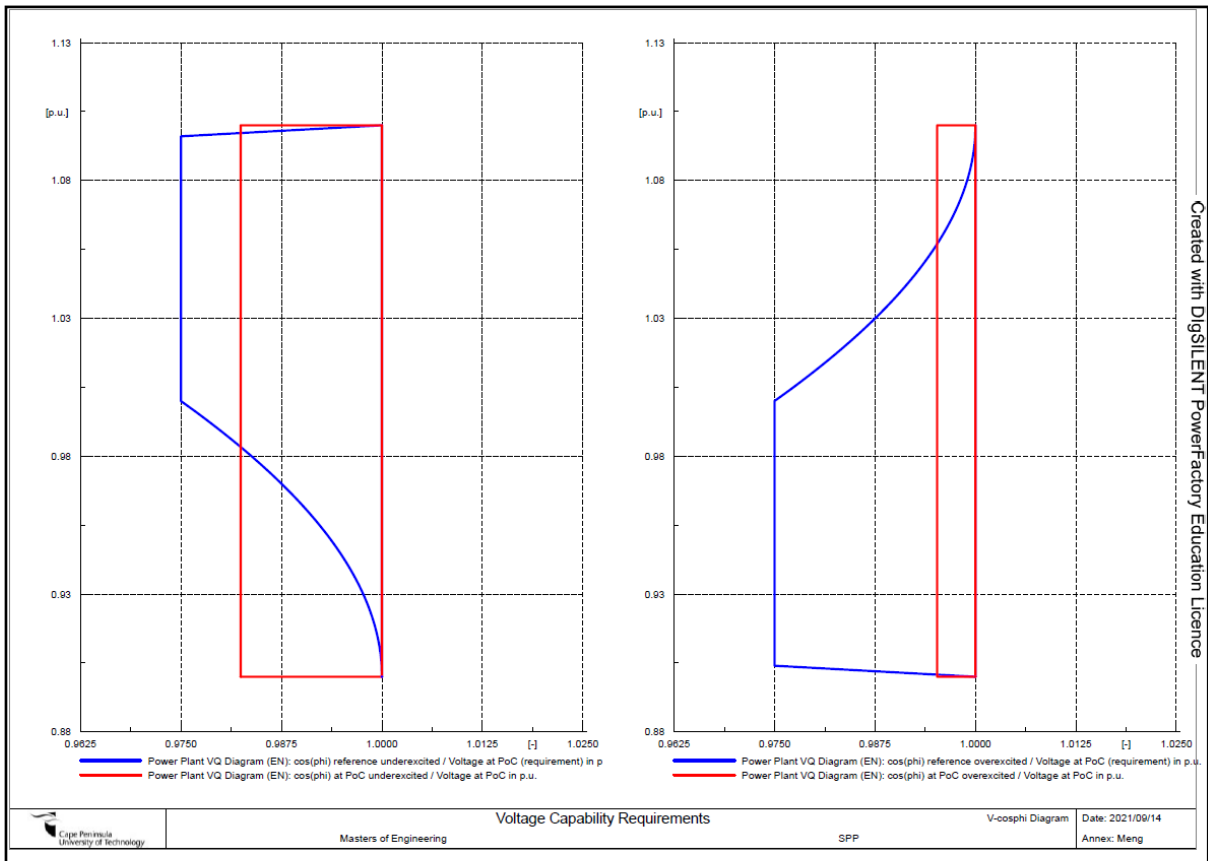


Figure C.13: Power factor and voltage requirement at POC indicating underexcited (left) conditions and overexcited conditions (right)

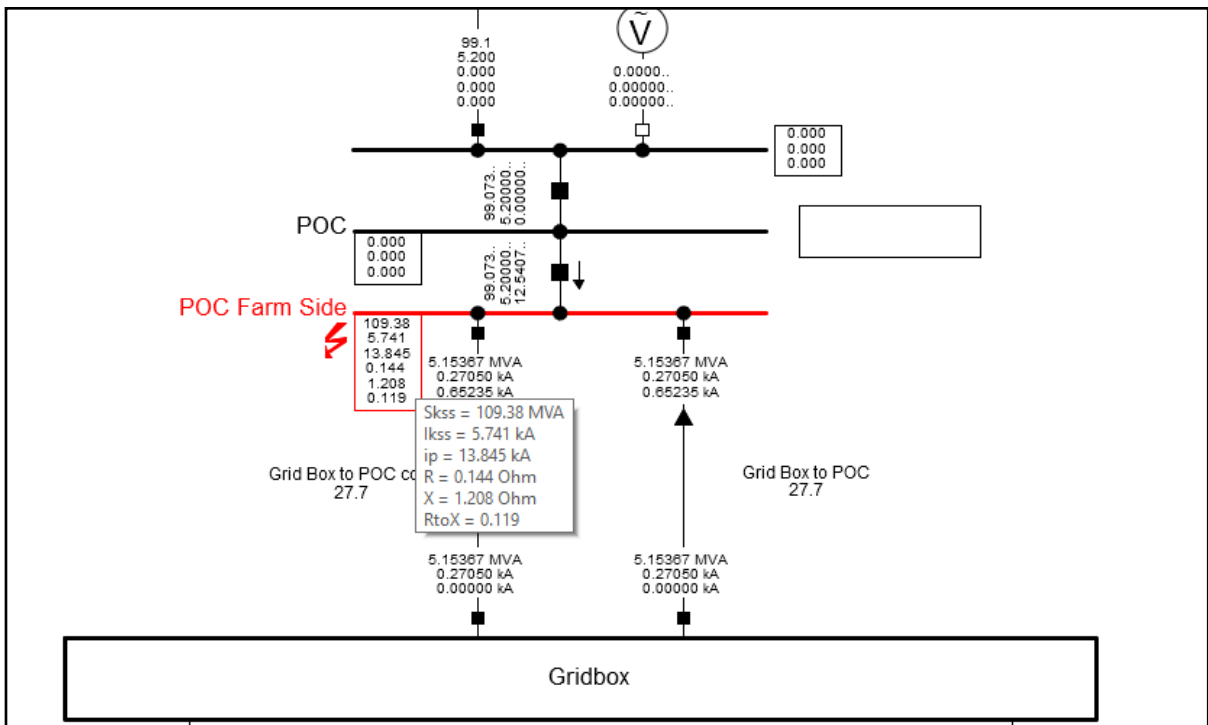


Figure C.14: Fault level study at POC (total contributions)

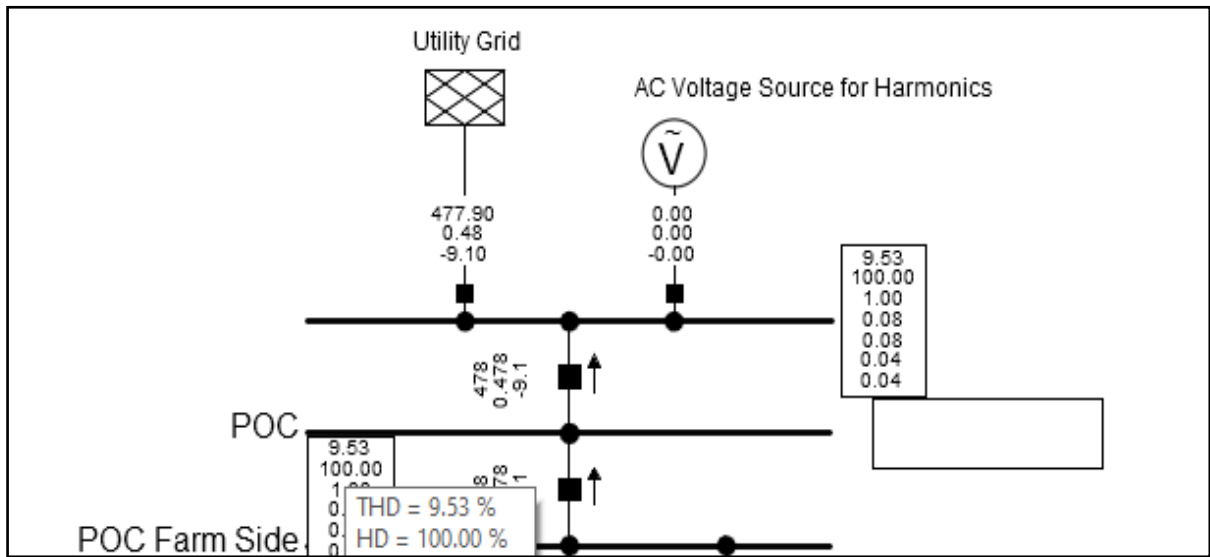


Figure C.15: THD at POC for maximum fault level

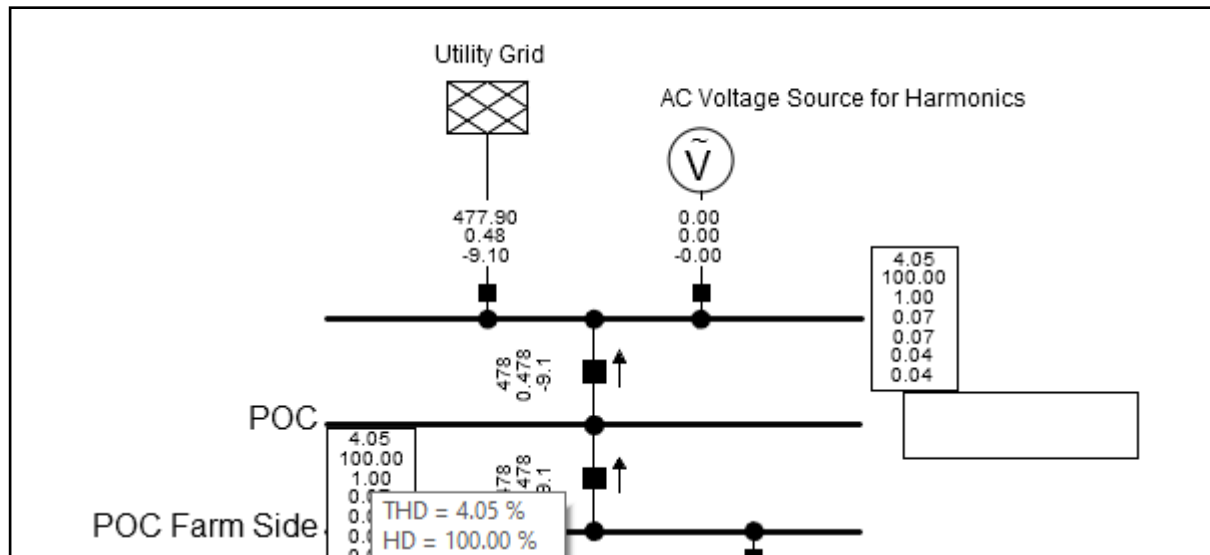


Figure C.16: THD at POC for minimum fault level

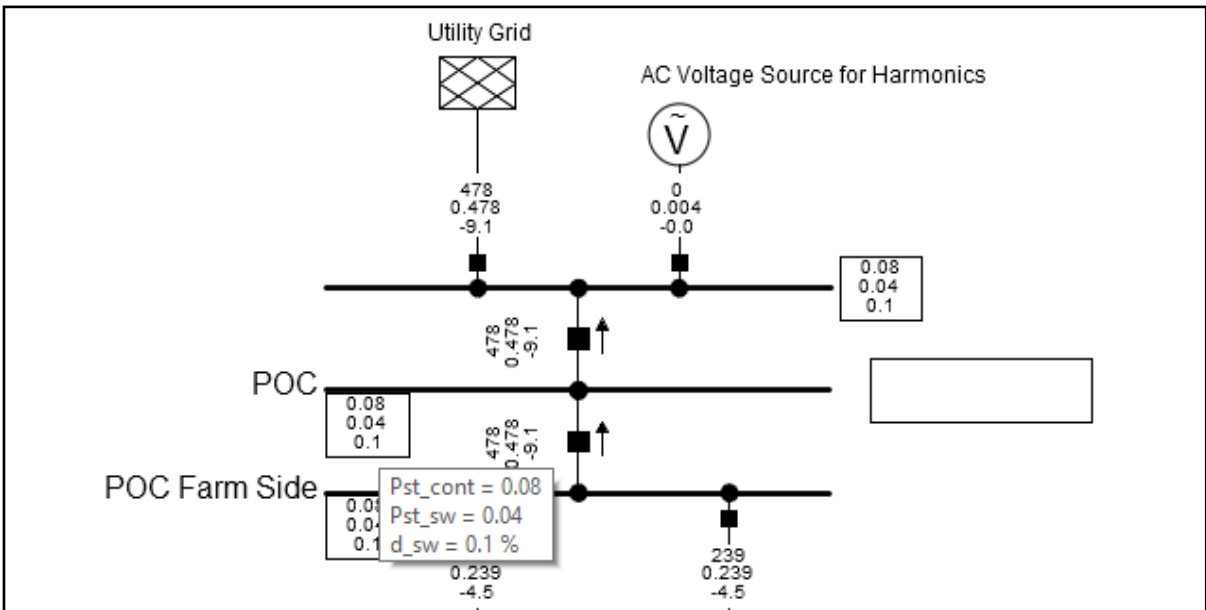


Figure C.17: Flicker at maximum fault level - Short-term continuous and switching operation results

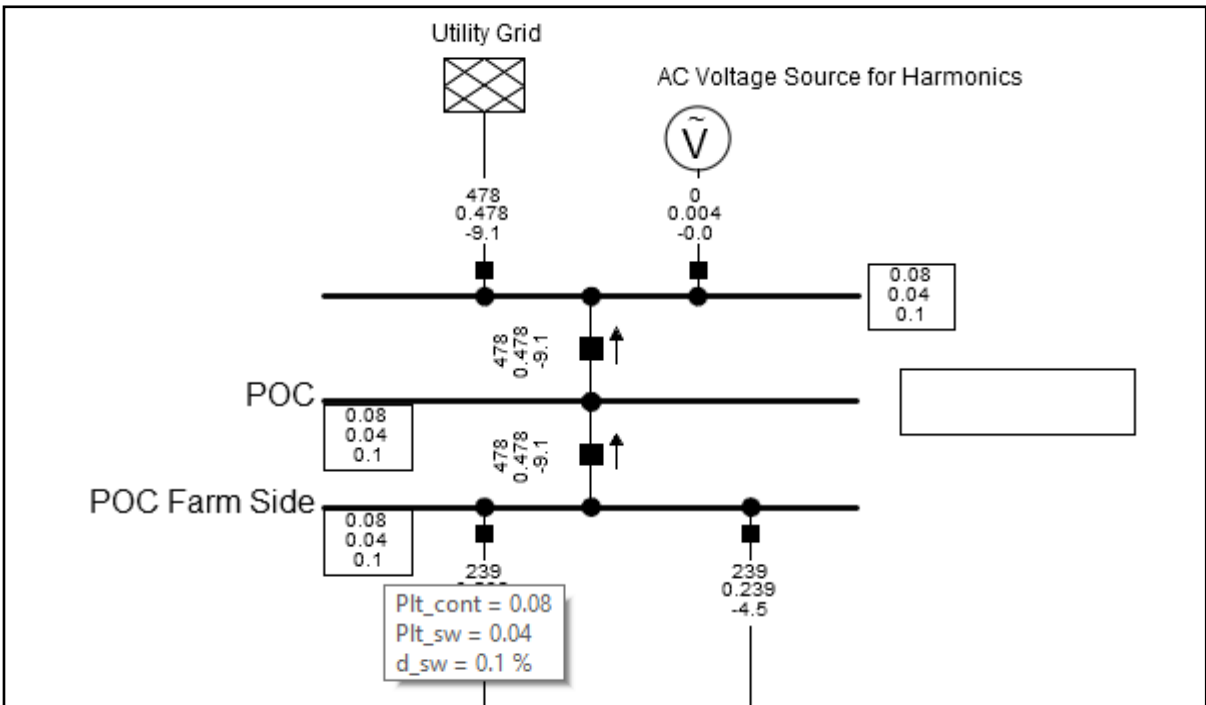


Figure C.18: Flicker at maximum fault level - Long-term continuous and switching operation results

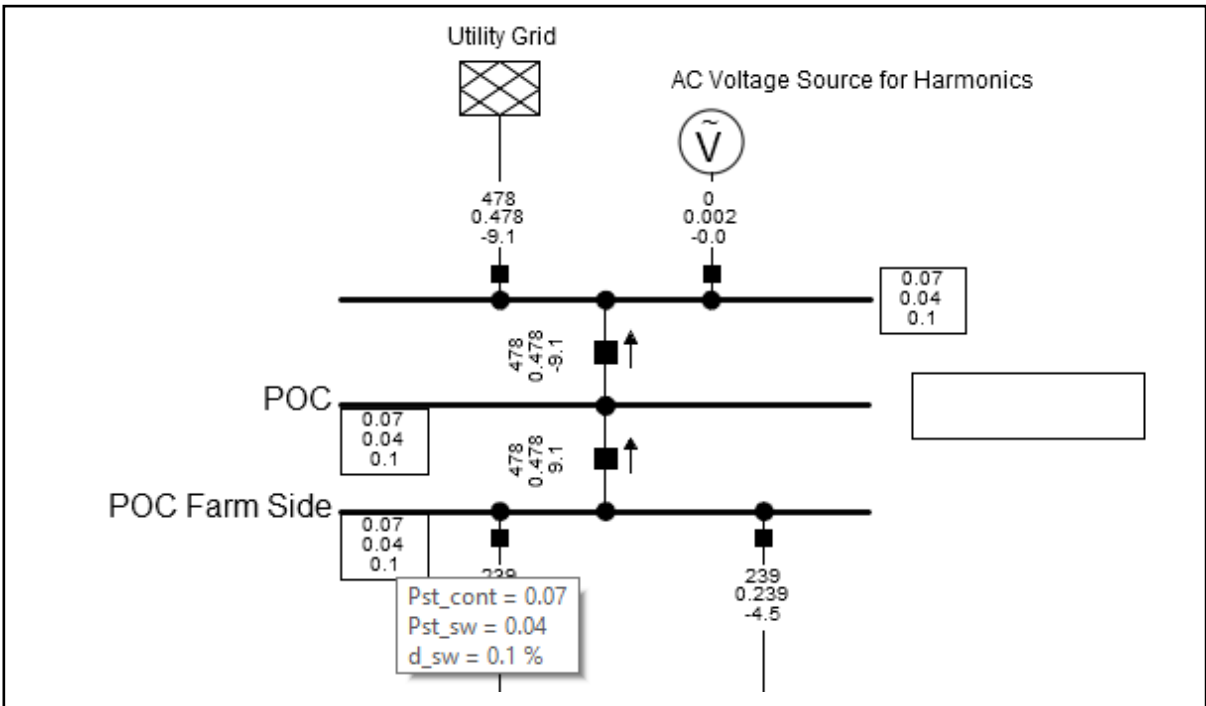


Figure C.19: Flicker at minimum fault level - Short-term continuous and switching operation results

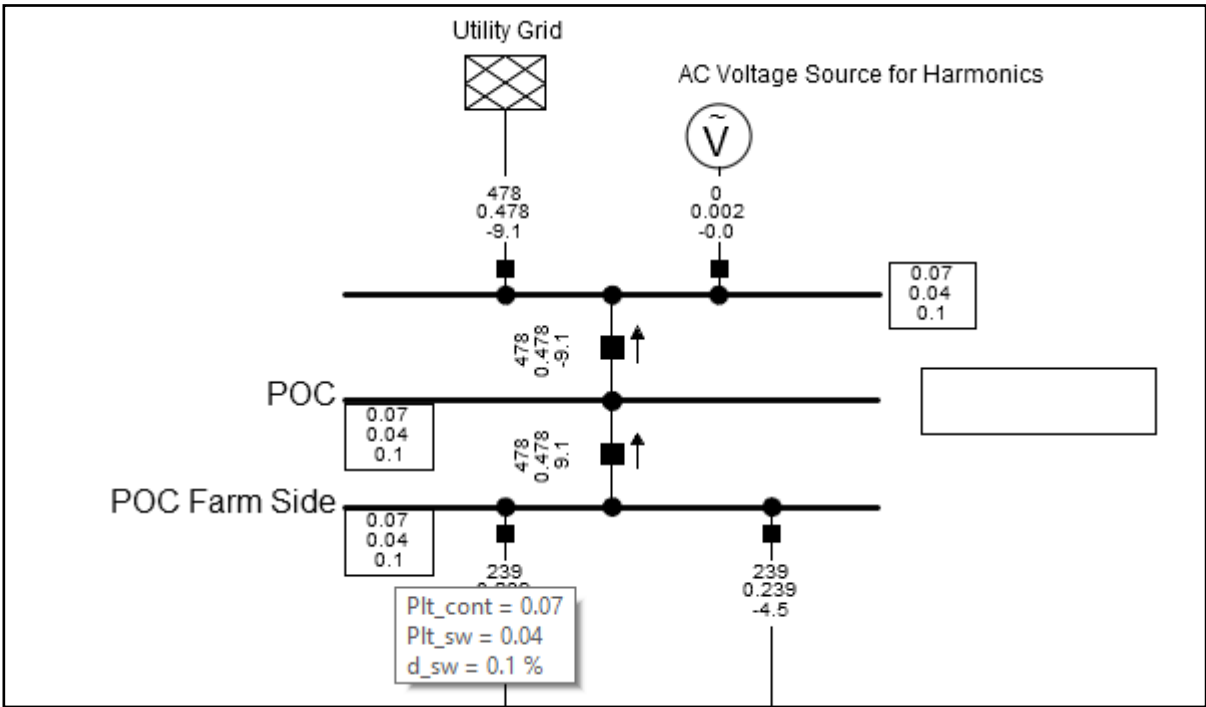


Figure C.20: Flicker at minimum fault level - Long-term continuous and switching operation results

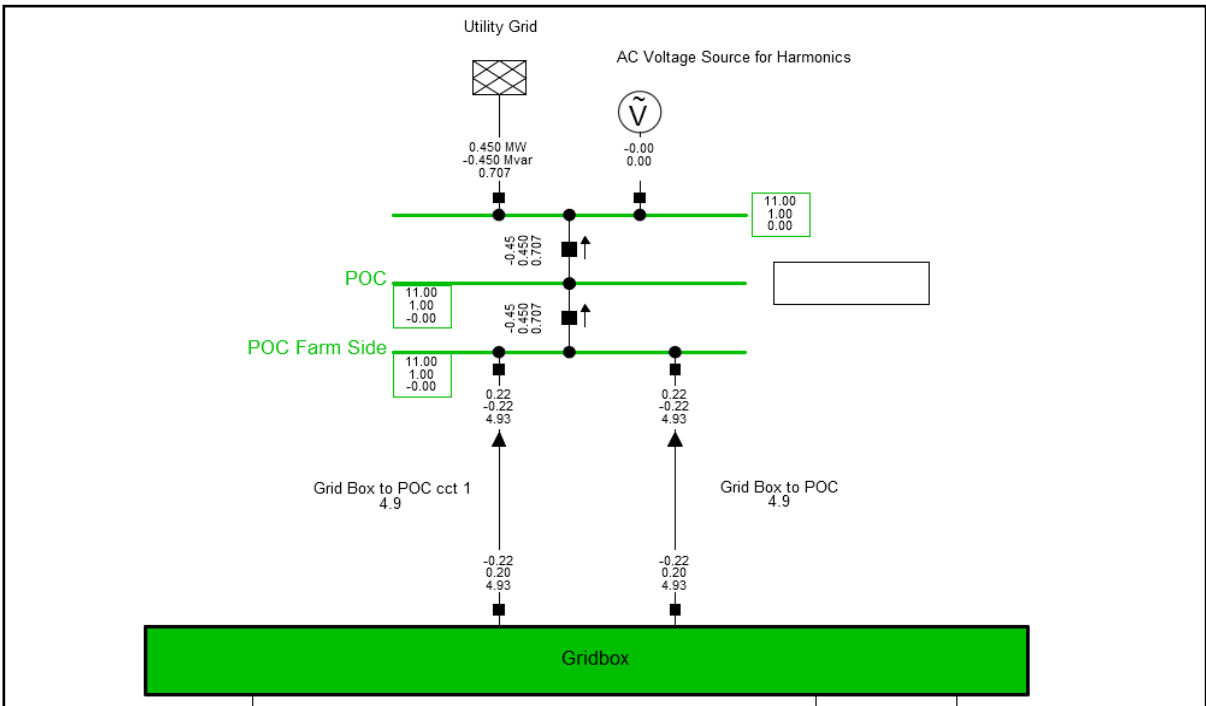


Figure C.21: Case study 1 - reactive power requirements for $Q = -0.450$ MVar & $P = 0.450$ MW at POC

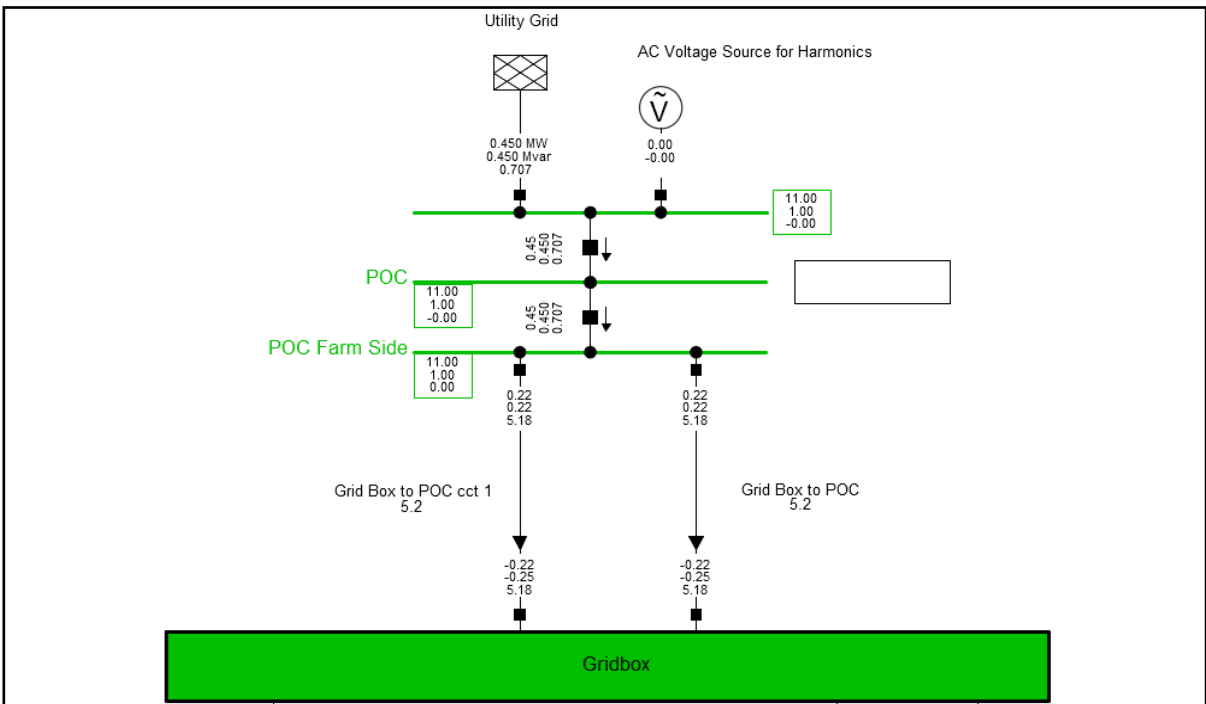


Figure C.22: Case study 1 - reactive power requirements for $Q = 0.450$ MVar & $P = 0.450$ MW at POC

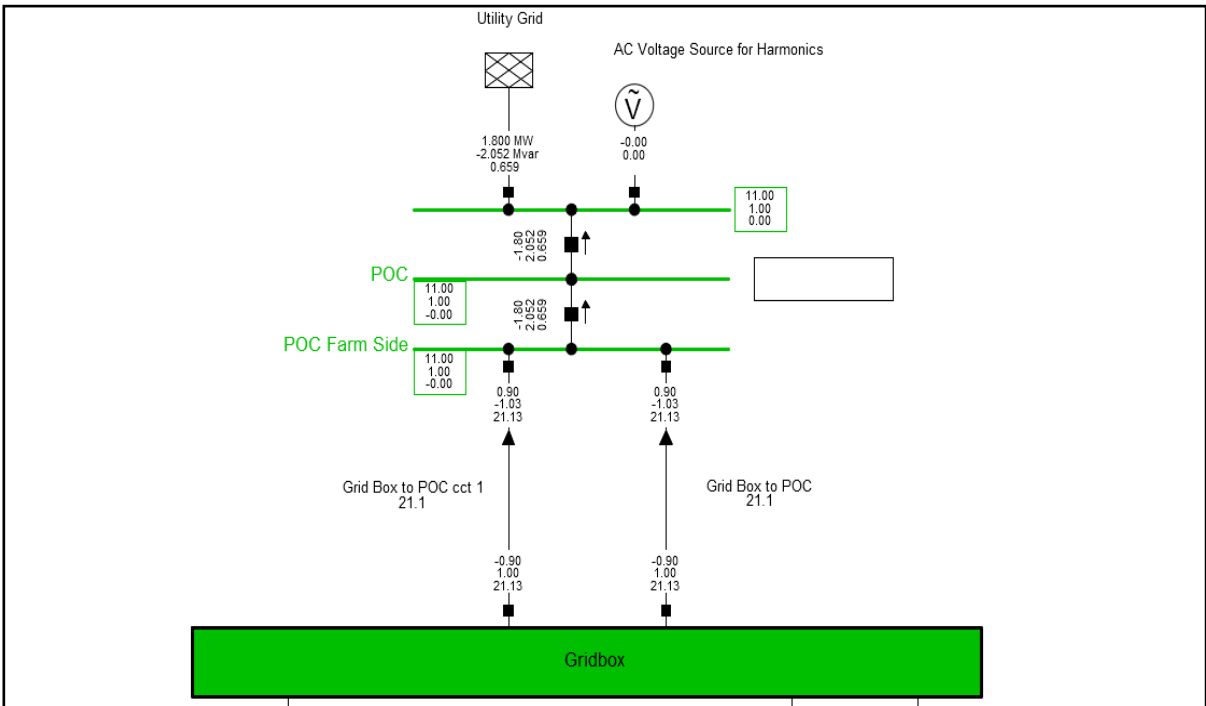


Figure C.23: Case study 1 - reactive power requirements for $Q = -2.052$ MVar & $P = 1.800$ MW at POC

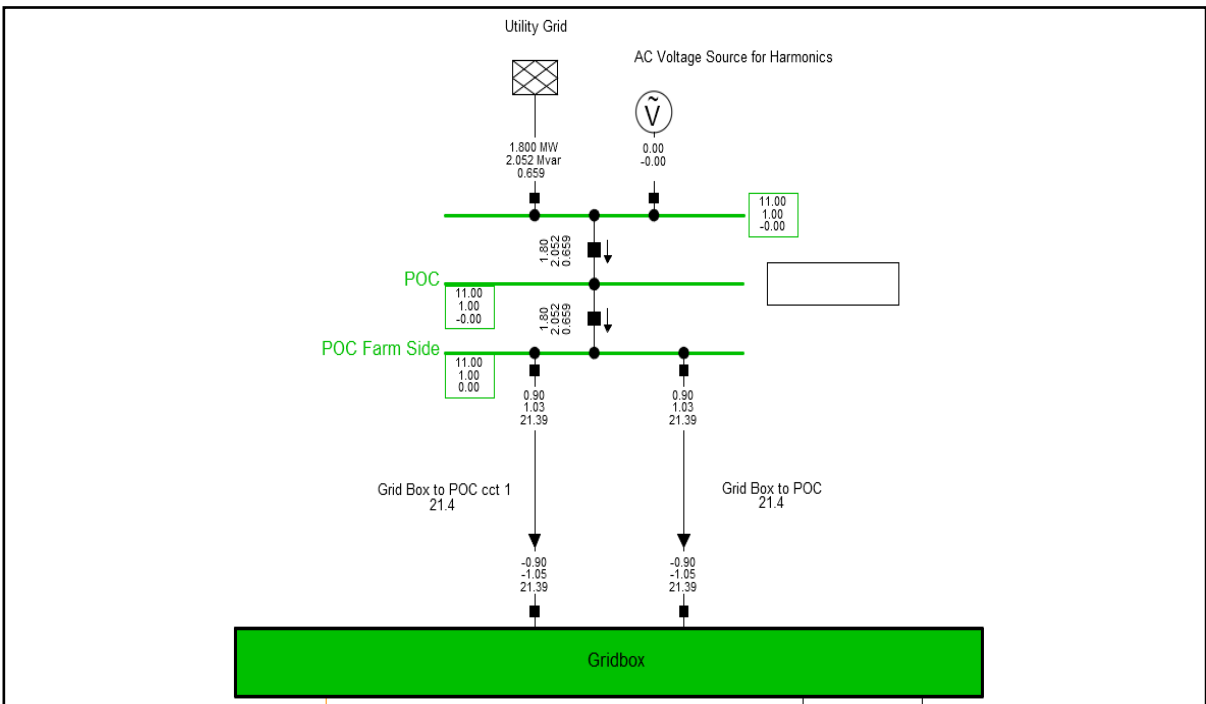


Figure C.24: Case study 1 - reactive power requirements for $Q = 2.052$ MVar & $P = 1.800$ MW at POC

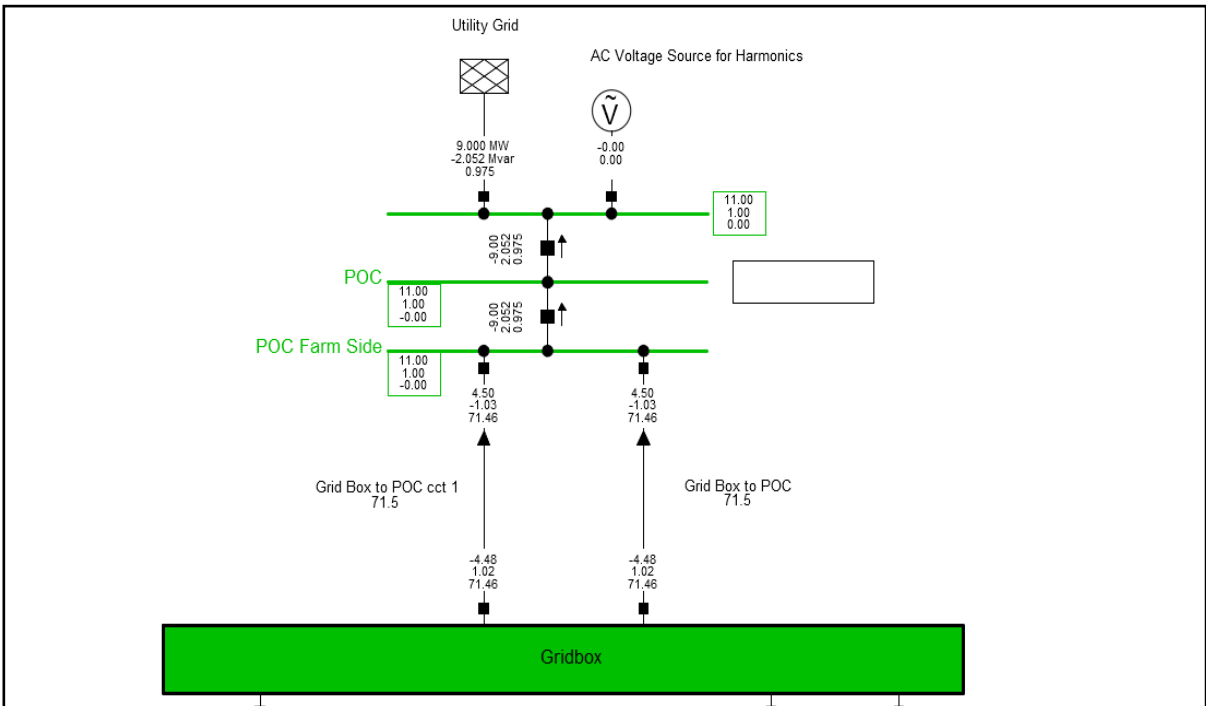


Figure C.25: Case study 1 - reactive power requirements for Q = -2.052 MVar & P = 9.000 MW at POC

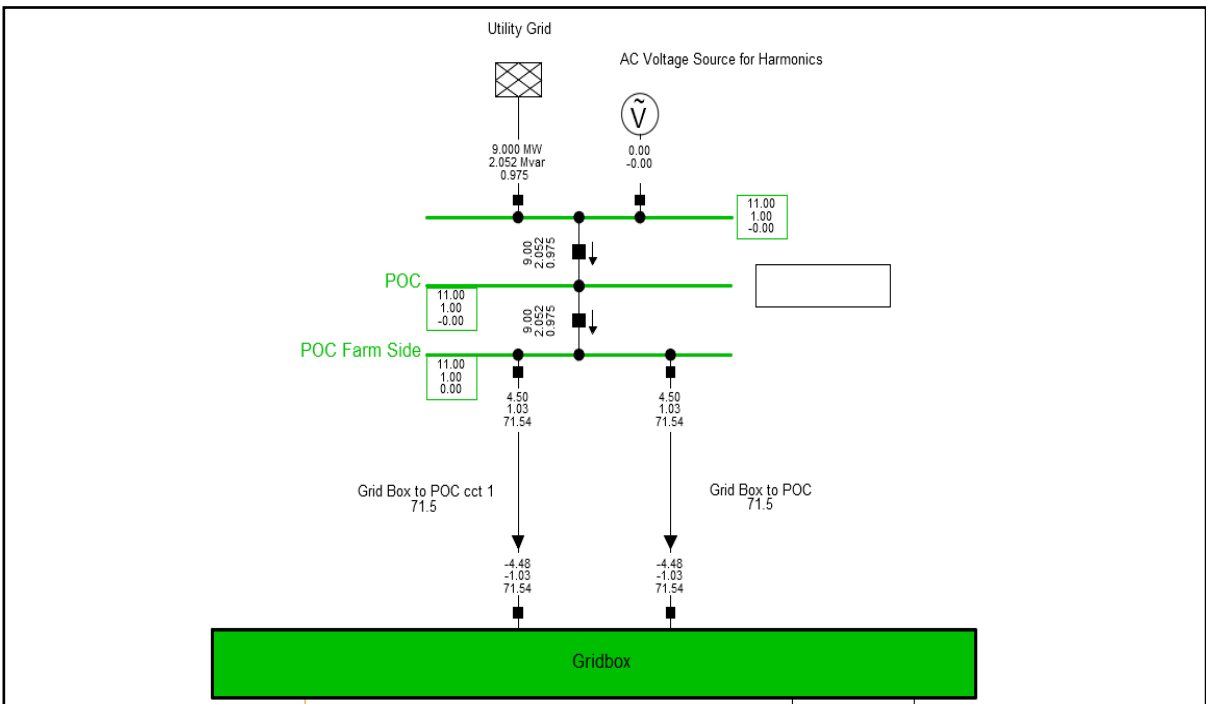


Figure C.26: Case study 1 - reactive power requirements for Q = 2.052 MVar & P = 9.000 MW at POC

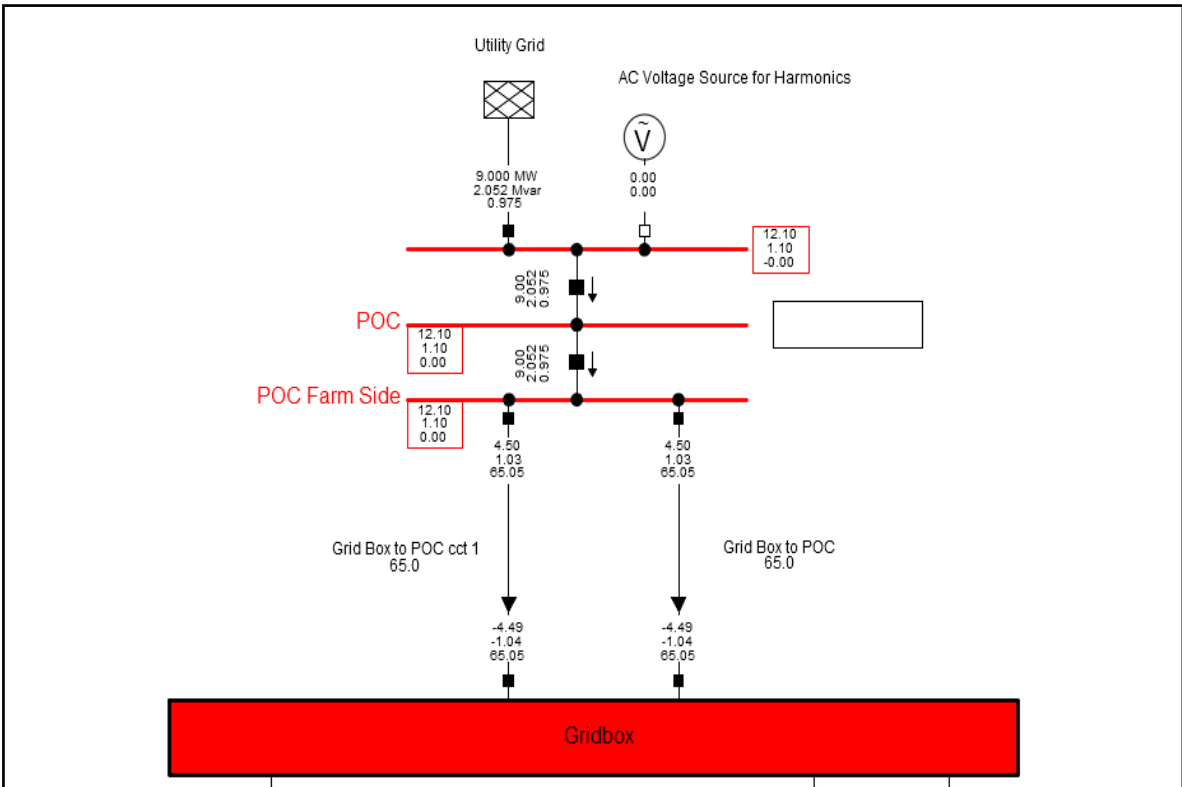


Figure C.27: Case study 1 - voltage capability at 1.1 p.u. for Q = 2.052 MVar & P = 9.000 MW at POC

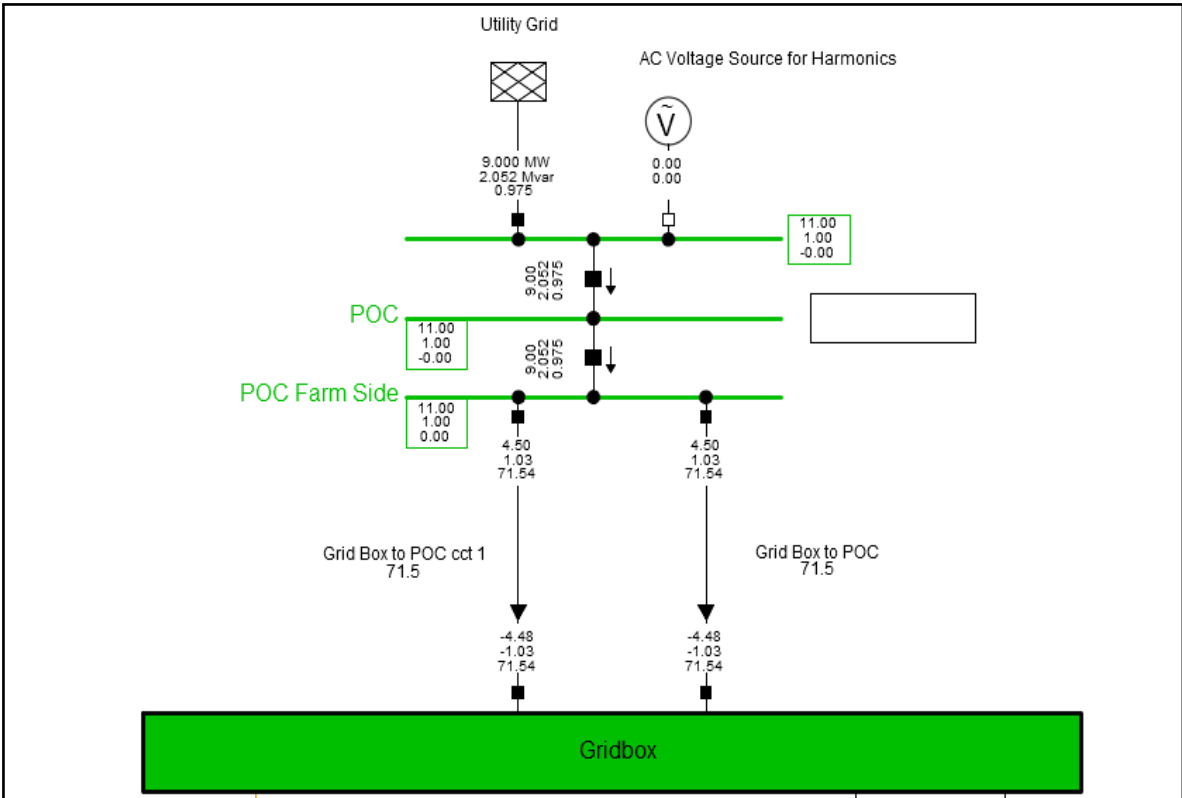


Figure C.28: Case study 1 - voltage capability at 1.0 p.u. for Q = 2.052 MVar & P = 9.000 MW at POC

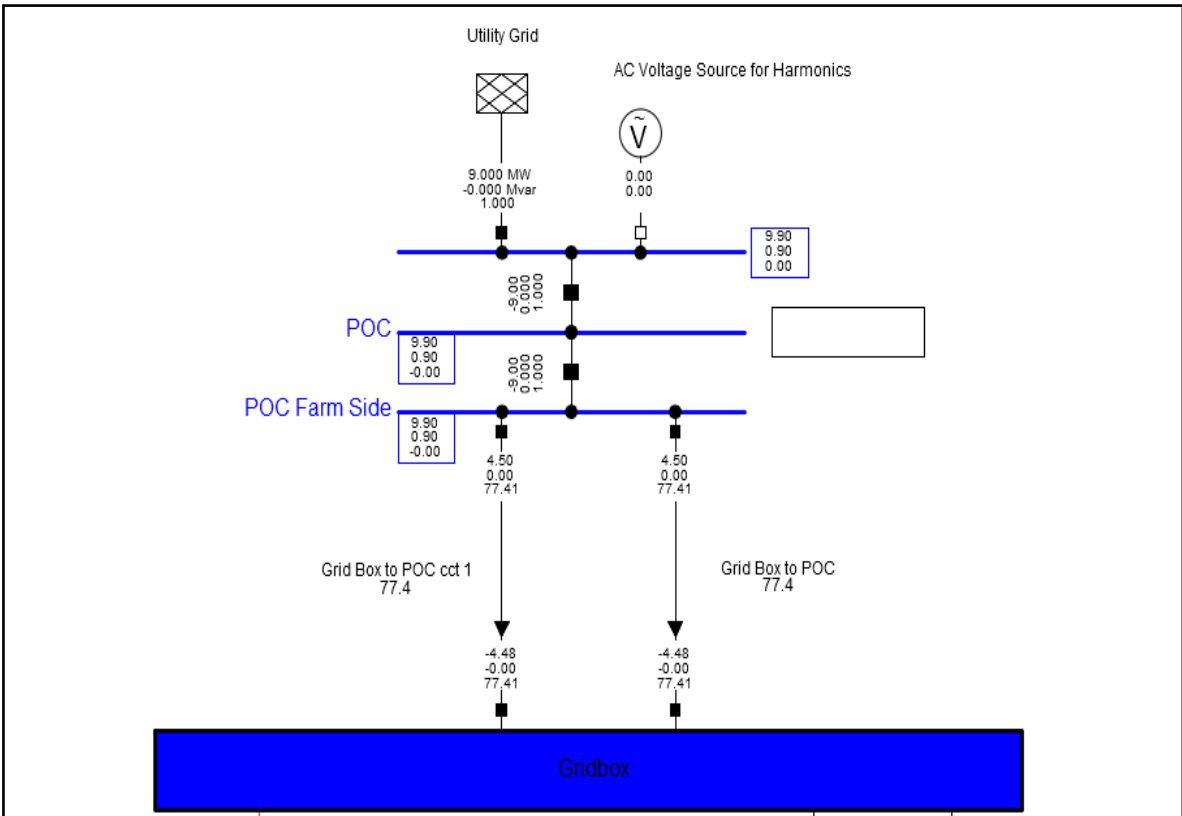


Figure C.29: Case study 1 - voltage capability at 0.9 p.u. for Q = -0.000 MVar & P = 9.000 MW at POC

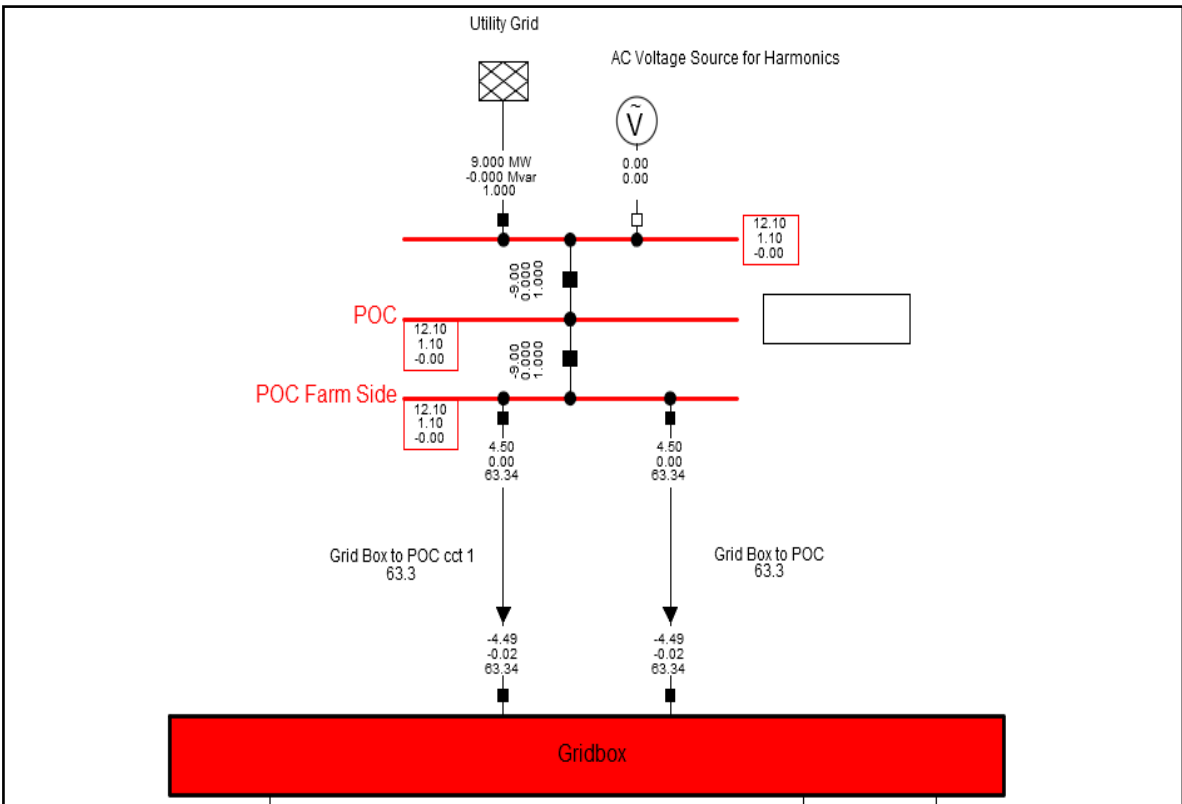


Figure C.30: Case study 1 - voltage capability at 1.1 p.u. for Q = 0.000 MVar & P = 9.000 MW at POC

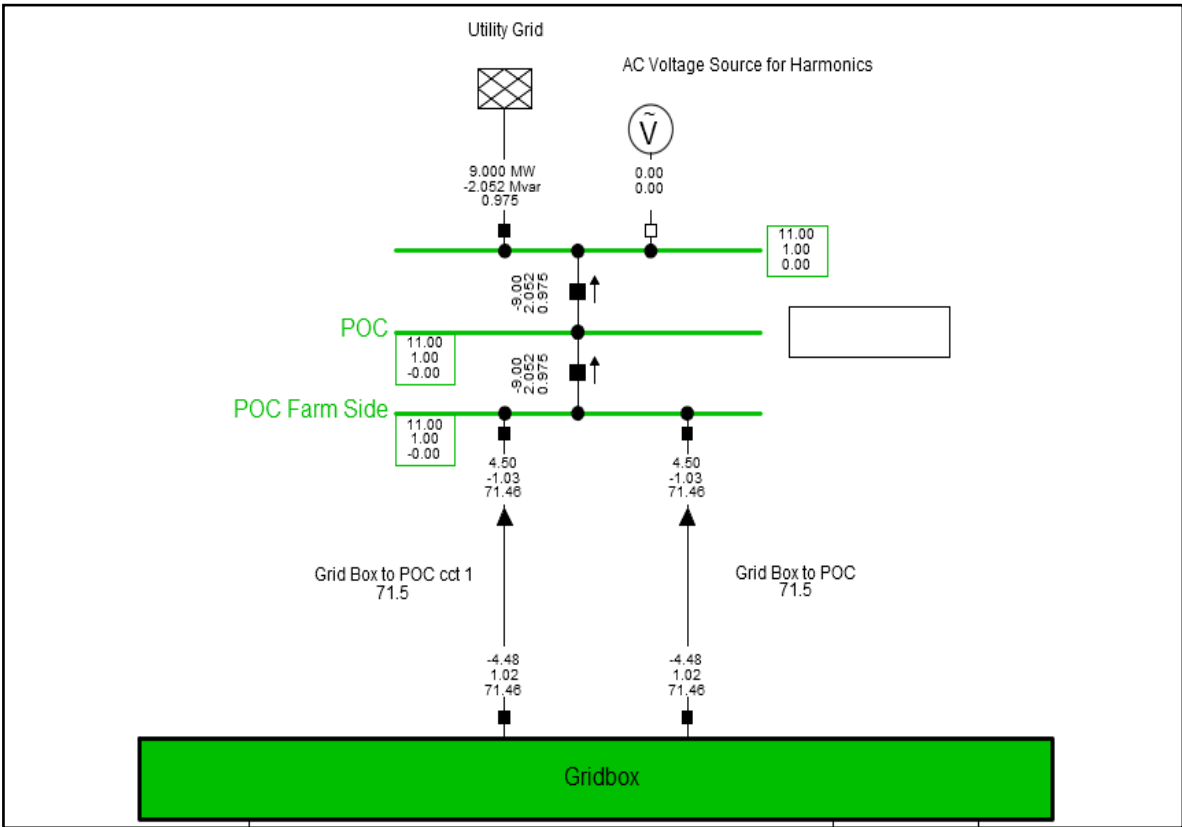


Figure C.31: Case study 1 - voltage capability at 1.0 p.u. for Q = -2.052 MVar & P = 9.000 MW at POC

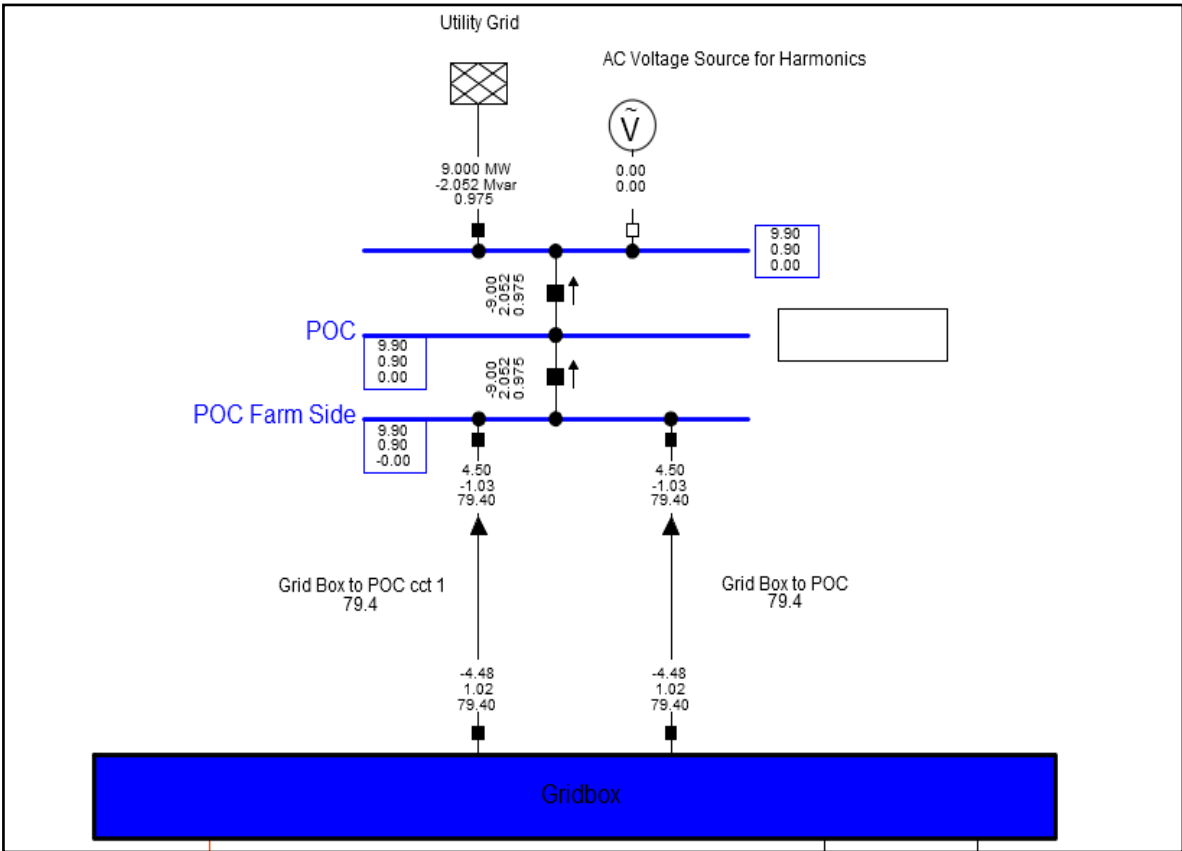


Figure C.32: Case study 1 - voltage capability at 0.9 p.u. for Q = -2.052 MVar & P = 9.000 MW at POC

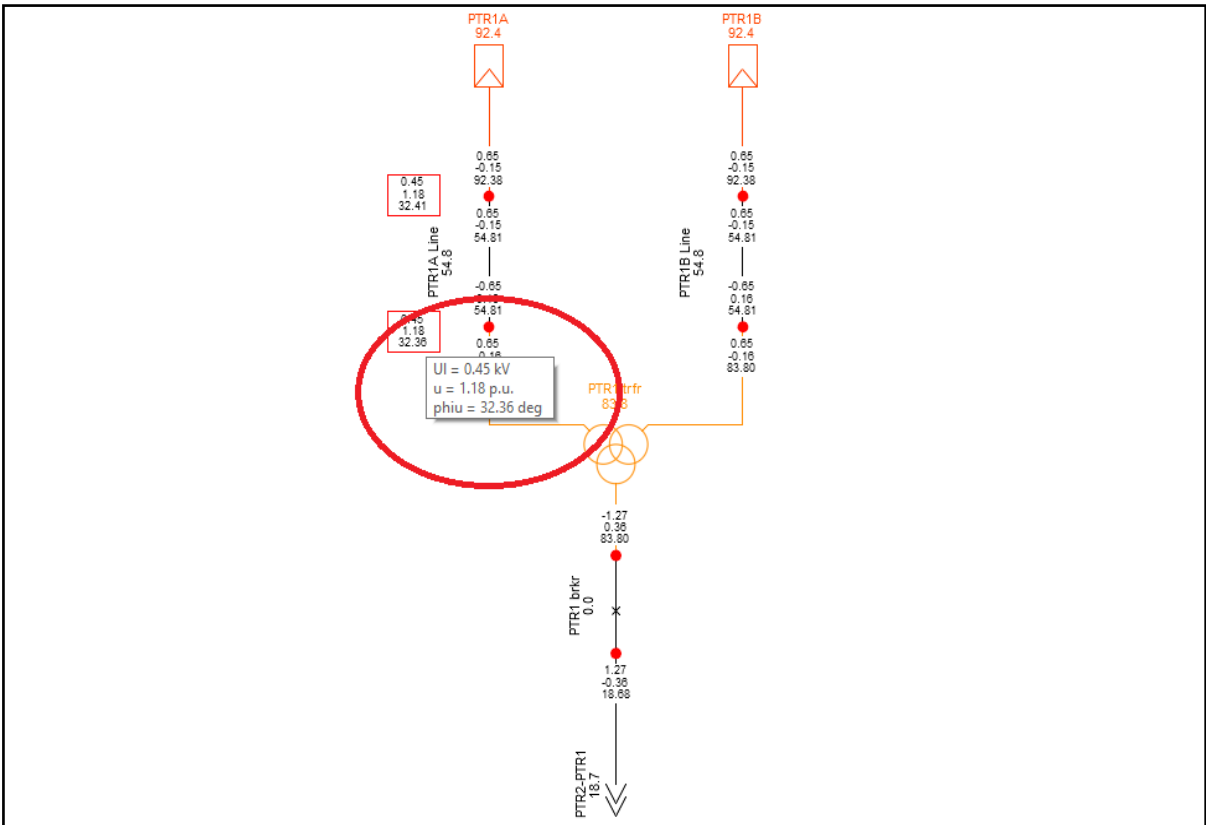


Figure C.33: Case study 1 - study point 1 during a voltage of 1.1 p.u. at the POC – inverter voltage within operational requirements

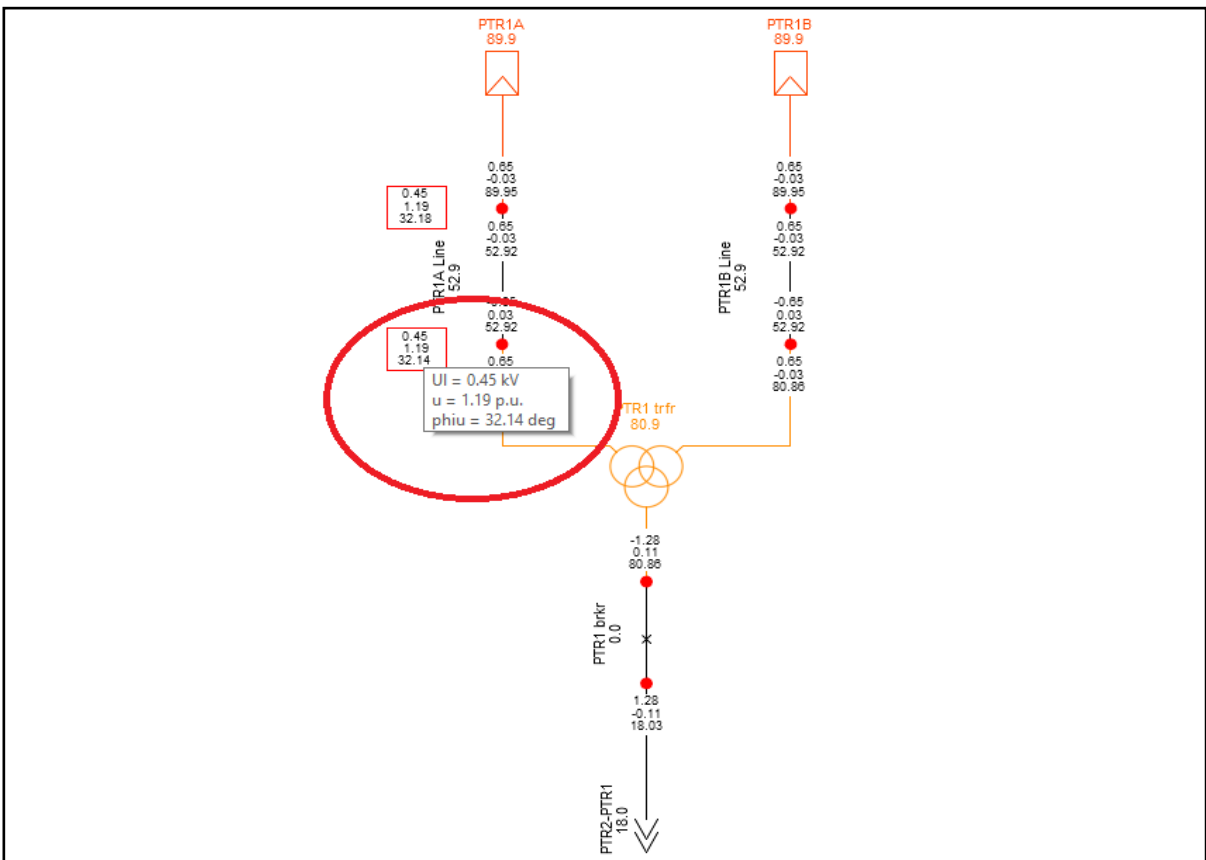


Figure C.34: Study case 1 - study point 4 during a voltage of 1.1 p.u. at the POC – inverter voltage within operational requirements

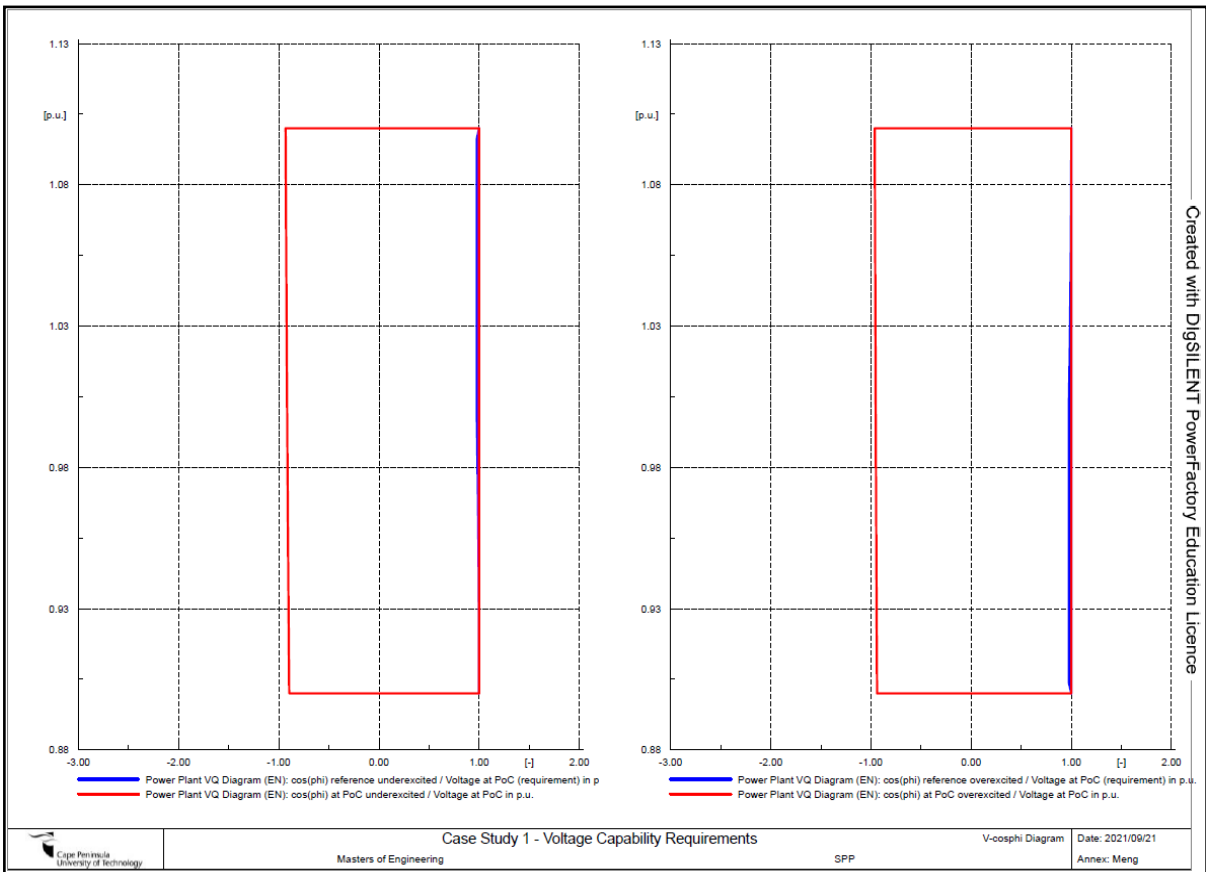


Figure C.35: Case study 1 - power factor and voltage requirement at POC indicating under excited (left) conditions and overexcited conditions (right)

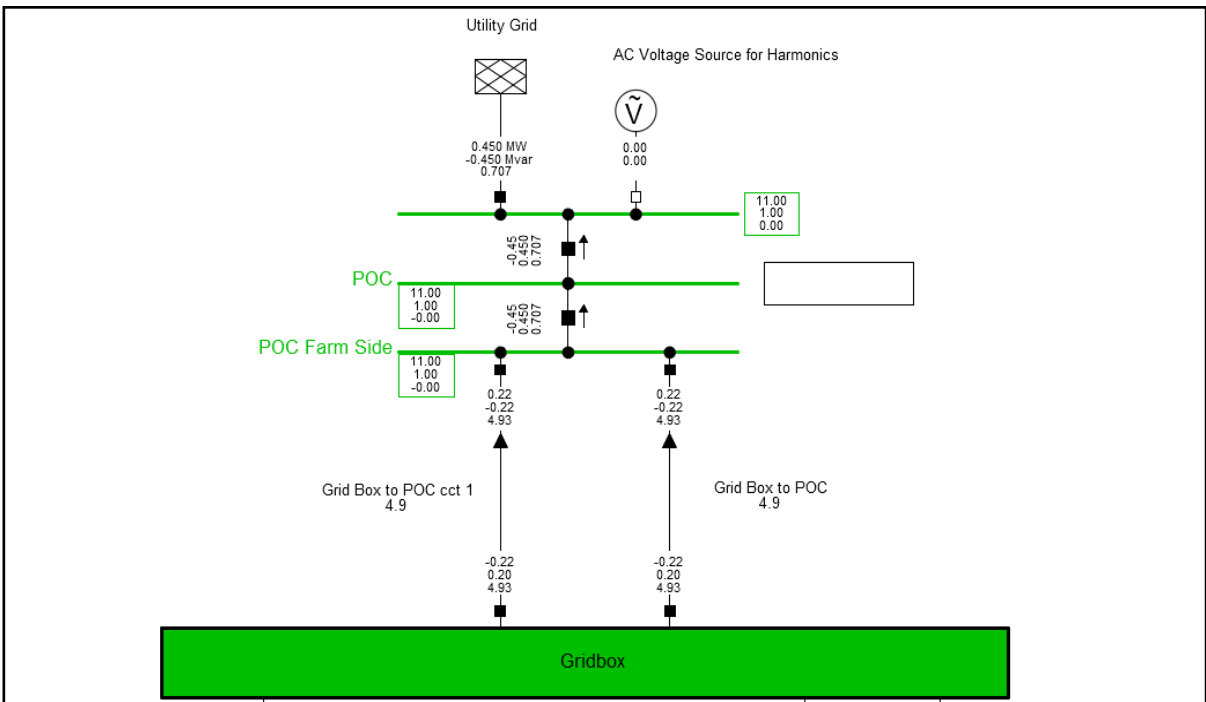


Figure C.35: Case study 2 - reactive power requirements for $Q = -0.450$ MVar & $P = 0.450$ MW at POC

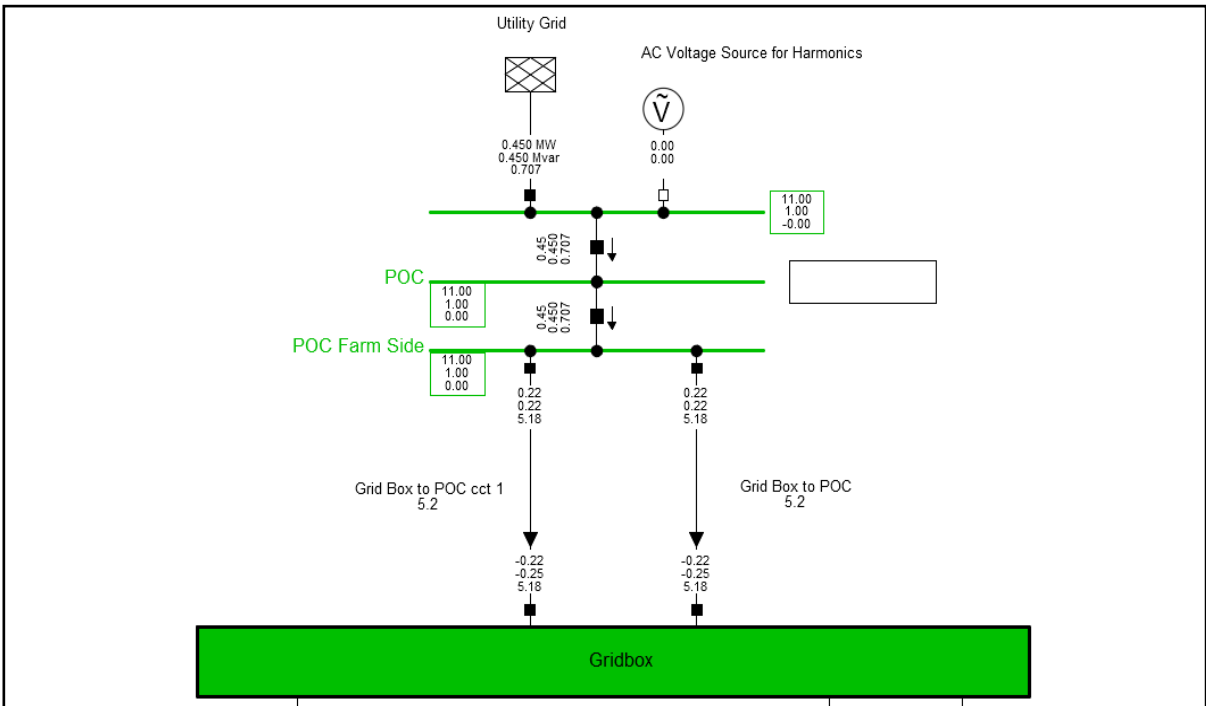


Figure C.37: Case study 2 - reactive power requirements for $Q = 0.450$ MVar & $P = 0.450$ MW at POC

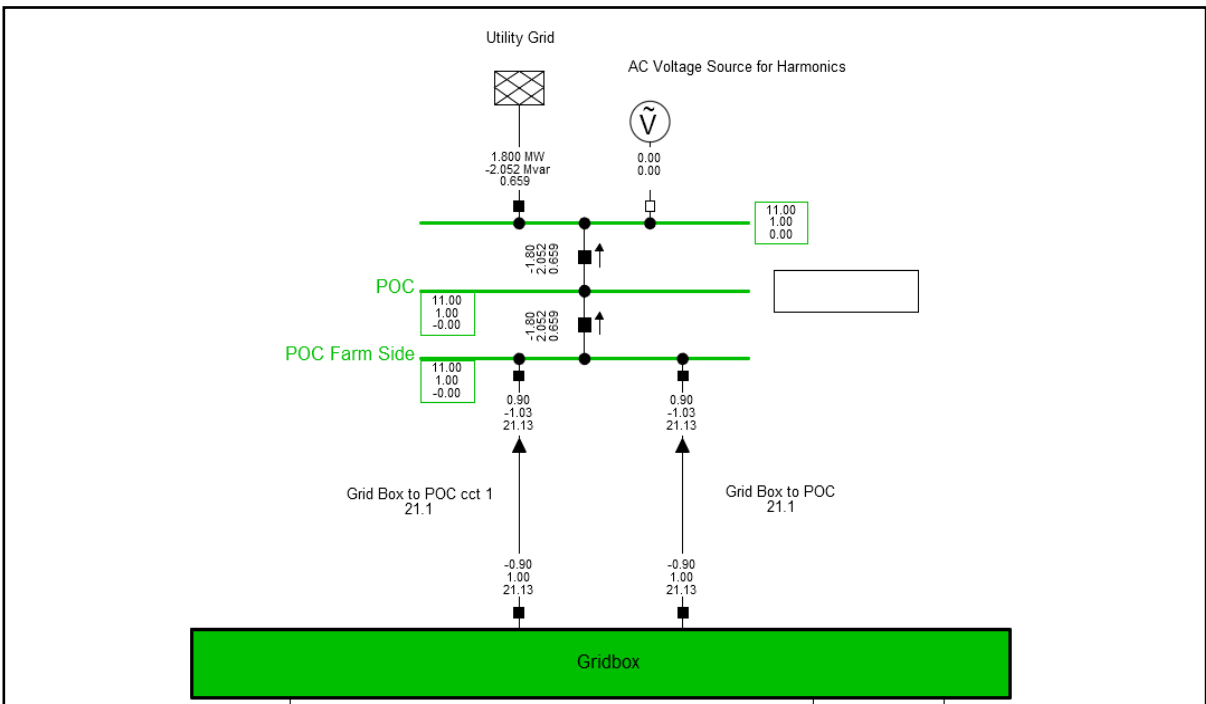


Figure C.38: Case study 2 - reactive power requirements for $Q = -2.052$ MVar & $P = 1.800$ MW at POC

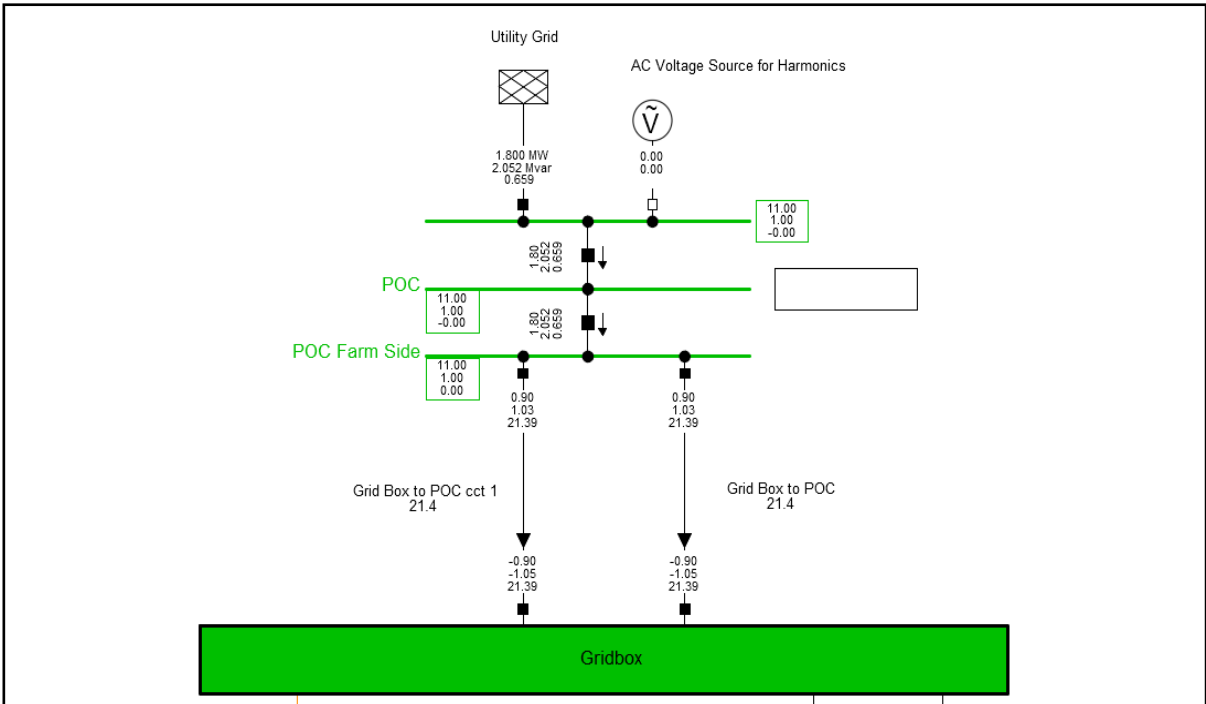


Figure C.39: Case study 2 - reactive power requirements for Q = 2.052 MVar & P = 1.800 MW at POC

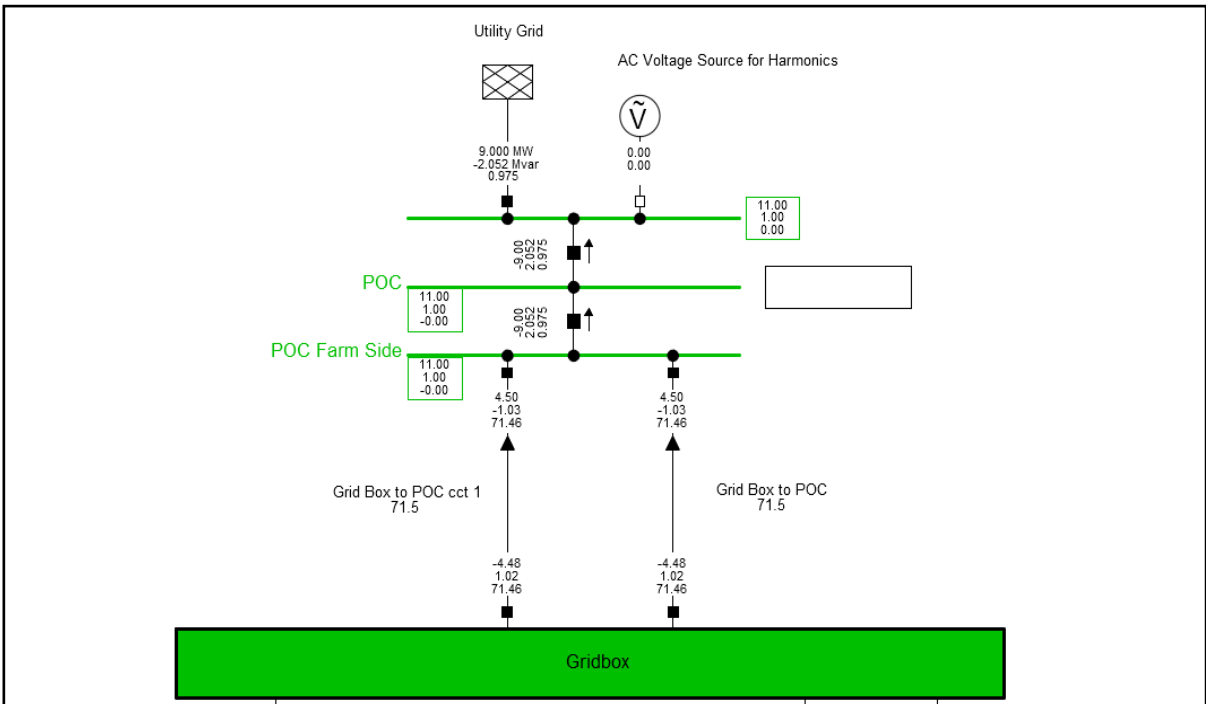


Figure C.40: Case study 2 - reactive power requirements for Q = -2.052 MVar & P = 9.000 MW at POC

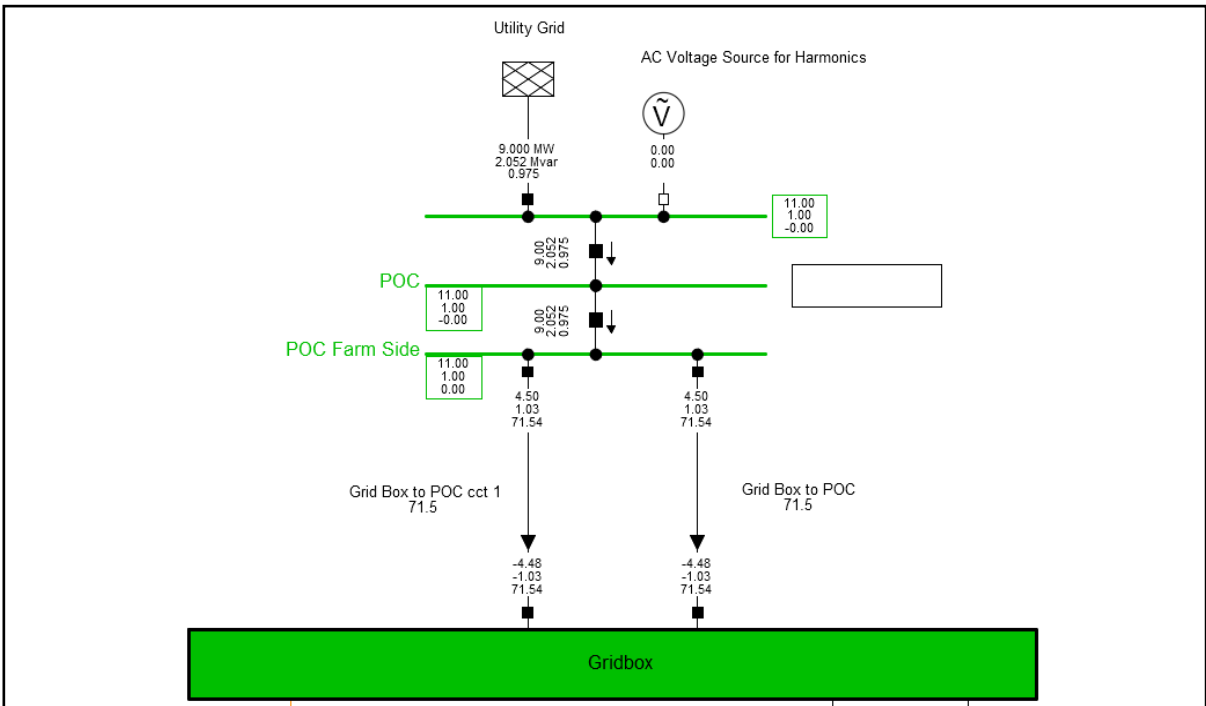


Figure C.41: Case study 2 - reactive power requirements for $Q = 2.052$ MVar & $P = 9.000$ MW at POC

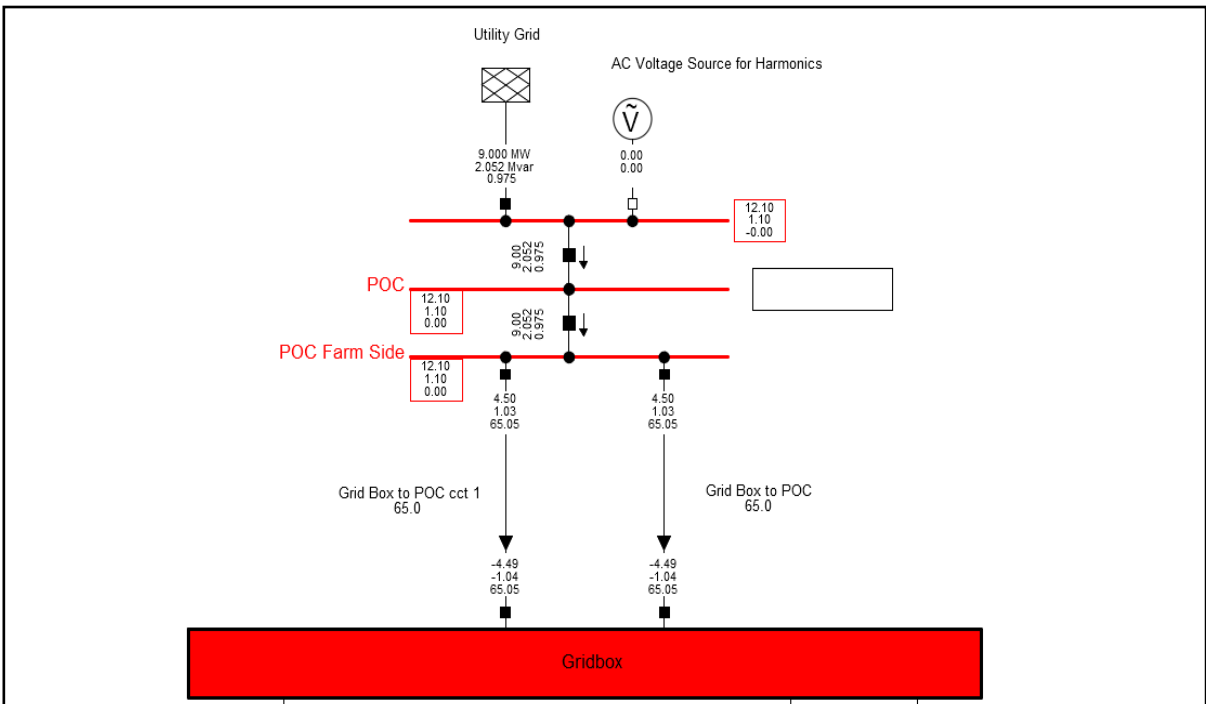


Figure C.42: Case study 2 - voltage capability at 1.1 p.u. for $Q = 2.052$ MVar & $P = 9.000$ MW at POC

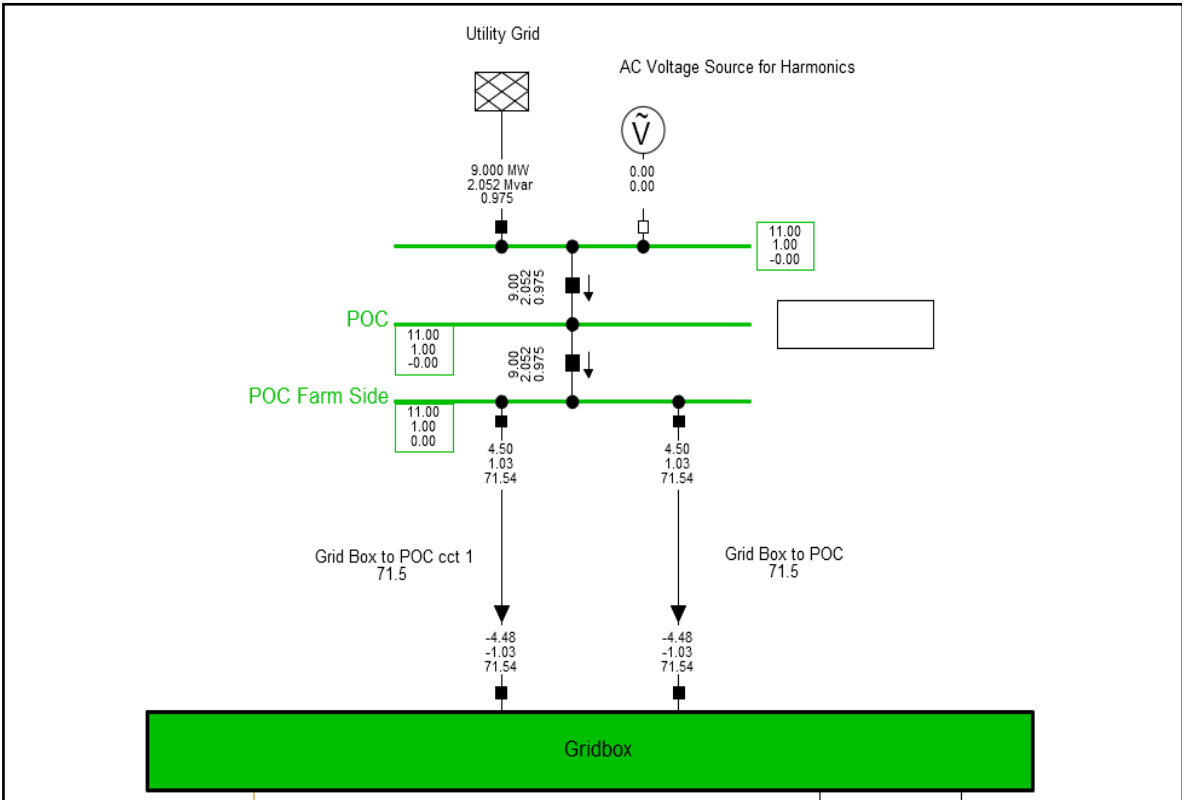


Figure C.43: Case study 2 - voltage capability at 1.0 p.u. for Q = 2.052 MVar & P = 9.000 MW at POC

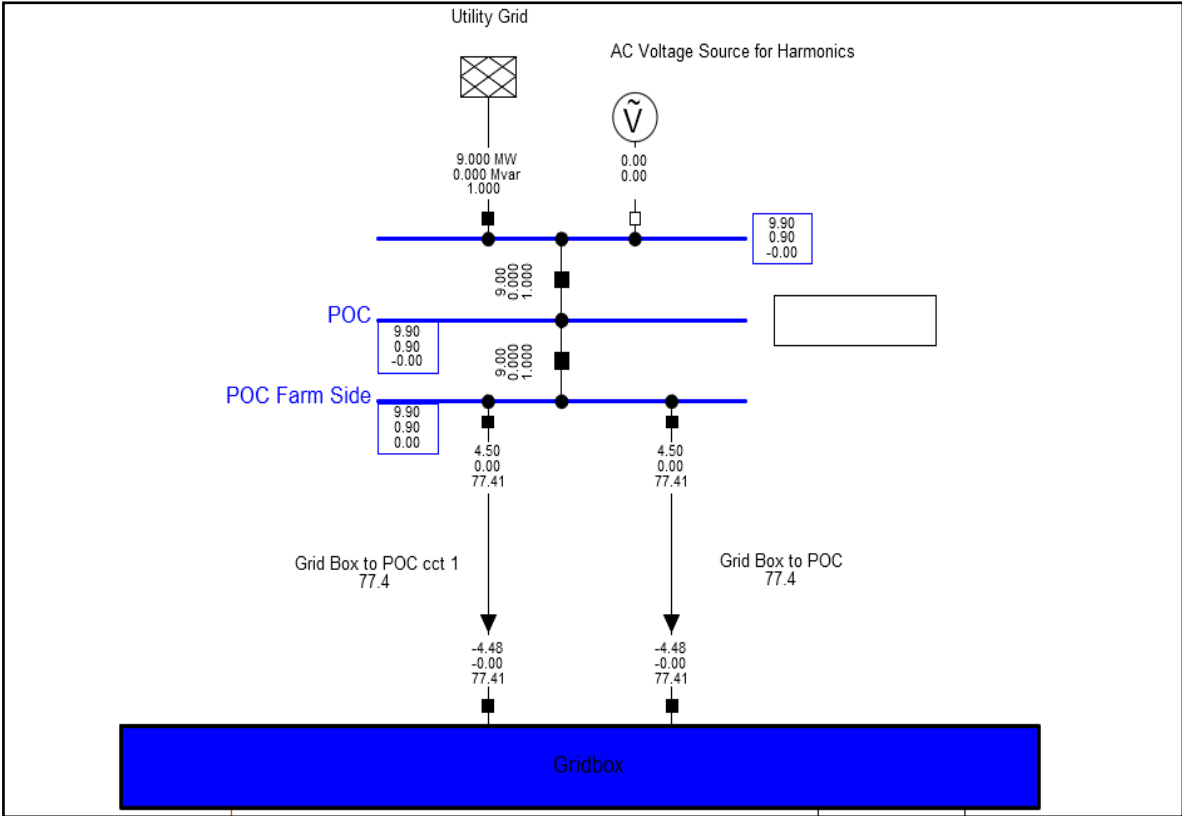


Figure C.44: Case study 2 - voltage capability at 0.9 p.u. for Q = -0.000 MVar & P = 9.000 MW at POC

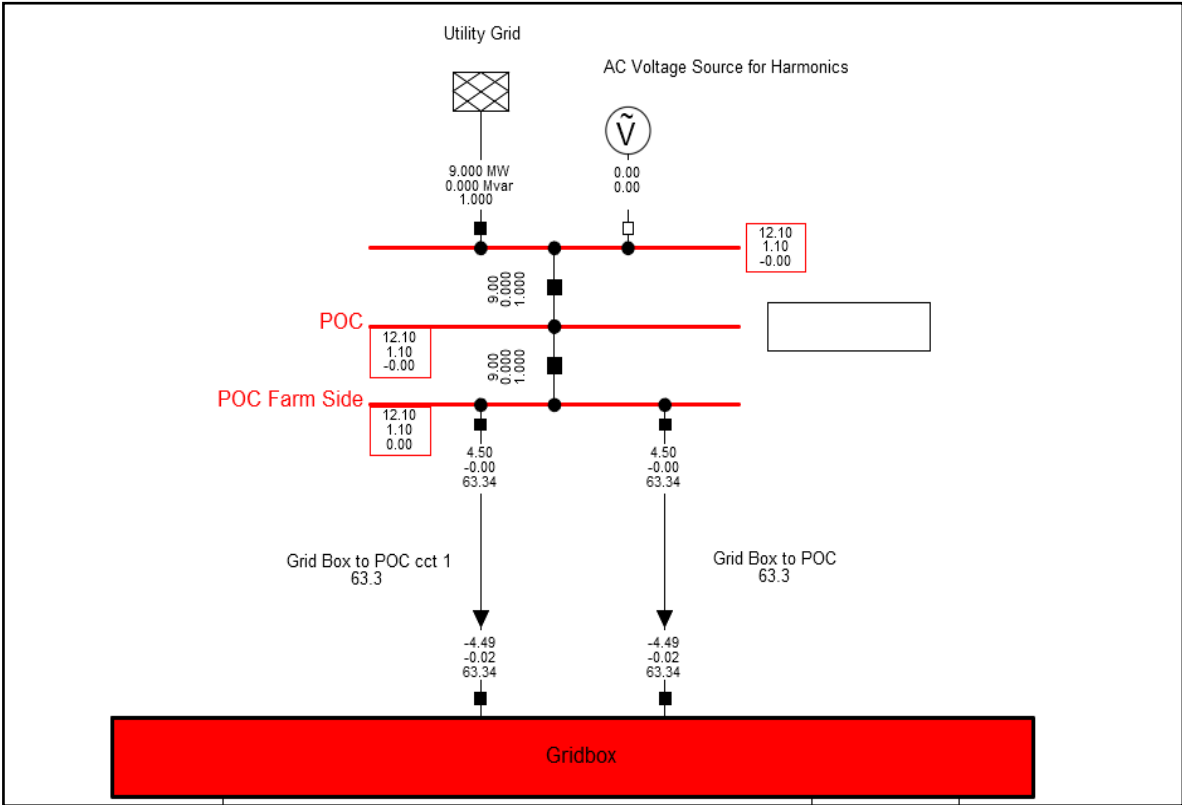


Figure C.45: Case study 2 - voltage capability at 1.1 p.u. for Q = 0.000 MVar & P = 9.000 MW at POC

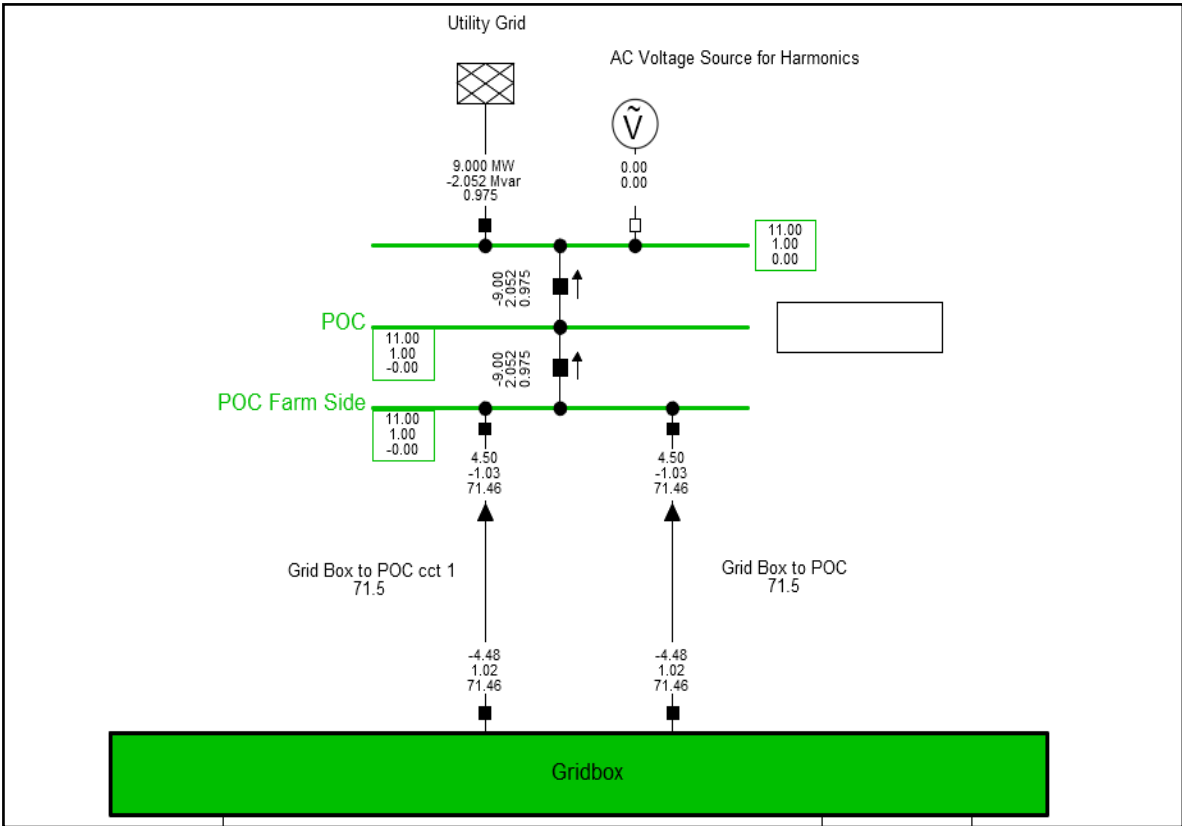


Figure C.46: Case study 2 - voltage capability at 1.0 p.u. for Q = -2.052 MVar & P = 9.000 MW at POC

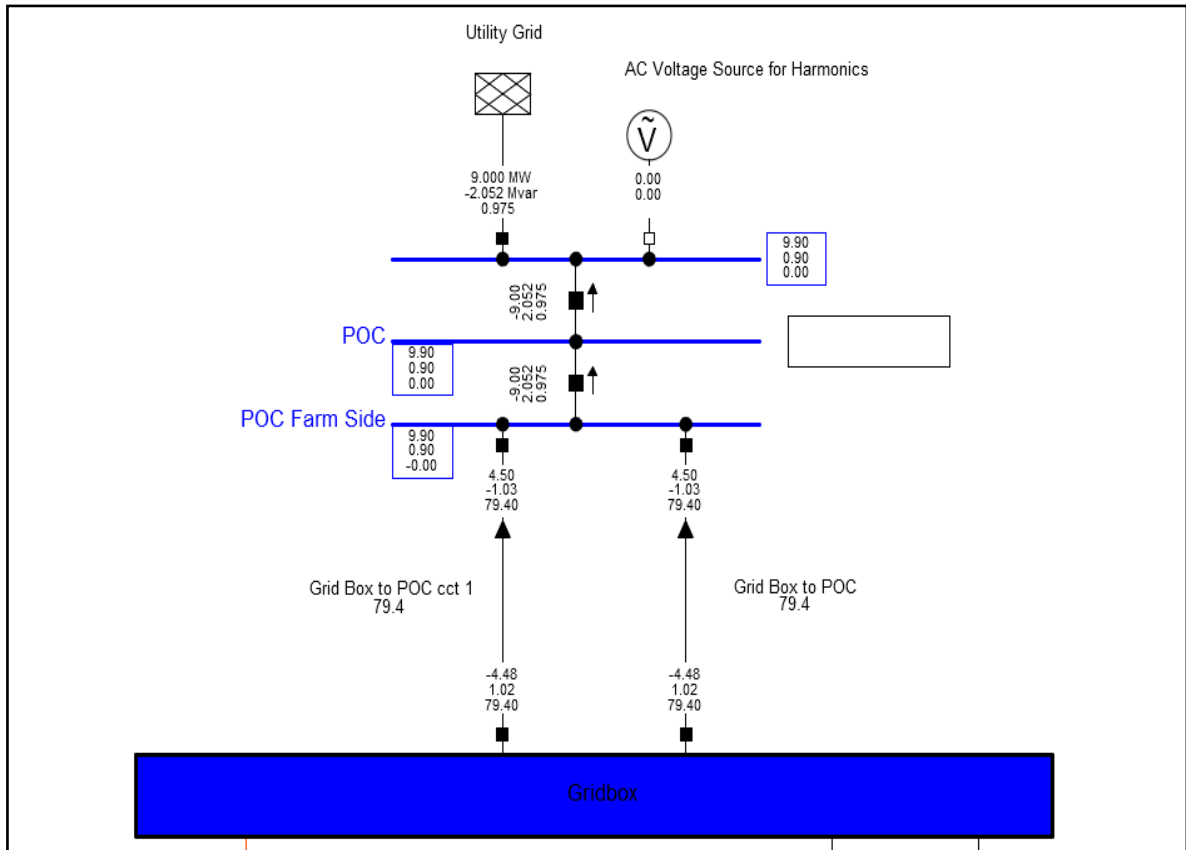


Figure C.47: Case study 2 - voltage capability at 0.9 p.u. for Q = -2.052 MVar & P = 9.000 MW at POC

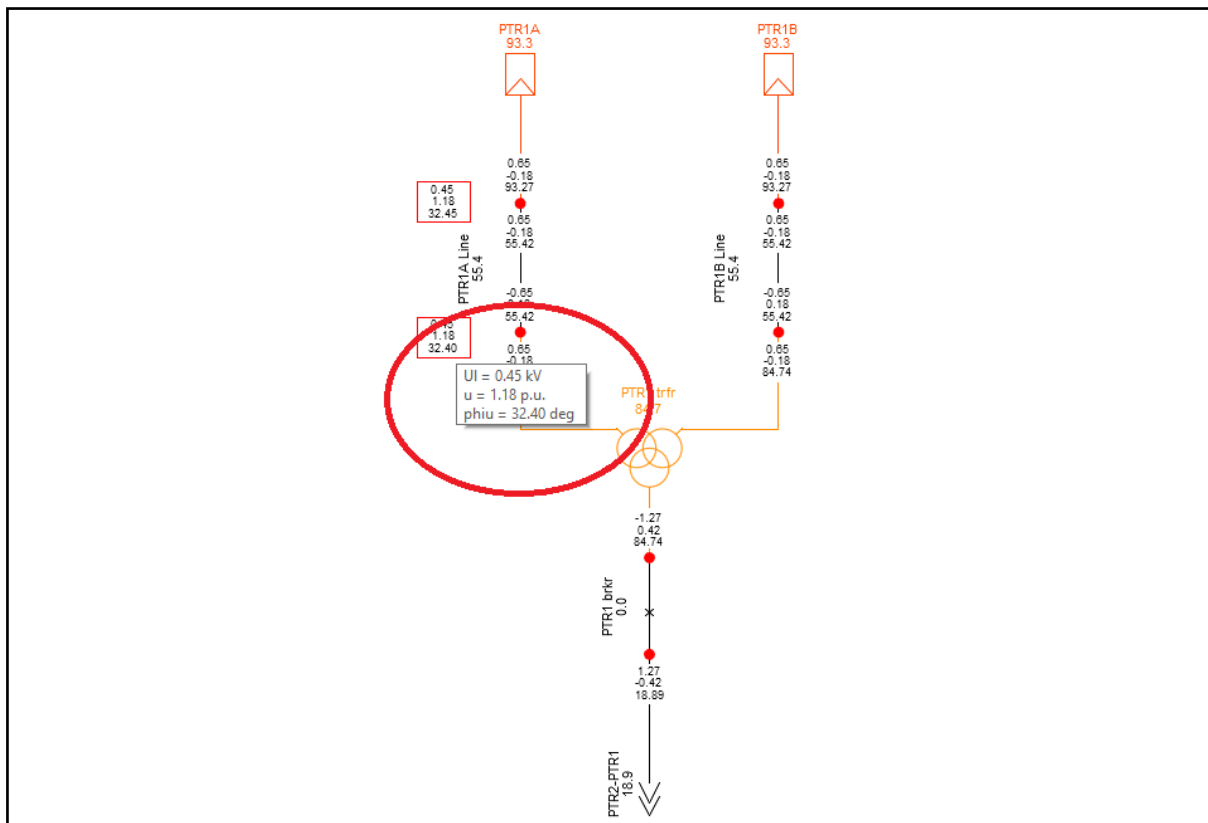


Figure C.48: Case study 2 - study point 1 during a voltage of 1.1 p.u. at the POC – inverter voltage within operational requirements

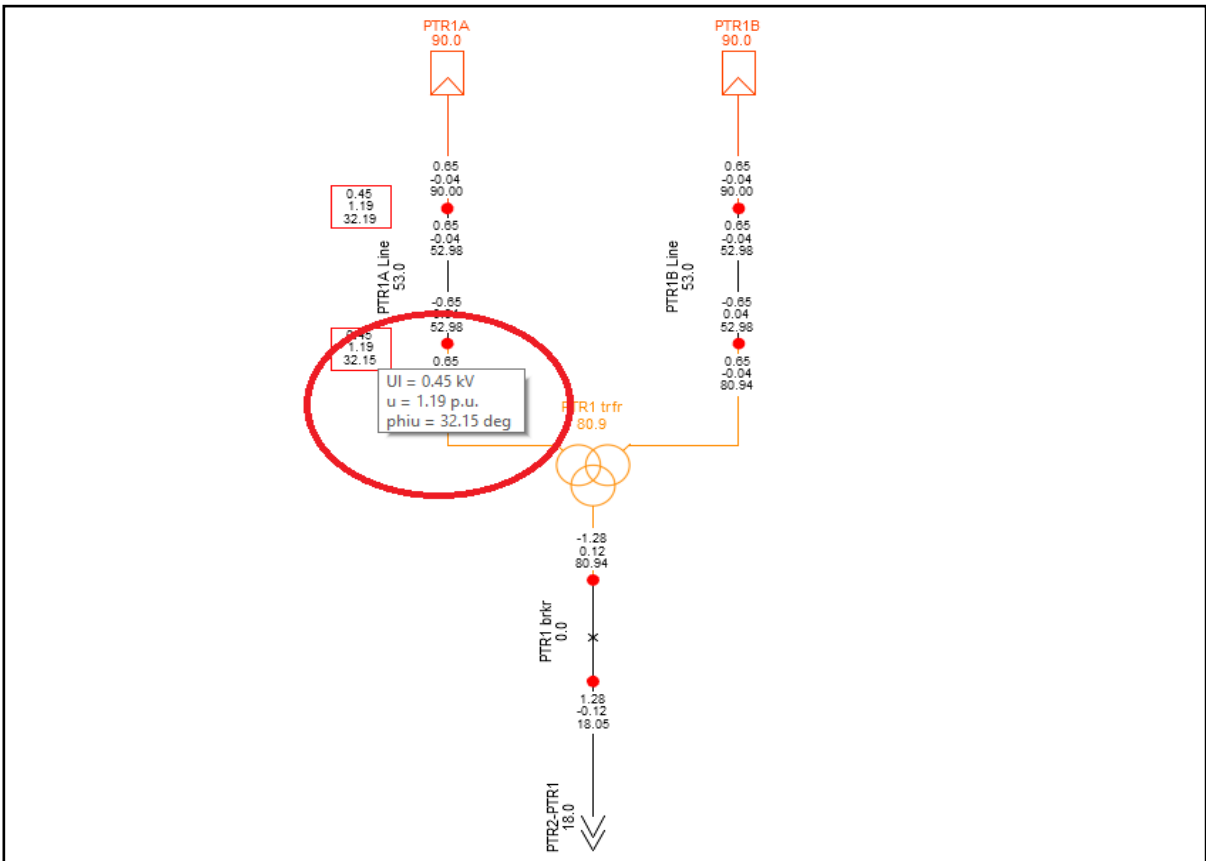


Figure C.49: Study case 2 - study point 4 during a voltage of 1.1 p.u. at the POC – inverter voltage within operational requirements

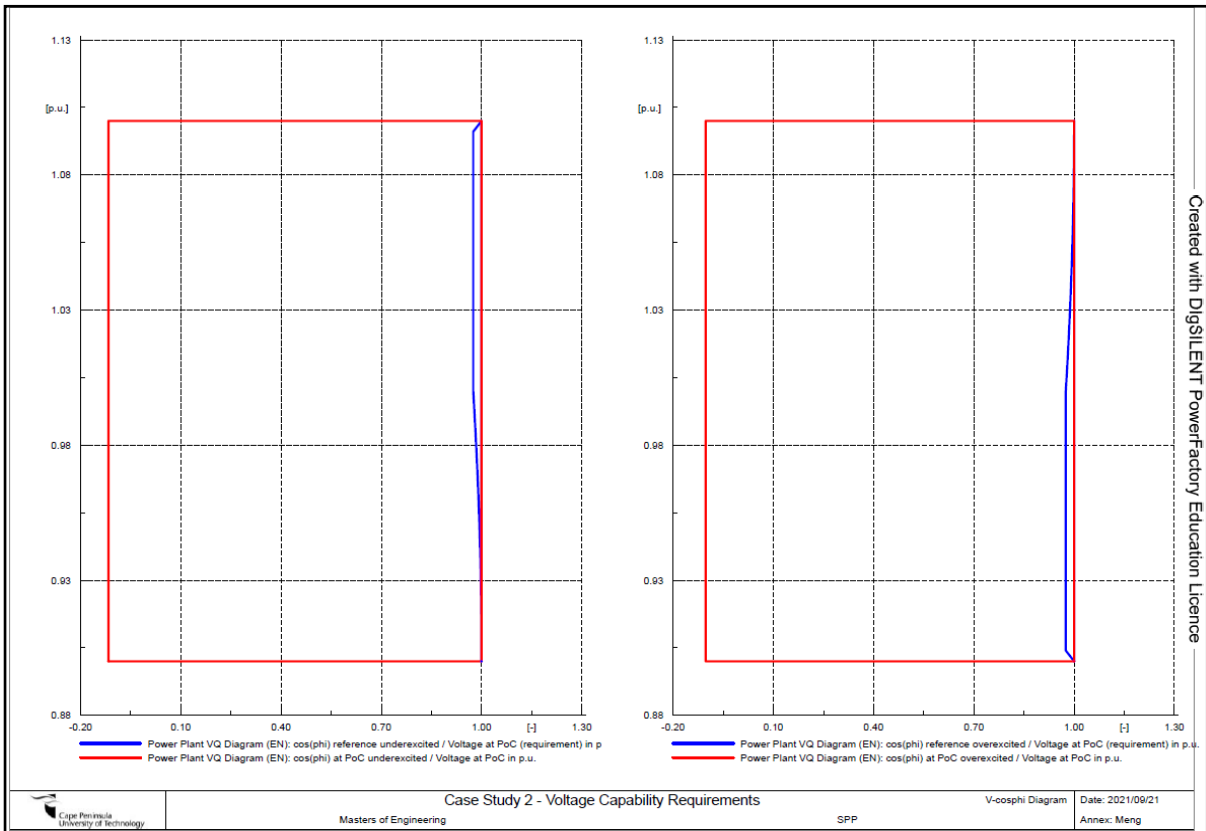


Figure C.50: Case study 2 - power factor and voltage requirement at POC indicating under excited (left) conditions and overexcited conditions (right)

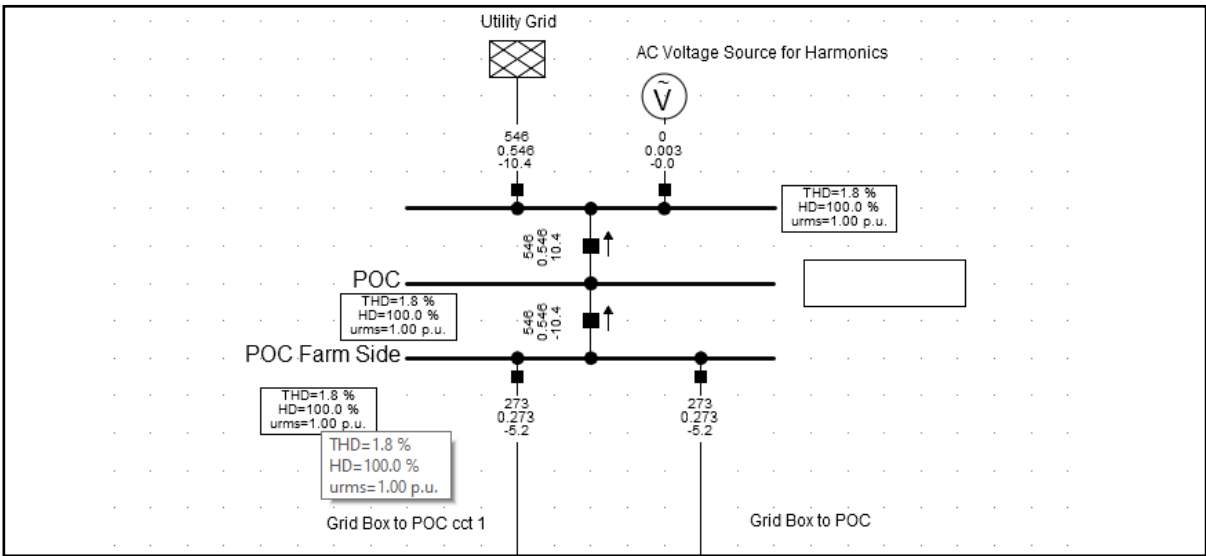


Figure C.51: Case study 3 - THD at POC for maximum fault level with shunt filter 1

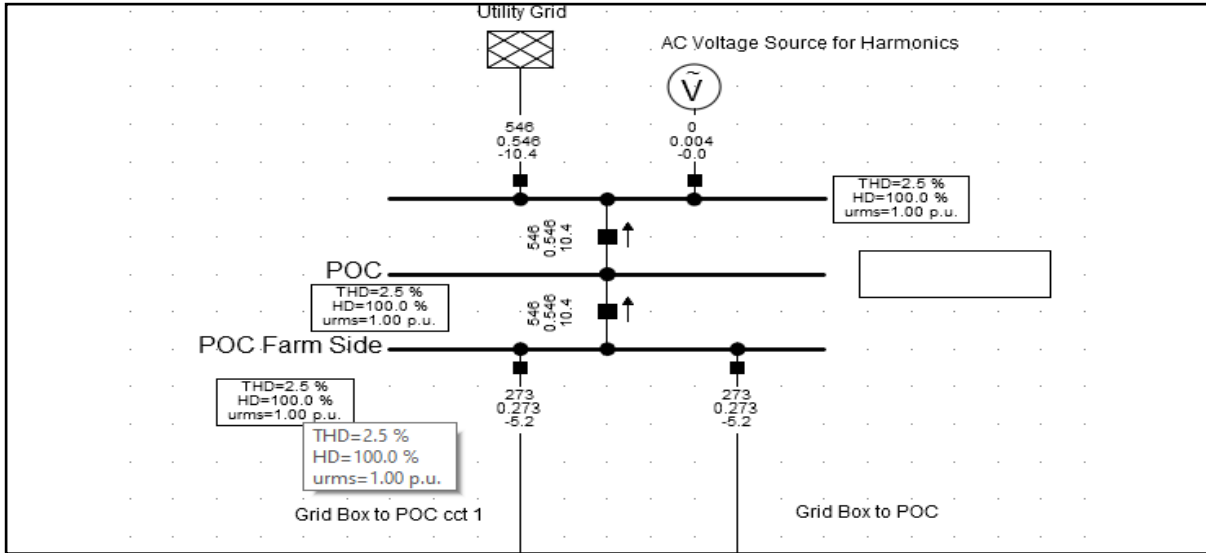


Figure C.52: Case study 3 - THD at POC for minimum fault level with shunt filter 1

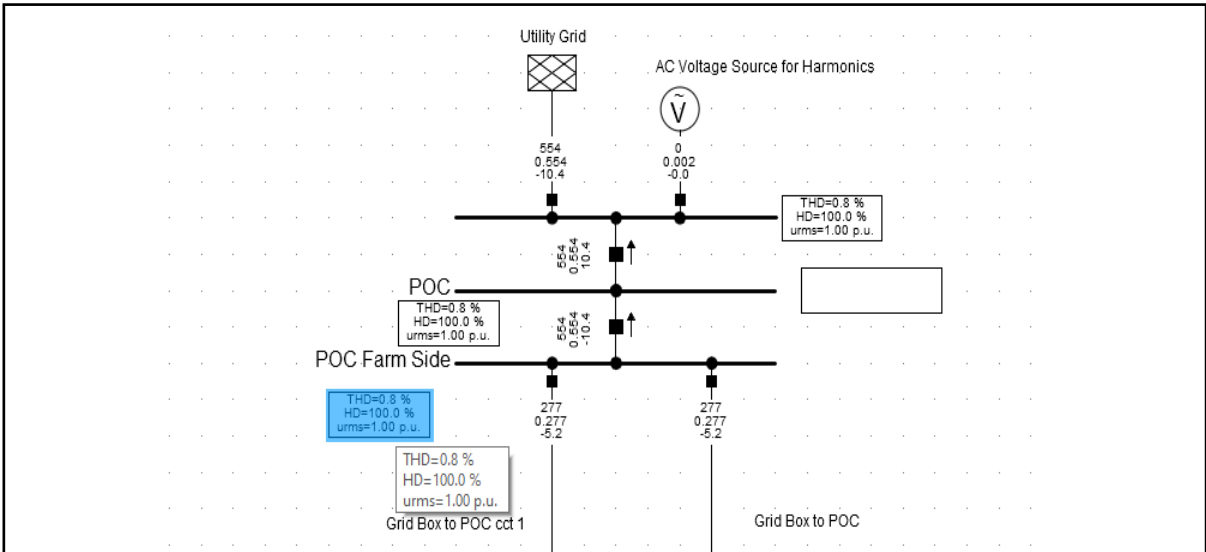


Figure C.53: Case study 3 - THD at POC for maximum fault level with shunt filter 2

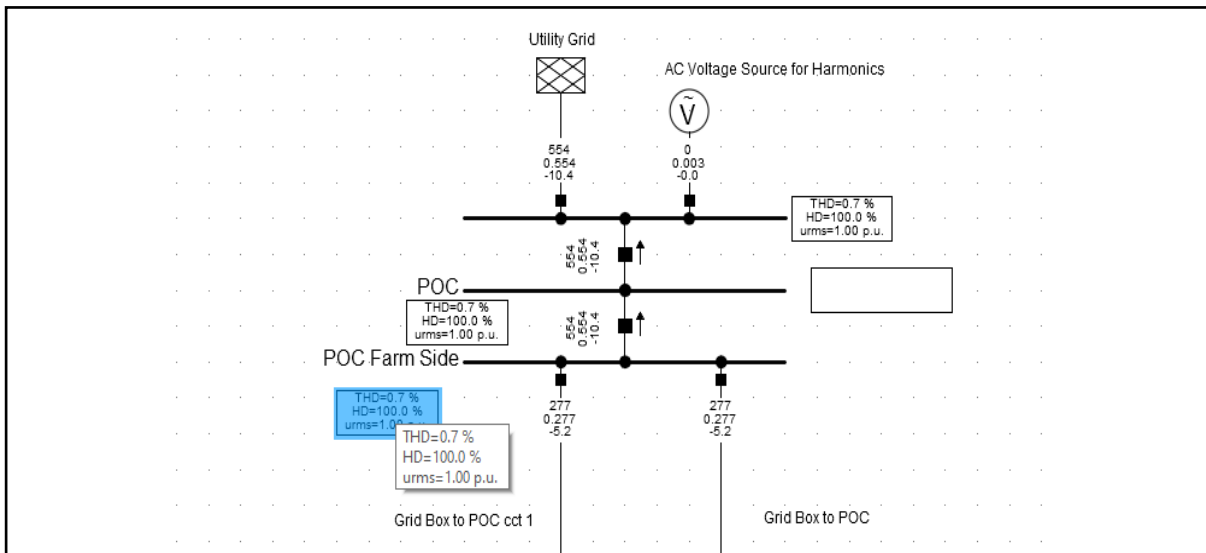


Figure C.54: Case study 3 - THD at POC for minimum fault level with shunt filter 2